LACTOFERRIN INTERACTS WITH THE AMYLOID-β PRECURSOR PROTEIN AND EXACERBATES Aβ PRODUCTION

Andrew Tsatsanis

The University of Leeds

School of Biomedical Sciences

August 2019

Submitted in accordance with the requirements for the degree of

Doctor of Philosophy

The candidate confirms that the work submitted is his own and that appropriate credit has been given where reference has been made to the work of others.

Specific contributions from others are as follows:

Dr Tim Ryan (The University of Melbourne, Australia) performed sedimentation velocity experiments relevant to Chapter 3.0.

Dr Bruce Wong (The University of Melbourne, Australia) performed tryptophan fluorescence experiments relevant to Chapter 3.0 and all aspects related to animal work relevant to Chapter 3.0, Chapter 4.0 and Chapter 5.0.

ACKNOWLEDGEMENTS

First and foremost, I would like to acknowledge and thank Alzheimer's Society with support from the Healthcare Management Trust for without their vital funding none of this research would have been possible. A heartfelt thank you to my Alzheimer's Society monitors, Sandra Barker and Eric Deeson. Their support and excitement during our progress meetings always made me feel my research was something more than just 'results'.

A huge thank you to my primary supervisor, James Duce. You are not only my mentor but also my friend. You are an incredible role model and I always admired your integrity and belief in fair dealing. You rescued me multiple times of distress and I always wondered what kind of emotional intelligence you must have to tolerate my unique personality. You always had my best interests at heart even though I was totally oblivious to what they were at the time. Your maddening attention to detail and inability to accept sub-par research inspired me to grow into a critical, knowledgeable, skilled and independent researcher. Thank you for your patient guidance, encouragement and advice in how to tackle such a complex research project. To my co-supervisor, Asipu Sivaprasadarao (Rao). Thank you for 'adopting' me into your lab during the second half of my PhD. I am forever grateful for your continuous support, patience, motivation and immense knowledge. You inspired me multiple times during our many discussions and I truly appreciate your critical feedback and suggestions regarding my work. Not only did you treat me like a fellow scientist, you taught me how to think like one, and for that I am eternally grateful.

I would like to thank and acknowledge Bruce Wong for performing the tryptophan fluorescence experiments and all aspects of animal work which has contributed to this thesis. An additional acknowledgement to Tim Ryan for performing the sedimentation velocity experiments, Anthony Turner for kindly providing cell lines for *in vitro* experimentation, and Robert Evans for generously providing purified human lactoferrin. Thank you to Sally Boxall for assistance in analysing flow cytometry data and for providing expertise on confocal microscopy.

I wish to express my gratitude to Sreenivasan Ponnambalam (Vas) and Mike Harrison for their experimental advice. An honourable mention goes to Christos

Pliotas. Thank you for letting me use your coffee machine which kept me going during times of immense stress. Your friendship and words of encouragement meant a lot.

To my wonderful friends I have made here in the United Kingdom that I now consider as family; Izma Abdul Zani (‘The Iz’), Faheem Shaik (‘Faheemi’), Robert Bedford (‘Robbie’), Gareth Fearnley (‘Gazza’), and Gina Smith (‘Gina’). Thank you for accepting and loving me the way I am. I gratefully appreciate your words of wisdom, advice and support. Cheers for always requesting Kylie Minogue songs to the DJ at the dance clubs (even though I was the only one dancing). A further acknowledgement goes to ‘The Iz’. You will always be my ‘Queen B’.

To my Australian friends; John (‘Yovan’), Dijana (‘Dude’), Daniella (‘Dan’), Diana (‘Dashe’), and Melissa (‘Mia’). Thank you for your love and encouragement. To my mother and father, Anastasia (‘Ma’) and George (‘Ba’). I love you both to the moon and back. Your love and support, both emotional and financial (especially financial) helped me so much. To my sister Jenny (‘Sultana’), brother-in-law Peter, brother Anthony (‘Donche’) and sister-in-law Laura, thank you for your love and words of wisdom. To my nephews and nieces; Geordie, Natasha, Olivia, George and Isabella. I love you all so much and thank you for always making me laugh. You are the pericardium that protects my heart.

This might seem silly but in my first month of starting my PhD, I found a fortune cookie on my desk that read ‘competence like yours is underrated’. I have kept that strip of paper with me ever since as a source of motivation. I would also like to acknowledge the following songs and artists I listened to ad nauseam at particular times during my PhD. Thank you to the following: ‘You’re The Best Around’ by Joe Esposito, ‘Weird Science’ by Oingo Boingo, ‘Blind’ by Hercules and Love Affair, ‘I’m Still Standing’ by Elton John, ‘All By Myself’ by Jamie O’Neal, ‘Enough Is Enough’ by Barbra Streisand and Donna Summer, and ‘Perfect Day’ by Lou Reed. Finally, for those particular experiments that seemed impossible to accomplish, there was a voice within me that repeatedly said ‘don’t lose hope’. I honestly believe that voice came from above and I couldn’t have accomplished this PhD without you. Thank you.

ABSTRACT

One of the predominant neuropathological hallmarks of Alzheimer's disease (AD) is extracellular senile plaques, the major component of which is the amyloid-β (Aβ) peptide, produced by the amyloidogenic processing of amyloid-β precursor protein (APP). Additional early indicators of AD include neuroinflammation and iron dyshomeostasis, but how each contributes to AD pathogenesis remains unclear. Lactoferrin (Lf) is an acute phase protein that is elevated in the AD brain and has been linked to neuroinflammation, stifling pathogen growth in part by sequestering free iron. Through a series of biophysical techniques, the conformational modification to Lf caused when iron is bound (holo-Lf) enabled a complex to be formed with the E2 domain of APP. Holo-Lf deviated cell surface APP from the classical clathrin-dependent internalisation route to a clathrin-independent route requiring ADP ribosylation factor 6 (ARF6). This directed APP to (Rab11-positive) vesicles for amyloidogenic processing, leading to increased Aβ production. Masking the holo-Lf binding sites of APP using either an antibody recognising Lf or peptides derived from APP that recognise the binding site on holo-Lf, alleviated the amyloidogenic processing of APP that was evident when holo-Lf alone was present. The removal of APP from the cell surface upon addition of exogenous holo-Lf also altered iron homeostasis via impairing APP associated surface stabilisation of the iron exporter ferroportin (FPN). By directly associating with APP, an acute phase role for Lf could be to sequester iron from invading pathogens. Furthermore, with Aβ being reported as an antimicrobial, an additional protective response of initiating this pathway may be the secretion of this peptide to destroy the pathogens. While this may initially be beneficial, this is likely not to be sustainable with a progressive build-up of intracellular iron, leading to iron-associated lipid peroxidation, and persistent elevated Aβ production further contributing to cell death. We reveal a physiologically novel sequence of events in which Lf via APP may lead to detrimental hallmarks related to AD when persistently induced by the presence of Lf. The identification of this novel therapeutic target that not only modulates the processing of APP but is also involved in the associated mechanisms implicated in AD leads hope for potential therapy.

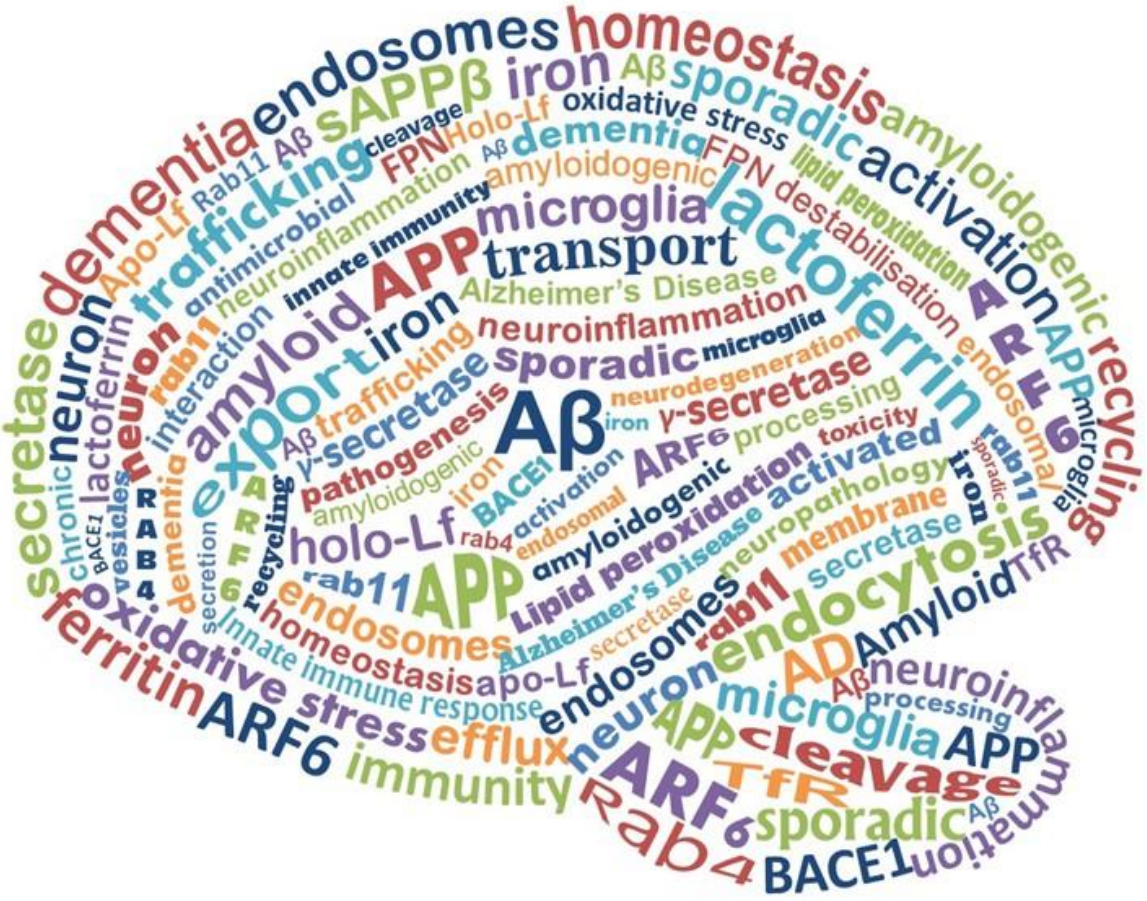
secretase
dementia
endosomes
homeostasis
amyloidogenic
recycling
neuron
chronic
lactoferrin
Apo-Lf
Rab11
Aβ
sAPPβ
iron
Aβ
sporadic
activation
APP
microglia
trafficking
cleavage
FPN
Holo-Lf
oxidative stress
dementia
FPN
lipid peroxidation
ARF6
vesicles
RAB4
antimicrobial
neuroinflammation
amyloidogenic
destabilisation
endosomal
rab11
interaction
innate immunity
amyloid
APP
transport
lactoferrin
export
iron
Alzheimer's Disease
neuroinflammation
microglia
trafficking
sporadic
neurodegeneration
γ-secretase
Aβ
iron
processing
pathogenesis
γ-secretase
toxicity
activated
rab11
sporadic
amyloidogenic
iron
BACE1
ARF6
activation
endosomal
rab4
Lipid peroxidation
neuropathology
iron
membrane
holo-Lf
APP
amyloidogenic
Alzheimer's Disease
secretase
endocytosis
TfR
Amyloid
AD
rab11
endosomes
Aβ
neuroinflammation
processing
neuron
microglia
APP
cleavage
TfR
ARF6
sporadic
Aβ
Rab4
BACE1
inflammation
ferritin
ARF6
oxidative stress
efflux
immunity
Innate immune response
homeostasis
apo-Lf
endosomes
rab11
recycling
secretion
dementia

TABLE OF CONTENTS

LIST OF TABLES

LIST OF FIGURES

CHAPTER 7.0

CHAPTER 8.0

ABBREVIATIONS

α2-M	α2-macroglobulin
Aβ	Amyloid-β
AβO	Aβ oligomer
ABC	ATP-binding cassette
AD	Alzheimer’s disease
ADAM	A disintegrin and metalloprotease
AICD	APP intracellular domain
ANOVA	Analysis of variance
APH-1	Anterior pharynx defective 1
APLP	Amyloid precursor-like protein
APOE	Apolipoprotein-E
APOER2	APOE receptor 2
APP	Amyloid-β precursor protein
APPKO	APP knockout
APPL	APP-like
ARF6	ADP ribosylation factor 6
BACE1	β-site APP cleaving enzyme 1
BBB	Blood brain barrier
BBCEC	Bovine brain capillary endothelial cell
BCA	Bicinchoninic acid
BIN1	Bridging integrator 1

BRI2	Integral membrane protein 2B
CAM1	Cell adhesion molecule 1
CAPPD	Central APP domain
CD2AP	CD2-associated protein
CD33	Sialic acid-binding immunoglobulin-like lectin
CHC	Clathrin heavy chain
CLU	Clusterin
CNS	Central nervous system
COX-2	Cycloxygenase-2
Cp	Ceruloplasmin
CR1	Complement receptor 1
CSF	Cerebrospinal fluid
CTF	C-terminal fragment
DAPI	4’,6-diamidino-2-phenylindol dihydrochloride
DFP	Deferiprone
DMEM	Dulbecco’s modified eagle medium
DMT1	Divalent metal transporter-1
DR6	Death receptor 6
DYM	Dynamin
ECL	Enhanced chemiluminescence
ELISA	Enzyme-linked immunosorbent assay
EMEM	Eagle’s minimum essential medium

eNOS	Endothelial NOS
EPHA1	Ephrin receptor A1
ERK1/2	Extracellular signal-regulated kinases 1 and 2
FAC	Ferric ammonium citrate
FACS	Fluorescence-activated cell sorting
FAD	Familial Alzheimer’s disease
FBS	Foetal bovine serum
FIP3	Family interacting protein 3
FPN	Ferroportin
Ft	Ferritin
FTD	Frontotemporal dementia
GAP	GTPase activating protein
GEF	Guanine nucleotide exchange factor
GFLD	Growth factor-like domain
Gpx4	Glutathione peroxidase 4
GWAS	Genome-wide association study
HBD	Heparin-binding domain
HBSS	Hank’s balanced salt solution
HFE	Human hemochromatosis protein
HMC3	Human microglial clone 3
HRP	Horseradish peroxidase
IFN-γ	Interferon-γ

IL-1	Interleukin-1
IP	Immunoprecipitation
IRE	Iron regulatory element
IRP	Iron response protein
KPI	Kunitz-protease inhibitor
LDLR	Low density lipoprotein receptor
Lf	Lactoferrin
LfKO	Lf knockout
LfR	Lf receptor
LIP	Labile iron pool
LPS	Lipopolysaccharides
LRP1	LDLR-related protein 1
LTP	Long term potentiation
MβCD	Methyl-β-cyclodextrin
MAP	Mitogen-activated protein
MeSNa	2-mercaptoethane sulfonic acid
MHC class II	Major histocompatibility complex class II
MPP^+	1-methyl-4-phenylpyridinium
MRI	Magnetic resonance imaging
MS4A cluster	Membrane-spanning 4-domains subfamily A
N2a	Neuro-2a
NF-κB	Nuclear factor-κB

NFT	Neurofibrillary tangle
NMDA	N-methyl-D-aspartate
NO	Nitric oxide
NOS	Nitric oxide synthase
NSAID	Non-steroidal anti-inflammatory drug
PDGFB	Platelet derived growth factor β polypeptide
PEN-2	PSEN enhancer-2
PET	Positron emission tomography
PICALM	Phosphatidylinositol-binding clathrin assembly protein
PKC	Protein kinase C
PNS	Peripheral nervous system
PRR	Pattern recognition receptor
PSEN	Presenilin
PSP	Progressive supranuclear palsy
PVDF	Polyvinylidene difluoride
Rab GDI	Rab GDP dissociation inhibitor
RAGE	Receptor for advanced glycation end products
RAP	Receptor associated protein
RIN3	Ras and Rab interactor 3
RIPA	Radioimmunoprecipitation assay
RNAi	RNA interference
ROS	Reactive oxygen species

RSL3	RAS-selective lethal 3
SAD	Sporadic Alzheimer’s disease
sAPP	Soluble APP
SDS-PAGE	Sodium dodecyl sulfate-polyacrylamide gel electrophoresis
SE	Standard error
sLRP1	Soluble LRP1
SORLA	Sorting protein-related receptor
Tf	Transferrin
TfR	Tf receptor
TGN	trans-Golgi network
TM	Transmembrane
TMB	3,3',5,5'-tetramethylbenzidine
TNF-α	Tumour necrosis factor-α
tPA	Tissue-type plasminogen activator
TREM2	Triggering receptor expressed on myeloid cells 2
UK	United Kingdom
UTR	Untranslated region

CHAPTER 1.0 INTRODUCTION

1.1 Alzheimer's Disease

Dementia is a general term that outlines a group of brain disorders that impedes cognitive function. Not only is it devastating to the sufferer but family, friends and carers are also affected. There is an estimated 46.8 million dementia sufferers worldwide with one new case of dementia being diagnosed every 3 seconds (Prince et al., 2015). Within the United Kingdom (UK), there are 850,000 people suffering from dementia, which leaves the UK with a financial burden of £26.3 billion per annum (Prince et al., 2014). This number of dementia sufferers is expected to increase to over 1 million by the year 2025 (Prince et al., 2014). The most common type of dementia is AD which accounts for 60-80 % of all cases (Prince et al., 2014).

What triggers the onset of AD still remains unclear, but several cohort studies have shown age, sex, family history and genetics, lifestyle and education level to be major risk factors (Kukull et al., 2002; Lobo et al., 2000; Qiu et al., 2009). Symptoms usually start with memory loss, ultimately leading to changes in personality, a decrease in cognitive function, a decline in language and motor function and finally death (Tarawneh and Holtzman, 2012). Studies have also estimated the disease process to begin 10-20 years before any symptoms appear (Perrin et al., 2009). Therefore, in order to fully understand the pathogenesis of AD and to develop new therapeutic treatments, further research is vital for a better understanding of disease progression, from pre-symptomatic to post-symptomatic.

It has been over 100 years since the first diagnosis of AD and to date there is still no cure, biomarker, or therapeutic treatment to detect, halt or reverse disease progression (Tanzi and Bertram, 2005). It can be very difficult to distinguish between the various forms of dementia in living patients. Sadly, the only definitive way to diagnose a person with AD is via autopsy. In addition to *post mortem* analysis, advanced brain scanning of living AD patients are beginning to illustrate clearer signs of atrophy in the cerebral cortex, lateral ventricles and hippocampus of the brain, and these correlate with mental decline (Jahn, 2013; Sabuncu et al.,

2011). A loss of synapses, axons and dendrites ultimately leads to neuronal deterioration and death (Kern and Behl, 2009).

There are two known forms of AD: familial which is early onset (FAD) and sporadic which is late onset (SAD) (Gotz and Ittner, 2008; McGowan et al., 2006; Murrell et al., 1991). FAD is hereditary (usually an autosomal dominant mutation), extremely rare and accounts for less than 5 % of all AD cases (Citron et al., 1992; Gotz and Ittner, 2008; McGowan et al., 2006; Murrell et al., 1991; Tomita et al., 1997). It is caused by mutations in 3 genes: APP, presenilin (PSEN) 1 or 2, all of which are involved in the overproduction of Aβ; a peptide known to be a neuropathological hallmark of AD (Citron et al., 1992; Gotz and Ittner, 2008; McGowan et al., 2006; Murrell et al., 1991; Tomita et al., 1997). SAD has a less clear aetiology but a number of risk factors are related to this form of the disease. One major risk factor gene is the apolipoprotein-E (APOE) (Gotz and Ittner, 2008; McGowan et al., 2006). The ε3 allele of APOE seems to be the most common within individuals while ε2 allele shows a decreased risk (Gotz and Ittner, 2008; McGowan et al., 2006). Individuals displaying the APOE ε4 allele do not necessarily suffer from SAD but factors such as environment and diet increase the risk of developing the disease. Genome-wide association studies (GWAS) have also identified a number of other potential risk factor genes associated with SAD. The following nine genes have been estimated to explain up to 50 % of SAD genetics (Hollingworth et al., 2011a; Morgan, 2011): clusterin (CLU), phosphatidylinositol-binding clathrin assembly protein (PICALM), complement receptor 1 (CR1), bridging integrator 1 (BIN1), ATP-binding cassette (ABC) transporter A7, membrane-spanning 4-domains subfamily A (MS4A cluster), CD2-associated protein (CD2AP), sialic acid-binding immunoglobulin-like lectin (CD33), and ephrin receptor A1 (EPHA1) (Dong et al., 2017; Harold et al., 2009; Hollingworth et al., 2011b; Lambert et al., 2009; Lambert et al., 2013; Naj et al., 2011; Seshadri et al., 2010). Individuals suffering from Down syndrome also have an increased risk from developing early onset SAD. Down syndrome is caused from having an extra copy of chromosome 21 (trisomy 21) that encodes the APP gene (Robakis et al., 1987a). Sufferers of Down syndrome exhibit an accumulation of Aβ (processed from APP) and exhibit AD symptoms before the age of 60 (Cataldo et al., 2000; Masters et al., 1985).

1.1.1 Hallmarks of AD

The two main neuropathological hallmarks of AD are extracellular senile plaques formed by the aggregation of the Aβ peptide and intracellular neurofibrillary tangles (NFTs) consisting mainly of hyperphosphorylated tau, a microtubule associated protein (Bertram et al., 2010; Gendron and Petrucelli, 2009; Hardy and Allsop, 1991; Mandelkow and Mandelkow, 1998; Serrano-Pozo et al., 2011a; Trojanowski and Lee, 2000).

NFTs are deposited within neurons of the entorhinal cortex, hippocampus, amygdala and the deeper layers of the neocortex (Morrison and Hof, 1997). There are also other minor components found in NFTs which include a number of proteins such as ubiquitin, APOE, kinases and other cytosolic enzymes, transition metal ions and other stress related molecules. Aβ and Aβ binding proteins can also be present in these aggregates (Hyman et al., 1989; Perry et al., 1987; Shin et al., 1994; Strittmatter et al., 1993). NFTs are not exclusively found in AD as they are also present in tauopathies such as frontotemporal dementia (FTD), progressive supranuclear palsy (PSP), Neimann-Pick disease, and certain forms of Parkinsonism (Perl, 2010).

Senile plaques are predominantly composed of Aβ fibrils but additional proteins and molecules include APOE, cell adhesion molecule 1 (CAM1), heparin sulphate proteoglycans and various acute phase proteins such as α2-macroglobulin (α2-M) (Armstrong, 2009; Strittmatter et al., 1993). Plaques form in an orderly and progressive manner over time (Thal et al., 2006) and deposit primarily within the subiculum to the outer CA1 area of the hippocampus (Serrano-Pozo et al., 2011a). Deposits then spread to the entorhinal cortex and ultimately to the CA4 central region of the hippocampus (Serrano-Pozo et al., 2011a).

1.1.2 The amyloid cascade hypothesis

The amyloid cascade hypothesis states that the overproduction of Aβ peptide in the brain is the initial, fundamental, driving event that causes AD (Hardy and Allsop, 1991). It was first proposed in 1991 by John Hardy and David Allsop and further updated and re-evaluated by John Hardy and Gerry Higgins (Hardy and Higgins, 1992). Since then, the amyloid cascade hypothesis has been generally

widely accepted, referenced and re-appraised several times (Armstrong, 2011; Hardy, 2009; Karran et al., 2011).

Mutations in APP or the presenilin proteins in FAD causes an accumulation and aggregation of Aβ, essential for AD pathogenesis (Citron et al., 1992; Murrell et al., 1991; Tomita et al., 1997). It was this finding that gave rise to the amyloid cascade hypothesis.

There are two major Aβ toxic species: $A\beta_{40}$ and $A\beta_{42}$ (40 and 42 amino acids long respectively) (Carrillo-Mora et al., 2014). $A\beta_{42}$ possesses more hydrophobic properties and therefore is more susceptible to aggregate and form fibrils (Citron et al., 1992; Dahlgren et al., 2002; Murrell et al., 1991; Tomita et al., 1997). A characteristic feature of AD progression is a reduction in cerebrospinal fluid (CSF) $A\beta_{42}$ (Motter et al., 1995; Rosen et al., 2013; Shaw et al., 2009). It is thought that the aggregated state of $A\beta_{42}$ inhibits it from being transported from the brain interstitial fluid to the CSF (Menendez-Gonzalez et al., 2018; Padayachee et al., 2016). However, since CSF $A\beta_{42}$ levels can also be low in non-AD individuals, the use of $A\beta_{42}$ alone as a neurodegeneration biomarker is of limited use (Dumurgier et al., 2013; Knopman et al., 2001). Replacing $A\beta_{42}$ by the $A\beta_{42}/A\beta_{40}$ ratio which is also decreased in AD (Janelidze et al., 2016) has a higher association with amyloid deposition in the brain as assessed by positron emission tomography (PET) (Janelidze et al., 2017; Lewczuk et al., 2017; Niemantsverdriet et al., 2017).

Most of the Aβ produced is secreted from brain cells in a monomeric state, however in AD, these Aβ peptides aggregate to form toxic species responsible for neuronal death which leads to synaptic dysfunction, impaired long term potentiation (LTP) and oxidative stress (Shankar and Walsh, 2009), in addition to triggering immune cells such as microglia to elicit an inflammatory response (Ballatore et al., 2007; Hardy and Selkoe, 2002). The combination of these events is what causes dementia (Hardy and Selkoe, 2002). Monomeric Aβ aggregate to form oligomers (AβOs) that range in shape and size from dimers and trimers to multimers, which then aggregate further to give rise to Aβ fibrils (Ballatore et al., 2007; Hardy and Selkoe, 2002). Aggregated Aβ and activated microglia stimulate stress pathways in neurons, altering kinase and phosphorylase activity, leading to the hyperphosphorylation of the protein tau (Ballatore et al., 2007). Under

normal physiological conditions, the microtubule binding ability of tau is post-translationally regulated by serine/threonine-directed phosphorylation (Mietelska-Porowska et al., 2014). Phosphorylated tau is unable to bind to microtubules, allowing for the movement of vesicles and other cellular components (Cho and Johnson, 2004; Kadavath et al., 2015). Conversely, dephosphorylated tau binds and stabilises microtubules (Kadavath et al., 2015). Hyperphosphorylated tau is locked into a cytosolic form, causing it to destabilise and aggregate to form NFTs within the neuron (Metaxas and Kempf, 2016; Simic et al., 2016; Umeda et al., 2014). More damage is caused and protein transport within the neuron is impeded, resulting in a greater likelihood of neuronal death and microglia activation (Ballatore et al., 2007; Hardy and Selkoe, 2002).

The amyloid cascade hypothesis also applies to SAD. However, the triggering mechanism that increases or aggregates Aβ still remains elusive.

1.1.2.1 Critical analysis of the amyloid cascade hypothesis

Since its publication, there has been some controversy regarding the amyloid cascade hypothesis, questioning its validity and whether or not Aβ accumulation is the primary event that causes AD.

The amyloid cascade hypothesis clearly states that Aβ deposition triggers the formation of NFTs (Hardy and Higgins, 1992). The topographical distribution of Aβ plaques and NFTs in both FAD and SAD show a poor correlation and there is evidence to suggest that Aβ aggregation is not sufficient to cause NFTs (Irvine et al., 2008; Morris et al., 2014; Nisbet et al., 2015; Struble et al., 2010). Several groups have shown Aβ deposits to infiltrate the cortex and then progress through the brain in an inward fashion whilst NFTs show an opposite progression (Braak and Braak, 1991; Price et al., 1991). Studies have shown a strong correlation between cholesterol homeostasis and Aβ accumulation and also NFT formation. Elevating membrane cholesterol levels *in vitro* increases the interaction between APP and BACE1, promoting β-cleavage of APP and Aβ production (Burns et al., 2003; Cordy et al., 2003). In addition, rat hippocampal neurons depleted of cholesterol affects the phosphorylation of tau and causes NFTs without the influence of Aβ (Koudinov and Koudinova, 2001). This evidence suggests that cholesterol metabolism might be a primary event that triggers AD pathogenesis, causing the hyperphosphorylation of tau and NFT formation as well as an

increase in Aβ production eventually giving rise to senile plaques. Therefore, Aβ may merely be a toxic by-product that contributes to neurodegeneration and not responsible for initiating AD pathology. This might be a plausible explanation regarding SAD but in FAD patients, mutations in APP and the presenilin proteins directly cause an increase in toxic $A\beta_{42}$. Furthermore, mouse models exhibiting these mutations show significant amyloid deposition and symptoms associated with AD such as memory loss, signifying that Aβ alone is enough to cause AD (Citron et al., 1992; Murrell et al., 1991; Tomita et al., 1997). Altering cholesterol levels is known to have detrimental effects on multiple proteins besides APP and Aβ, making any attempt for a therapeutic target extremely difficult (Wood et al., 2014). Also, other neurodegenerative diseases such as tauopathies do not exhibit any amyloid deposition (Perl, 2010), implying that NFTs in AD develop subsequent to amyloid deposits (Bolmont et al., 2007; Oddo et al., 2003). More evidence to suggest that Aβ deposition is responsible for NFT formation comes from the work performed by the groups of Hardy and Selkoe. When authors introduced APP mutations into transgenic tau mice, hyperphosphorylated tau and NFT formation increased, demonstrating amyloid pathology instigates tau hyperphosphorylation and NFT formation (Hardy, 2006; Hardy and Selkoe, 2002). Fibroblast cells acquired from AD patients, reprogrammed into stem cells and differentiated into neurons exhibited an increase in Aβ and phosphorylated tau levels, again acknowledging the relationship between the two and their importance in AD pathology (Israel et al., 2012).

A major flaw of the amyloid cascade hypothesis is that senile plaques and NFTs can be present in non-demented elderly individuals regardless of their cognitive state. This attributes to a poor correlation between AD symptoms and Aβ or NFT load (Arriagada et al., 1992; Ohm et al., 1995). Indeed, it is the synaptic dysfunction in AD patients that appear to have better correlation with cognitive decline (Coleman and Yao, 2003; Koffie et al., 2011; Tampellini, 2015). However, studies have shown that the species of Aβ is crucial for AD pathology and that AD patients contain the oligomeric form of Aβ at the synapse whereas non-demented elderly individuals do not (Bjorklund et al., 2012). This suggests that the biophysical state and location of Aβ play a significant role in AD pathogenesis.

Questions still remain unanswered regarding the amyloid cascade hypothesis and even though drug treatments that are based on this hypothesis have shown

a reduction in Aβ load in mouse models exhibiting AD-like symptoms, they have not been successful in human clinical trials (Pimplikar, 2009).

1.2 The amyloid precursor protein

1.2.1 APP isoforms and homologues

APP is an integral type I transmembrane protein that produces Aβ when cleaved in a particular way (Kang et al., 1987). It is located on chromosome 21 (21q21) and is highly conserved (Goldgaber et al., 1987; Kang et al., 1987; Robakis et al., 1987b). The APP gene consists of 19 exons and alternative splicing of exons 7, 8 and 15 gives rise to three major isoforms, each differing in their extracellular domain (Yoshikai et al., 1991). The three major isoforms of APP are APP695, APP751 and APP770 (695, 751 and 770 amino acids long respectively) (Ponte et al., 1988). The APP695 isoform lacks the Kunitz-protease inhibitor (KPI) and OX-2 domains and is mainly expressed in neurons, whereas the APP751 and APP770 isoforms are expressed mostly in non-neuronal cells (Kang and Muller-Hill, 1990; Ponte et al., 1988; Weidemann et al., 1989).

There are human homologues of APP which are amyloid precursor-like protein (APLP) 1 and 2 which share 56 % and 68 % amino acid sequence homology to APP, respectively (Jacobsen and Iverfeldt, 2009; Slunt et al., 1994; Wasco et al., 1993; Wasco et al., 1992). There are also orthologs in a variety of other species such as APP-like (APPL) protein in fruit flies with 43 % homology (Luo et al., 1990; Rosen et al., 1989), and APL-1 in nematode worms with 46 % homology to APP (Daigle and Li, 1993). APLP-1, APLP-2 and APP all share a similar structure (Sandbrink et al., 1994; Walsh et al., 2007) and post-translationally all are glycosylated and phosphorylated in a similar way (Eggert et al., 2004; Suzuki et al., 1997; Walsh et al., 2007). In addition, the secretase enzymes responsible for the processing of APP are also able to cleave APLP-1 and 2 proteins and γ-cleavage of either produce an intracellular transcriptionally active fragment that translocates to the nucleus in a similar way as the cytosolic APP intracellular domain (AICD) produced from APP (Cong et al., 2011; Eggert et al., 2004; Endres et al., 2005; Gu et al., 2001; Hogl et al., 2011; Li and Sudhof, 2004; Scheinfeld et al., 2002; Walsh et al., 2003). However, one major difference between these family members is that APLP-1 and APLP-2 lack the Aβ region and therefore do not possess this proteolytic fragment that is toxic or prone to aggregation (Eggert

et al., 2004; Minogue et al., 2009). Whilst both APP and APLP-2 are ubiquitously expressed in the body, APLP-1 is solely expressed in the central nervous system (CNS) (Crain et al., 1996; McNamara et al., 1998). All three proteins show an overlapping expression pattern in the brain, suggesting redundancy or an intersecting function (Crain et al., 1996; McNamara et al., 1998). However, further studies using knockout mice have revealed variant phenotypes and subcellular localisations, suggesting that each protein could possess distinct functions as well as intersecting ones (Heber et al., 2000; Kim et al., 1995).

1.2.2 APP structure

The APP protein consists of a large extracellular amino-terminal domain, a single transmembrane (TM) domain and a small intracellular carboxy-terminal domain (Figure 1.1) (Reinhard et al., 2005). The structure of full-length APP or its entire intact extracellular domain have yet to be determined (Gralle and Ferreira, 2007). However, atomic resolution structures for the majority of APP regions (E1, KPI, E2, Aβ, TM, AICD) have been solved (Barnham et al., 2003; Dahms et al., 2010; Hynes et al., 1990; Luhrs et al., 2005; Nadezhdin et al., 2011; Rossjohn et al., 1999; Tomaselli et al., 2006; Wang and Ha, 2004). Structural studies suggest that the extracellular domain contains regions that are highly adaptable, representing individual folding units and therefore are able to undergo conformational changes, making them accessible for new, undiscovered, highly specific ligands (Botelho et al., 2003; Gralle et al., 2002; Gralle and Ferreira, 2007). The binding of these ligands could encourage a conformational change and stabilise the extracellular domain or possibly uncover cleavage sites of APP, resulting in an increase in ectodomain shedding (Gralle and Ferreira, 2007). However, whether the conformational shape of each characterised domain remains conserved with the additional domains present in regards to full-length membrane-bound APP remains to be seen.

The extracellular domain of APP has three major regions: the E1 region, the acidic region and the E2 region, also known as the central APP domain (CAPPD) (Figure 1.1) (Reinhard et al., 2005). Studies have confirmed protein-protein interactions within these regions. From the N-terminal region, the E1 domain contains a growth factor-like/heparin-binding domain (GFLD/HBD) followed by Cu^{2+} and Zn^{2+} metal binding sites (Ciuculescu et al., 2005; Dahms et al., 2010;

Kong et al., 2007; Rossjohn et al., 1999). The GFLD/HBD is cysteine-rich, contains disulphide bonds, a heparin binding site and a hydrophobic patch that serves as an important site for protein-protein interactions (Rossjohn et al., 1999). Adjacent to the E1 region is the unstructured and highly flexible acidic region. The significance of this region remains elusive. However, studies suggest that the acidic region regulates heparin-induced dimerisation of the E1 domain (Hoefgen et al., 2014). Following the acidic region is the KPI and OX-2 domain, which are absent in some isoforms of APP due to alternative splicing (KPI and OX-2 being absent in APP695; and OX-2 being absent in APP751) (Kang and Muller-Hill, 1990). *In vitro*, the KPI domain is known to inhibit various serine proteases (Sinha et al., 1990), and is also implicated in the coagulation cascade in human plasma (Smith et al., 1990; Van Nostrand et al., 1990). The role of the OX-2 domain still remains unclear. The E2 region is linked to the transmembrane domain by an unstructured linker domain and consists of a carbohydrate region containing a heparin binding site (Ninomiya et al., 1993; Wang and Ha, 2004) and a RERMS motif important for cell growth and differentiation (Li et al., 1997; Ninomiya et al., 1993). This remains speculative since structural studies have shown that access to the RERMS motif is limited and therefore a conformational change is required to expose the motif for interaction (Wang and Ha, 2004). The Aβ region is located partially within the extracellular linker domain and partially within the transmembrane domain (Figure 1.1). The transmembrane domain contains a GxxxG motif that determines the length of Aβ peptide produced from APP processing (Munter et al., 2007). Following the transmembrane domain is the intracellular cytoplasmic region (AICD), containing phosphorylation sites and a YENPTY motif that is involved in cell signalling and transcriptional regulation (Kerr and Small, 2005; Russo et al., 2005).

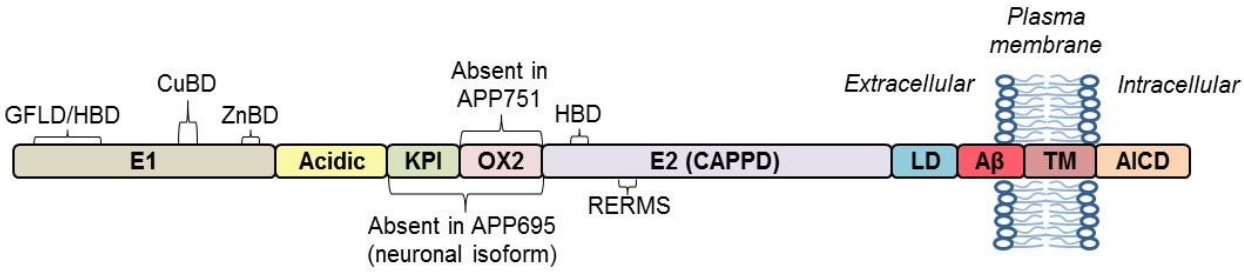

Figure 1.1. Schematic representation of the APP structure. The extracellular domain of APP is composed of the E1, acidic, and E2 (CAPPD) domains, each containing multiple subdomains. Alternative splicing of APP gives rise to various isoforms, namely APP770, APP751 and APP695. The KPI and OX-2 are absent in APP695 and the OX-2 domain is absent in APP751. The Aβ region is located partially within the extracellular LD and partially within the TM domain. Abbreviations: APP, amyloid-β precursor protein; CAPPD, central APP domain; BD, binding domain; GFLD, growth factor-like domain; HBD, heparin binding domain; KPI, Kunitz-protease inhibitor; TM, transmembrane; LD, linker domain; Aβ, amyloid-β; AICD, APP intracellular domain.

1.2.3 The maturation and trafficking of APP

APP is transported along the axon to nerve endings via fast anterograde transport which localises to synaptic terminals in the brain (Szodorai et al., 2009). APP is synthesised and translated on rough endoplasmic reticulum ribosomes within the cell body, before travelling to the Golgi/trans-Golgi network (TGN) where nascent APP undergoes maturation via the constitutive secretory pathway and trafficked to the plasma membrane (Lai et al., 1995; Lyckman et al., 1998; Tienari et al., 1996). Immature APP undergoes maturation via a series of post-translational modifications, including N- and O-linked glycosylation, ectodomain and cytoplasmic phosphorylation and tyrosine sulphation (Caporaso et al., 1994; Lassek et al., 2013; Sisodia et al., 1990; Tomita et al., 1998). Within neurons, the majority of APP is stored at the TGN (Graebert et al., 1995; Weidemann et al., 1989). The remaining APP (approximately 10 %) is transported from the Golgi to the cell surface via TGN derived secretory vesicles, where a small portion (approximately 30 %) undergoes α-cleavage (Koo et al., 1996) whilst the majority is re-endocytosed within clathrin-coated vesicles to the Rab5-positive early endosome (Cossec et al., 2010; Culvenor et al., 1995; Jung et al., 1996; Marquez-Sterling et al., 1997). Cell surface APP endocytosis requires the cytoplasmic YENPTY internalisation motif (Lai et al., 1995; Yamazaki et al., 1996). A small portion of APP that is trafficked to the endosome undergoes β-cleavage (Schrader-Fischer and Paganetti, 1996) whilst the rest is either transported back to the TGN, recycled back to the cell surface via Rab4-positive vesicles or delivered to Rab7-positive late endosomes and lysosomes where APP and/or its derived products are completely degraded (Figure 1.2) (Caporaso et al., 1992a; Lai et al., 1995; Yamazaki et al., 1996). For β-cleavage, the endosome's acidic pH provides an optimal environment for β-secretase processing of APP (Schrader-Fischer and Paganetti, 1996). In this processing pathway, APP subsequently undergoes γ-secretase processing in a variety of subcellular locations (Haass et al., 2012).

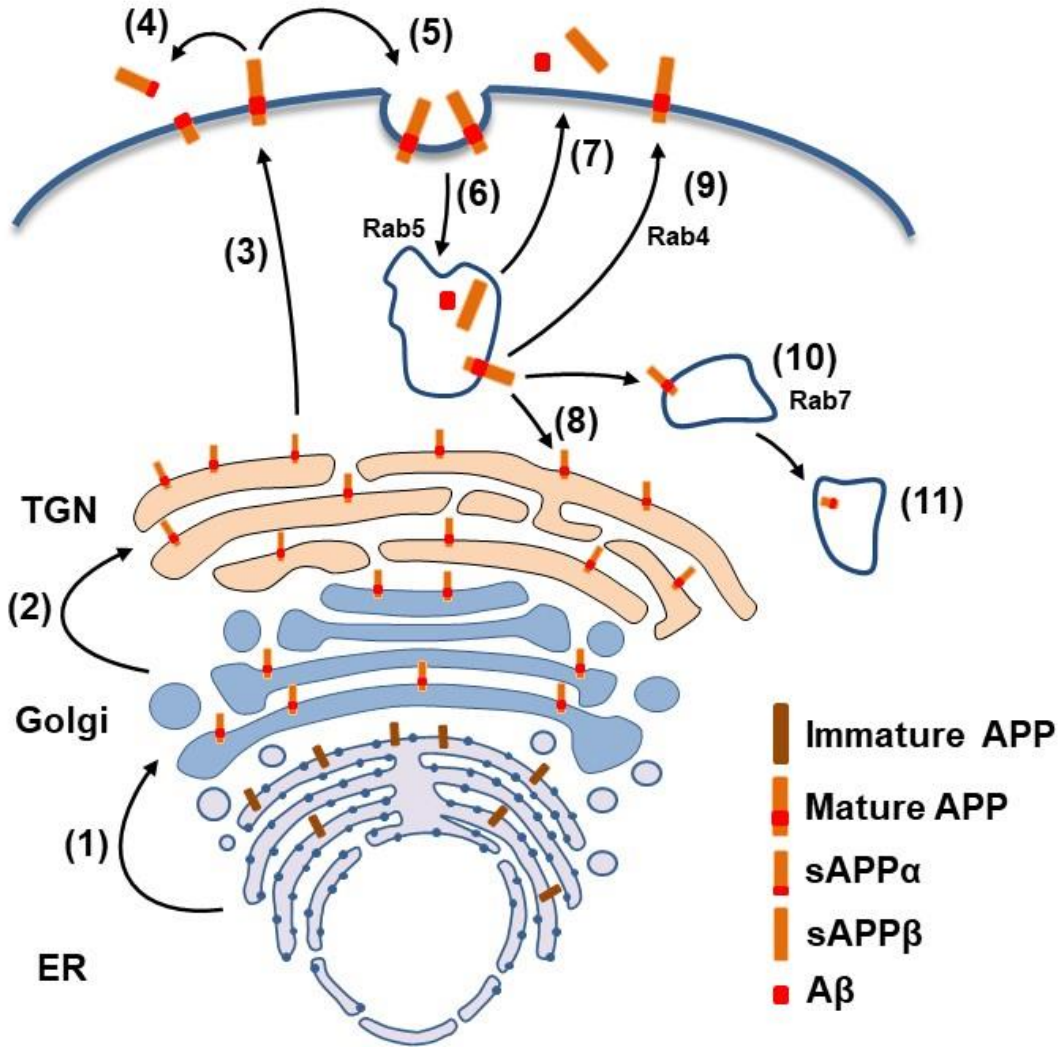

Figure 1.2. Schematic representation of APP trafficking. APP is synthesised and translated in the rough ER, before travelling to the Golgi (1) where immature APP undergoes maturation via a series of post-translational modifications. Whilst the majority of mature APP is stored within the TGN (2), a small portion may be trafficked to the cell surface via TGN derived secretory vesicles (3). Some APP on the cell surface can undergo α-cleavage to generate sAPPα (4) or be re-internalised (5) and trafficked to the Rab5-positive early endosome (6) to undergo β- and γ-cleavage to generate sAPPβ and Aβ, which are both secreted (7). After re-internalisation, most of the APP can also be transported back to the TGN (8), recycled back to the cell surface via Rab4-positive vesicles (9) or delivered to Rab7-positive late endosomes (10) and lysosomes (11) for degradation. Abbreviations: APP, amyloid-β precursor protein; ER, endoplasmic reticulum; TGN, trans-Golgi network; sAPP, soluble APP; Aβ, amyloid-β.

1.2.4 Rab GTPases involved in neuronal APP transport

Rab GTPases are small active proteins of the Ras superfamily and are associated with cellular vesicular trafficking. They are involved in vesicle formation and transport as well as tethering and docking to target compartments (Luo, 2000; Mitra et al., 2011; Takai et al., 2001). Rab proteins function as molecular switches and are able to shift back and forth from the inactive cytoplasmic GDP-bound state to the active membrane associated GTP-bound state; a process mediated by activator proteins called guanine nucleotide exchange factors (GEFs) (Cabrera and Ungermann, 2013; Stenmark and Olkkonen, 2001; Ullrich et al., 1994; Zerial and McBride, 2001). Once activated, Rab-GTP recruits cytosolic effector proteins that stabilise the Rab protein in its GTP state and aids in the docking and fusion of transport vesicles to their specific target membrane (Grosshans et al., 2006; Kaddai et al., 2008; Seabra et al., 2002; Stenmark and Olkkonen, 2001). After vesicle transport, Rab-GTP undergoes hydrolysis by GTPase activating proteins (GAPs) and returns to its inactive GDP-bound state (Alory and Balch, 2001; Markgraf et al., 2007). Rab GDP dissociation inhibitors (Rab GDIs) regulate Rab protein activity and localisation, and prevents the conversion of Rab-GDP to its active GTP state and facilitates the recycling of Rab-GDP back to its place of origin (Alory and Balch, 2001; Markgraf et al., 2007; Seabra et al., 2002).

There are over 60 known Rab GTPases and a considerable number have been identified to play a role in the trafficking and processing of APP (Diekmann et al., 2011; Li, 2011). A number of Rab GTPase proteins have been specifically associated with distinct subcellular compartments involved in the intracellular pathways of APP and many have become standard markers for these compartments. For instance, Rab5 is the major marker associated with early endosomes (Bucci et al., 1992; Gorvel et al., 1991; Markgraf et al., 2007), Rab7 is linked to late endosomes (Feng et al., 1995; Vanlandingham and Ceresa, 2009), and Rab4 and Rab11 are connected with fast and slow recycling endosomes, respectively (Daro et al., 1996; Goldenring, 2015; Grant and Donaldson, 2009; Trischler et al., 1999; van der Sluijs et al., 1992; Wilcke et al., 2000).

1.2.4.1 Rab5 Early Endosome

Rab5 has undeniably been the most studied endosomal Rab GTPase protein and has been associated with the pathogenesis of AD (Grbovic et al., 2003; Xu et al., 2018). Rab5 is linked with the early endocytic pathway and is predominantly localised in early/sorting endosomes and clathrin-coated vesicles (Bucci et al., 1992; Gorvel et al., 1991; Li and Stahl, 1993; Somsel Rodman and Wandinger-Ness, 2000). Major functions of Rab5 include vesicle tethering and docking for endocytic and recycling events as well as the fusion of endocytic vesicles to early endosomes (Gorvel et al., 1991; Somsel Rodman and Wandinger-Ness, 2000; Woodman, 2000). Studies have demonstrated Rab5 overexpression *in vitro* leads to an increase in APP endocytosis with subsequent formation of enlarged early endosomes that result in an increase in Aβ production (Grbovic et al., 2003; Li et al., 2012). *Post mortem* sporadic AD brain tissue also exhibit enlarged Rab5-positive early endosomes along with an increase in Rab5 expression, indicating an upregulation of the early endocytic pathway in sporadic AD (Cataldo et al., 2004; Ginsberg et al., 2010b). In support, GWAS analysis on sporadic AD identified Ras and Rab interactor 3 (RIN3) as a risk factor for the disease (Karch et al., 2014; Rosenthal and Kamboh, 2014). RIN3 functions as a Rab5 GEF which is known to activate Rab5 GTPase activity, potentially attributing to the upregulation of the early endocytic pathway in sporadic AD (Kajiho et al., 2003; Karch et al., 2014). Disruptions to the early endocytic pathway and changes in endosomal size have been shown to occur in areas of the brain independent of Aβ deposits, indicating alterations in the endocytic pathway may be involved in disease progression from an early stage (Cataldo et al., 2001; Grbovic et al., 2003; Nixon, 2005).

1.2.4.2 Rab7 Late Endosome

Rab7 GTPase is linked to the late endocytic pathway and is primarily associated with the transport of late endosomes to lysosomes (Feng et al., 1995). It is also involved in lysosome biogenesis and autophagy pathways (Bucci et al., 2000; Feng et al., 2014; Feng et al., 1995; Gutierrez et al., 2004; Jager et al., 2004). The cellular mechanisms involved in the transfer of cargo through the endocytic pathway requires further investigation. Two models have been proposed: the vesicular trafficking model and the maturation model. The vesicular trafficking

model suggests Rab7 is recruited to early endosomes where fusion of Rab5-positive cargo containing endocytic vesicles to the early endosome undergo sorting to Rab7-positive domains (Gruenberg, 2001; Meresse et al., 1995; Vonderheit and Helenius, 2005). These domains begin to bud and detach to form Rab7-positive carrier vesicles, where they are trafficked to pre-existing distinct late endosomes in the perinuclear region under microtubule dependent transport and subsequent degradation in lysosomes (Feng et al., 1995; Griffiths and Gruenberg, 1991; Gruenberg, 2001; Gruenberg et al., 1989; Gruenberg and Stenmark, 2004; Heinrich and Rapoport, 2005; Hu et al., 2015). In the maturation model, cargo destined for degradation are sorted into intralumenal vesicles, formed by the inward invagination and budding of the early endosomal membrane, to give an appearance of a multivesicular endosome (Hu et al., 2015; Hyttinen et al., 2013). As the endosome migrates to the perinuclear region along microtubules, the endosome matures via dissociation of Rab5 domains and replacement with Rab7. This process is aided by GAPs, GEFs and associated effector proteins (Hyttinen et al., 2013; Rink et al., 2005). Rab7-positive compartments that are devoid of Rab5 then fuse with one another, along with autophagosomes and other cytoplasmic vesicles containing degrading enzymes, to form the lysosome (Bucci et al., 2000; Hyttinen et al., 2013; Rink et al., 2005; Storrie and Desjardins, 1996). Both proposed models are yet to be fully elucidated and it is still unclear as to which of these two mechanisms form the basis of the late endocytic trafficking pathway. Co-existence as separate mechanisms could be possible in the same cell type or tissue (Sriram et al., 2006) but evidence pointing toward the maturation model has recently grown in momentum and is beginning to become widely accepted. This has largely arisen from several groups' pulse-chase experimental findings in a variety of cell lines using fluorescently labelled ligands (Bright et al., 2005; Dunn and Maxfield, 1992; Racoosin and Swanson, 1993; Sriram et al., 2003; Stoorvogel et al., 1991). After cellular uptake and a variable chase, individual endosomes retain their original endocytic load with numbers remaining constant. In addition, progressive gain and loss of characteristic endocytic vesicle markers were also apparent, making these findings incompatible with the vesicular trafficking concept (Dunn and Maxfield, 1992; Humphries et al., 2011; Poteryaev et al., 2010; Racoosin and Swanson, 1993; Sriram et al., 2003; Stoorvogel et al., 1991; Vonderheit and Helenius, 2005).

Similar to Rab5-positive early endosomes, *post mortem* sporadic AD brain tissue exhibit enlarged Rab7-positive late endosomes and lysosomes along with an increase in Rab7 expression, indicating an upregulation of the late endocytic pathway in sporadic AD (Cataldo et al., 2008; Ginsberg et al., 2010a). Furthermore, Rab7 overexpression *in vitro* leads to an accumulation in Aβ production within the late endosome and lysosome (LeBlanc and Goodyer, 1999; Liu et al., 2010; Yang et al., 1998). Taken together, these findings are in support of the maturation model of the late endocytic pathway since enlarged early endosomes serve as the precursor and eventually mature into enlarged late endosomes and lysosomes (Huotari and Helenius, 2011; Poteryaev et al., 2010). Physiologically, the Aβ that results from the amyloidogenic processing of APP is mostly degraded within lysosomes (Baranello et al., 2015; Saido and Leissring, 2012; Yuyama and Yanagisawa, 2009). In neurons, autophagosomes containing waste components and hydrolases (degrading enzymes) and late endosomes carrying cargo for degradation such as Aβ are present near synapses and require retrograde axonal transport to lysosomes (Gutierrez et al., 2004; Muresan and Muresan, 2006; Nixon, 2007). In AD, there is an accumulation of autophagic vacuoles present in neurites and synaptic terminals, suggesting a disruption of autophagy and lysosome pathways (Nixon, 2005; Nixon et al., 2005). Studies have also shown that disruption of these pathways induce AD-like axonal dystrophy in mouse primary neurons (Lee et al., 2011a). Disrupting the late endocytic pathway *in vitro* by Rab7 knockdown and exogenously adding soluble Aβ significantly resulted in amyloid fibril formation whilst blocking the early endocytic pathway by Rab5 knockdown had no effect on the aggregation state of Aβ (Yuyama and Yanagisawa, 2009). Taken together, these findings indicate that dysfunction of the late endocytic pathway involving Rab7 could be a contributing factor in the aggregation of Aβ and axonal degeneration in AD.

1.2.4.3 Rab4 and Rab11 Recycling Endosomes

Rab4 and Rab11 GTPases both regulate the recycling of intracellular cargo back to the plasma membrane (Hsu and Prekeris, 2010; Li and DiFiglia, 2012). Rab4 is predominantly localised with Rab5 on early/sorting endosomes (Sonnichsen et al., 2000). The exact function of Rab4 remains poorly understood but it has been shown to mediate a fast recycling process which involves direct transport of carrier vesicles formed from the tubular regions of the early endosome to the

plasma membrane (Sheff et al., 1999; van der Sluijs et al., 1992). Rab11 is primarily associated with perinuclear recycling compartments which are formed from the budding, detachment and maturation of the early endosome's extended tubules whilst the globular portion of the early endosome starts to undergo maturation to form the late endosome (Allison et al., 2013; Goldenring, 2015; Maxfield and McGraw, 2004; Ullrich et al., 1996). Rab11 mediates slow recycling which involves trafficking of cargo proteins from perinuclear localised recycling compartments to the plasma membrane (Ullrich et al., 1996; Urbe et al., 1993). Although not entirely understood how, Rab11 also transports cargo from the recycling compartment to the TGN (Chen et al., 1998; Urbe et al., 1993). Rab4 has also been shown to co-localise with Rab11 on perinuclear recycling compartments (Sonnichsen et al., 2000; Ward et al., 2005a). However, whether Rab4 mediates the transport of carrier vesicles from the early endosome to Rab11-positive recycling compartments or whether it's involved in the process of forming the recycling compartment remains to be established.

Overexpression of Rab4 does not affect endocytosis but does result in an accumulation of intracellular cargo proteins destined for recycling (van der Sluijs et al., 1992). Enlargement of Rab5-positive early endosomes observed in *post mortem* sporadic AD brain tissue also exhibit an increase in Rab4 expression, suggesting an upregulation of the rapid recycling pathway (Cataldo et al., 2000; Ginsberg et al., 2011). Rab4 has been shown to be involved in Aβ secretion rather than production. For instance, silencing Rab4 *in vitro* results in an accumulation of intracellular Aβ and a decrease within the media, suggesting Rab4-positive vesicles mediate the secretion of Aβ generated from early endosomes (Udayar et al., 2013). Other independent studies have also demonstrated co-localisation between Rab4-positive compartments and exogenously added Aβ (Arriagada et al., 2007; Arriagada et al., 2010).

Unlike Rab4, Rab11 has been shown to regulate Aβ production rather than secretion whereby silencing Rab11 results in a decrease in sAPPβ and Aβ generation (Udayar et al., 2013). Interestingly, exome sequencing performed by Udayar *et al* revealed a genetic link between Rab11 and sporadic AD, and a network analysis of GWAS genes associated with sporadic AD identified Rab11 as an interacting component (Udayar et al., 2013). To reinforce Rab11 being an important regulator of Aβ production, there is also evidence linking Rab11 to

BACE1 trafficking and the γ-secretase complex. Buggia-Prevot *et al* revealed BACE1 sorting to be Rab11-dependent, evidenced by the co-localisation of fluorescently stained BACE1 and Rab11 in the axons of primary neurons (Buggia-Prevot et al., 2014). Whilst Dumanchin *et al* showed an *in vitro* interaction between Rab11 and PSEN1 (Dumanchin et al., 1999).

1.2.5 APP knockout mice

Zheng *et al* were one of the first groups to generate APP knockout (APPKO) mice (Zheng et al., 1996; Zheng et al., 1995). The endogenous APP gene was disrupted by insertion of a neomycin resistance gene which substituted a short 3.8 kb sequence encoding the promotor region and first exon of APP (Zheng et al., 1995). APPKO mice do not exhibit any serious physical or behavioural defects at birth (Li et al., 1996; Muller et al., 1994; Zheng et al., 1995). However, compared to aged match wild-type mice, APPKO mice have decreased body weight (Magara et al., 1999; Muller et al., 1994), forelimb grip strength and locomotor activity (Ring et al., 2007; Zheng et al., 1995) as well as LTP impairment and deficits in cognition (Dawson et al., 1999; Ring et al., 2007; Seabrook et al., 1999). By 4 months of age they exhibit reactive gliosis, indicating signs of neuronal damage (Seabrook et al., 1999; Zheng et al., 1995).

Given the relatively subtle phenotype of APP single gene knockout mice, earlier studies suggested that APP either had no relevant physiological function or that its function has redundancy or an intersecting function with another protein. The latter was eventually supported from studies involving knockouts of other members of the APP family; APLP-1 and APLP-2 (Crain et al., 1996; Heber et al., 2000; McNamara et al., 1998; von Koch et al., 1997). As with APP, mice with a single gene knockout of APLP-1 or APLP-2 are viable and fertile (Li et al., 1996; Muller et al., 1994; von Koch et al., 1997; Zheng et al., 1995). However, further studies involving APP and APLP-2 or APLP-1 and APLP-2 (but not APP and APLP-1) double gene knockout mice revealed an early postnatal lethal phenotype (Heber et al., 2000; von Koch et al., 1997). These findings indicate an overlapping functional capability of APLP-2 with both other family members and thus may be able to functionally compensate for their loss whilst also having a separate developmental role in the absence of APP or APLP-1.

1.2.6 The physiological function of APP

The physiological function of APP still remains unclear. APP contains a number of different binding domains and therefore is thought to be multifunctional. Several possible functions have been proposed. For example, based on the structure of membrane-bound APP, there is evidence to suggest APP to function as a cell surface receptor (Kang et al., 1987). Studies suggest F-spondin to be an attractive extracellular ligand for APP. F-spondin is a signalling molecule that is involved in neuronal development and repair. By binding to the extracellular central region of APP (E2 domain) it regulates APP cleavage to reduce Aβ production (Hafez et al., 2012; Ho and Sudhof, 2004). Other examples of proteins that bind and modulate APP metabolism are summarised in Table 1.1.

There is also substantial evidence to suggest that APP functions as a cell adhesion molecule (Evin and Weidemann, 2002). APP co-localises and interacts with adhesion molecules that are organised into 'patches' (Storey et al., 1996). The cell adhesion molecule integrin β1, which is located in these patches (Storey et al., 1996; Yamazaki et al., 1997), binds to APP via an RHDS motif at the C-terminal region to promote cell adhesion (Ghiso et al., 1992). Further support for APP's involvement in cell adhesion is through its ability to bind to various components of the extracellular matrix such as heparin, collagen and laminin (Beher et al., 1996; Kibbey et al., 1993; Multhaup, 1994), as well as dimerising with itself and other members of the APP family in a homo- or hetero-philic fashion (Soba et al., 2005).

APP is also known to be involved in synaptogenesis (Hung et al., 1992; Leyssen et al., 2005). APP expression is elevated at neuronal synaptic regions, and this is further upregulated after neuronal damage and during neuronal differentiation (Hung et al., 1992; Leyssen et al., 2005). This may explain why APPKO mice show LTP impairment and deficits in cognition (Dawson et al., 1999) which can be rescued by the reintroduction of soluble APPα (sAPPα) (Ring et al., 2007; Weyer et al., 2011). These studies also suggest that it is the ectodomain of APP that plays a crucial role in memory.

More recent studies have suggested APP to be involved in iron homeostasis (Ayton et al., 2015b; Belaidi et al., 2018; Duce et al., 2010; McCarthy et al., 2014; Needham et al., 2014; Wong et al., 2014b). APP has a role in iron efflux via

binding and forming a complex with the iron export protein FPN to stabilise and promote its retention on the cell surface (Duce et al., 2010; Wong et al., 2014b). Absence of APP on the surface leads to a reduction in surface presented FPN and thus neuronal iron accumulates within the cell (Belaidi et al., 2018; Duce et al., 2010; Wong et al., 2014b).

1.2.7 The proteolytic processing of APP

The proteolytic processing of APP is performed by specific secretases in different subcellular locations. There are two proteolytic pathways that physiologically process APP into smaller, soluble fragments. These pathways can be classed as either amyloidogenic or non-amyloidogenic, depending on whether or not the neurotoxic Aβ species is produced (Chow et al., 2010; Zheng and Koo, 2011). However, there has been recent developments regarding the processing pathways of APP with the identification of a number of novel secretases, including δ- (Zhang et al., 2015) and η-secretase (Baranger et al., 2016; Willem et al., 2015), and the alternative β-secretase meprin-β (Bien et al., 2012; Jefferson et al., 2011). These secretases have been shown to process APP into soluble fragments including Aβ (Baranger et al., 2016; Bien et al., 2012; Zhang et al., 2015) but the amount of APP that is processed by each secretase and whether this contributes to the pathogenesis of AD remains uncertain.

1.2.7.1 The amyloidogenic processing of APP

The type I transmembrane aspartyl protease, β-site APP cleaving enzyme 1 (BACE1), is the β-secretase responsible for the amyloidogenic processing of APP (Evin and Weidemann, 2002; Vassar et al., 1999). BACE1 contains a pro-peptide domain that requires to be cleaved by a furin within the Golgi before forming mature BACE1 (Benjannet et al., 2001). The protease domain contains the active site which is made from two separate motifs (Vassar et al., 1999). BACE1 is ubiquitously expressed at low levels throughout the body with highest expression in the brain (Rossner et al., 2001; Vassar et al., 1999). In the brain, BACE1 is predominantly expressed in the hippocampus, cortex and cerebellum regions (Rossner et al., 2001) and studies have shown an upregulation of BACE1 in response to neuronal stress such as oxidative stress and hypoxia (O'Connor et al., 2008). BACE1 is located mostly in the TGN and within endosomes (Huse et al., 2002). APP, BACE1 and γ-secretase components can be found within lipid

rafts (Cataldo et al., 2004; Chow et al., 2010; Daugherty and Green, 2001; Zheng and Koo, 2011); small localised domains within the cellular membrane, containing high levels of cholesterol and sphingolipids (Lingwood and Simons, 2010). It is within these specialised membrane microdomains that APP undergoes amyloidogenic processing (Figure 1.3A) (Ehehalt et al., 2003). Whilst APP and BACE1 may be at separate regions of the lipid raft domains, endocytosis brings APP and BACE1 together within endosomes (Cataldo et al., 2004; Chow et al., 2010; Daugherty and Green, 2001; Giannone et al., 2010; Zheng and Koo, 2011) where the environment is more conducive for the pH-dependent activity of BACE1 to optimally cleave APP (Ellis and Shen, 2015; Prasad and Rao, 2015; Vassar et al., 1999). BACE1 cleaves APP at the D1 site of the Aβ domain (Figure 1.3C) to produce a soluble, N-terminal extracellular domain known as sAPPβ (Figure 1.3A) (Chow et al., 2010; Vassar et al., 1999; Zheng and Koo, 2011). After the initial cleavage of APP by BACE1, the remaining C-terminal transmembrane fragment known as C99 or CTF-β is further processed by the γ-secretase complex (Figure 1.3A) which consists of nicastrin, anterior pharynx defective 1 (APH-1), PSEN1 or PSEN2 and presenilin enhancer-2 (PEN-2) (De Strooper et al., 2012; Edbauer et al., 2003). The aspartyl protease, presenilin, contains the active site that cleaves the CTF-β to produce the neurotoxic Aβ peptide, and the AICD (De Strooper et al., 2012; Edbauer et al., 2003). Although γ-secretase can still function in the absence of nicastrin (Zhao et al., 2010), PEN-2 is needed to activate the proteolytic cleavage capability of presenilin whilst the additional components are thought to be required for the maturation and stability of the complex (De Strooper, 2003). γ-Secretase cleaves the CTF-β at different sites, thereby altering the lengths of Aβ and AICD (Wolfe et al., 1999). For instance, γ-secretase initially cleaves the CTF-β at a region known as the ‘ε-site’, producing $A\beta_{48}$ or $A\beta_{49}$ and continues to cleave the Aβ C-terminus every 3 amino acids to generate $A\beta_{42}$ or $A\beta_{40}$ respectively (Figure 1.3C) (Takami et al., 2009; Vardy et al., 2005; Weidemann et al., 2002). Historically, $A\beta_{40}$ and $A\beta_{42}$ have been considered the most abundant forms, with $A\beta_{40}$ being most prevalent in normal brain and the aggregation prone $A\beta_{42}$ increasing in the AD brain (Haass and Selkoe, 2007; Klein et al., 1999; Pike et al., 1995). However, more sensitive ways of detecting the different forms of Aβ have recently identified a more complex profile of forms in the normal and diseased brain (Esparza et al., 2016; Ji et al., 2018; Wildburger et al., 2017).

1.2.7.2 The non-amyloidogenic processing of APP

Several proteases that belong to the ADAM (a disintegrin and metalloprotease) group, such as ADAM9, ADAM10, and ADAM17 exhibit α-secretase activity and are involved in the non-amyloidogenic processing of APP (Roberts et al., 1994). Approximately 30 % of cell surface presented APP undergoes constitutive cleavage by α-secretase, predominantly outside lipid raft regions (De Strooper and Annaert, 2000; Koo et al., 1996; Taylor and Hooper, 2007). APP is cleaved within the Aβ region at L17 (Figure 1.3C) thereby preventing Aβ formation, and produces a large soluble ectodomain known as sAPPα (Figure 1.3B) (Roberts et al., 1994; Simons et al., 1996). Constitutive cleavage predominantly occurs at the cell surface (Parvathy et al., 1999) and multiple reports have shown ADAM10 to be the main secretase involved in this cleavage, particularly in neurons (Kuhn et al., 2010). In contrast, ADAM17 is the predominant α-secretase enzyme involved in regulated cleavage of APP and is thought to be dependent on the activation of protein kinase C (PKC) (Buxbaum et al., 1998; Jolly-Tornetta and Wolf, 2000; Zhu et al., 2001). Various studies have shown that the activation of PKC via phorbol ester treatment or muscarinic acetylcholine receptor stimulation increases sAPPα formation as well as reducing levels of sAPPβ and Aβ *in vitro* (Caporaso et al., 1992b; Farber et al., 1995; Nitsch et al., 1992). ADAM17 along with PKC-regulated α-secretase activity predominantly resides within intracellular compartments such as the TGN (Skovronsky et al., 2000), indicating ADAM17 to be involved in stimulated rather than constitutive α-cleavage of APP. After the initial cleavage of APP by α-secretase, the remaining C-terminal transmembrane fragment known as C83 or CTF-α is further processed by the γ-secretase complex to produce a short, non-toxic peptide fragment known as p3 in addition to the AICD (Figure 1.3B). Physiologically, the majority of APP is processed through the non-amyloidogenic pathway, resulting in low levels of Aβ from being typically produced (Chow et al., 2010; Zheng and Koo, 2011).

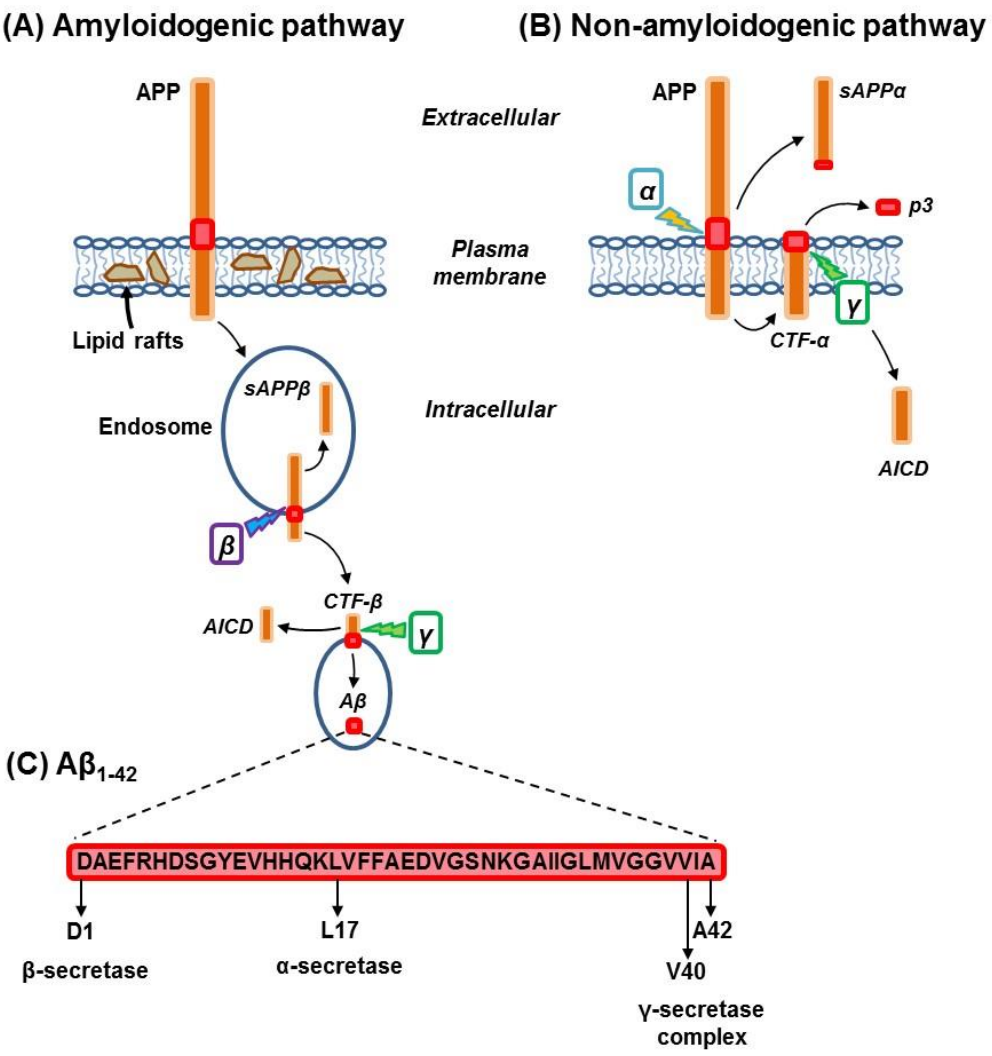

Figure 1.3. The predominant proteolytic processing pathways of APP. (A) In the amyloidogenic pathway, APP is present in lipid raft rich regions of the plasma membrane and is cleaved by β-secretase (β) within the early endosome, producing sAPPβ and CTF-β. CTF-β is cleaved by γ-secretase (γ), generating Aβ and AICD. (**B)** In the non-amyloidogenic pathway, cell surface APP is cleaved by α-secretase (α) producing sAPPα and CTF-α. CTF-α is cleaved by γ-secretase, generating p3 and AICD. **(C) The cleavage points of Aβ$_{1-42}$ by α-, β-, and γ-secretase.** Residue numbering corresponds to the Aβ sequence which typically begins at D1 and ends at V40/A42. Cleavage at L17 by α-secretase following γ-secretase cleavage precludes Aβ formation while cleavage at D1 by the β-secretase and either of the γ-sites generates Aβ peptides typically 40-42 amino acids in length (shown in black). Abbreviations: APP, amyloid-β precursor protein; sAPP, soluble APP; CTF, C-terminal fragment; Aβ, amyloid-β; AICD, APP intracellular domain.

1.2.7.3 The functions of the APP proteolytic fragments

The processing of APP is an important determining factor in the development of AD. The predominantly studied non-amyloidogenic and amyloidogenic processing pathways of APP leads to the generation of secreted and intracellular protein fragments carrying potential roles within the cell.

sAPPα has been shown to be neuroprotective and counterbalance the damaging effects of Aβ production (Roberts et al., 1994). Studies have demonstrated sAPPα to increase cell proliferation (Caille et al., 2004), keratinocyte motility (Kirfel et al., 2002), and also increase LTP *in vivo* (Taylor et al., 2008). AD mouse models with an overexpression of the α-secretase enzyme ADAM10 have elevated sAPPα levels with subsequent enhanced LTP and improved learning and memory (Postina et al., 2004). sAPPα cleaved from APP695 protects neurons from Aβ induced oxidative stress (Goodman and Mattson, 1994), promotes cell adhesion and synaptogenesis (Stahl et al., 2014), and neurite outgrowth (Gakhar-Koppole et al., 2008; Mattson et al., 1997) whereby administration of sAPPα to primary neuronal cultures increases axonal and dendritic growth (Jin et al., 1994). sAPPα has also been shown to mediate neuronal differentiation in embryonic stem cells (Freude et al., 2011), implying that sAPPα (and APP) may have roles in embryonic brain development, although APP single gene knockout mice fail to exhibit embryonic lethality (Zheng et al., 1995). sAPPα has also been shown to be involved in iron homeostasis where extracellular administration of sAPPα stabilises surface FPN and stimulates iron export in vascular endothelial cells (McCarthy et al., 2014).

Unlike its non-amyloidogenic counterpart, sAPPβ does not possess any neuroprotective functions and so the biological function of sAPPβ and its role in AD still remain unclear. However, studies have suggested sAPPβ to have a role in axon pruning during neuronal development (Nikolaev et al., 2009). Trophic deprivation induces APP cleavage by BACE1 to produce sAPPβ which can be further cleaved (by an unknown protease) to produce a 35 kDa fragment termed N-APP. N-APP was shown to bind to Death Receptor 6 (DR6) and activate caspase activity, triggering axonal pruning and degeneration of developing neurons (Nikolaev et al., 2009). However, further investigation is required to establish its physiological significance in developing neurons and in the adult

brain. Previous experiments have primarily focussed on neurons cultured from the peripheral nervous system (PNS) and therefore would need to be repeated and validated in CNS neurons (Nikolaev et al., 2009). Whether the 35 kDa N-APP fragment and DR6 interaction has any bearing to AD pathology would also need to be further explored.

Whether both CTF-α and CTF-β merely serve as substrates for the γ-secretase or whether they possess any biological role remains to be established. The p3 peptide generated from α- and γ-cleavage of APP has also not been attributed to any biological role and has long been regarded as a harmless non-toxic by-product secreted in the extracellular environment (Chow et al., 2010). While Aβ is implicated in AD pathogenesis, the physiological function of Aβ remains unclear (Hiltunen et al., 2009). Studies have suggested Aβ to be involved in cell survival (Plant et al., 2006) and regulate cholesterol transport (Igbavboa et al., 2009; Yao and Papadopoulos, 2002). However, further investigation to elucidate the potential mechanisms of Aβ is required since various animal studies have shown that the absence of Aβ is not associated with any loss of physiological function (Luo et al., 2003; Morris et al., 2014). Nevertheless, increasing attention has been on the antimicrobial properties of Aβ and its potential role in innate immunity (Bourgade et al., 2016; Eimer et al., 2018; Gosztyla et al., 2018; Kumar et al., 2016; Lukiw et al., 2010; Soscia et al., 2010; Spitzer et al., 2016; White et al., 2014) (further discussed in section 1.6.1).

The AICD may be involved in cell signalling and transcriptional regulation of several genes. AICD binds to the intracellular adaptor protein Fe65 where it is transported from the cytoplasm to the nucleus of the cell. In the nucleus it binds to the histone acetyltransferase Tip60, forming the AFT transcriptional complex (a multi-protein complex consisting of AICD, Fe65 and Tip60) (Cao and Sudhof, 2001; Konietzko et al., 2010; von Rotz et al., 2004). Nuclear AICD has been shown to regulate the expression of several genes such as neprilysin, p53, BACE1 and many others (Beckett et al., 2012; Belyaev et al., 2010; Ohkawara et al., 2011; Pardossi-Piquard et al., 2005) by targeting the MED12 subunit of RNA polymerase II to promoter sites (Xu et al., 2011). However, only AICD generated from β- and γ-cleavage of APP695 has been reported to translocate to the nucleus and regulate gene expression (Belyaev et al., 2010; Goodger et al., 2009). Furthermore, there are inconsistencies within the literature as to the

identification of particular genes regulated by AICD (Chen and Selkoe, 2007; Hass and Yankner, 2005; Hebert et al., 2006), and some studies have even reported that the AICD does not translocate to the nucleus and therefore fails to activate gene transcription (Waldron et al., 2008).

1.3 Proteins that regulate APP trafficking and processing

There are various proteins that have been shown to regulate the trafficking and processing of APP, and therefore alter levels of sAPPα, sAPPβ and Aβ secreted by cells (Tang and Liou, 2007). However, despite these initial reports, a consensus of a functional ligand for APP that reveals the precise mechanisms that regulate APP processing and function are yet to be made.

Below are several candidate proteins that have been shown to affect the trafficking and/or proteolytic processing of APP.

1.3.1 LRP1/LRP1B

The low density lipoprotein receptor-related protein 1 (LRP1) is part of the low density lipoprotein receptor (LDLR) family and is involved in lipoprotein metabolism, protease degradation, lysosomal enzyme activation and can also act as a cellular entry point for bacterial toxins and viruses (Marzolo and Bu, 2009). LRP1 is an endocytotic receptor that recognises more than thirty ligands including APOE, APP, Aβ, and a number of adaptor proteins (Herz and Bock, 2002). Studies have shown LRP1 to have a role in Aβ clearance (Kanekiyo et al., 2013; Liu et al., 2017; Storck et al., 2016). It is able to bind and mediate Aβ endocytosis, directing it to lysosomes for degradation (Kanekiyo et al., 2013). Initially, LRP1 was only known to bind to cell surface APP containing the KPI domain (Knauer et al., 1996). Subsequent studies have now shown LRP1 to bind directly to the intracellular C-terminal region of APP695 (lacking the KPI domain) or indirectly through the adaptor protein Fe65 (Lakshmana et al., 2008). This facilitates the amyloidogenic processing of APP by directing APP to lipid rafts for early endocytosis with LRP1 (Lakshmana et al., 2008; Marzolo and Bu, 2009). The interaction between APP and LRP1 may be prevented by the receptor associated protein (RAP) (Knauer et al., 1996). RAP is known to chaperone LRP1 from the endoplasmic reticulum to the Golgi, and then separates due to the low pH environment in the secretory pathway (Cam and Bu, 2006; Knauer et al., 1996;

Prasad et al., 2015). RAP therefore can act as an LRP1 antagonist, preventing APP itself from binding, resulting in a decrease in Aβ production (Cam and Bu, 2006; Fuentealba et al., 2010; Prasad et al., 2015). Conversely, LDLR-related protein 1B (LRP1B) has the opposite effect and competes with LRP1 for APP binding and since LRP1B has a much slower rate of endocytosis than LRP1, retains APP on the plasma membrane for the non-amyloidogenic processing by α-secretase, preventing Aβ formation (Cam and Bu, 2006).

1.3.2 SORLA

Sorting protein-related receptor (SORLA) is another well-known member of the LDLR family and is thought to transport proteins between the Golgi and endosomes, and also bind to a variety of adaptor proteins (Andersen et al., 2005; Gustafsen et al., 2013). The frontal cortex of AD brains reveal a decreased expression of SORLA, indicating a possible role in AD (Andersen et al., 2005; Gustafsen et al., 2013; Spoelgen et al., 2006). There is also evidence to suggest that SORLA has a potential role in the processing of APP (Andersen et al., 2005; Gustafsen et al., 2013). *In vitro* studies have shown a reduction in sAPPα, sAPPβ and Aβ secreted by neuronal cells overexpressing SORLA (Gustafsen et al., 2013). APP is known to co-localise with SORLA in endosomes and Golgi compartments (Andersen et al., 2005; Gustafsen et al., 2013; Spoelgen et al., 2006). This interaction results in a reduction in cell surface APP and an increase in intracellular APP, obstructing both the trafficking of APP to the cell surface and the amyloidogenic and non-amyloidogenic processing pathways (Andersen et al., 2005). Additionally, to disrupt SORLA function, cells transfected with a mutated form of SORLA showed an increase in cell surface APP via promoting APP trafficking to the cell surface instead of maintaining APP in the intracellular vesicles (Andersen et al., 2005; Gustafsen et al., 2013). The association between SORLA and APP has further been established *in vivo* by co-localisation experiments in mouse brain (Andersen et al., 2005). Studies involving SORLA knockout mice show an increase in sAPPα and Aβ levels further suggesting that SORLA has an effect on APP localisation and processing (Andersen et al., 2005).

1.3.3 APOER2

APOE receptor 2 (APOER2) is also part of the LDLR family and is predominantly expressed in the hippocampus and cortex of the brain (Kim et al., 1996). It has

important roles in cell migration during neuronal development and is involved in the regulation of LTP (Duit et al., 2010; Masiulis et al., 2009; Reddy et al., 2011). Multiple studies have published contradictory effects of APOER2 on the processing of APP. This comes as no surprise since APOER2 possesses several isoforms that are present in specific tissues, each interacting with different ligands (Brandes et al., 1997; Fuentealba et al., 2007). APOER2 is an important receptor for a number of soluble ligands including APOE, F-spondin and reelin, and studies suggest APOER2 binds and regulates cell surface proteins, such as APP (Fuentealba et al., 2007; Hoe and Rebeck, 2005; Hoe et al., 2005). For example, Hoe *et al* has shown various APOER2 isoforms to bind to cell surface APP via F-spondin, resulting in decreased levels of Aβ and increased APP CTF production (Hoe et al., 2005). In contrast, Fuentealba *et al* has demonstrated that there is a direct interaction of APOER2 to APP that is mediated by the cytoplasmic domain of APOER2 (Fuentealba et al., 2007). APOER2 co-localises and binds to APP on the cell surface, shifting towards lipid raft rich regions of the membrane, promoting β- and γ-secretase processing, resulting in an increase in Aβ production (Fuentealba et al., 2007).

1.3.4 BRI2

Integral membrane protein 2B (BRI2) is a transmembrane protein and like APP, is expressed within the brain along the axons of neurons. In AD, concentrated levels of BRI2 can be found in dystrophic neurites surrounding plaques (Fotinopoulou et al., 2005). Although the function of BRI2 remains unclear, studies have shown an interaction between BRI2 and APP on the cell surface, resulting in a reduction in Aβ production (Fotinopoulou et al., 2005). Cell lines overexpressing BRI2 exhibit a decrease in Aβ, sAPPα and CTF-α, and an increase in sAPPβ. AD mouse models expressing BRI2 also show a reduction in Aβ levels. BRI2 is able to interact with only the post-translational form of APP in addition to CTF-β (Fotinopoulou et al., 2005). Furthermore, cells transfected with a mutated form of BRI2, designed to alter its location, causes it to be detained in the endoplasmic reticulum and does not associate with APP or alter its processing (Matsuda et al., 2011). This suggests that APP must be transported to the cell surface in order to bind with BRI2. On the cell surface, the binding of BRI2 to APP blocks the α-cleavage site, resulting in reduced levels of sAPPα and CTF-α. Additionally, γ-cleavage sites are also blocked, precluding Aβ formation.

However, the β-cleavage site remains accessible and so APP is preferentially cleaved by β-secretase, giving rise to an increase in sAPPβ (Fotinopoulou et al., 2005; Matsuda et al., 2005; Matsuda et al., 2011).

Other examples of proteins that are known to regulate the trafficking and processing of APP are summarised in Table 1.1.

1.4 The APP interactome

APP interactome studies have played a major role in the discovery of putative APP ligands. Bai *et al* performed an *in vivo* brain interactome by perfusing mouse brain tissue with paraformaldehyde and cross-linking any interacting proteins present. With the use of C- and N-terminal APP antibodies (C-terminal to capture intracellular associations and N-terminal to capture extracellular binding proteins), immunoprecipitation studies revealed APP and any cross-linked proteins present within the homogenised mouse tissue sample. Liquid chromatography and mass spectrometry methods were carried out to recognise proteins that were co-purified with APP. Not only did this study uncover new APP interacting proteins but also confirmed existing APP interactions previously published (Bai et al., 2008). Unlike *in vitro* studies that use an artificial environment to establish APP interacting proteins, the *in vivo* brain interactome showed APP interactions within a relevant physiological environment. However, various novel APP interacting proteins discovered by Bai *et al* may not be direct interactions and could possibly involve other complexed proteins. Another group, Perreau *et al*, established a protein interaction network by collating all relevant published data that identified new and existing APP interacting ligands and reported which APP binding domain was involved in the protein interaction (Perreau et al., 2010).

Various examples of candidate APP ligands identified by interactome studies, showing where they bind and how they influence APP metabolism are listed in Table 1.1.

Table 1.1. Examples of proteins that modulate APP metabolism

Protein	Direct or indirect APP interaction	Effect	Mechanism
Contactin	E1 and E2	↑ AICD, CTF-α and CTF-β	Mediates AICD release in γ-secretase dependent manner; stimulates α- and β-secretase processing (Ma et al., 2008)
DAB1	Cytoplasmic domain	↑ sAPPα and CTF-α; ↓ CTF-β and Aβ	Promotes and retains APP on the cell surface, increasing α-cleavage and decreasing β-cleavage (Hoe et al., 2006)
DISC1	Cytoplasmic domain	↓ sAPPα and CTF-α; ↑ Aβ	Increases APP endocytosis, promoting β-secretase cleavage. DISC1 knock down reduces APP endocytosis and retains APP on the cell surface for α-secretase cleavage (Shahani et al., 2015)
Flotillin-2	Indirect	↑ Aβ	Regulates APP endocytosis and β-secretase processing (Schneider et al., 2008)
Lingo-1	E1; KPI; E2; transmembrane domain; cytoplasmic domain	↑ CTF-β and Aβ; ↓ CTF-α	Modulates β-cleavage of APP by promoting access of BACE1 to APP (Bai et al., 2008)
LRP10	E1; E2; cytoplasmic domain	↓ sAPPα, CTF-α, sAPPβ, CTF-β and Aβ	Regulates APP trafficking and processing. Retains APP in the Golgi, preventing APP transport to endosomes and cell surface (Brodeur et al., 2012)
Nogo receptor	E1; E2; Aβ	↓ Aβ, sAPPβ and sAPPα	Binds APP, blocking access for α- and β-secretase processing (Park et al., 2006; Park and Strittmatter, 2007)
Prion protein	Indirect	↓ Aβ	Interacts with BACE1 via glycosaminoglycans, inhibiting interaction with APP (Parkin et al., 2007)
SNX33	Indirect	↑ sAPPα	Blocks APP endocytosis, retaining APP on the cell surface, preventing β-secretase cleavage and increasing α-secretase cleavage (Schobel et al., 2008)

1.5 Endocytosis of APP

APP endocytosis is necessary for the generation of Aβ given that Aβ production can be minimised upon inhibiting APP internalisation (Cirrito et al., 2008; Ehehalt et al., 2003; Koo and Squazzo, 1994; Schneider et al., 2008). The C-terminus of APP contains a YENPTY motif that is necessary for the endocytosis of APP (Lai et al., 1995). Apart from surface APP endocytosis, the YENPTY motif is also required for APP internalisation into TGN vesicles and transfer to the cell surface during APP trafficking (Rebelo et al., 2008; Vieira et al., 2009). APP endocytosis is influenced by the phosphorylation state of the Y^{687} residue (tyrosine) within the $YENPTY^{687}$ motif and plays a crucial role in the regulation of APP endocytosis (Barbagallo et al., 2010; Rebelo et al., 2007). For example, phosphorylation of Y^{687} decreases APP endocytosis, resulting in reduced β-cleavage and Aβ production. Conversely, the dephosphorylation of Y^{687} increases APP endocytosis, giving rise to increased β-cleavage (Barbagallo et al., 2010; Rebelo et al., 2007). The phosphorylation state of interacting proteins also impacts the processing and trafficking of APP. Mint proteins which are highly expressed in neurons are adaptor proteins known to bind to the C-terminal region of APP, affecting APP endocytosis and preventing APP from localising in lipid rafts, thereby reducing β-secretase processing and Aβ generation (Chaufty et al., 2012; Ho et al., 2008). Mint2 phosphorylated by Src kinase increases APP endocytosis and accelerates APP transport to endosomes, resulting in an increase in intracellular $Aβ_{42}$ (Chaufty et al., 2012).

1.5.1 Cholesterol mediated Endocytosis

Cholesterol is crucial for maintaining cell membrane fluidity and enhancing mechanical stability of lipid bilayers (Cooper, 1978; Rog et al., 2009). Lipid rafts are small localised domains within the cellular membrane, containing high levels of cholesterol and sphingolipids (Lingwood and Simons, 2010). APP, BACE1 and γ-secretase components can be found within lipid rafts and it is within these specialised microdomains that APP undergoes amyloidogenic processing (Cataldo et al., 2004; Chow et al., 2010; Daugherty and Green, 2001; Ehehalt et al., 2003; Zheng and Koo, 2011). Protein mobility is restricted within lipid rafts as opposed to non-raft regions of the cell membrane, where proteins are much more dispersed and mobile (Giannone et al., 2010). Protein interactions from one lipid

raft to another can be achieved by lipid rafts coming together and forming clusters (Simons and Gerl, 2010). This might be one way of regulating protein interactions on the plasma membrane and also controlling APP processing by the secretases.

APP endocytosis is strongly influenced by cholesterol levels. In AD brains, there is an accumulation of total cholesterol, particularly in the membrane fraction (Cutler et al., 2004; Xiong et al., 2008). Studies have shown altering cholesterol levels affects clathrin-dependent endocytosis of APP and in turn modulates Aβ formation (Ehehalt et al., 2003; Kojro et al., 2001; Simons et al., 1998; Xiong et al., 2008). For instance, increasing membrane cholesterol content results in both an increase in APP internalisation (Cossec et al., 2010) and interaction between APP and BACE1, promoting β-cleavage of APP and Aβ production (Cossec et al., 2010; Marquer et al., 2011; von Arnim et al., 2008). Silencing the clathrin heavy chain, required for the formation of clathrin-coated vesicles increases cell surface APP and prevents APP endocytosis (Cossec et al., 2010; Motley et al., 2003). Increasing membrane cholesterol did not affect APP internalisation, signifying that cholesterol regulates APP endocytosis through a clathrin-dependent manner (Cossec et al., 2010). Conversely, a reduction in membrane cholesterol minimised the formation of lipid rafts, prompting APP to be re-located to non-lipid raft regions of the plasma membrane (Ehehalt et al., 2003; Kojro et al., 2001). Since APP is preferentially cleaved by α-secretase instead of BACE1 in non-lipid raft regions, α-cleavage was increased (Ehehalt et al., 2003; Kojro et al., 2001).

APP binds to cholesterol in a 1:1 ratio (Barrett et al., 2012; Marquer et al., 2011). The transmembrane domain of APP contains both cholesterol and α-secretase binding sites that are located alongside each other (Barrett et al., 2012). Studies suggest binding of cholesterol to APP inhibits α-secretase from binding, favouring the amyloidogenic pathway. Cholesterol levels are also involved in the production of Aβ by the γ-secretase complex (Osenkowski et al., 2008). Osenkowski *et al* demonstrated increasing levels of cholesterol stimulated γ-secretase activity, which not only resulted in an increase in Aβ production, but also resulted in the production of longer Aβ peptides ($A\beta_{40}$) (Osenkowski et al., 2008).

Cholesterol exporting channels ABCA7 and G1 are both expressed in the hippocampus and have been shown to alter the processing of APP (Chan et al.,

2008; Tansley et al., 2007). Cells overexpressing APP695 transiently transfected with ABCA7 exhibited an increase in cholesterol efflux from the cell and a decrease in membrane cholesterol, resulting in a reduction of sAPPα, sAPPβ, Aβ and APP CTF (Chan et al., 2008). In contrast, cells over-expressing ABCG1 altered the distribution of membrane cholesterol and increased cell surface presented APP, resulting in an increase in sAPPα, sAPPβ and Aβ production (Tansley et al., 2007). The proposed mechanism of ABCG1 is yet to be determined. How ABCG1 is involved in APP trafficking and whether ABCG1 either directly affects secretase activity, or the association between APP and the secretases requires further investigation.

1.5.2 Receptor mediated Endocytosis

Receptor mediated endocytosis may be classified as being clathrin-dependent or clathrin-independent. As reported earlier, APP and BACE1 may be located in separate lipid raft regions on the plasma membrane, restricting protein mobility (Giannone et al., 2010). Endocytosis of both proteins brings the two together into the early endosome, which provides the optimal acidic environment for BACE1 to cleave APP (Cataldo et al., 2004; Chow et al., 2010; Zheng and Koo, 2011). APP is internalised via clathrin-dependent endocytosis (Ehehalt et al., 2003; von Arnim et al., 2008; Yap and Winckler, 2015) while BACE1 undergoes clathrin-independent endocytosis and is sorted to the early endosome via the endocytic trafficking regulator ARF6 (Sannerud et al., 2011; Tang et al., 2015).

1.5.2.1 Clathrin-dependent Endocytosis of APP

Clathrin consists of three heavy and light chains, forming a triskelion-shaped scaffolding-like protein (Brodsky et al., 2001; Fotin et al., 2004; Kirchhausen, 1999; Schmid, 1997). It self-polymerises (Fotin et al., 2004; Gilbert et al., 1997; Schmid, 1997) and forms complexes with assembly and adaptor proteins AP-2 (McNiven and Thompson, 2006; Morris and Cooper, 2001) and Dab2 (Morris and Cooper, 2001). This forms a ‘cage’ like structure around the vesicle, initiating budding of the cell membrane and undergoes scission by dynamin GTPase (Carey et al., 2005). The tyrosine residue within the YENPTY motif of APP acts as a sorting signal recognised by various clathrin adaptor proteins such as AP-2 which aids in the regulation of clathrin-dependent endocytosis (Bonifacino and Traub, 2003; Prabhu et al., 2012). The clathrin-coated vesicle containing APP is

then transported, sorted and fuses with the early endosome (Damke et al., 1994; Henley et al., 1998). Studies have shown manipulating the associated proteins involved in clathrin-mediated endocytosis results in altered APP internalisation. For example silencing the clathrin heavy chain (Cossec et al., 2010; Motley et al., 2003) or transfecting cells with a mutated form of dynamin (Carey et al., 2005; Damke et al., 1994), prevents APP internalisation and results in an accumulation of APP on the cell surface.

1.5.2.2 Clathrin-independent Endocytosis of BACE1

ARF6 is a small GTPase and like other GTPases is able to shift back and forth from its inactive GDP form to its active GTP-bound state (Gaschet and Hsu, 1999; Klein et al., 2006; Pasqualato et al., 2001). Normally, ARF6 expression is predominantly found within the CA1 and CA2 regions of the hippocampus (Tang et al., 2015). In AD brains, ARF6 expression is increased and spreads to the hippocampal CA3 and CA4 regions (Tang et al., 2015). ARF6 is located on the plasma membrane and endosomes, managing endocytic trafficking of a variety of endogenous cell membrane proteins that do not possess the classical clathrin binding motif. ARF6 GDP is activated by GEFs on the plasma membrane (Chesneau et al., 2012; Macia et al., 2004) and facilitates BACE1 internalisation from the cell surface (Sannerud et al., 2011). RNAi knockdown studies have shown silencing ARF6 *in vitro* prevents BACE1 internalisation into the early endosome, blocking the capability of BACE1 to cleave APP to produce sAPPβ (Sannerud et al., 2011). ARF6 is also directly associated with Rab11-positive recycling compartments (Fielding et al., 2005; Nieuwenhuis and Eva, 2018; Schonteich et al., 2007), and shares some of the cytosolic effector proteins with Rab11, such as family interacting protein 3 (FIP3), that is primarily involved in the docking and fusion of vesicles to the recycling compartment (Fielding et al., 2005; Hickson et al., 2003; Schonteich et al., 2007; Takahashi et al., 2011). ARF6 has been shown to facilitate transport of clathrin-independent internalised proteins from the cell surface directly to Rab11-positive compartments, bypassing the early endosome (Chen et al., 2014; Maldonado-Baez et al., 2013; Radhakrishna and Donaldson, 1997).

1.5.2.3 A new Endocytic mechanism of APP

There has recently been some controversy and conflicting evidence regarding the role of ARF6 and whether it only regulates the endocytic trafficking of cell surface proteins like BACE1 that do not contain the clathrin binding motif to undergo clathrin-dependent endocytosis. Tang *et al* has shown ARF6 to influence APP internalisation via another endocytic mechanism known as macropinocytosis, avoiding delivery to the early endosome and transporting APP to the lysosome for β-processing (Tang et al., 2015). Macropinocytosis involves the formation of endocytic vacuoles termed macropinosomes from cell membrane budding via actin-based membrane protrusions, engulfing large volumes of extracellular fluid and plasma membrane (Jones, 2007; Sun et al., 2003; Tang et al., 2015). These internalised vacuoles vary in size (100-1000 nm in diameter), and are considered much larger than the vesicles formed via receptor-mediated endocytosis (Tang et al., 2015). Live cell imaging and electron microscopy demonstrated an increase in cell surface APP internalisation via macropinosomes (> 500 nm in diameter) and an increase in Aβ production within the lysosome. This was significantly inhibited by co-transfection with a dominant negative mutated form of ARF6, which reduced levels of Aβ production (Tang et al., 2015). This evidence suggests that ARF6 is required for APP macropinocytosis to occur and is also involved in delivery to the lysosome where APP can undergo β-cleavage. There is also a correlation between ARF6 expression and neurotoxic Aβ formation in the hippocampus of AD brains, suggesting that ARF6 may be involved in AD pathology (Braak et al., 2006; Tang et al., 2015). However, there is still an overwhelming majority of studies that demonstrate the internalisation pathway of APP to be ARF6-independent (Cossec et al., 2010; Ehehalt et al., 2003; von Arnim et al., 2008; Yap and Winckler, 2015) and therefore before any conclusions are drawn on any new mechanism on APP endocytosis and trafficking, further investigation is required.

1.6 Neuroinflammation in AD

Activation of the innate immune system in the brain protects against infectious insult or unwanted stimuli but persistent neuroinflammation, as seen in AD, can exacerbate underlying chronic pathology (Hensley, 2010). Despite the involvement of inflammation in AD being acknowledged for some time, it has only

recently been recognised to contribute to early pathogenesis. Neuroinflammation is now considered a primary factor in disease progression (McGeer and McGeer, 2010).

AD is characterised by reactive gliosis; activated microglia and astrocytes located around plaques and tangle-bearing neurons (Serrano-Pozo et al., 2011b). Once activated, these cells produce a range of inflammatory mediators including cytokines, prostanoids, chemokines and cycloxygenase-2 (COX-2) (Heneka and O'Banion, 2007). Astrocytes are involved in Aβ clearance and degradation, and provide a supportive barrier between Aβ aggregates and neurons (Rossner et al., 2005). Microglia are also involved in Aβ clearance and degradation by migrating to the infected area and clearing unwanted stimuli such as Aβ via phagocytosis (Frautschy et al., 1998; Mandrekar-Colucci and Landreth, 2010; Qiu et al., 1998). However, persistent activation of these cells leads to the production of inflammatory molecules in addition to toxic products such as reactive oxygen species (ROS), nitric oxide (NO), and complement factors. These not only target infected cells and unwanted debris for elimination and clearance but can also target surrounding unaffected viable cells, inducing further neuronal dysfunction and cell death (Atwood et al., 2003; Fassbender et al., 2000; Halliday et al., 2000).

Microglia are the resident immune cells of the brain and upon activation adopt two apparent phenotypes; the M1 and M2 (Crain et al., 2013; Orihuela et al., 2016). However, this is now considered as an oversimplification since (single cell) transcriptome and epigenome studies have revealed a continuum of activation phenotypes, such as the sub-classification of the M2 into M2a (tissue repair and phagocytosis), M2b (recruitment of regulatory T cells), and M2c (anti-inflammatory and healing) (Dubbelaar et al., 2018; Eggen et al., 2019; H et al., 2017). Nevertheless, for simplicity, references within this thesis are made to the generalised M1/M2 activation phenotypes. The M2 activated phenotype is anti-inflammatory and is involved in tissue repair and phagocytosis of Aβ protein aggregates and cell debris (Michell-Robinson et al., 2015; Tang and Le, 2016), while the M1 activated phenotype is pro-inflammatory and is involved in the secretion of pro-inflammatory mediators such as acute phase proteins, cytokines, chemokines and the generation of ROS (Loane and Byrnes, 2010; Tang and Le, 2016). The M1 phenotype is thought to be detrimental to the brain since these

pro-inflammatory mediators are known to induce neuronal toxicity, causing neuronal dysfunction and cell death (Fassbender et al., 2000; Orihuela et al., 2016). It is thought that the M1 activated microglial phenotype takes precedence in the AD brain, whilst M2 microglia typically emerge downstream for tissue repair and remodeling (Tang and Le, 2016). Studies have shown a mixed population of microglial activated phenotypes in *post mortem* sporadic AD brain tissue as well as in transgenic AD mouse model brains (Colton et al., 2006). However, AD individuals carrying a mutation in the Triggering receptor expressed on myeloid cells 2 (TREM2) gene exhibit a predominance of the M1 activated phenotype (Tanzi, 2015; Walter, 2016; Zhong et al., 2015). Individuals carrying TREM2 mutations such as the TREM2 R47H variant exhibit microglial dystrophy, decreased phagocytosis, and an increase in the M1 microglial reactive phenotype (Hickman and El Khoury, 2014; Tanzi, 2015; Walter, 2016). Analysis of GWAS genes associated with sporadic AD has identified TREM2 as an AD risk factor (Guerreiro et al., 2013; Jonsson et al., 2013; Walter, 2016). TREM2 is a transmembrane glycoprotein solely expressed by the brains immune cells, particularly microglia and is involved in the regulation of phagocytosis and promotion of the M2 activated microglial phenotype, inducing anti-inflammatory signaling to promote survival and repair pathways (Mecca et al., 2018; Neumann and Takahashi, 2007; Zheng et al., 2017). Studies have also shown disruption in TREM2 expression leads to an increase in LPS-induced pro-inflammatory cytokine production and secretion in microglia (Hickman and El Khoury, 2014; Zhong et al., 2015), suggesting TREM2 abnormalities promote the activation state of microglia towards an M1 pro-inflammatory reactive phenotype.

The production of inflammatory mediators have also been shown to increase APP synthesis and the amyloidogenic processing of APP. In turn, this produces more toxic Aβ and reduces α-secretase cleavage as well as the production of neuroprotective sAPPα (Atwood et al., 2003; Del Bo et al., 1995; Fassbender et al., 2000; Misonou et al., 2000; Ringheim et al., 1998). Elevated production of Aβ is then able to increase glial activation (Fassbender et al., 2000; Krabbe et al., 2013; Meda et al., 1995), inevitably causing the generation of more inflammatory mediators leading to a vicious cycle of neuronal dysfunction and cell death (Fassbender et al., 2000; Krabbe et al., 2013). Ablation of APP results in less reactive microglia with reduced levels of cytokine production (Carrano and Das,

2015), suggesting APP and/or its cleaved products are required for an efficient innate immune response. Tumour necrosis factor-α (TNF-α), interleukin-1 (IL-1) and interleukin-6 (IL-6) are pro-inflammatory cytokines produced from activated microglia in response to Aβ deposition (Meraz-Rios et al., 2013). TNF-α stimulates glial activation, promotes excitotoxicity and is known to contribute to synaptic loss in AD (Olmos and Llado, 2014; Rao et al., 2012; Rubio-Perez and Morillas-Ruiz, 2012). TNF-α also increases production and secretion of other pro-inflammatory cytokines such as IL-1 and IL-6 which in turn promote chronic inflammation when unopposed by anti-inflammatory cytokines (Neta et al., 1992; Szczepanik et al., 2001). IL-1 is involved in dystrophic neurite formation in plaques and NFT development (Griffin et al., 1995; Mrak and Griffin, 2001) while IL-6 has been shown to be present in the early stages of plaque formation (Hull et al., 1996) and is primarily involved in the production of acute phase proteins such as α2-M (Wood et al., 1993). *In vitro*, these cytokines affect the amyloidogenic pathway of APP by enhancing APP and BACE1 expression, thereby promoting sAPPβ and Aβ peptide production (Blasko et al., 1999; Buxbaum et al., 1992; Del Bo et al., 1995; Ringheim et al., 1998; Spooren et al., 2011; Yamamoto et al., 2007). Supporting the amyloid cascade hypothesis, the production of these pro-inflammatory cytokines might not be the primary cause of AD but may indeed be involved in a detrimental cycle of APP metabolism enhancement and neuronal death, further accelerating the development of AD (Griffin et al., 1998; Lindberg et al., 2005).

COX-2 production is stimulated by inflammatory cytokines and growth factors and is involved in prostaglandin synthesis which in turn promotes neuroinflammation (Choi and Bosetti, 2009; Meraz-Rios et al., 2013). COX-2 is linked to neurotoxicity and high expression of COX-2 in microglia in the hippocampus correlates with an increase in plaque load, NFT formation and cognitive dysfunction (Xiang et al., 2002). AD mouse models expressing COX-2 exhibit an increase in amyloid plaque formation and levels of the inflammatory mediator prostaglandin E2. This correlated with an increase of toxic $A\beta_{42}$ and an upregulation of γ-secretase processing with unaltered APP expression levels (Xiang et al., 2002).

Nitric oxide synthase (NOS) is an enzyme that catalyses L-arginine in the presence of oxygen to produce L-citrulline and NO (Bishop and Anderson, 2005; Liu et al., 2002; Meraz-Rios et al., 2013). There are three isoforms of NOS. The

endothelial isoform (eNOS) can be found in hippocampal neurons, endothelial cells and some astrocytes (Bishop and Anderson, 2005; Liu et al., 2002). NO formation by activated astrocytes and microglia in response to neuroinflammation may be involved in protein and lipid oxidative damage, excitotoxicity and neuronal cell death (Bishop and Anderson, 2005; Calabrese et al., 2007; Liu et al., 2002). *In vivo*, eNOS deficient mice exhibit an increase in APP and BACE1 protein expression and an increase in BACE1 activity compared to wild-type mice (Austin et al., 2010), thereby promoting β-secretase processing of APP as well as $A\beta_{40}$ and $A\beta_{42}$ peptide production. Expression of the α- and γ-secretases were unchanged (Austin et al., 2010), suggesting that NO selectively effects BACE1 activity.

Nuclear factor-κB (NF-κB) is a redox sensitive DNA transcription factor and upon activation is involved in cytokine synthesis (Jana et al., 2002; Nakajima et al., 2006), NO formation in microglia (Bhat et al., 2002) and COX-2 production in astrocytes (Dai et al., 2006). In neurons and astrocytes, NF-κB is activated by TNF-α (Mir et al., 2008), IL-1 (Koo et al., 2010) and Aβ (Yamamoto and Gaynor, 2001), and is upregulated in AD brains (Chen et al., 2012). *In vitro*, NF-κB binds to the human BACE1 promoter region and facilitates BACE1 gene expression, increasing β-secretase processing of APP and Aβ generation, which could explain the irregular BACE1 gene expression and increase BACE1 activity observed in AD (Chen et al., 2012). This can be prevented by the use of non-steroidal, anti-inflammatory drugs (NSAIDs) (Chen et al., 2012) which suggests NF-κB to be a possible therapeutic target for AD.

1.6.1 Aβ as an antimicrobial peptide

While Aβ is implicated in AD pathogenesis, many have regarded it as a pathological by-product produced by an abnormal proteolytic pathway with no real physiological function. However, increasing attention has been on the antimicrobial properties of Aβ and its potential role in innate immunity (Bourgade et al., 2016; Kumar et al., 2016; Soscia et al., 2010; Spitzer et al., 2016; White et al., 2014). A study conducted by Soscia *et al* compared synthetic forms of Aβ in different aggregation states with another antimicrobial peptide termed LL-37 which is also a part of the innate immune response (Soscia et al., 2010) involved in bacterial phagocytosis by macrophages (Wan et al., 2014). They demonstrated

in vitro that Aβ oligomers prevented pathogen growth similar or even more effectively than LL-37. Aβ extracted from human AD brains also provided similar results. The authors proposed that the binding of Aβ to the microbial surface caused Aβ to aggregate, disturbing the microbial cell membrane and preventing the microbe from binding to its host cell and spreading infection (Soscia et al., 2010). Subsequent studies also reveal the antimicrobial properties of Aβ against a range of other bacterial (Kumar et al., 2016; Spitzer et al., 2016), fungal (Kumar et al., 2016; Spitzer et al., 2016) and viral agents (Bourgade et al., 2015; Bourgade et al., 2016; Lukiw et al., 2010; White et al., 2014), indicating that the antimicrobial effects of Aβ is not confined to a specific pathogen. These findings were explored *in vivo* when Kumar *et al* demonstrated Aβ fibril formation in AD mouse brains infected with *Salmonella typhimurium* bacteria (Kumar et al., 2016). Potential mechanisms of action were in accordance with other studies where authors found Aβ oligomers bound to the pathogenic (*Salmonella typhimurium* bacteria or *Candida albicans* pathogenic yeast) surface and aggregated to form fibrils. This mechanism alleviated infection by preventing pathogen binding to the host cell (Kumar et al., 2016). These studies suggest how an overload of microbial presence in the brain could trigger neuroinflammation to drive Aβ generation, and under a sustained presence, the initiation and progression of AD. However, more experimental data on the role of microbes in AD is required before drawing any conclusions on the possibility of microbes being involved in the etiology and progression of AD. Instead of a continuing microbe presence, another possibility could be a transient infection that the brain might mistakenly perceive as an ongoing threat, initiating and sustaining the production of Aβ to mount an ongoing innate immune response (Le Page et al., 2018; Moir et al., 2018). On the other hand, a non-infectious inflammatory triggering mechanism, for example, head trauma (Blennow et al., 2016; Mendez, 2017; Washington et al., 2016) or stroke (Vijayan and Reddy, 2016; Zhou et al., 2015), which have both been linked to AD, could also pose as the initiating event that drives neuroinflammation and subsequent Aβ production (Le Page et al., 2018; Moir et al., 2018). The amyloidogenic proteolytic processing of APP that leads to the generation of Aβ is through receptor mediated APP endocytosis (Cirrito et al., 2008; Ehehalt et al., 2003; Koo and Squazzo, 1994). However, further investigation is required to identify a functional cognate ligand that can promote

the amyloidogenic pathway of APP through receptor mediated endocytosis and exacerbate widespread Aβ deposition within an inflammatory environment.

1.7 Iron dyshomeostasis in AD

Iron is a vital nutrient required as a cofactor in metabolic processes throughout the body and specifically in tissues of high oxygen consumption, such as the CNS. The ability of iron to freely receive and donate electrons is critical for neurotransmitter regulation as well as oxidative phosphorylation, nitric oxide metabolism and oxygen transport (Zecca et al., 2004). An iron imbalance can lead to metabolic stress on these processes and through Fenton and Haber-Weiss chemistry, high levels of unbound iron may react with molecular oxygen to generate toxic ROS that can lead to severe cell damage and eventual death (Conrad and Umbreit, 2000; McCarthy and Kosman, 2013; Sharpe et al., 2003). Increased cellular susceptibility to oxidative stress associated with iron accumulation leads to neurodegeneration within patients and animal models of dementia related disorders (Connor et al., 1992b; Jack et al., 2005; LeVine, 1997). In AD, an accumulation of iron has been shown in both plaques and tangles (Connor et al., 1992a; Meadowcroft et al., 2009; Smith et al., 1997) where several studies have shown iron to promote Aβ oligomerisation and aggregation (Bousejra-ElGarah et al., 2011; Liu et al., 2011; Mantyh et al., 1993). Iron also induces toxic ROS production through Fenton chemistry by binding and forming a redox-active complex with Aβ (Rival et al., 2009; Rottkamp et al., 2001).

Iron elevation in affected cortical regions of AD has also been characterised in living patients using magnetic resonance imaging (MRI), and in *post mortem* brains using multiple techniques (Du et al., 2018; Zecca et al., 2004). Furthermore, higher brain iron levels are associated with faster disease progression (Ayton et al., 2015a, 2017a; Ayton et al., 2017b). However until recently, it was unclear to what extent iron contributes to AD pathogenesis. The impact of iron on longitudinal AD outcomes was recently revealed by using ferritin (Ft; a major iron binding protein) levels in CSF as an index. High brain-iron load was associated with poorer cognition and brain atrophy over a 6-year period (Ayton et al., 2015a). The magnitude impact of CSF ferritin on these and other AD outcomes is comparable to the tau/$A\beta_{42}$ ratio, previously the best diagnostic CSF biomarker for AD (Shaw et al., 2009; Toledo et al., 2013). This has

introduced the utility of CSF iron reporters in predicting both cognitive deterioration and atrophy along the pathway to dementia (Ayton et al., 2015a).

Since iron imbalance can compromise cell viability, cellular iron homeostasis is tightly regulated by iron uptake, transport, storage and enzymatic proteins that are themselves regulated by iron (Hare et al., 2013; Zecca et al., 2004). The primary source of iron for neurons is through receptor mediated endocytosis of the transferrin (Tf) and transferrin receptor-1 (TfR1) complex (Crichton and Ward, 1992; Deane et al., 2004b; Moos et al., 2007; Rouault et al., 2009). Tf is the major iron transporter in the brain and when bound to ferric iron (holo-Tf), uses its cell surface receptor (TfR1) to internalise into the cell (Hentze et al., 2004; Zhang et al., 2012). Following internalisation, the Tf/TfR1 complex is transported to endosomes via endocytic carrier vesicles where the acidic environment of the endosome facilitates iron release (Hentze et al., 2004). The iron is then reduced to Fe(II) (De Domenico et al., 2008; Knutson, 2007) and exported to the cytosol by divalent metal transporter-1 (DMT1) (Burdo et al., 2001; Ward et al., 2014), contributing to the labile iron pool (LIP) which serves as a source of redox-active iron in addition to an indicator of the amount of iron present within the cell (Breuer et al., 2012; Breuer et al., 2008; Brissot et al., 2012; Cabantchik, 2014; De Domenico et al., 2008). The iron proceeds to be either utilised by the cell, oxidised and stored in the iron storage protein Ft (Arosio et al., 2009) or effluxed via FPN (De Domenico et al., 2011).

One regulatory route for maintaining intracellular iron homeostasis is through the cellular expression and location of proteins such as APP (Duce et al., 2010; McCarthy et al., 2014; Wong et al., 2014b), ceruloplasmin (Cp) (Patel et al., 2002) and hephaestin (Vulpe et al., 1999), which facilitate the movement of iron across the plasma membrane, partly through their ability to complex with the iron exporter FPN and stabilise its expression on the cell surface. The predominant modulator of iron efflux in neurons is APP and has been confirmed transcriptionally using APPKO models (Duce et al., 2010; Wong et al., 2014b). Hephaestin and the membrane-associated form of Cp are ferroxidase proteins that oxidise Fe(II) to Fe(III) for Tf loading and transport, and are the predominant modulators of iron efflux from oligodendrocytes and astrocytes respectively (Yang et al., 2011), while the mechanism of how APP is involved in the oxidation of iron in the efflux process remains uncertain. One possible way is that the iron

is auto-oxidised by the anion environment (Wong et al., 2014a; Wong et al., 2014b) or there is the use of other ferroxidases such as hephaestin which has recently been reported to oxidise iron and facilitate iron efflux from FPN in primary rat hippocampal neurons (Ji et al., 2018).

Intracellular iron levels are regulated by cytoplasmic RNA-binding proteins known as iron response proteins (IRPs) that act as cytosolic LIP sensors (Anderson et al., 2012). IRPs bind to specific regions called iron regulatory elements (IREs) located in the 3' or 5' untranslated region (UTR) of mRNAs encoding several proteins responsible for iron uptake, storage and export, and either enhance or diminish translation according to the cells metabolic requirements (Anderson et al., 2012; Pantopoulos, 2004). When intracellular iron levels become low, IRPs bind IREs located in the 3' UTR of TfR1 and DMT1 mRNA and increase translation to promote iron import, while binding to the IREs in the 5' UTR of Ft and FPN prevents translation and therefore downregulates iron storage and export mechanisms respectively. In contrast, when intracellular iron levels are high within the cell, iron from the LIP binds to the IRPs, preventing their interaction with IREs which results in an increase in Ft and FPN translation to accommodate iron storage and export respectively, while TfR1 and DMT1 translation are reduced through mRNA degradation (Aisen et al., 2001; Muckenthaler et al., 2008; Wong and Duce, 2014). APP is also classed as an iron response protein containing IREs located in the 5' UTR of its mRNA, where translation is directly regulated by cellular iron levels (Rogers et al., 2002). Iron imbalance plays a major role in the pathogenesis of AD (Christen, 2000; Greenough et al., 2013). Studies have shown AD affected neurons to exhibit an increase in intracellular iron, possibly attributed by the dysregulation of associated iron regulatory proteins (Atwood et al., 2003; Bonda et al., 2011; Bush, 2013; Duce et al., 2010; Li et al., 2017; Myhre et al., 2013). For example, a decrease in FPN expression has been shown in *post mortem* AD brain tissue (Manolov et al., 2017; Raha et al., 2013; Urrutia et al., 2013), indicating a disruption to the iron export pathway that could be a contributing factor in the accumulation of intracellular iron levels (Connor et al., 1992b; Duce et al., 2010; Maynard et al., 2002; Wong et al., 2014b).

Competitive binding for the cell surface stabilisation rate to FPN may also regulate both cellular iron efflux as well as export of iron into the plasma/blood.

Studies have suggested the circulating peptide hormone called hepcidin to be involved in regulating iron export by direct association with FPN (De Domenico et al., 2011; Ganz, 2003). Hepcidin is predominantly expressed by and excreted from hepatocytes in response to a wide range of stimuli including Tf saturation levels in the periphery (Anderson et al., 2009). Under high levels of Tf saturation, iron bound Tf displaces human hemochromatosis protein (HFE) from TfR1. HFE then binds and forms a complex with TfR2, activating various signalling pathways that induce expression and release of hepcidin which binds to FPN in iron exporting cells and triggers FPN internalisation and degradation. In contrast, when iron saturation of Tf is low, HFE is complexed to TfR1 and hepcidin production is minimised for efficient iron export by cell surface FPN (Anderson et al., 2009; De Domenico et al., 2009; Ganz and Nemeth, 2011; Pietrangelo, 2011; Zhang et al., 2011). Other molecular mechanisms as well as the signalling pathways that are involved in the regulation of hepcidin expression can be found in reviews Rishi *et al* (2015) and Sangkhae *et al* (2017) (Rishi et al., 2015; Sangkhae and Nemeth, 2017). Physiologically, hepcidin expression within the brain has been documented, although at minimal levels in cells such as neurons, glial and endothelial cells (Hanninen et al., 2009; Pigeon et al., 2001; Raha-Chowdhury et al., 2015; Zechel et al., 2006). However, studies have documented a significant increase in hepcidin levels within the brain during inflammation and iron overload (Lu et al., 2017; Pigeon et al., 2001; Sun et al., 2012; Wang et al., 2008; Xiong et al., 2016; You et al., 2017). There has been increasing debate on whether hepcidin has any role in iron homeostasis within AD as several studies have also reported minimal levels of hepcidin expression. As an example, Manolav *et al* reported an increase of hepcidin expression in the AD brain which could contribute to an increase in intracellular iron levels from the reduction of the iron exporter FPN (Manolov et al., 2017), whereas Raha *et al* demonstrated low levels of hepcidin (and FPN) within the AD brain (Raha et al., 2013), suggesting an alternative mechanism of FPN regulation. Clearly, further investigation is required to elucidate the precise mechanism of hepcidin within physiological and pathophysiological states of the brain.

Accumulation of lipid peroxidation products and lethal ROS derived from iron metabolism can lead to regulated cell death termed ferroptosis (Cao and Dixon, 2016; Dixon et al., 2012) and has been recently suggested as a

neurodegenerative disease mechanism (Stockwell et al., 2017). This has created significant interest in the possibility that disturbances of brain iron levels can lead to a selective form of cell death separate from apoptosis or necrosis. Ferroptosis is an iron and ROS-dependent form of non-apoptotic cell death that can be triggered by conditions that inhibit glutathione biosynthesis or the lipid repair enzyme glutathione peroxidase 4 (Gpx4) (Dixon et al., 2012). Ferroptosis was determined through a pharmacological approach where high-throughput screening identified two molecules, erastin (Dolma et al., 2003) and RAS-selective lethal 3 (RSL3) (Yang and Stockwell, 2008) that could instigate a form of cell death distinct from apoptotic and necrotic pathways (Dixon et al., 2012). Multiple studies have indicated system X_c^- and Gpx4 to be important regulators of ferroptosis (Dixon et al., 2012; Yang et al., 2014). Erastin triggers cell death by inhibiting the cystine-glutamate antiporter system X_c^-, subsequently leading to a reduction in Gpx4 activity, whereas RSL3 directly interacts with Gpx4 to inhibit its enzymatic activity (Dixon et al., 2012; Yang et al., 2014; Yang and Stockwell, 2008). Resulting cell toxicity through such pathways trigger oxidative stress, mitochondrial fragmentation and loss of plasma membrane integrity, all of which are key features of AD (Montine et al., 2002; Park et al., 2015; Sanchez Campos et al., 2015). However, a direct link between ferroptosis and AD has yet to be determined.

The precise role of iron in ferroptosis is yet to be fully elucidated but multiple studies have demonstrated iron to be a fundamental requirement (Dixon et al., 2012; Stockwell et al., 2017). Furthermore, the fact that ferroptosis can be inhibited by deferoxamine and deferiprone (DFP), well known iron chelators (Kontoghiorghe and Kontoghiorghes, 2016), also reinforces an integral role for iron in the ferroptotic pathway. Treatment with these iron chelators *in vitro* depletes iron and prevents iron-dependent lipid peroxidation and restores Gpx4 levels (Dixon et al., 2012; Do Van et al., 2016; Feng and Stockwell, 2018; Wu et al., 2018).

Recently, there has been growing evidence in the possible role of iron regulatory proteins on the regulation of ferroptosis. For instance, Gao *et al* described a prominent component in serum, which was later identified as the iron transporter Tf that could potentiate erastin-induced ferroptotic cell death *in vitro* (Gao et al., 2015). This enhanced cell death was confirmed upon exogenously adding

recombinant holo-Tf but not iron-unbound Tf (apo-Tf) to cells without serum. Furthermore, immunodepletion of Tf from the serum, RNAi knockdown of TfR, and treatment with the ferroptosis inhibitor ferrostatin-1, all distinctively prevented ferroptotic cell death. Although the underlying cellular mechanisms remain unclear, results illustrate the iron import capability of Tf to enhance iron-associated ferroptotic cell death (Gao et al., 2015). Another example of an iron regulatory protein involved in modulating ferroptosis was when Geng *et al* revealed that FPN knockdown in neuroblastomas facilitated ferroptosis induction. Erastin treatment of FPN depleted neuroblastomas resulted in an increase in intracellular iron levels, lipid ROS, and cell death all of which could be prevented by ferrostatin-1 and deferoxamine but not with apoptotic and necroptotic associated inhibitors (Geng et al., 2018). These results highlight the importance of FPN in modulating iron efflux in neuroblastomas whereby disrupting FPN expression, prompts an accumulation of intracellular iron which accelerates ferroptosis induction (Geng et al., 2018).

1.8 Lactoferrin

Lf is a glycoprotein that is considered a member of the transferrin family (Metz-Boutigue et al., 1984), sharing approximately 60 % amino acid sequence homology to Tf (Harmsen et al., 1995). Tf and Lf maintain iron in its stable oxidation state, preventing it from inducing toxic ROS formation through Fenton chemistry (Chung and Raymond, 1993). Lf consists of a polypeptide chain folded into two globular lobes (N and C lobes), each containing one iron binding site. The two lobes are connected by a linker peptide that forms a rigid 3-turn α-helix to stabilise the binding of iron within each lobe (Anderson et al., 1987; Anderson et al., 1989; Baker and Baker, 2005). This is unlike Tf where the linker peptide is irregular and highly flexible (T. A. MacGillivray et al., 1998). There are six ligands contained in each lobe required for iron binding. Four of the ligands are from the polypeptide chain (one aspartic acid residue, two tyrosine residues, and one histidine residue) whilst the other two are formed from the oxygen atoms of an anion, usually carbonate, required to facilitate iron release at low pH (Baker, 1994; Baker et al., 2002; Rosa et al., 2017; T. A. MacGillivray et al., 1998). Similar to Tf, there are two predominant forms of Lf; iron-bound holo and iron-unbound apo, each differing in their tertiary structure. For instance, apo-Lf has an ‘open’ conformation in which the iron binding site is near the protein surface and

exposed to the surrounding environment, whereas holo-Lf mainly has a compact ‘closed’ conformation in which the iron is well below the protein surface and therefore inaccessible to potential ligands (Jameson et al., 1998; Querinjean et al., 1971). The iron binding affinity of Lf has been shown to be 260 times greater than that of Tf at physiological pH, likely due to its binding off rate (Aisen and Leibman, 1972; Chung and Raymond, 1993), and as such Tf may act as an iron donor for Lf (Aisen and Leibman, 1972; Baker and Baker, 2004; Metz-Boutigue et al., 1984; Valenti and Antonini, 2005).

The incorporation of iron into Tf or Lf is instrumental in controlling the level of free iron within biological fluids; acting as an extracellular transporter of iron that both delivers iron to cells and facilitates the removal of iron from cells (Crichton and Charloteaux-Wauters, 1987). Similar to holo-Tf, holo-Lf interacts with its cell surface bound receptors such as the Lf receptor (LfR), leading to targeted cellular iron delivery via receptor mediated endocytosis (Dautry-Varsat et al., 1983).

First described as the major protein found in colostrum and breast milk, Lf is also excreted by various exocrine glands and specific granules of neutrophils (Kruzel et al., 2007) as well as being present within plasma (Hansen et al., 1975) and tissues such as the liver (McAbee and Ling, 1997). Within the brain, it is reportedly expressed in glia, neurons, and endothelial cells (Fischer et al., 2007; Kawamata et al., 1993). Lf may also promote other physiological functions through interactions with various proteins within mammalian cells (de Lillo et al., 1992), some secretory proteins (Lampreave et al., 1990; Watanabe et al., 1984), receptors on bacterial cell surfaces (Schryvers et al., 1998; Wong and Schryvers, 2003) and metal ions (Crichton and Charloteaux-Wauters, 1987). For example, Lf has been shown to participate in growth and differentiation of osteoblasts by both increasing the proliferation and inhibiting apoptotic cell death, resulting in an increase in bone matrix synthesis and mineralisation (Naot et al., 2005). Lf is also anti-inflammatory. Lf proteolytic cleavage by pepsin digestion produces short functional peptides capable of binding to outer-membrane structures such as lipopolysaccharides (LPS), resulting in bacterial membrane permeabilisation and disruption, attenuating the immunostimulatory response of LPS (Schryvers et al., 1998). Lf also protects against carcinogenesis via stimulating natural killer cells, modulating G1 proteins and suppressing vascular endothelial growth factor-mediated angiogenesis (Sakamoto et al., 2006; Siebert and Huang, 1997).

Tf is the predominant iron transporter in the body while Lf is thought to play a limited role in normal iron homeostasis (Sanchez et al., 1992). Lf is more involved in cellular iron management during neuroinflammation and the immune response (Grossmann et al., 1992; Jameson et al., 1998; Sanchez et al., 1992). Its expression is rapidly increased during infection and inflammation which contributes to alterations in iron metabolism (Levay and Viljoen, 1995). As an acute phase protein, Lf stifles pathogen growth by sequestering free iron (Grossmann et al., 1992; Jameson et al., 1998; Levay and Viljoen, 1995). The sites of infection and inflammation creates a pH environment low enough to accommodate the iron binding capability of Lf whereas holo-Tf is unable to retain its bound iron at acid pH (Aisen and Leibman, 1972; Sanchez et al., 1992). Of significance, Lf is increased with AD in neurons and glia and accumulates around lesions of neuronal damage, including plaques (Kawamata et al., 1993; Leveugle et al., 1994; Qian and Wang, 1998; Wang et al., 2010) but it is yet to be determined whether this is protective by sequestering free iron or deleterious by signalling inflammation.

1.9 Aims

The processing of APP is an important determining factor in the development of AD given that APP amyloidogenic proteolytic processing leads to the generation of Aβ that accumulates in extracellular plaques in the AD brain (Cras et al., 1991). A functional cognate ligand that promotes the amyloidogenic pathway of APP has yet to be widely confirmed even though multiple groups have shown various proteins to regulate APP metabolism, altering levels of Aβ secreted by cells (Tang and Liou, 2007). Discovering a cognate ligand for APP is challenging because one must find a ligand that has a role and an interrelationship within the associated mechanisms involved in AD and one that corrects the multiple facets of the pathobiology. Studies often provide experimental evidence that partially characterise potential ligands and APP interactions. These often lack experimental data relating to whether the interaction is direct or indirect, the affinity and specificity of the target ligand to APP and whether the interaction offers any insight to the possible physiological function of APP and its amyloidogenic processing pathway. The identification of a novel ligand that not only associates with APP and modulates it’s trafficking and processing but is also

involved in the associated mechanisms implicated in AD will not only increase our understanding of the disease but will also reveal potential therapeutic targets.

The major hypothesis of this study is to investigate whether Lf-signalled inflammation could provide an ‘inflammatory hit’ that shifts APP towards the amyloidogenic pathway, resulting in Aβ production and subsequent intracellular iron retention. This study will determine whether Lf is a key player connecting neuroinflammation, iron accumulation, APP processing, and Aβ secretion which will reveal a unified mechanism relevant to AD.

Direct binding of Lf with the major isoforms of APP with and without the presence of iron will be investigated. This will determine whether the conformational change to Lf in the presence of iron impacts the binding of APP and whether the interaction is APP isoform specific. APP peptide arrays will be carried out to identify the minimal binding domain of APP for Lf in the hope of identifying small peptides that block the interaction and alleviate the associated Lf effects on APP metabolism.

Whether the binding of Lf to APP requires a protein complex involving a third component will also be addressed. Studies have demonstrated LRP1 to act as an APP ligand and promote amyloidogenic processing (Rushworth et al., 2013). An extracellular domain that also competitively binds Lf is required for this endocytosis (Dautry-Varsat et al., 1983; Grey et al., 2004; Vash et al., 1998). Therefore, whether the binding between Lf and APP is mediated by LRP receptors will be determined.

Whether Lf is involved in APP receptor mediated endocytosis will be investigated along with the impact of Lf on the predominant processing pathways of APP. Manipulating the major proteins and cellular components required for clathrin-dependent and independent internalisation into the cell will provide insight to the internalisation route of Lf and APP. The precise intracellular location within the endosomal system of Lf and APP after internalisation will also be ascertained by manipulating some of the major Rab GTPases involved in the various APP trafficking pathways (Kiral et al., 2018). Studies will provide further insight into the intracellular location of the amyloidogenic processing of APP directed by Lf. Evaluating the endocytosis, intracellular trafficking, and processing of APP

mediated by Lf will also help define the mode of action of Lf at the cellular level and provide critical insight into the precise cellular mechanism.

To confirm findings in a more physiological cellular environment, a cellular model using transwell co-culture of microglia and neuroblastomas will be developed to interrogate the signalling cross-talk between different populations of cells and confirm the effects of inflammation induced Lf on the amyloidogenic processing pathway of APP. Data obtained will not only resemble physiological conditions but also provide a stronger biological relevance.

Whether Lf could possibly be considered as a therapeutic target will be explored by masking the Lf binding sites of APP and investigating what effect this has on the amyloidogenic pathway and production of Aβ.

Whether APP is involved in the ability of Lf to alter iron homeostasis will be investigated. Similar to the previous aims that use an acute dose, a more chronic administration of Lf at varying doses will be used to determine whether the persistent presence of Lf causes an accumulation of intracellular iron resulting in iron-associated oxidative stress and cell death.

The identification of a new connection between APP and Lf along with unravelling the precise cellular mechanism that may cause increased presence of Aβ and iron, both elevated in AD (Duce et al., 2010; Murphy and LeVine, 2010; Zhu et al., 2009), will determine whether this process can be responsible for the neurodegeneration prevalent in AD. Outcomes obtained from this study will strengthen our understanding of a mechanism as to how levels of iron and Aβ may be altered in a population of people that have no pre-existing family history of the disease.

CHAPTER 2.0 METHODOLOGY

2.1 Materials

Chemicals and reagents were all analytical grade or tissue culture grade and obtained from Sigma-Aldrich, unless otherwise stated.

2.2 Protein production

2.2.1 APP recombinant protein expression and purification

The recombinant fragments of the human soluble APP695α, APP751α, and APP770α were all expressed in the methylotrophic yeast *Pichia pastoris* strain GS115 and purified as previously described (Cappai et al., 1999; Henry et al., 1997) by Dr Bruce Wong (The University of Melbourne, Australia). Media containing APP required a two-step purification procedure using an AKTA FPLC (GE Healthcare), involving anion exchange on a Q-Sepharose column (1.6 x 25 cm column; GE Healthcare) followed by hydrophobic exchange with phenyl-Sepharose (0.5 x 5 cm column; GE Healthcare) (Henry et al., 1997).

2.2.2 Holo-Lf preparation from apo-Lf

Purified human apo-Lf was generously provided by Prof Robert Evans (Brunel University, UK). Saturation of iron in apo-Lf to produce the holo-form was carried out with freshly prepared FeNTA solution (9.9 mM ferric nitrate, 8.5 mM nitrilotriacetic acid adjusted to pH 7.0) as previously described (van Berkel et al., 1995). To determine the concentration of holo-Lf, the absorbance ratio at 280 and 466 nm was measured using a NanoDrop™ 2000c spectrophotometer (Thermo Fisher Scientific). Total protein concentration was determined using the absorption coefficient at 280 nm (ε^{280} = 135,000 $M^{-1}cm^{-1}$) while the concentration of the holo form was determined using the molar absorption coefficient at 466 nm (ε^{466} = 2300 $M^{-1}cm^{-1}$) (Majka et al., 2013).

2.3 Biophysical methods

2.3.1 Sedimentation velocity

Sedimentation experiments were performed by Dr Tim Ryan (The University of Melbourne, Australia) and were conducted using an XL-I analytical ultracentrifuge

(Beckman Coulter Instruments), an An-Ti60 rotor, and double-sector 12-mm path length cells containing Quartz windows and charcoal-filled epon centrepieces. Samples were centrifuged at 50,000 rpm, with radial 280 nm absorbance scans acquired from 6-7.25 cm every 7 minutes. Data were analysed with the c(S) model from Sedfit 9.4 with maximum entropy regularisation to produce sedimentation coefficient distributions (Schuck, 2000). The resulting c(S) distributions were integrated to obtain the weight average sedimentation coefficient and dissociation constants were obtained from this data as previously described (Dam et al., 2005) (Appendix I).

2.3.2 Tryptophan fluorescence

Tryptophan fluorescence experiments were carried out by Dr Bruce Wong (The University of Melbourne, Australia). Tryptophan fluorescence spectra were measured in a 96-well quartz microplate using a Flexstation 3 fluorescence plate reader (Molecular Devices). Fluorescence spectra were acquired, in triplicate, using an excitation wavelength of 295 nm and scanning the emission monochromator from 320-450 nm in 1 nm steps, with a bandwidth of 5 nm and an averaging time of 1 second. Titration data of the change in fluorescence intensity at 340 nm as a function of Lf concentration were fitted to a model describing the binding of a ligand to 2 independent sites on an acceptor, as described by Bailey *et al* (Bailey et al., 2007) (Appendix I) to obtain estimates of the $Kd_{1:1}$ and $Kd_{1:2}$, with the assumption that the change in fluorescence intensity is entirely representative of the fraction of complex formed.

2.3.3 APP770 peptide array

To identify the minimal binding domains of APP for holo-Lf, 15-mer APP peptides were custom synthesised on a cellulose membrane by the Spot technique (GenScript). Full length APP770 was represented as overlapping peptides of 5 αα in length, each shifting by 10 αα (Table 2.1). Hence, each peptide was identical with the previous peptide in 5 out of 15 residues. The peptide membrane was rehydrated in methanol for 5 minutes at room temperature before being thoroughly washed in PBS. Membrane was blocked for 2 hours at room temperature in PBS containing 0.1 % (v/v) Tween-20 (PBS-T) with 3 % (w/v) BSA and then incubated with 1 µg/ml holo-Lf in blocking buffer for 24 hours at 4°C. After thoroughly washing, the membrane was incubated with rabbit anti-Lf (1:500;

bs-5810R; Bioss) primary antibody in blocking buffer for 2 hours at room temperature. Membrane was washed in PBS-T before incubation with horseradish peroxidase (HRP)-conjugated anti-rabbit secondary antibody at a dilution of 1:5000 in blocking buffer for 1 hour at room temperature. After extensive washing, protein on membrane was visualised with enhanced chemiluminescence (ECL) reagent (Thermo Scientific), following the manufacturer's instructions and images were captured using a LAS-3000 Imaging suite (Fujifilm Life Sciences). To determine non-specific binding of holo-Lf, the above was repeated with recombinant apo-Lf (1 µg/ml) as a substitute for holo-Lf, rabbit anti-Lf primary antibody alone (1:500), and finally HRP-conjugated anti-rabbit secondary antibody alone (1:5000). The structure of the APP E2 domain (PDB code 3NYJ) highlighting the interactive binding sites for holo-Lf (marked in yellow, red, and green) determined from the APP peptide array was examined using UCSF Chimera 1.13.1 software (http://www.rbvi.ucsf.edu/chimera).

Table 2.1. 15-mer APP peptides covering the full length APP770 sequence

peptide_1 MLPGLALLLLAAWTA	**peptide_27** PYEEATERTTSIATT	**peptide_53** KKAAQIRSQVMTHLR
peptide_2 AAWTARALEVPTDGN	**peptide_28** SIATTTTTTTESVEE	**peptide_54** MTHLRVIYERMNQSL
peptide_3 PTDGNAGLLAEPQIA	**peptide_29** ESVEEVVREVCSEQA	**peptide_55** MNQSLSLLYNVPAVA
peptide_4 EPQIAMFCGRLNMHM	**peptide_30** CSEQAETGPCRAMIS	**peptide_56** VPAVAEEIQDEVDEL
peptide_5 LNMHMNVQNGKWDSD	**peptide_31** RAMISRWYFDVTEGK	**peptide_57** EVDELLQKEQNYSDD
peptide_6 KWDSDPSGTKTCIDT	**peptide_32** VTEGKCAPFFYGGCG	**peptide_58** NYSDDVLANMISEPR
peptide_7 TCIDTKEGILQYCQE	**peptide_33** YGGCGGNRNNFDTEE	**peptide_59** ISEPRISYGNDALMP
peptide_8 QYCQEVYPELQITNV	**peptide_34** FDTEEYCMAVCGSAM	**peptide_60** DALMPSLTETKTTVE
peptide_9 QITNVVEANQPVTIQ	**peptide_35** CGSAMSQSLLKTTQE	**peptide_61** KTTVELLPVNGEFSL
peptide_10 PVTIQNWCKRGRKQC	**peptide_36** KTTQEPLARDPVKLP	**peptide_62** GEFSLDDLQPWHSFG
peptide_11 GRKQCKTHPHFVIPY	**peptide_37** PVKLPTTAASTPDAV	**peptide_63** WHSFGADSVPANTEN
peptide_12 FVIPYRCLVGEFVSD	**peptide_38** TPDAVDKYLETPGDE	**peptide_64** ANTENEVEPVDARPA
peptide_13 EFVSDALLVPDKCKF	**peptide_39** TPGDENEHAHFQKAK	**peptide_65** DARPAADRGLTTRPG
peptide_14 DKCKFLHQERMDVCE	**peptide_40** FQKAKERLEAKHRER	**peptide_66** TTRPGSGLTNIKTEE
peptide_15 MDVCETHLHWHTVAK	**peptide_41** KHRERMSQVMREWEE	**peptide_67** IKTEEISEVKMDAEF
peptide_16 HTVAKETCSEKSTNL	**peptide_42** REWEEAERQAKNLPK	**peptide_68** MDAEFRHDSGYEVHH
peptide_17 KSTNLHDYGMLLPCG	**peptide_43** KNLPKADKKAVIQHF	**peptide_69** YEVHHQKLVFFAEDV
peptide_18 LLPCGIDKFRGVEFV	**peptide_44** VIQHFQEKVESLEQE	**peptide_70** FAEDVGSNKGAIIGL
peptide_19 GVEFVCCPLAEESDN	**peptide_45** SLEQEAANERQQLVE	**peptide_71** AIIGLMVGGVVIATV
peptide_20 EESDNVDSADAEEDD	**peptide_46** QQLVETHMARVEAML	**peptide_72** VIATVIVITLVMLKK
peptide_21 AEEDDSDVWWGGADT	**peptide_47** VEAMLNDRRRLALEN	**peptide_73** VMLKKKQYTSIHHGV
peptide_22 GGADTDYADGSEDKV	**peptide_48** LALENYITALQAVPP	**peptide_74** IHHGVVEVDAAVTPE
peptide_23 SEDKVVEVAEEEEVA	**peptide_49** QAVPPRPRHVFNMLK	**peptide_75** AVTPEERHLSKMQQN
peptide_24 EEEVAEVEEEEADDD	**peptide_50** FNMLKKYVRAEQKDR	**peptide_76** KMQQNGYENPTYKFF
peptide_25 EADDDEDDEDGDEVE	**peptide_51** EQKDRQHTLKHFEHV	**peptide_77** TYKFFEQMQN
peptide_26 GDEVEEEAEEPYEEA	**peptide_52** HFEHVRMVDPKKAAQ	

2.4 Transgenic mice and treatments

Mice were raised in a controlled environment (22-25°C room temperature, 50-60 % relative humidity, and 12 hour light/dark cycles) with free access to food and water. All mouse studies were performed by Dr Bruce Wong (The University of Melbourne, Australia) with the approval of the IACUC and in accordance with statutory regulations. APPKO mice (Zheng et al., 1995) and background C57BL6/SV129 control mice aged 12 months were used. For iron-fed mice, carbonyl iron was freshly prepared daily and administered at 120 µg/g/day in an 8 % sucrose solution for 8 days before sacrifice. Controls were administered with

8 % sucrose solution only and the dose was orally applied with the use of an olive-tipped oroesophageal needle.

2.4.1 Mouse brain tissue preparation

Mouse brain tissue was prepared by Dr Bruce Wong (The University of Melbourne, Australia). Brain tissue was homogenised in PBS containing 1 % Triton X-100 (PBS-TX100) and centrifuged at 100,000 *g* for 30 minutes at 4°C. Supernatants were collected and protein content was determined by Bicinchoninic acid (BCA; Method 2.6.3). Brain supernatants were then stored -80°C until required for immunoprecipitation experiments.

2.5 Cell lines

Human SH-SY5Y expressing endogenous APP along with SH-SY5Y and mouse Neuro-2a (N2a) cells stably transfected with APP695 (SH-SY5Y-APP695 and N2a-APP695 respectively), were kindly provided by Prof Anthony Turner (The University of Leeds, UK). Human microglial clone 3 (HMC3) cells were purchased from American Type Culture Collection (ATCC®; CRL-3304™).

2.5.1 Cell culture maintenance

SH-SY5Y, SH-SY5Y-APP695 and N2a-APP695 cell lines were maintained in complete growth medium consisting of Dulbecco's Modified Eagle Medium containing 4.5 g/L glucose with L-glutamine (DMEM; Lonza) supplemented with 10 % foetal bovine serum (FBS; Biosera). HMC3 cells were maintained in Eagle's Minimum Essential Medium (EMEM; ATCC®) supplemented with 10 % FBS. All cell lines were sustained in a humidified chamber at 37°C with 5 % CO_2.

2.5.2 Mouse primary neuronal cultures

Preparation and isolation of mouse primary neuronal cultures was carried out as per our previous report (Wong et al., 2014b) by Dr Bruce Wong (The University of Melbourne, Australia).

2.5.3 Co-culture of SH-SY5Y-APP695 cells with Microglial HMC3 cells

A transwell co-culture device was used to investigate the effect of Lf secretion from induced microglia (Fillebeen et al., 2001; Wang et al., 2015) on the

amyloidogenic pathway of APP in SH-SY5Y-APP695 cultures. The cell culture insert which contains a semi-permeable polycarbonate membrane (0.4 µm pore size; Transwell plate; Corning Inc.) was pre-incubated in HMC3 complete growth medium at 37°C overnight to improve cell attachment and distribution. SH-SY5Y-APP695 cells were seeded in 6-well plates at a density of 8.0 x 10^5 cells/ml while HMC3 cells were seeded into pre-incubated cell culture inserts (4.0 x 10^5 cells/ml) both in their respective complete growth media and left overnight at 37°C with 5 % CO_2 to adhere. Cell culture inserts were then placed into wells to start a non-contact co-culture of upper-well HMC3 and lower-well SH-SY5Y-APP695. For HMC3 activation, the medium of the upper insert well was replaced with serum-free EMEM containing 10 ng/ml recombinant human interferon-γ (IFN-γ) (PeproTech) for 24 hours, while the medium in the lower plate well was replaced with fresh serum-free DMEM.

2.5.4 RNA interference (RNAi)

2.5.4.1 Forward transfection

Cells were seeded in 6-well plates at 70 % confluency one day before being transiently forward transfected. APP, BACE1, LRP1, dynamin (DYM), ARF6, Rab5a, Rab7a, Rab11a, Lf (SMARTpool: ON-TARGETplus Human siRNA; Thermo Scientific), or control non-target (ONTARGETplus Non-targeting Pool; Thermo Scientific) RNAi were prepared at a final concentration of 20 nM in siRNA buffer (Thermo Scientific) and Opti-MEM (Life Technologies) to a volume of 150 µl. In turn, this was added to 150 µl of Opti-MEM containing 4 µl of Lipofectamine® RNAiMAX (Life Technologies), prepared separately. After a 5 minute incubation at room temperature, the 300 µl RNAi mixture was added dropwise to cells per well in 1 ml complete growth medium and incubated for 48 hours at 37°C prior to experimental conditioning.

2.5.4.2 Reverse transfection

For RNAi directed against clathrin heavy chain (CHC), cells were transiently reverse transfected. CHC (SMARTpool: ON-TARGETplus Human CHC siRNA; Thermo Scientific) or control non-target RNAi was prepared at a final concentration of 40 nM in siRNA buffer and added to 500 µl Opti-MEM containing 9 µl of Lipofectamine® RNAiMAX and incubated at room temperature for 20

minutes. During this incubation, cells were seeded in 6-well plates at 8.0 x 10^5 cells/well in a 1 ml volume in complete growth medium. The 500 µl RNAi mixture was then immediately added dropwise to the freshly re-suspended cells and incubated for 30 minutes at room temperature and then a further 6 hours at 37°C. Media was replaced with fresh complete growth medium and cells were further incubated for 72 hours prior to experimental conditioning.

2.5.4.3 RNAi reverse and forward co-transfection

For RNAi directed against both LRP1 and APP, ARF6 and APP or Rab4a and Rab11a and control non-target, cells were transiently reverse transfected with 20 nM APP, Rab4a (SMARTpool: ON-TARGETplus Human Rab4a siRNA; Thermo Scientific) or control non-target using 4 µl of Lipofectamine® RNAiMAX as described above and on the following day, transiently forward transfected with 20 nM LRP1, ARF6 or Rab11a RNAi using 4 µl of Lipofectamine® RNAiMAX. Cells were incubated with the RNAi mixture for a further 48 hours prior to experimental conditioning.

2.5.5 Lf titration and time course

For the Lf titration experiment, SH-SY5Y cells were incubated in Hank's Balanced Salt solution (HBSS) media containing 0, 50, 100, 250, 500, and 1000 nM holo-Lf for 2 hours at 37°C. To confirm the optimal time for Lf treatment, cells were incubated with 500 nM holo-Lf in HBSS for 0.5, 1, 2, and 4 hours at 37°C.

2.5.6 Iron bound and unbound forms of Lf and Tf treatment

Cells were incubated for 2 hours with HBSS containing apo-Lf, holo-Lf, apo-Tf or holo-Tf (500 nM) at 37°C, unless otherwise stated. The procedure for holo-Lf exposure to N2a-APP695 cells was performed according to Guo *et al* (Guo et al., 2017). Cells were incubated with serum-free DMEM for 24 hours, then incubated with fresh serum-free DMEM containing 0.1 mg/ml holo-Lf for an additional 24 hours at 37°C.

2.5.7 Methyl-β-cyclodextrin (MβCD) treatment

Cells were incubated in serum-free DMEM containing 1 mM MβCD for 3 hours at 37°C. Live cells were assayed for cholesterol depletion using the Amplex Red

Cholesterol assay kit (Life Technologies) as described in the manufacturer's instructions. Fluorescence was measured at an excitation of 560 nm and emission of 590 nm using a FlexStation 3 with SoftMax Pro 5.4.6 software (Molecular Devices). A standard curve was used to calculate cholesterol concentrations of each sample. For each point, background fluorescence was corrected by subtracting the values derived from the no-cholesterol control.

2.5.8 APP blocking peptides

The 15-mer APP peptides from the peptide array that specifically interacted with holo-Lf were custom made with > 95 % purity from GenScript. Peptides were dissolved in DMSO and pre-incubated at varying concentrations with holo-Lf (500 nM) in serum-free DMEM containing 0.01 % BSA for 2 hours at 4°C. Bound APP peptide to holo-Lf was then applied to SH-SY5Y-APP695 cells and incubated for another 2 hours at 37°C.

2.5.9 Antibody neutralisation of Lf

For antibody neutralisation experiments, 20 µg/ml of rabbit anti-Lf antibody or rabbit IgG isotype control was added to SH-SY5Y-APP695 cells in the lower wells of the co-culture device in serum-free DMEM, while serum-free EMEM with human IFN-γ was added in the upper wells containing HMC3 cells for 24 hours at 37°C.

2.6 Protein analysis by Western blot

2.6.1 Preparation of condensed media

Serum-free conditioned media was collected and centrifuged for 5 minutes at 2500 *g* at room temperature to pellet any unwanted cells and debris. Media samples were concentrated approximately 10-fold using a 3,000 Da molecular weight cut off Amicon Ultra-0.5 centrifugal filter unit with an Ultracel-3 membrane (Millipore) by centrifugation at 14,000 *g* for 30 minutes at room temperature. Condensed media samples were stored at -20°C until further analysis.

2.6.2 Preparation of cell lysates

Cells were washed twice with ice-cold PBS, collected and pelleted by centrifugation at 2500 *g* for 5 minutes at 4°C. Cells were re-suspended and lysed

in ice-cold radioimmunoprecipitation assay (RIPA) buffer (150 mM NaCl, 1 % (v/v) Nonidet P-40, 1 % (w/v) sodium deoxycholate, 0.1 % (v/v) SDS, 25 mM Tris-HCl, pH 7.6) with a complete, EDTA-free protease inhibitor cocktail mixture (Roche) for 15 minutes on ice. To increase protein yields, each sample was homogenised using a 29 G x 13 mm needle and syringe. Cell lysates were clarified by centrifugation at 14,000 *g* for 15 minutes at 4°C. Supernatants were transferred to a fresh 1.5 ml tube and stored at -20°C until further analysis.

2.6.3 BCA protein assay

Total protein concentrations of cell lysate and conditioned media samples were determined using the BCA protein assay kit (Thermo Fisher Scientific) according to the manufacturer's instructions. All measurements were performed in duplicates and conducted in a clear 96-well microplate. A standard curve was prepared by diluting the BSA standard in dH_2O. Both standards and samples were diluted 1:10 in dH_2O and pipetted into the microplate wells. A working reagent was made by mixing 50 parts of Reagent A with 1 part of Reagent B. 200 µl of this mixture was added to each well and the microplate was incubated at 37°C for 30 minutes. After cooling the plate to room temperature, the absorbance was measured at 562 nm using a Varioskan Flash spectral scanning multimode reader and analysed using SkanIt 2.5.1 software (Thermo Fisher Scientific). By taking the dilution factors into account, the BSA standard curve was used to calculate the concentrations of the unknown protein samples using the blank subtracted data.

2.6.4 Sodium Dodecyl Sulfate-Polyacrylamide Gel Electrophoresis (SDS-PAGE) and Western blotting

10 µg of total protein in media and cell lysates or equal volumes of conditioned media containing purified holo-Lf protein from each experimental condition were denatured in Laemmli sample buffer (62.5 mM Tris-HCl pH 6.8, 25 % glycerol, 2 % SDS, 0.01 % bromophenol blue, 5 % 2-mercaptoethanol) and boiled at 90°C for 5 minutes. Samples were separated on 10 % PAGE (Tris-Glycine; BioRad) for sAPP/APP, ADAM10, BACE1, LRP1, CHC, DYM, ARF6, sAPPβ, Lf, TfR, and Ft detection or 4-20 % PAGE (Tris-Glycine; BioRad) for Rab4, Rab5, Rab7, Rab11, and major histocompatibility complex class II (MHC class II) detection

using the Mini Protean Tetra system (BioRad), and electrophoresed at 120 V in 25 mM Tris, 192 mM Glycine, 0.1 % (w/v) SDS, pH 8.3 buffer. Resolved proteins were transferred to polyvinylidene difluoride (PVDF) 0.45 µm membranes (Hybond-P; GE Healthcare Life Sciences) at 120 V for 75 minutes at 4°C in 25 mM Tris, 192 mM glycine buffer containing 20 % methanol. For Lf detection, resolved proteins were transferred to nitrocellulose 0.45 µm membranes (Protran; GE Healthcare Life Sciences). For Aβ detection, protein samples were separated on 4-12 % PAGE (Bis-Tris; Life Technologies), electrophoresed at 120 V in 50 mM MES, 50 mM Tris, 0.1 % (w/v) SDS, 1 mM EDTA, pH 7.3 buffer, and transferred to PVDF 0.2 µm membranes at 25 mA for 2 hours and 15 minutes at 4°C. PVDF membranes were blocked for 1 hour at room temperature in PBS-T with either 5 % (w/v) dried milk powder or 2 % (w/v) BSA (Table 2.2). For Aβ detection, PVDF membranes were boiled in PBS for 10 minutes before blocking to expose epitopes for antibody binding. Membranes were then incubated overnight at 4°C with primary antibody diluted in blocking buffer (Table 2.2). Membranes were then washed in PBS-T before incubation with HRP-conjugated secondary antibody at a dilution of 1:5000 in PBS-T for 1 hour at room temperature. Membranes were washed in PBS-T once again and proteins were visualised with ECL reagent and images were captured using a LAS-3000 Imaging suite. For re-probing membranes, antibodies were stripped by incubating the blots for 30 minutes at room temperature in Re-Blot Plus Strong Antibody Stripping solution (Millipore) diluted 1:10 in dH_2O, before repeating the immunoblotting procedure with either β-actin or Na^+/K^+ ATPase antibody (Table 2.2). Densitometry using Image J (v1.48k; NIH) was performed in triplicate or duplicate on 3 separate experiments unless otherwise stated and all quantification was standardised against β-actin levels or Na^+/K^+ ATPase for surface protein analysis.

Table 2.2. Antibodies and conditions used in Western blotting

Antigen	Antibody	Dilution	Blocking agent	Secondary
sAPP/APP	22C11 (Millipore)	1:2000	5 % (w/v) milk	Rabbit anti-Mouse
ADAM10	ab1997 (Abcam)	1:1000	2 % (w/v) BSA	Goat anti-Rabbit
BACE1	ab108394 (Abcam)	1:1000	2 % (w/v) BSA	Goat anti-Rabbit
LRP1	ab92544 (Abcam)	1:5000	2 % (w/v) BSA	Goat anti-Rabbit
CHC	ab21679 (Abcam)	1:1000	5 % (w/v) milk	Goat anti-Rabbit
DYM	ab52611 (Abcam)	1:1000	5 % (w/v) milk	Goat anti-Rabbit
ARF6	ab131261 (Abcam)	1:1000	2 % (w/v) BSA	Goat anti-Rabbit
sAPPβ	1A9 (GlaxoSmithKline)	1:2500	5 % (w/v) milk	Rabbit anti-Mouse
Lf	bs-5810R (Bioss)	1:500	2 % (w/v) BSA	Goat anti-Rabbit
TfR	H68.4 (Invitrogen)	1:2000	5 % (w/v) milk	Rabbit anti-Mouse
Ft	FTH1 (Cell Signalling Technology)	1:1000	2 % (w/v) BSA	Goat anti-Rabbit
Rab4	ab13252 (Abcam)	1:1000	5 % (w/v) milk	Goat anti-Rabbit
Rab5	ab109534 (Abcam)	1:1000	5 % (w/v) milk	Goat anti-Rabbit
Rab7	ab137029 (Abcam)	1:1000	5 % (w/v) milk	Goat anti-Rabbit
Rab11	ab3612 (Abcam)	1:500	5 % (w/v) milk	Goat anti-Rabbit
MHC class II	ab157210 (Abcam)	1:5000	5 % (w/v) milk	Goat anti-Rabbit
sAβ/Aβ	6E10 (BioLegend)	1:2000	2 % (w/v) BSA	Rabbit anti-Mouse
Na^+/K^+ ATPase	ab7671 (Abcam)	1:1000	5 % (w/v) milk	Rabbit anti-Mouse
β-actin	AC15	1:5000	5 % (w/v) milk	Rabbit anti-Mouse

2.7 Double-Antibody capture Enzyme-Linked Immunosorbent Assay (ELISA)

The level of Aβ in cell lysates and conditioned media were quantified using the double-antibody capture ELISA as previously described (Haugabook et al., 2001). Monoclonal antibodies W02 (recognising amino acids 4-10 of the N-terminal region of Aβ) and HRP-conjugated 1E8 (recognising amino acids 18-22 of Aβ) were kindly provided by Dr Bruce Wong (The University of Melbourne, Australia). Nunc MaxiSorp® flat-bottom 96 well plates (eBioscience) were coated overnight at 4°C with 0.5 µg/well of monoclonal W02 Aβ capture antibody in PBS (100 µl per well). Plates were blocked for 4 hours at room temperature with PBS containing 0.5 % (w/v) casein. After blocking, plates were washed twice with PBS, and 50 µg total cell lysate, 100 µl neat conditioned media samples and $A\beta_{42}$ standards (Bachem) diluted in assay buffer (5.75 mM NaH_2PO_4, 15 mM Na_2HPO_4, 2 mM EDTA, 0.4 M NaCl, 0.2 % (w/v) BSA, 0.05 % (w/v) CHAPS, 0.5 % (w/v) casein, 0.05 % (w/v) NaN_3, pH 7.0) were placed in the appropriate wells and incubated at 4°C for 24 hours. Wells were washed twice with PBS and incubated in HRP-conjugated 1E8 Aβ detection antibody (1:1000) diluted in 3.4 mM NaH_2PO_4, 17 mM Na_2HPO_4, 2 mM EDTA, 1 % (w/v) BSA, pH 7.0 and incubated overnight at 4°C. Wells were washed three times with PBS-T and developed using 3,3',5,5'-tetramethylbenzidine (TMB) according to the manufacturer's instructions (Insight Biotechnology). The reaction was stopped with 1 M H_3PO_4 and absorbance was read at 450 nm using a FlexStation 3 with SoftMax Pro 5.4.6 software. Aβ values in the unknowns were calculated by comparison to the values obtained from the synthetic $A\beta_{1-42}$ standards.

2.8 Cell surface Biotinylation assay

Cells were rinsed once with ice-cold PBS (Mg/Ca) and labelled with 0.5 mg/ml sulfosuccinimidyl-2-[biotinamido] ethyl-1,3-dithiopropionate (Sulfo-NHS-SS-Biotin; Thermo Scientific) in PBS (Mg/Ca) for 30 minutes on ice. Unreacted biotin was quenched with ice-cold 100 mM glycine for 20 minutes on ice and cells were rinsed three times with ice-cold PBS (Mg/Ca). Cells were then lysed using RIPA buffer and BCA protein assayed as previously described (Methods 2.6.2 & 2.6.3). To precipitate biotinylated surface proteins, equal amounts of protein from cell lysates were incubated with 50 µl High Capacity Neutravidin Agarose (Thermo

Scientific) overnight at 4°C. Agarose was pelleted by brief centrifugation and supernatants containing non-bound 'intracellular' proteins were removed. Agarose was then washed twice with ice-cold RIPA buffer followed by ice-cold 'high salt' wash buffer (500 mM NaCl, 5 mM EDTA, 50 mM Tris-HCl pH 7.5) and then finally with ice-cold 'no salt' wash buffer (10 mM Tris-HCl pH 7.5). Bound proteins were eluted with 40 µl Laemmli sample buffer containing 50 mM DTT for 30 minutes at room temperature. The procedure for cell surface biotinylation on isolated mouse primary cortical neurons was carried out by Dr Bruce Wong (The University of Melbourne, Australia).

2.9 Fluorescence-activated cell sorting (FACS)

SH-SY5Y cells were washed and collected using PBS at room temperature. After cells were pelleted by centrifugation at 800 *g* for 5 minutes at room temperature, the remaining procedure was performed at 4°C. Cells were re-suspended in ice-cold FACS buffer (PBS, 2.5 mM EDTA pH 8.0) and incubated with a primary antibody against N-terminal APP (1:50; ab15272; Abcam) or FPN (1:50; LifeSpan Biosciences) for 30 min. APP and FPN antibodies used were raised to epitopes on extracellular domains and intensity of fluorescence was compared to cells stained with secondary only to minimise the detection of non-specific binding. Cells were washed with FACS buffer before lightly fixing with 1 % paraformaldehyde (Alfa Aesar) for 5 minutes. Cells were then re-suspended in FACS buffer containing AlexaFluor 488 goat anti-rabbit IgG secondary antibody (1:200; Life Technologies) for 30 minutes in the dark. Cells were further washed with FACS buffer before incubating with 4',6-diamidino-2-phenylindol dihydrochloride (DAPI; 1:2000; Cell Signaling Technology) to differentiate dead cells. Cells were sorted by forward and side scatter on a BD-LSR-Fortessa (BD Biosciences) with a 488 nM blue laser according to fluorescence at 530±30 nM. A minimum of 10,000 cells were recorded in each experiment, having gated the cell population to ensure that only live cells were monitored. Experiments were carried out in duplicate on 3 separate occasions and data were analysed using BD FACS DiVa 6.0 and FlowJo 7.6.4 software.

2.10 Ligand internalisation assay

SH-SY5Y cells were incubated in Opti-MEM for 2 hours at 37°C. During this incubation, sulfo-NHS-SS-Biotin was added to holo-Lf in 20-fold molar excess

and incubated at room temperature for 30 minutes. Removal of non-reacted sulfo-NHS-SS-Biotin was performed by gel filtration using Zeba™ Spin Desalting Columns with a 40,000 Da molecular weight cut off (Thermo Scientific), according to the manufacturer's instructions. Opti-MEM was removed and replaced with fresh Opti-MEM containing 0.5 mg/ml biotinylated holo-Lf and cells were further incubated for 60 minutes at 37°C to allow internalisation. Internalisation was stopped by incubating cells with ice-cold NT buffer (150 mM NaCl, 1 mM EDTA, 0.2 % (w/v) BSA, 20 mM Tris-HCl pH 8.5) on ice for 5 minutes. Residual surface biotin was stripped by incubating cells with 20 mM of the membrane impermeant reducing agent 2-mercaptoethane sulfonic acid (MeSNa) in ice-cold NT buffer twice for 30 minutes each on ice. Cells were washed with ice-cold HBSS then incubated in fresh HBSS containing 20 mM iodoacetic acid for 15 minutes to inactivate residual MeSNa. To examine total biotinylated Lf, MeSNa treatment was omitted. PBS-T containing 2 % (w/v) BSA with High Sensitivity Streptavidin-HRP antibody (1:5000; Thermo Scientific) was used to detect biotinylated holo-Lf. Refer to Figure 2.1 for a schematic overview of the ligand internalisation assay.

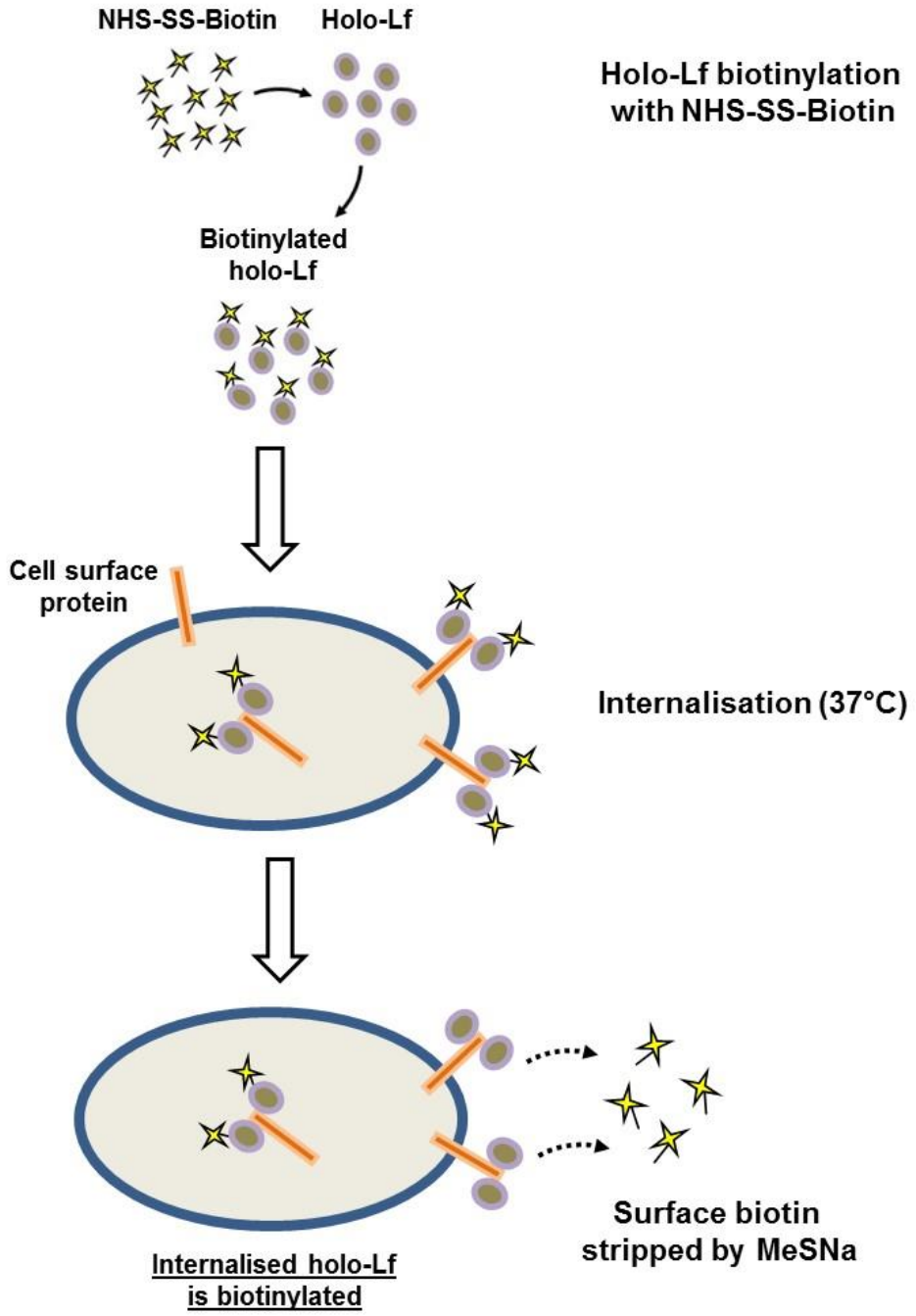

Figure 2.1. Schematic overview of the ligand internalisation assay. Holo-Lf (purple circles) was biotinylated with NHS-SS-Biotin (yellow stars) and then added to cells at 37°C to allow internalisation. Surface biotin was cleaved with the membrane impermeant reducing agent MeSNa to distinguish between internalised and surface localised proteins.

2.11 Immunoprecipitation (IP)

For IP experiments, the IP Dynabeads™ protein G kit (Thermo Scientific) was used as per the manufacturer's instructions with minor modifications. After treatment with each experimental condition, media was collected or cells were lysed and each sample was BCA protein assayed as previously described (Methods 2.6.2 & 2.6.3). Equal concentrations of media or cell lysate were pre-cleared for any non-specific binding with 50 µl protein G Dynabeads for 1 hour at 4°C. Capture antibody (anti-LRP1; 1:100 or anti-Lf; 1:200; LifeSpan BioSciences) was incubated with 50 µl protein G Dynabeads for 2 hours to allow sufficient antibody binding. Pre-cleared media or cell lysates were then added to each tube containing protein G Dynabeads bound to antibody and mixed for a further 24 hours at 4°C. Beads were then thoroughly washed and bound proteins were either eluted with 50 µl Laemmli sample buffer for 10 minutes at 70°C or 100 mM citrate buffer pH 2.0 for 10 minutes at room temperature. Unbound fractions were concentrated approximately 10-fold using a 3,000 Da molecular weight cut off Amicon Ultra-0.5 centrifugal filter unit with an Ultracel-3 membrane as previously described (Method 2.6.1). As a negative control, mouse anti-β-actin (1:100) was used as the capture antibody to confirm specificity of protein interaction. For co-culture IP experiments, each fraction was buffer exchanged with HBSS using Zeba™ Spin Desalting Columns and an aliquot from each fraction was tested for Lf expression via Western blot before being applied to SH-SY5Y-APP695 cells for 2 hours at 37°C. Immunoprecipitation of Lf with APP in mouse brain tissue was performed by Dr Bruce Wong (The University of Melbourne, Australia). Equal concentrations of supernatant from each experimental condition were pre-cleared for non-specific binding with protein G agarose beads for 1 hour at 4°C before being incubated with capture antibody (anti-Lf; 1:200; LifeSpan BioSciences) for a further 1 hour at 4°C. Fresh equilibrated protein G agarose beads were then added to each sample and mixed for a further 2 hours at 4°C. Beads were then thoroughly washed in PBS-TX100 and bound proteins were eluted with Laemmli sample buffer for 10 minutes at 70°C.

2.12 Double Immunofluorescence and Confocal Microscopy

Double immunofluorescence staining was performed to examine co-localisation of APP with CHC, ARF6, Rab4 and Rab11 in the presence of holo-Lf. After RNAi

transfection (Method 2.5.4), SH-SY5Y-APP695 cells were re-platted on poly-L-lysine coated coverslips. Cells were rinsed once with DMEM and blocked in DMEM containing 1 % (w/v) BSA on ice for 30 minutes to halt surface protein internalisation. Cells were then incubated with mouse anti-APP (22C11; 1:50; in-house) antibody in blocking buffer for 20 minutes on ice to label surface presented APP. Non-permeabilised cells were rinsed in PBS (Mg/Ca) and incubated with HBSS media containing 1 µM holo-Lf for 1 hour at 37°C. Cells were washed with PBS (Mg/Ca) and fixed with 4 % paraformaldehyde for 10 minutes at room temperature. Excessive fixative was quenched with 50 mM NH_4Cl. Cells were washed thoroughly and permeabilised in PBS (Mg/Ca) containing 0.1 % Triton X-100 for 15 minutes at room temperature to gain entry to internalised proteins. After thoroughly washing with PBS (Mg/Ca), cells were blocked again in PBS (Mg/Ca) containing 5 % (v/v) donkey serum for 30 minutes at room temperature. Cells were then incubated with the appropriate primary antibodies diluted in blocking buffer for a further 24 hours at 4°C. Primary antibodies used were anti-CHC (1:100), anti-ARF6 (1:100), anti-Rab4 (1:100), and anti-Rab11 (1:50). Cells were then incubated with fluorescently conjugated secondary antibodies for 1 hour in blocking buffer after further washes in PBS (Mg/Ca). Alexa Fluor 488 Donkey anti-Mouse IgG and Alexa Fluor 568 Donkey anti-Rabbit IgG (Life Techologies) were used in combination at 1:500. Cells were washed in PBS (Mg/Ca) and at a final time in ‘no salt’ wash buffer before being mounted onto slides using FluorSave™ mounting reagent (Millipore). A Zeiss LSM700 inverted confocal microscope under an oil-immersed 63x objective lens (NA = 1.40) was used to collect z-stacks of immunofluorescent stained cells, deconvoluted using ZEN 2.3 SP1 (Black) software (Carl Zeiss Microscopy GmbH), and each stack compiled using Image J software. Refer to Figure 2.2 for a schematic representation of the double immunofluorescence staining procedure.

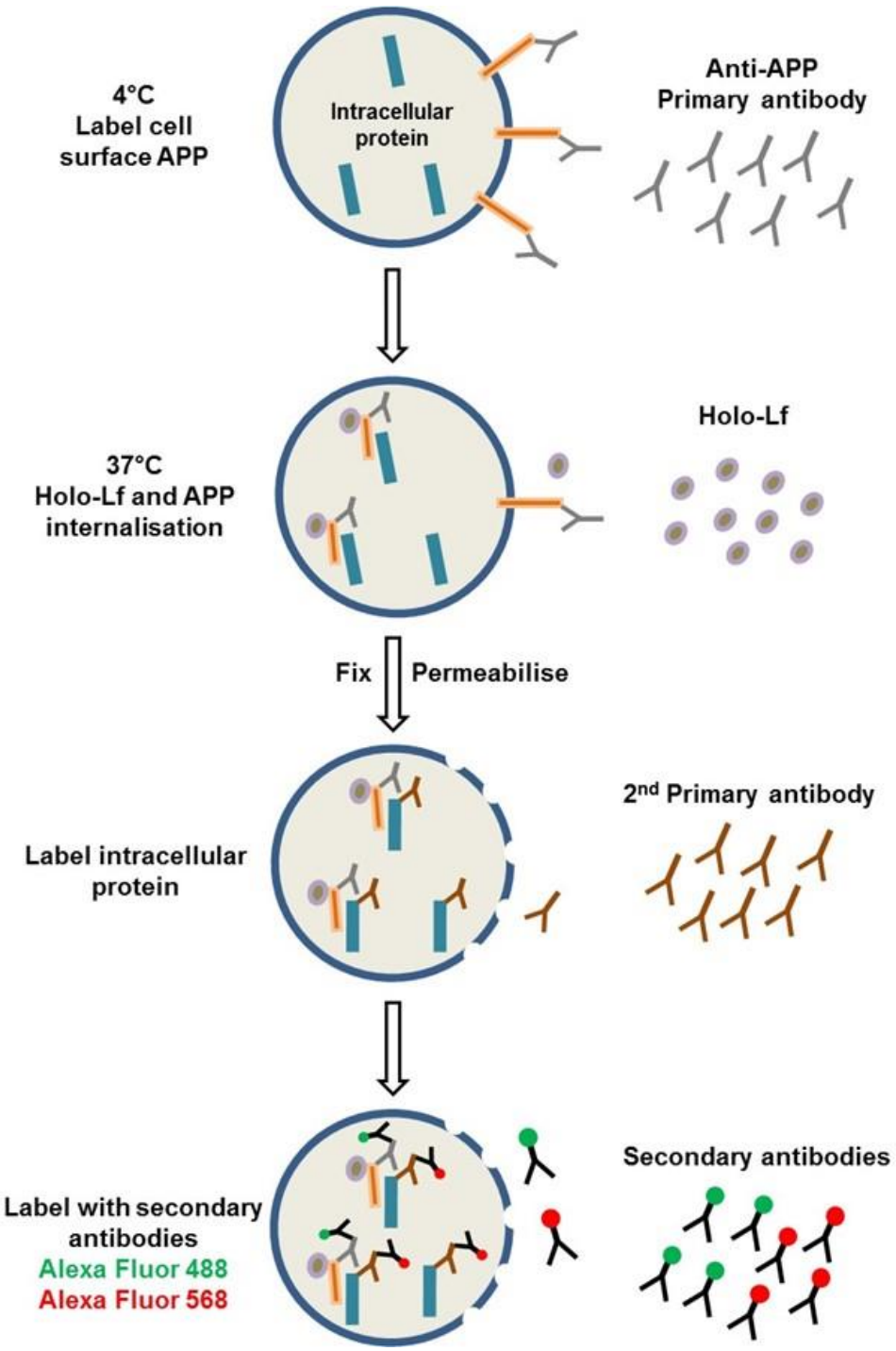

Figure 2.2. Schematic overview of the double immunofluorescence staining procedure. Cell surface APP (orange bars) were labelled with primary antibody at 4°C before being allowed to internalise at 37°C in the presence of holo-Lf (purple circles). Cells were fixed and permeabilised to allow access to internalised proteins. Cells were labelled with the appropriate second primary antibody and then stained with Alexa Fluor 488 (green) and 568 (red) conjugated secondary antibodies to detect co-localisation of proteins.

2.13 Fluorometric BACE1 activity assay

Total BACE activity using human recombinant BACE1 enzyme (Invitrogen) in the presence of apo- and holo-Lf was determined using the TruPoint™ β-Secretase Assay kit (PerkinElmer Life Sciences) according to the manufacturer's instructions. All measurements were performed in black 384-well OptiPlates (PerkinElmer Life Sciences) in a final reaction volume of 50 µl. Both BACE1 enzyme and substrate were diluted in reaction buffer (included in the kit) and reactions were initiated by the addition of 20 µl of BACE1 enzyme (10 µM/reaction) to wells containing 10 µl of either apo- or holo-Lf (20 µM). 20 µl of substrate was added to each well at a final concentration of 200 nM. Fluorescence at an excitation of 340 nm and emission of 615 nm measurements were started immediately and taken every 2 minutes for a total time of 90 minutes using a FlexStation 3 with SoftMax Pro 5.4.6 software. Control wells were prepared without BACE1 enzyme (background) or Lf proteins (enzyme alone). In the presence of the BACE1 enzyme, the peptide substrate is cleaved, separating the fluorescent europium chelate from the quencher (QSY 7), generating a time-resolved fluorescent signal (Gopalakrishnan et al., 2002).

2.14 Calcein-AM assay

The use of Calcein-AM to measure the cytoplasmic LIP was adapted from a previously reported procedure (Kakhlon and Cabantchik, 2002). Cells were plated at 20,000 cells/well in a black 96-well microplate (Greiner Bio-One) in complete growth medium before treatment with each experimental condition. Cells were washed twice with PBS after which 100 µl of PBS containing a final concentration of 60 nM Calcein-AM (Life Techologies) was added. Fluorescence at an excitation of 485 nm and emission of 535 nm measurements were started immediately and taken every minute using a FlexStation 3 with SoftMax Pro 5.4.6 software for 10 min or until a consistent minimum reading had been reached. In triplicate, the iron chelating agent DFP was rapidly added at a final concentration of 100 µM and fluorescence measurements were started again immediately. Readings were continued for a further 5 min or until a plateau had been reached. The fold change of LIP chelated was calculated as the ΔF (the difference in fluorescence from before and after DFP addition) for each condition compared to control under endogenous iron homeostatic regulation.

2.15 Lipid peroxidation assay

Oxidative stress was measured with the lipid peroxidation sensor BODIPY-C11 (Thermo Scientific) according to the manufacturer's instructions. SH-SY5Y-APP695 cells were incubated with complete growth medium containing 0, 0.1, 0.25, 0.5, 1, 3, 5 and 10 µM holo-Lf for either 2 or 72 hours at 37°C. After treatment, cells were rinsed once with PBS (Mg/Ca) and then incubated with DMEM containing 1 µM BODIPY-C11 for 30 minutes at 37°C in the dark. Cells were washed twice with PBS (Mg/Ca) and then incubated with DAPI (1:2000) to measure cell death. BODIPY-C11 was read in tandem with DAPI using a BD-LSR-Fortessa with a 488 nM blue laser according to fluorescence at 530±30 nM. Flow cytometry data were analysed using BD FACS DiVa 6.0 and FlowJo 7.6.4 software.

2.16 Statistical analysis

Statistical analysis and graphical presentation was performed with GraphPad Prism v7.0 software. All data are expressed as means ± standard error (SE). Analysis was carried out with a two-tailed t-test, one-way analysis of variance (ANOVA) followed by Tukey's post-hoc test or two-way ANOVA followed by Bonferroni multiple comparison test, and p-values < 0.05 were considered statistically significant.

CHAPTER 3.0 IRON-BOUND HOLO-LF DIRECTLY BINDS TO THE E2 DOMAIN OF APP

3.1 Introduction

How neuroinflammation and iron dyshomeostasis contribute to AD pathogenesis remains poorly understood. There are a variety of proteins and cellular components associated with these mechanisms that modulate Aβ production, directly or indirectly interacting with APP (Tang and Liou, 2007). However, a functional cognate ligand that promotes the amyloidogenic pathway of APP is yet to be widely confirmed. The identification of a novel therapeutic target that not only associates with APP and modulates it's trafficking and processing but is also involved in the associated early AD pathological mechanisms offers hope for potential therapy.

Lf is an iron transporting protein which is secreted by activated microglia in response to inflammatory stimuli (Fillebeen et al., 2001; Wang et al., 2015) and plays an important role in modulating an innate immune response (Actor et al., 2009). Lf is increased in AD within neurons and glia, and accumulates around lesions of neuronal damage, including plaques (Kawamata et al., 1993; Leveugle et al., 1994; Qian and Wang, 1998; Wang et al., 2010). The upregulation of Lf within the AD brain suggests a potential role for Lf in AD. Furthermore, APP was found to be co-localised with Lf in the affected regions of the AD brain (Kawamata et al., 1993; Tuccari et al., 2002), suggesting a potential physical interaction between Lf and APP. However, at present, there has been no evidence of a direct interaction of APP with Lf or with any of the other members of the Tf family.

Iron imbalance is tightly linked with inflammation and the immune response and many proteins involved in cellular iron management are altered by inflammatory stimuli that ultimately lead to cellular iron retention (Sheng et al., 2003; Urrutia et al., 2013). Indicators of an inflammatory response are associated with iron accumulation as early hallmarks of AD (Rogers et al., 1996; Smith et al., 1997). Both APP and Lf are involved in cellular iron management and have been linked with neuroinflammation and the immune response. APP binds to the iron efflux protein FPN, tethering it to the membrane for efficient neuronal iron export (Ayton et al., 2015b; Ayton et al., 2014; Duce et al., 2010; McCarthy et al., 2014;

Needham et al., 2014; Wong et al., 2014b), and APPKO mice exposed to an inflammatory stimulus, exhibit less reactive microglia (Carrano and Das, 2015) indicating an altered innate immune response. Lf, as an acute phase protein isolates pathogens from its essential growth nutrient iron by sequestration and redistribution (Actor et al., 2009; Kruzel et al., 2007; Kruzel et al., 2017).

LRP1 is part of the LDLR family and is involved in lipoprotein metabolism, protease degradation, lysosomal enzyme activation and can also act as a cellular entry point for bacterial toxins and viruses (Marzolo and Bu, 2009). LRP1 is one of the gene hits discovered by GWAS associated with sporadic AD (Shinohara et al., 2017). It is an endocytotic receptor that recognises more than thirty ligands (Spuch et al., 2012) including APP (Lakshmana et al., 2008) and Lf (Grey et al., 2004). The amyloidogenic processing of APP by β-secretase in the lipid raft is via receptor mediated endocytosis involving LRP1 (Lakshmana et al., 2008). An extracellular domain that also competitively binds Lf is required for this endocytosis (Dautry-Varsat et al., 1983; Grey et al., 2004; Vash et al., 1998).

In the present chapter, we demonstrate the inflammatory response protein Lf as a new binding partner to APP. Since conformational differences have been shown between iron-free apo-Lf and iron bound holo-Lf (Jameson et al., 1998; Querinjean et al., 1971), direct binding of Lf with the major isoforms of APP with and without the presence of iron was investigated *in vitro*. Information obtained was further validated *in vivo*, demonstrating physiological relevance of the interaction between Lf and APP. The minimal binding domain of APP for Lf was identified and through a series of biophysical techniques, the affinity of holo-Lf for APP was observed to be comparable to that of another previously reported interaction of Lf with the copper-carrying ferroxidase protein Cp (Ha-Duong et al., 2010; White et al., 2012). Whether the binding of Lf to APP requires a protein complex involving LRP receptors was also investigated.

3.2 Results

3.2.1 Sedimentation velocity analysis of the interaction between Lf and APP

To confirm the interaction between Lf and APP, sedimentation velocity analysis was performed. sAPPα (sAPP695) alone sedimented as a single homogenous distribution with a modal sedimentation coefficient of 3.92 S (f/f0 = 1.4, molecular weight ≈ 61,000 Da), while holo-Lf alone provided a similar Gaussian distribution with a modal sedimentation coefficient of 5.1 S (f/f0 = 1.38, molecular weight ≈ 79,000 Da) (Figure 3.1A). Mixing of sAPP695 with holo-Lf at molar ratios of 1:1 or less resulted in a bimodal distribution with maximal sedimentation coefficients at approximately 4 S and 6.9 S, (f/f0 = 1.39, molecular weights of ≈ 61,000 and 142,000 Da) (Figure 3.1A). The significant shift in the second Gaussian distribution to a higher sedimentation coefficient suggests a strong interaction. Example data sets showing data quality, and the fit of the c(s) model to the data are shown in Appendix I (Figure S1).

Increasing the ratio of holo-Lf:sAPP695 to 1.5:1 and 2:1, resulted in the emergence of a third peak in the c(S) distribution with a maxima at ≈ 9.8 S (f/f0 = 1.36, molecular weight ≈ 223,000 Da) (Figure 3.1A), consistent with a stoichiometry of 2 Lf molecules per sAPP695 molecule. Weight average sedimentation coefficients for these samples were obtained by integrating the c(S) distributions in Figure 3.1A (Figure 3.1B). The data were fitted to a two-site binding model (Appendix I: Eq. 1) to obtain estimates of $Kd_{1:1}$ and $Kd_{1:2}$ (Table 3.1), giving an R^2 of 0.998. Single site models were also trialled, however the quality of the fit to this model was poor with a non-random distribution of residuals and $R^2 < 0.92$ (data not shown). To determine if alternative isoforms of APP had different binding affinities to holo-Lf, the larger sAPPα isoforms sAPP751 and sAPP770, which are preferentially expressed in the periphery were also examined. In the presence of equimolar holo-Lf, all three isoforms produced similar bimodal c(S) distributions with maxima at approximately 4 S and 7 S (Figure 3.1C) indicating that the additional domains present in the larger APP isoforms did not alter the interaction with Lf.

To investigate the interaction of APP with apo-Lf, the sedimentation behaviour of apo-Lf was analysed in the presence of sAPP695. The unbound-iron did not affect the rate of sedimentation of apo-Lf alone, giving a very similar

sedimentation distribution to that of holo-Lf. Mixing apo-Lf with sAPP695 at a 1:1 or 5:1 molar ratio resulted in a bimodal distribution with modal sedimentation coefficients of 3.95 S and 5.0 S (Figure 3.1D), which correspond to the modal sedimentation values of APP alone and apo-Lf alone, respectively. This indicates that there is no significant interaction between these two molecules in the absence of iron.

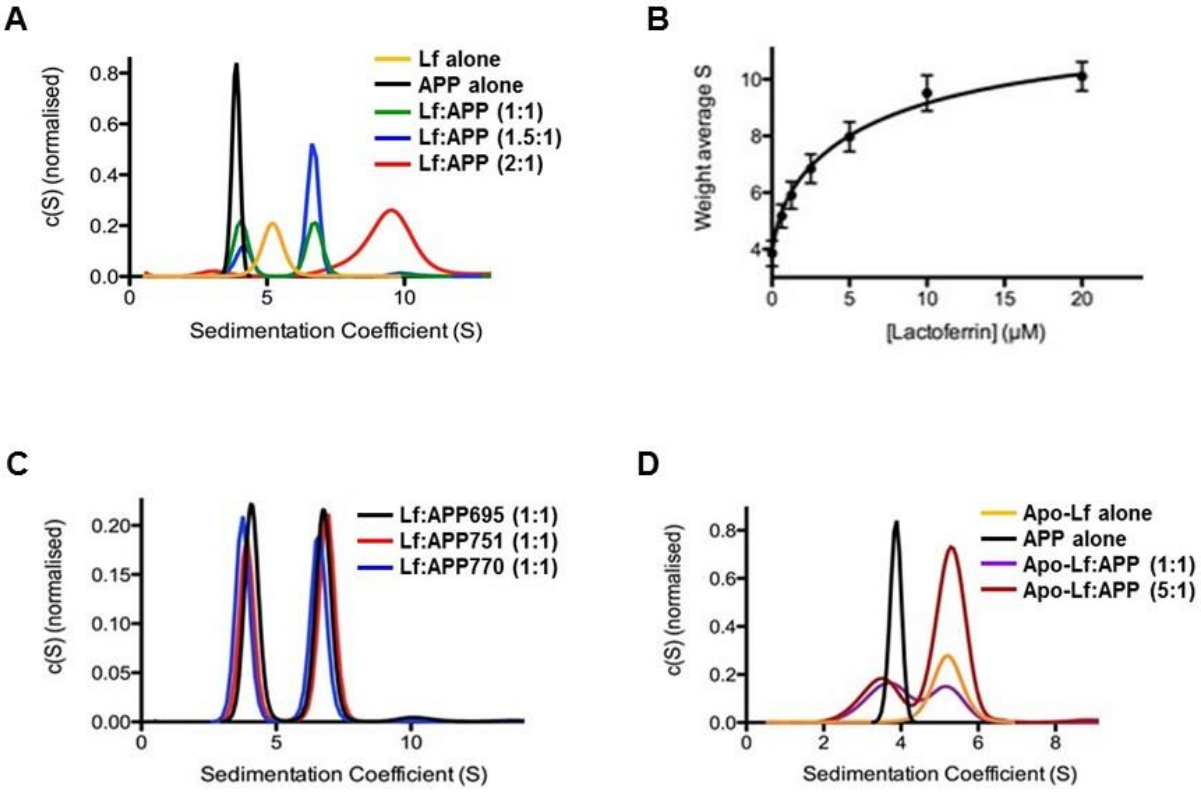

Figure 3.1. Biophysical interaction of Lf with APP via sedimentation velocity. (A) Sedimentation coefficient distributions of holo-Lf alone (5 μM; orange) and APP (2.5 μM) in the absence (black) and presence of holo-Lf (green: 2.5 μM; blue: 3.75 μM; red: 5 μM). The c(S) distributions indicate two different complexes which form in a concentration dependent manner. (**B)** The weight average sedimentation coefficient obtained by integrating the c(S) distribution as a function of Lf concentration. Data was analysed using Eq. 1 found in Appendix I, with the assumption that APP contains two binding sites for Lf with two different dissociation constants. **(C)** Sedimentation coefficient distributions of APP695 (black), APP751 (red) and APP770 (blue) (2.5 μM) in the presence of holo-Lf (2.5 μM). **(D)** Sedimentation velocity analysis of apo-Lf alone (2.5 μM; orange) and APP (2.5 μM) in the absence (black) and presence of apo-Lf (purple: 2.5 μM; maroon: 12.5 μM). Data are means of 3 experiments performed in triplicate. **Sedimentation velocity experiments were performed by Dr Tim Ryan (The University of Melbourne, Australia).**

3.2.2 Intrinsic fluorescence analysis of the interaction between Lf and APP

The interaction of sAPP695 with holo-Lf was investigated further using intrinsic tryptophan fluorescence spectroscopy. Fluorescence spectra (Figure 3.2A) showed that the tryptophan fluorescence intensity of sAPP695 in the presence of an excess of holo-Lf was approximately 1.15 fold greater than the simple addition of the tryptophan fluorescence spectra of these two macromolecules. In addition, while the maxima of the 2 spectra are not significantly different, the spectrum of the mixture of sAPP695 and holo-Lf is more intense in the longer wavelength region than that of the addition spectra of the two macromolecules (Figure 3.2B), indicating that there is a blue shift in one or more of the 15 tryptophan residues present in these macromolecules. This increased sharpening and fluorescence intensity suggests that at least one of these residues is being protected from solvent as part of this interaction. The change in fluorescence intensity as a function of Lf concentration is presented in Figure 3.2C. While a single site model could fit the data (R^2 of 0.97) a better fit was obtained using a 2-site model (R^2 = 0.99), giving estimates of $Kd_{1:1}$ and $Kd_{1:2}$ that were in accordance with those obtained from sedimentation analysis (Table 3.1).

Similar results in both intrinsic fluorescence and sedimentation velocity analyses were obtained with bovine Lf (data not shown).

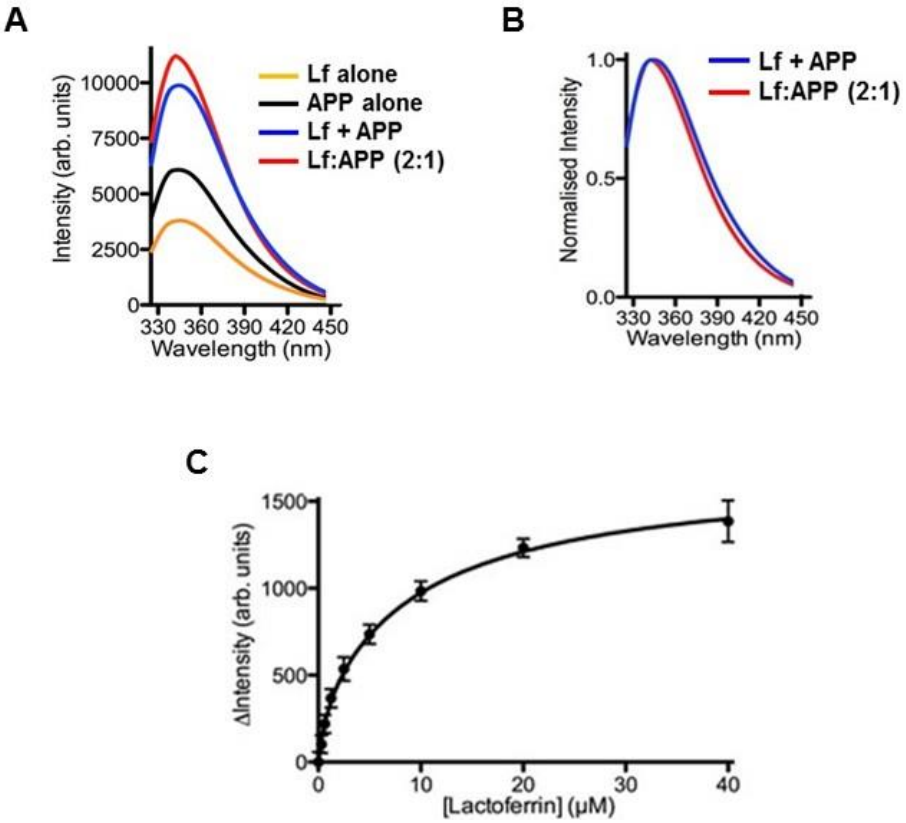

Figure 3.2. Confirmation of biophysical interaction of APP with Lf via fluorescence spectroscopy. (A) Tryptophan fluorescence spectra were acquired using an excitation wavelength of 295 nm for APP alone (2.5 μM) (black), holo-Lf alone (5 μM) (orange) and a mixture of APP and holo-Lf (2.5 μM and 5 μM, respectively) (red). To determine the total expected intensity an addition spectrum of APP alone and holo-Lf alone spectra was also calculated (blue). **(B)** Normalised spectra for the addition spectrum (blue) and the spectra of the APP and Lf mixture (red). **(C)** The difference in fluorescence intensity between the addition spectrum and the spectra of the mixture of APP and Lf plotted as a function of Lf concentration. The data were analysed according to Eq. 2 (Appendix I) assuming a 2-site model with two different dissociation constants. Data are means of 3 experiments performed in triplicate. **Fluorescence spectroscopy experiments were carried out by Dr Bruce Wong (The University of Melbourne, Australia).**

Table 3.1. Dissociation constants determined from sedimentation velocity and fluorescence analysis

	Sedimentation velocity analysis	Fluorescence analysis
$Kd_{1:1}$ (μM)	0.62	0.69
$Kd_{1:2}$ (μM)	8.2	9.4

3.2.3 Identification of APP binding sites for holo-Lf

A peptide array of 15-mer APP peptides, each with a 5 αα overlap covering the full length human APP770 sequence was prepared by using the Spot technique and then tested for reactivity with purified holo-Lf (1 μg/ml; 24 hours). In comparison to apo-Lf (Figure 3.3B), anti-Lf primary (Figure 3.3C) and anti-rabbit (Figure 3.3D) secondary antibody treatment controls, we identified five reactive sequences that bound to holo-Lf (Figure 3.3A). Peptide 49 (QAVPPRPRHVFNMLK), corresponding to region 481-495 of the APP770 sequence, showed to be most reactive. This was followed by peptide 40 (FQKAKERLEAKHRER), located at 391-405 of APP770, peptide 55 (MNQSLSLLYNVPAVA), located at 541-555 of APP770, and finally peptide 50 (FNMLKKYVRAEQKDR) and 48 (LALENYITALQAVPP), corresponding to regions 491-505 and 471-485 of APP770 respectively (Figure 3.3E). These regions were mapped and located within the α-helix rich E2 domain of APP (Figure 3.3F & G). Since our *in vitro* biophysical studies indicate holo-Lf to interact with APP in a 2:1 ratio (Table 3.1), these results suggest that the amino acid sequence of peptide 49 and the flanking peptides 48 and 50 could be the predominant interacting site for holo-Lf, whilst the second interacting site contains the amino acid sequence of either peptide 40 or 55.

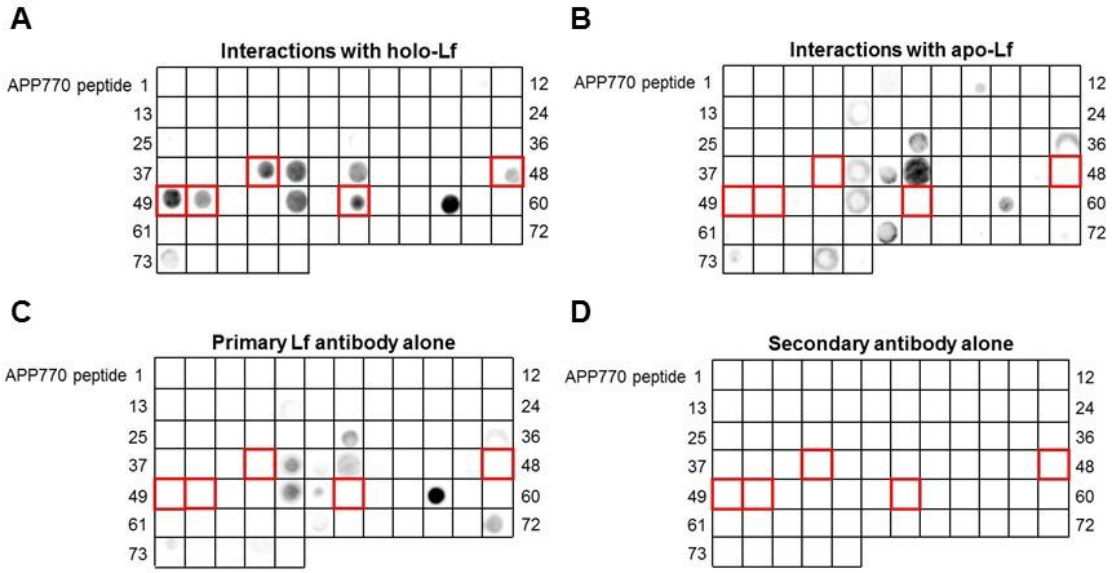

E

APP770 peptide #	Sequence	Reactivity*	Sequence localisation
40	FQKAKERLEAKHRER	++	391-405
48	LALENYITALQAVPP	+	471-485
49	QAVPPRPRHVFNMLK	+++	481-495
50	FNMLKKYVRAEQKDR	+	491-505
55	MNQSLSLLYNVPAVA	++	541-555

Peptide reactivity was determined by visual observation: +++ strong, ++ moderate, + weak reactivity

F

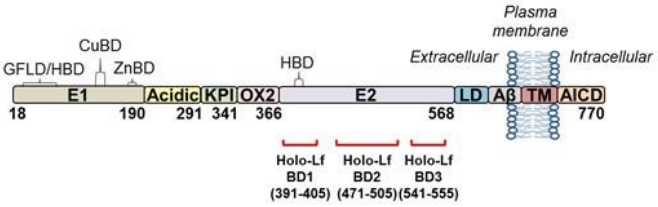

G

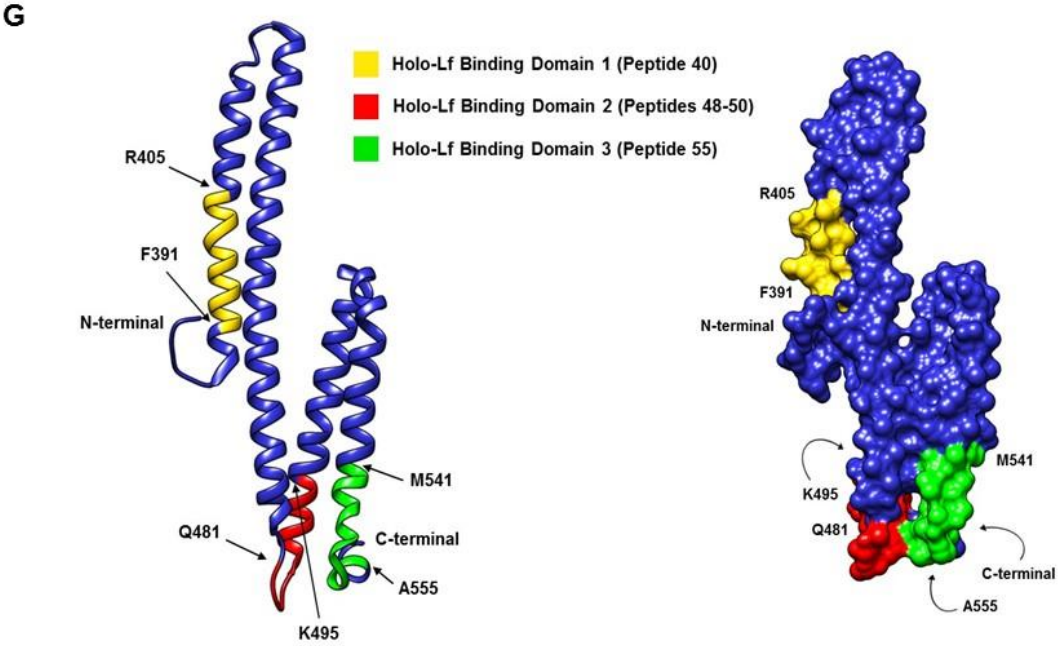

Figure 3.3. Holo-Lf binds to the E2 domain of APP. Peptide array consisting of 15-mer peptides with a 5 αα overlap covering the full length APP770 protein were custom synthesised on a cellulose membrane by the Spot technique. **(A)** APP peptide reactivity was revealed by incubation with 1 µg/ml holo-Lf for 24 hours. APP peptides 40, 48, 49, 50 and 55 (highlighted in red squares) correspond to sequences specific for holo-Lf binding which did not cross-react with **(B)** apo-Lf (1 µg/ml), **(C)** anti-Lf primary antibody alone (1:500), or **(D)** anti-rabbit secondary antibody alone (1:5000) treatment controls. The corresponding sequence and reactivity of each minimal motif is indicated in **(E)**. Peptide reactivity was scored by visual observation as: +++ strong, ++ moderate, + weak reactivity. **(F)** Schematic representation of the multiple subdomains of full length APP770 highlighting the interactive binding sites within the E2 domain for holo-Lf binding (red bars). Highlighted in black numbering below the schematic diagram indicates amino acid sequence (18-770). **(G)** The colour blue represents the structure and surface representation of the APP-E2 domain (PDB code 3NYJ) from the N- to the C-terminus. Peptide 40 corresponding to residues 391-405 (FQKAKERLEAKHRER), residing in domain 1 is shown in yellow. Peptides 48-50 corresponding to residues 471-505 incorporates three overlapping binding motifs (LALENYITALQAVPP; QAVPPRPRHVFNMLK; and FNMLKKYVRAEQKDR), residing in domain 2, shown in red. Peptide 55 corresponding to residues 541-555 (MNQSLSLLYNVPAVA), residing in domain 3 is shown in green. The first and last amino acid letter code along with the starting and ending residue number (according to **(E)**) for each respective binding site is labelled in black.

3.2.4 In vivo confirmation of the interaction between Lf and APP

To determine whether the interaction between Lf and APP occurred *in vivo*, immunoprecipitation of mouse brain extracts was performed. Lf was captured using an anti-Lf antibody bound to protein G agarose beads. APP was prominently co-captured with Lf immunoprecipitated from brain tissue, as detected by Western blot using a monoclonal antibody to the N-terminal of APP (Figure 3.4). As expected for an iron-related interaction, APP co-elution with Lf was exaggerated in mice fed a high-iron diet. Specificity of the interaction was confirmed when no APP was detected in Lf immunoprecipitation from brain of APPKO mice (Figure 3.4).

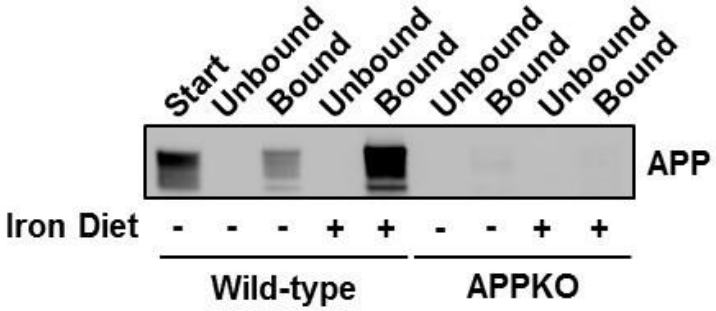

Figure 3.4. Demonstration of *in vivo* interaction between Lf and APP. Confirmation of an interaction of APP with Lf *in vivo* using anti-APP for detection (analysed by Western Blot) and anti-Lf for immunoprecipitation of brain homogenates from 12 month old APPKO mice and littermate controls either on a normal or high iron diet. The 'unbound' refers to the starting material ('start') remaining after separation from the agarose beads, and the 'bound' fraction refers to the eluted protein. Each immunoprecipitation for an individual mouse was performed on six different mouse brains (n = 6) from each mouse line. **Preparation of mouse brain homogenates followed by immunoprecipitation of Lf with APP was performed by Dr Bruce Wong (The University of Melbourne, Australia).**

3.2.5 LRP1 is not involved in the interaction between holo-Lf and APP

Immunoprecipitation was performed on SH-SY5Y cells treated with holo-Lf (500 nM; 2 hours) to determine whether the interaction between Lf and APP involved LRP1. As expected, anti-LRP1 antibody bound to protein G Dynabeads co-captured APP with LRP1 from non-treated SH-SY5Y cells, detected by Western blot using a monoclonal antibody to the N-terminal of APP. However, in the presence of holo-Lf, APP nor Lf was able to be co-captured with LRP1 (Figure 3.5A). To confirm this finding, immunoprecipitation was performed on SH-SY5Y cells depleted of either APP or LRP1 in the presence of holo-Lf. Cells were treated with control non-target (20 nM), APP (20 nM) or LRP1 (20 nM) RNAi followed by incubation of holo-Lf to media (500 nM; 2 hours). Antibodies targeting APP (22C11) or LRP1 confirmed knockdown in respective APP and LRP1 RNAi treated cells (Figure 3.5B). In the presence of holo-Lf, anti-Lf bound to protein G Dynabeads co-captured APP with Lf but not LRP1 in SH-SY5Y cells expressing both APP and LRP1. Only when endogenous APP was silenced did anti-Lf bound to protein G Dynabeads co-capture LRP1 with Lf. Specificity of the interaction was confirmed when no APP, Lf or LRP1 was immunoprecipitated when using anti-β-actin as the capture antibody (-ve) (Figure 3.5). Taken together, these results not only suggest that LRP1 is not involved in the interaction between Lf and APP, but Lf preferentially binds APP over LRP1.

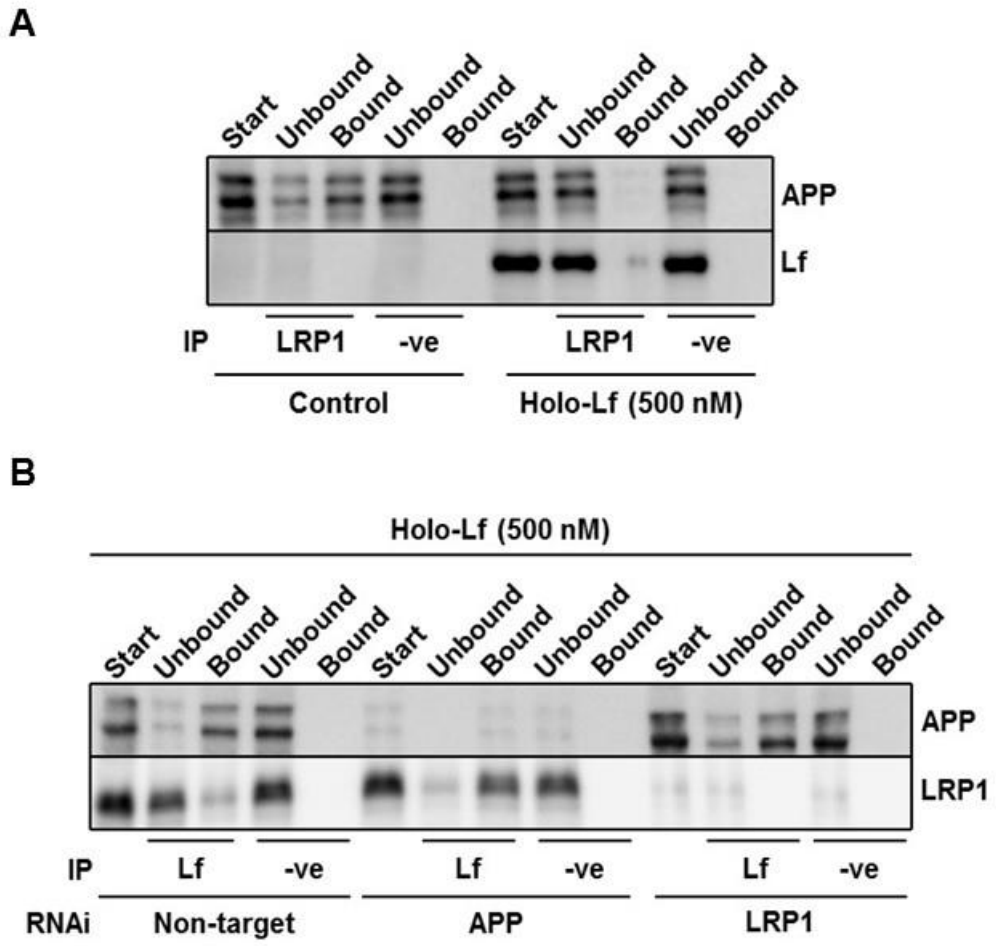

Figure 3.5. Holo-Lf preferentially binds APP over LRP1. To examine whether LRP1 is involved in the interaction between holo-Lf and APP, immunoprecipitation of LRP1 or Lf was carried out on SH-SY5Y cells in the presence and absence of holo-Lf. SH-SY5Y cells were treated with **(A)** ± holo-Lf (500 nM; 2 hours) or transfected with **(B)** control non-target, APP or LRP1 RNAi (20 nM; 48 hours) followed by holo-Lf treatment (500 nM; 2 hours). LRP1 or Lf was immunoprecipitated using **(A)** anti-LRP1 or **(B)** anti-Lf antibody followed by Western blot analysis. Anti-β-actin (-ve) was used to confirm antibody selectivity. The 'unbound' refers to the starting material ('start') remaining after separation from the protein G Dynabeads, and the 'bound' fraction refers to the eluted protein. Immunoprecipitation experiments were performed in duplicate on two separate occasions.

3.3 Discussion

In the present chapter, we describe the ability of Lf to form a complex with APP *in vitro* and *in vivo*. Further characterisation revealed the binding affinity of APP with Lf to be selective as only the holo form (iron bound) of Lf interacted with APP. No binding was evident with the apo form (iron unbound) of Lf. The E2 region of APP was identified as the minimal binding domain for Lf and through a series of biophysical techniques, the affinity of holo-Lf for APP was observed to be comparable to that of another previously reported interaction of Lf with the copper-carrying ferroxidase protein Cp (Ha-Duong et al., 2010; White et al., 2012). Furthermore, despite evidence demonstrating LRP1 as a common binding partner, it was found not to be involved in the interaction between Lf and APP.

The binding affinity and ratio of Lf with APP ($Kd_{1:1}$ ~ 0.6 μM and $Kd_{1:2}$ ~ 8.2 μM) (Table 3.1) obtained from sedimentation velocity (Figure 3.1A & B) and intrinsic fluorescence (Figure 3.2) analysis closely matched the affinity of Lf to another iron regulatory protein; the copper-carrying ferroxidase enzyme Cp (11.0 μM and 1.5 μM) (Ha-Duong et al., 2010). Studies revealed Lf to complex with and increase the ferroxidase activity of Cp for the incorporation of oxidised iron into Lf (Sokolov et al., 2005), possibly accounting for Lf's role in iron sequestration (Legrand et al., 2005). The dissociation of Cp with Lf can occur through a number of conditions including high salt and low pH which suggests an ionic interaction more than a conformational change in either protein (Ha-Duong et al., 2010; Pulina et al., 2002; Sokolov et al., 2006). This is also possibly reflected by the large difference in pI's between the two proteins (8.6 for Lf; 4.5 for Cp) (Sokolov et al., 2005). APP has a comparably low pI to Cp (ranging from 4.0-4.5) (Simons et al., 1995) and thus may similarly interact with Lf through the positively charged N-lobe (Sabatucci et al., 2007). However, APP is unlikely to require the arginine positive cluster within the N-lobe reportedly involved in the interaction with Cp (Pulina et al., 2002; Sokolov et al., 2006), as it interacted with both bovine and human Lf, and only human Lf contains this motif (Sinha et al., 2013).

The additional domains found in the larger isoforms of APP did not alter the interaction with Lf (Figure 3.1C), meaning that the APP interactive sites for holo-Lf binding must be in a region associated with all three isoforms. An array of APP peptides representing the full length sequence of APP770 allowed the

identification of the regions for holo-Lf interaction (Figure 3.3A-D). We identified the minimal binding interactive sites of APP for Lf to be located within the rigidly folded, highly conserved E2 extracellular domain (Figure 3.3F) (Coburger et al., 2013), a region known to contain several negatively charged residues (Wang and Ha, 2004). The peptide library revealed peptide sequence QAVPPRPRHVFNMLK (peptide 49) to be most reactive to holo-Lf (Figure 3.3E). The flanking peptide sequences LALENYITALQAVPP (peptide 48) and FNMLKKYVRAEQKDR (peptide 50) also showed detectable reactivity to holo-Lf (Figure 3.3E). Since each peptide was identical with the previous peptide in 5 out of 15 residues, we speculated that the minimal reactivity observed with peptides 48 and 50 was due to the overlapping sequence associated with peptide 49. Therefore, we assumed that amino acids within peptide 49 but also 48 or 50 formed the dominant interactive site for holo-Lf. In addition, two other APP 15-mer sequences were shown to be reactive to holo-Lf, peptides 40 (FQKAKERLEAKHRER) and 55 (MNQSLSLLYNVPAVA) (Figure 3.3E). In an effort to understand in more detail the location and proximity each interactive site had to one another, the binding sites were mapped on a surface representation of the APP E2 structure (Figure 3.3G). We found the APP binding site encompassing peptide 40 to be isolated from the 49 and 55 sites, with these latter sites being in very close proximity to each other (Figure 3.3G). Since our *in vitro* biophysical studies indicate holo-Lf to interact with APP in a 2:1 ratio (Table 3.1), there are a number of possible binding scenarios available. Whilst the most likely scenario involves site 40 forming one binding region while 49 and 55 forming another, without knowing how these proteins interact in their native structure, this remains speculative. What also requires further investigation is whether the entire 15-mer sequence of each peptide or merely just a few residues of APP are required for holo-Lf to bind to the associated E2 region. Further inspection of the properties of the amino acids encompassing each binding site identifies that peptide 49 mostly contains hydrophobic residues (A, L, M, F, V, P), peptide 40 predominantly has charged residues (R, K, D, E) and peptide 55 contains mostly neutral uncharged polar residues (Q, N, H, S). Hydrophobic residues are typically not involved in conformational changes upon ligand binding (Ruvinsky et al., 2012), while accessible charged and polar residues exposed on the protein interface are beneficial for ligand binding (Ruvinsky et al., 2012; Zhao et al., 2011). Therefore, the interactive site of peptide 49 may act to stabilise the binding

once the interactive binding motif of holo-Lf is bound to the associated APP-E2 region. It must be noted that these observations on the possible binding arrangements between APP and holo-Lf are merely assumptions and are in no way definitive. Therefore, structural studies are warranted to not only determine the potential binding pockets and specific residues needed for holo-Lf binding, but also determine how the conformational shape of each protein contours and aligns itself for binding to the interactive sites proposed in this study.

Only the iron saturated holo form of Lf interacted with APP whereas no interaction was evident with apo-Lf (Figure 3.1D & Figure 3.3B). The diverse range of iron-independent roles for Lf may originate from the large conformational differences between apo-Lf and holo-Lf. Based on structure analysis, apo-Lf has an 'open' conformation whereas holo-Lf mainly has a compact 'closed' conformation (Grossmann et al., 1992; Jameson et al., 1998). These alterations in structure are believed to lead to the exposure of different binding sites and may cause alternative binding partners to interact with the different Lf forms. The APP interaction with Lf only in the presence of iron would be consistent with a role for Lf in iron export, but it must be noted that APP may still also be indirectly important for the other functions of apo-Lf via its ability to mediate the location of holo-Lf within the body. Notably, APPKO mice have previously been shown to have a significant impairment in immuno-response to infection and inflammation compared to their wild-type littermates (Puig et al., 2012), characteristics which Lf knockout (LfKO) mice also feature (Velusamy et al., 2013; Ward and Conneely, 2004).

Studies on APP-deficient mouse tissue signified that the interaction between Lf and APP occurred *in vivo* (Figure 3.4), demonstrating a physiological relevance. Supporting previous observations on the similar location of APP and Lf in the brain (Kawamata et al., 1993), anti-Lf co-immunoprecipitated with APP in wild-type mouse brain tissue and responded accordingly in mice fed on a high iron diet (Figure 3.4). This increase in iron load is known to drive rapid APP translation via the IRE of APP mRNA (Rogers et al., 2002) and is also likely to upregulate Lf expression in order to control the level of free iron via the formation of iron bound holo-Lf (Rosa et al., 2017; Wang et al., 2005). An age dependent accumulation in Lf has been observed in human brain, which is elevated in regions affected by AD and in APP transgenic models of AD (Kawamata et al., 1993; Wang et al.,

2010). The study conducted by Kawamata *et al* also revealed increased Lf expression within neurons and glia in affected AD brain tissue (Kawamata et al., 1993). Our data could explain the co-localisation of Lf and APP in the enlarged granules observed by the authors, who originally attributed this finding to the variety of functional roles Lf encompasses in association with the innate immune response involved in AD (Kawamata et al., 1993).

Despite evidence of a direct interaction between Lf and APP *in vitro* and *in vivo*, it is yet to be identified whether holo-Lf and APP form part of a multi-complex with a third component. Multiple studies have shown Lf (Grey et al., 2004; Vash et al., 1998) and APP (Pietrzik et al., 2002; Rushworth et al., 2013) to interact with the ubiquitously expressed multifunctional cell surface receptor LRP1. Confirming previous reports, we showed APP to interact with LRP1 in the absence of holo-Lf (Figure 3.5A). However, in the presence of holo-Lf, no binding occurred between LRP1 and APP (Figure 3.5). In APP depleted cells, an interaction between holo-Lf and LRP1 was evident, while in LRP1 depleted cells, holo-Lf still bound to APP (Figure 3.5B). These results indicate that holo-Lf preferentially binds APP over LRP1 and that LRP1 is not required for the interaction between APP and holo-Lf. After an extensive literature search, the binding affinity between Lf and LRP1 could not be found, but it is feasible to assume the binding affinity between holo-Lf and APP ($Kd_{1:1}$ ~ 0.6 μM) (Table 3.1) is greater than that of holo-Lf and LRP1. This could have potential implications on the signalling pathways previously associated with LRP1 and Lf. Various studies have shown specific ligands to directly bind cell surface LRP1 to initiate intracellular cell signalling (Boucher et al., 2003; Shi et al., 2009; Webb et al., 2001; Zilberberg et al., 2004). For instance, Qiu *et al* showed treatment of the LRP1 ligand α2-M to primary neurons increased LRP1 expression and stimulated neurite outgrowth through the mitogen-activated protein (MAP) extracellular signal-regulated kinases 1 and 2 (ERK1/2) signalling pathway (Qiu et al., 2004). The fact that the addition of RAP, an LRP1 antagonist, could prevent α2-M from binding to LRP1 (Mantuano et al., 2008; Qiu et al., 2004; Strickland et al., 2002) implies a functional role for LRP1 in cell signalling. However, the resulting responses from LRP1 mediated MAP/ERK cell signalling may be dependent on the type of ligand and co-receptor expressed by the particular cell (Bacskai et al., 2000; May et al., 2004; Stiles et al., 2013). For example, Wan *et al* showed that through MAP/ERK1/2 signalling

N-methyl-D-aspartate (NMDA) receptors activate ADAM10 expression, one of the several proteases that exhibit α-secretase activity (Wan et al., 2012). Furthermore, Mantuano *et al* exhibited a NMDA multi-receptor complex with Trk that interacted with LRP1 through ligands α2-M and the tissue-type plasminogen activator (tPA) to induce MAP/ERK1/2 signalling (Mantuano et al., 2013). The activation and expression of ADAM10 by MAP/ERK1/2 signalling is able to cleave cell surface LRP1 to release soluble LRP1 (sLRP1) into the extracellular space (Liu et al., 2009; Quinn et al., 1997; Selvais et al., 2011) which can transport Aβ across the blood brain barrier (BBB), an important mechanism in Aβ clearance within the brain (Deane et al., 2004a; Sagare et al., 2007; Shibata et al., 2000). However, sLRP1 is also pro-inflammatory and can induce microglial activation (Brifault et al., 2017). Lf is synthesised and released by activated microglia (Fillebeen et al., 2001; Wang et al., 2015) and can also act as an LRP1 antagonist, binding cell surface LRP1 to block ERK signalling and therefore limit sLRP1 production (Laporte et al., 2004; Mantuano et al., 2016; Mantuano et al., 2013). This could possibly be a potential mechanism of Lf whereby binding to LRP1 and preventing sLRP1 production may downregulate microglial activation and lessen the inflammatory response. In chronic neuroinflammatory diseases such as AD (Zhang and Jiang, 2015), there is a reduction in sLRP1 and an increase in oxidised sLRP1 (Sagare et al., 2007; Sagare et al., 2011), rendering sLRP1 incapable of clearing Aβ through the BBB (Deane et al., 2008; E Donahue et al., 2006; Jeynes and Provias, 2008). Therefore, the preference of Lf binding to APP over LRP1 could be a contributing factor to the chronic inflammation and defected Aβ clearance by LRP1 observed in AD.

Even though LRP1 was not involved in the complex formation of APP and holo-Lf, there is still the possibility of another binding partner being involved in the interaction. One such example could be the ubiquitously expressed LfR (Suzuki et al., 2005). Like holo-Tf, holo-Lf also interacts with its cell surface receptor (LfR) and internalises into the cell via receptor mediated endocytosis (Dautry-Varsat et al., 1983; Jiang et al., 2011); a similar internalisation mechanism to APP (Cossec et al., 2010). Therefore, further investigation is required to identify whether the LfR is involved in the interaction between APP and holo-Lf.

Taken together, our results describe iron-bound holo-Lf as a novel binding partner to APP. The interacting regions of APP for holo-Lf binding were also determined.

However, complementary studies to determine the specific binding sites on holo-Lf for APP is also required. Determination of the structure of the APP and holo-Lf complex (via X-ray crystallography) is also warranted since the peptide library used to identify the interactive binding sites of APP were synthesised as short linear peptides and thus unobstructed by the proteins conformational shape. Since both the E2 portion of APP (Lee et al., 2011b) and holo-Lf (Haridas et al., 1995) have previously been crystallised individually, the probability of establishing a crystallised structure of the complex is high. Together, these approaches will reveal the structural basis for the interaction between holo-Lf and APP. The investigation of the downstream implications of this interaction in a cellular model and its AD-related significance will be further explored.

CHAPTER 4.0 HOLO-LF PROMOTES APP INTERNALISATION THROUGH AN ARF6-DEPENDENT PATHWAY TO RAB11 RECYCLING COMPARTMENTS

4.1 Introduction

Once synthesised, APP is trafficked through the constitutive secretory pathway to a functional location on the plasma membrane (Lai et al., 1995; Lyckman et al., 1998; Wong et al., 2014b). Cell surface APP may be cleaved by α-secretase (Koo et al., 1996) or be rapidly endocytosed due to the presence of the cytoplasmic YENPTY internalisation motif where it can be either amyloidogenically processed, recycled or degraded (Yamazaki et al., 1996).

By manipulating cell membrane cholesterol levels in addition to proteins required for endocytosis, studies have indicated APP internalisation to be a cholesterol (Ehehalt et al., 2003) and clathrin-dependent process requiring dynamin for the budding and scission of clathrin-coated vesicles from the cell membrane (Motley et al., 2003). The silencing of clathrin heavy chain (Koo and Squazzo, 1994) or reduction of membrane cholesterol levels via MβCD treatment (Cossec et al., 2010) prevents APP internalisation and results in an accumulation of APP on the cell surface.

The endocytosis of Lf is not very well established but there has been some evidence to suggest Lf internalises into the cell in a similar way to APP. Jiang *et al* showed a significant decrease in the uptake of radiolabelled Lf upon clathrin suppression (Jiang et al., 2011), while Florian *et al* demonstrated a lack of internalised Lf into the cell with MβCD treatment (Florian et al., 2012). These findings indicate clathrin and cholesterol, respectively, are required for Lf endocytosis.

Surface presented proteins can also be internalised by a variety of mechanisms that are clathrin-independent. For example, BACE1 responsible for APP β-cleavage undergoes a clathrin-independent process requiring the endocytic trafficking regulator ARF6. Reducing ARF6 prevents BACE1 internalisation, thereby hindering the amyloidogenic pathway of APP (Sannerud et al., 2011).

The trafficking of APP to the various intracellular compartments involves the participation of Rab GTPase endocytic regulators (Somsel Rodman and Wandinger-Ness, 2000). Rab5, Rab7, and Rab11 are major Rab GTPases associated with early (Bucci et al., 1992), late (Feng et al., 1995) and recycling (Takahashi et al., 2012) endosomes respectively. Exploiting the APP sorting and trafficking pathways has a profound effect on the cellular location of APP and therefore its metabolism. For example, by transiently transfecting Rab5 into APP overexpressing cells, Grbovic *et al* exhibited an increase in APP endocytosis which resulted in enlarged Rab5-positive early endosomes (Grbovic et al., 2003), a morphological feature commonly observed in neurons from *post mortem* sporadic AD brain tissue (Cataldo et al., 2004; Ginsberg et al., 2010b; Laifenfeld et al., 2007; Thinakaran and Koo, 2008). This also led to increased amyloidogenic processing of APP, resulting in increased Aβ generation (Grbovic et al., 2003).

In the present chapter, we further explored the relationship between holo-Lf and APP and found holo-Lf to internalise APP from the cell surface in a receptor mediated pathway. The internalisation route of Lf and APP was determined by manipulating the major proteins and cellular components required for clathrin-dependent and independent internalisation. The precise intracellular location within the endosomal system of Lf and APP after internalisation was also determined by manipulating some of the major Rab GTPases involved in the various APP trafficking pathways (Kiral et al., 2018). Data within this chapter provides a critical insight into the cellular mechanism of holo-Lf mediated internalisation and trafficking of APP.

4.2 Results

4.2.1 Holo-Lf decreases APP levels on the cell surface

Cell surface presented APP was measured by FACS in SH-SY5Y cells treated with iron bound holo-Lf and holo-Tf. Holo-Tf was investigated as a control to determine the specificity of the interaction observed with Lf. The iron-unbound (apo) isoforms of Lf and Tf were additional controls tested in this technique. SH-SY5Y cells were incubated for 2 hours with holo-Lf, apo-Lf, holo-Tf, and apo-Tf at either 37°C or 4°C. At physiological temperature (37°C), treatment with holo-Lf decreased surface levels of APP ($p < 0.0001$) (Figure 4.1A). However, there was no evidence of a change in cell surface APP with the addition of apo-Lf, apo-Tf or holo-Tf (Figure 4.1A). This observation was confirmed to be through energy dependent endocytosis (Peterson et al., 2007) by reducing the temperature to 4°C and inhibiting holo-Lf changes to cell surface APP expression levels (Figure 4.1B).

Cell surface APP levels in SH-SY5Y cells with holo-Lf treatment (500 nM; 2 hours) was also analysed by surface biotinylation. In support to Figure 4.1A, there was a significant reduction of cell surface APP in SH-SY5Y cells in the presence of holo-Lf ($p < 0.0001$) (Figure 4.2A). An increase in cell surface APP with holo-Tf treatment (500 nM; 2 hours) was also evident ($p < 0.05$) (Figure 4.2A). Changes in cell surface APP levels observed with holo-Lf was detected and confirmed in primary murine neurons by surface biotinylation. Holo-Lf altered the location of APP in the neuron, resulting in reduced neuronal surface APP ($p < 0.0001$), whereas treatment with holo-Tf remained unchanged (Figure 4.2B).

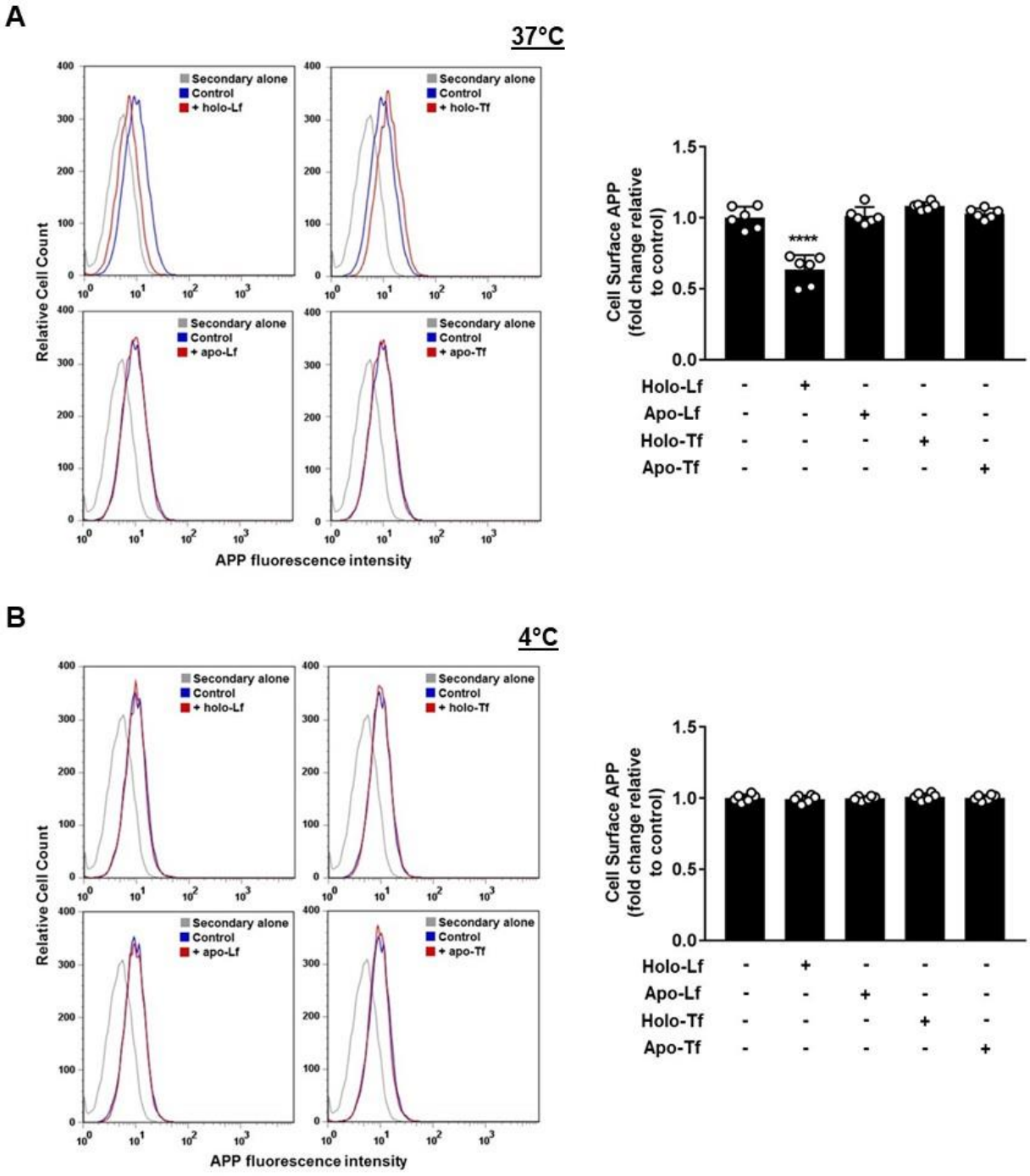

Figure 4.1. Holo-Lf decreases APP levels on the cell surface via an endocytic pathway. FACS was performed to measure APP levels on the cell surface of non-permeabilised SH-SY5Y cells after a 2 hour incubation with 500 nM holo-Lf, apo-Lf, holo-Tf and apo-Tf at either **(A)** 37°C or **(B)** 4°C using ab15272 to recognise N-terminal extracellular epitopes of APP. Data are means ± SE of 3 experiments performed in duplicate. Quantified histogram data depict fold change compared to non-treated control cells, * $p < 0.05$ and **** $p < 0.0001$.

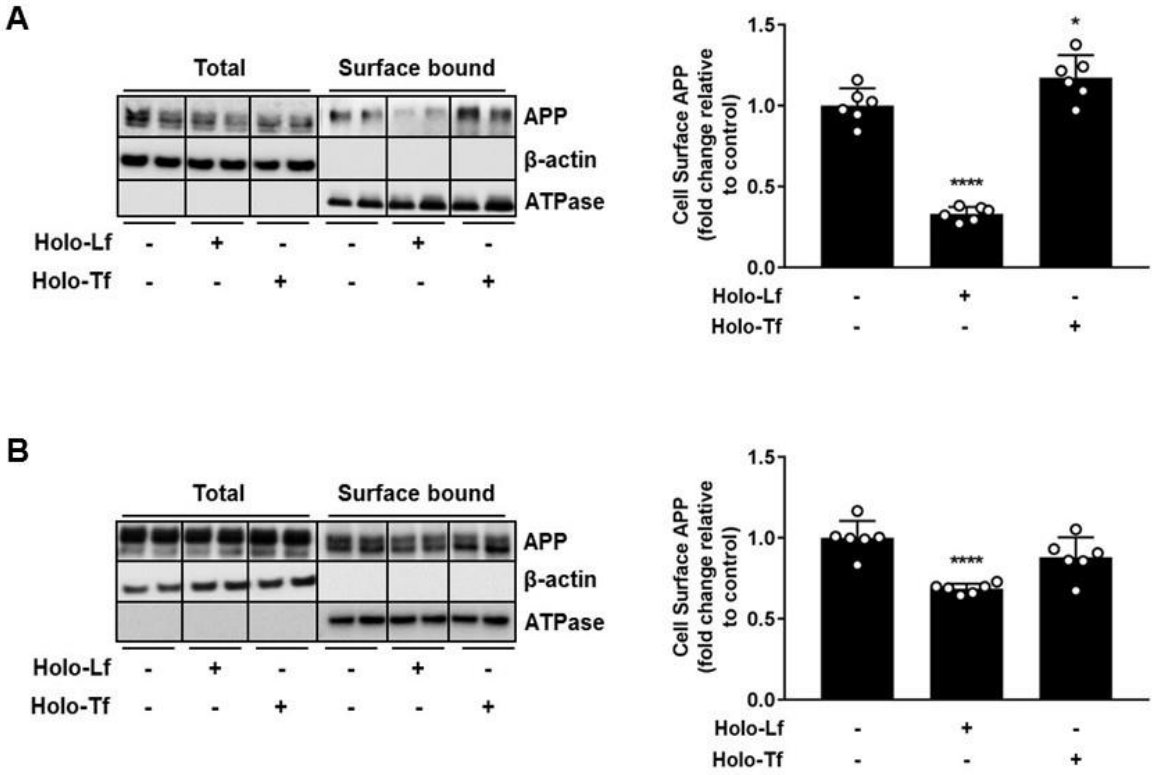

Figure 4.2. Confirmation that iron bound Lf decreases cell surface APP levels. APP location was examined in **(A)** SH-SY5Y cells and **(B)** primary murine neuronal cultures treated with holo-Lf (500 nM) and holo-Tf (500 nM) for 2 hours. Cell surface proteins on **(A)** SH-SY5Y cells and **(B)** primary neurons were biotinylated to identify changes to APP expression on the cell surface. Total and surface labelled APP were analysed by Western blot. Cell surface APP was normalised to Na^+/K^+ ATPase surface protein content. Data are means ± SE of 3 experiments performed in duplicate, * $p < 0.05$ and **** $p < 0.0001$ compared to non-treated control cells. **Preparation and isolation of mouse primary neuronal cultures followed by cell surface biotinylation (Figure 4.1B) was performed by Dr Bruce Wong (The University of Melbourne, Australia).**

4.2.2 Holo-Lf is internalised into SH-SY5Y cells in the presence of APP

The relationship between Lf and APP was further explored by investigating whether Lf internalisation in SH-SY5Y cells is influenced by the presence of APP. Biotinylated holo-Lf (0.5 mg/ml) was added to APP depleted SH-SY5Y cells (RNAi; 20 nM) for 60 minutes at 37°C. Surface biotin was stripped with the impermeable reducing agent MeSNa so that only internalised biotinylated Lf could be detected in the total cell lysate when analysed by Western blot. To examine total biotinylated Lf, MeSNa treatment was omitted. 22C11 antibody was used to confirm APP reduction in APP RNAi treated cells ($p < 0.0001$) and High Sensitivity Streptavidin-HRP was used to detect biotinylated Lf (Figure 4.3). The biotinylated Lf that was detectable in the total cell lysate (termed 'total') which consisted of surface and internalised biotinylated Lf significantly decreased in APP depleted cells ($p < 0.0001$). Cells treated with MeSNa (termed 'internal') signified internalised Lf which decreased when APP was depleted ($p < 0.0001$) (Figure 4.3). The surface fraction (termed 'surface') was calculated by subtracting the internal fraction data means from the total fraction. No significant change was observed between surface biotinylated Lf in cells with and without the presence of APP, symbolising equivalent amounts of biotinylated Lf distributed (Figure 4.3). These results reveal that not only is the internalisation of holo-Lf and APP a receptor mediated event, but APP stimulates holo-Lf internalisation into the cell.

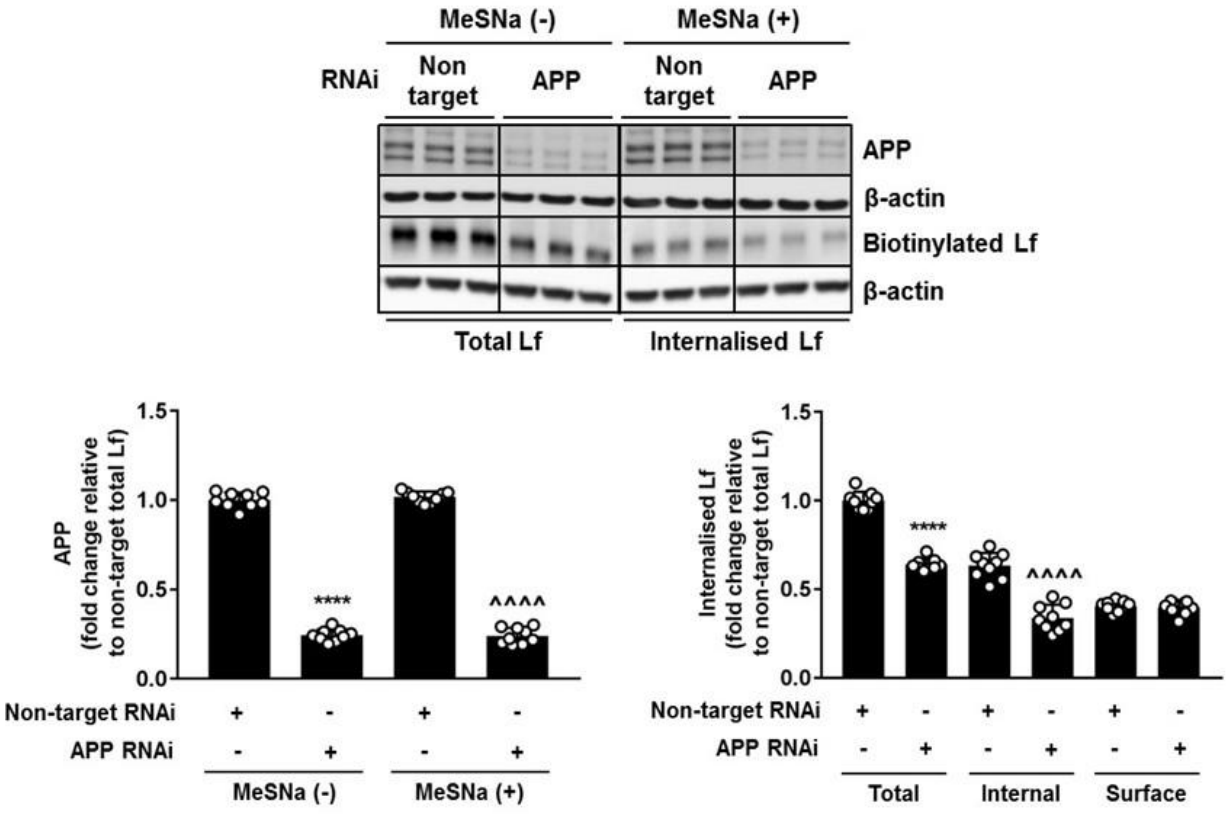

Figure 4.3. Holo-Lf internalisation is reduced by APP knockdown. SH-SY5Y cells were transfected with control non-target and APP RNAi (20 nM) for 48 hours before being subjected to the ligand internalisation assay. Total APP protein expression, total biotinylated holo-Lf (MeSNa (-)) and internalised holo-Lf (MeSNa (+)) were visualised by Western blot. Data are means ± SE of 3 experiments performed in triplicate normalised to β-actin. **** $p < 0.0001$ compared to the non-target total fraction and ^^^^ $p < 0.0001$ compared to the non-target internal fraction. Total fraction represents cell surface and internalised biotinylated Lf (cells without MeSNa treatment), internal fraction represents internalised biotinylated Lf (cells treated with MeSNa), and surface biotinylated Lf fraction was determined by subtracting the internal fraction data means from the total fraction.

4.2.3 Holo-Lf mediated APP endocytosis does not require LRP1

To confirm earlier findings that suggested LRP1 is not required for the interaction between Lf and APP (Chapter 3.2.5), FACS was performed to investigate changes in APP protein expression on the cell surface of LRP1 depleted (RNAi; 20 nM) non-permeabilised SH-SY5Y cells in the presence of holo-Lf (500 nM; 2 hours). In cells without holo-Lf but treated with LRP1 RNAi, surface APP significantly rose ($p < 0.0001$) (Figure 4.4A). However, cell surface APP levels still significantly decreased in LRP1 depleted cells when holo-Lf was added ($p < 0.0001$) (Figure 4.4A). This response to Lf by APP in the absence or presence of LRP1 was similar using the ligand internalisation assay as described in Results 4.2.2. Antibodies targeting APP (22C11) and LRP1 were confirmed by knockdown in APP and LRP1 RNAi treated cells, respectively ($p < 0.0001$) (Figure 4.4B). Whilst cells treated with APP RNAi alone showed a significant decrease in Lf internalisation ($p < 0.0001$), LRP1 depleted cells exhibited an increase ($p < 0.0001$) (Figure 4.4B). Co-transfection with APP and LRP1 RNAi showed a decrease in Lf internalisation, comparable to APP RNAi treated levels, demonstrating that APP mediated holo-Lf internalisation does not require LRP1.

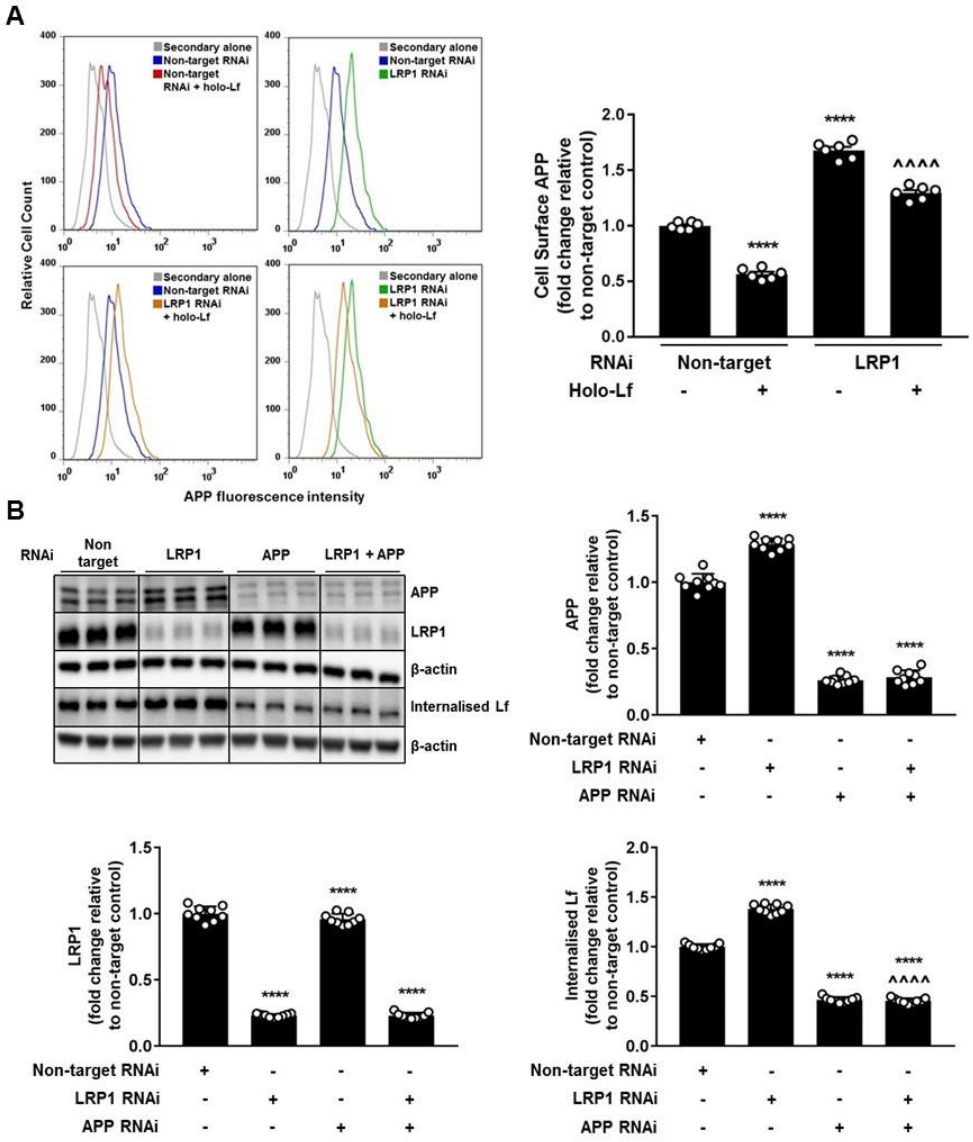

Figure 4.4. Holo-Lf mediated APP internalisation does not require LRP1. (A) Quantification of APP levels on the cell surface of non-permeabilised SH-SY5Y cells after being transfected with control non-target and LRP1 RNAi (20 nM) for 48 hours. Cells were then subjected to a 2 hour incubation with 500 nM holo-Lf. FACS was performed using ab15272 recognising N-terminal extracellular epitopes of APP. **(B)** SH-SY5Y cells were subjected to the ligand internalisation assay after being transfected with control non-target, APP and/or LRP1 RNAi (20 nM; 48 hours). Surface biotin was stripped with MeSNa to detect internalised biotinylated Lf. APP, LRP1 and internalised holo-Lf were visualised by Western blot. Data are means ± SE of 3 experiments performed in **(A)** duplicate and **(B)** triplicate normalised to β-actin. **** $p < 0.0001$ compared to non-target control and ^^^^ $p < 0.0001$ compared to LRP1 RNAi cells.

4.2.4 Depletion of cholesterol by MβCD disrupts holo-Lf mediated APP internalisation

To determine whether APP cell surface expression and holo-Lf mediated APP endocytosis are altered by shifting APP out of the lipid raft region of the cell membrane, cholesterol content in the SH-SY5Y plasma membrane was disrupted. MβCD was used to modify the membrane lipid raft content required for the endocytosis of APP. Amplex Red quantification illustrated that cholesterol was unchanged by the addition of holo-Lf (500 nM; 2 Hours) and confirmed depletion by MβCD (1 mM; 3 hours) ($p < 0.0001$) (Figure 4.5A). Cholesterol depletion caused a significant increase in surface presented APP levels in non-permeabilised SH-SY5Y cells ($p < 0.0001$) which persisted when holo-Lf was introduced (Figure 4.5B). Using the ligand internalisation assay as described in Results 4.2.2, depleting membrane cholesterol in SH-SY5Y cells showed a significant decrease in Lf internalisation ($p < 0.0001$) (Figure 4.5C), suggesting that holo-Lf and APP endocytosis are both cholesterol-dependent.

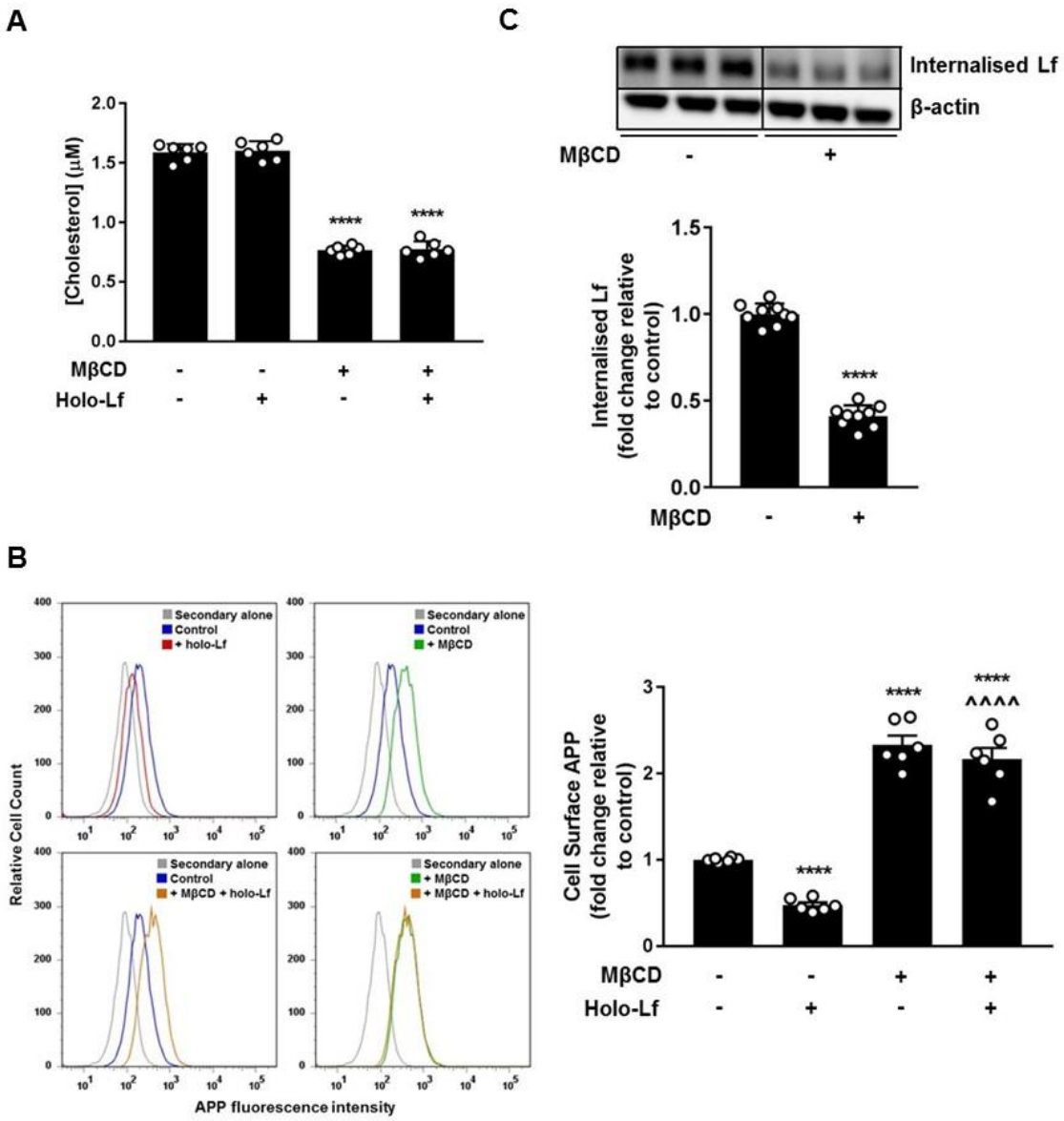

Figure 4.5. Holo-Lf mediated APP internalisation is cholesterol-dependent. **(A)** Live SH-SY5Y cells were assayed for cholesterol depletion (MβCD; 1 mM; 3 hours) followed by holo-Lf treatment (500 nM; 2 hours) in serum-free DMEM using the Amplex Red Cholesterol assay kit. SH-SY5Y cells treated in the same conditions as **(A)** were subjected to **(B)** FACS and **(C)** the ligand internalisation assay. Surface biotin was stripped with MeSNa to detect internalised biotinylated Lf. **(B)** Quantification of APP levels on the cell surface of non-permeabilised SH-SY5Y cells was performed using ab15272 recognising N-terminal extracellular epitopes of APP. **(C)** Internalised holo-Lf was visualised by Western blot normalised to β-actin content. Data are means ± SE of 3 experiments performed in **(A & B)** duplicate and **(C)** triplicate. **** $p < 0.0001$ compared to non-treated control and **(B)** ^^^^ $p < 0.0001$ compared to holo-Lf only treated cells.

4.2.5 Holo-Lf mediated APP internalisation is through a clathrin- and dynamin-independent mechanism involving ARF6

To obtain evidence as to whether CHC or DYM, the major proteins involved in clathrin-dependent endocytosis (Motley et al., 2003) are required for holo-Lf mediated APP internalisation, FACS was performed on CHC or DYM depleted (RNAi; 40 and 20 nM respectively) non-permeabilised SH-SY5Y cells in the presence of holo-Lf (500 nM; 2 hours). Cells without holo-Lf but treated with CHC or DYM RNAi resulted in an increase in surface presented APP ($p < 0.0001$ & $p < 0.01$ respectively) which significantly decreased when holo-Lf was added ($p < 0.0001$) (Figure 4.6A & B). These findings were investigated further using the ligand internalisation assay as described in Results 4.2.2. Antibodies targeting CHC and DYM were confirmed by knockdown in CHC and DYM RNAi treated cells, respectively ($p < 0.0001$) (Figure 4.6C & D). Cells treated with either CHC or DYM RNAi showed a significant increase in Lf internalisation ($p < 0.0001$) (Figure 4.6C & D).

Since previous results suggested CHC and DYM were not required for the internalisation of APP facilitated by holo-Lf, an alternative clathrin-independent ARF6 associated pathway (Gaschet and Hsu, 1999) was studied. Depleting ARF6 (RNAi; 20 nM) in non-permeabilised SH-SY5Y cells without the addition of holo-Lf had no effect on cell surface APP expression levels (Figure 4.7A). In contrast, cell surface APP significantly increased in ARF6 depleted cells treated with holo-Lf (500 nM; 2 hours) ($p < 0.001$) (Figure 4.7A). The endocytosis of APP mediated by holo-Lf was further examined using the ligand internalisation assay as described in Results 4.2.2. Antibodies targeting APP (22C11) and ARF6 confirmed knockdown in APP, ARF6, and double APP and ARF6 RNAi treated cells ($p < 0.0001$) (Figure 4.7B). Cells co-transfected with APP (20 nM) and ARF6 (20 nM) RNAi showed a decrease in Lf internalisation ($p < 0.0001$), comparable to APP and ARF6 RNAi alone treated levels ($p < 0.0001$) (Figure 4.7B), indicating Lf internalisation to be dependent on the presence of APP and ARF6.

The internalisation of APP mediated by holo-Lf was next demonstrated in SH-SY5Y-APP695 cells by double immunofluorescence confocal microscopy. After depleting CHC or ARF6 by RNAi treatment, SH-SY5Y-APP695 cells were placed at 4°C to halt protein internalisation and label surface bound APP with anti-APP

(22C11) antibody, and then incubated with 1 μM holo-Lf (1 hour) at 37°C to allow protein internalisation to occur. Cells were permeabilised for antibody access to internalised proteins and labelled with either anti-CHC or anti-ARF6 antibody. In the absence of holo-Lf, intracellular APP (green) was found to co-localise with CHC (red) and upon CHC RNAi, APP was retained on the cell surface (Figure 4.8). However, in the presence of holo-Lf, APP (green) co-localisation with CHC (red) was not apparent and RNAi treatment did not stop the internalisation of APP (Figure 4.8). In contrast, co-localisation was observed between APP (green) and ARF6 (red) in untreated conditions and in ARF6 RNAi treated cells, intracellular staining of APP was still evident (Figure 4.9). In the presence of holo-Lf, co-localisation of APP with ARF6 was observed and upon ARF6 RNAi treatment, APP accumulated on the cell surface (green) (Figure 4.9). Taken together, these results suggest clathrin is not required for the internalisation of APP by holo-Lf and that ARF6, which is also associated with the endocytosis of BACE1 (Sannerud et al., 2011), is necessary for holo-Lf mediated APP internalisation.

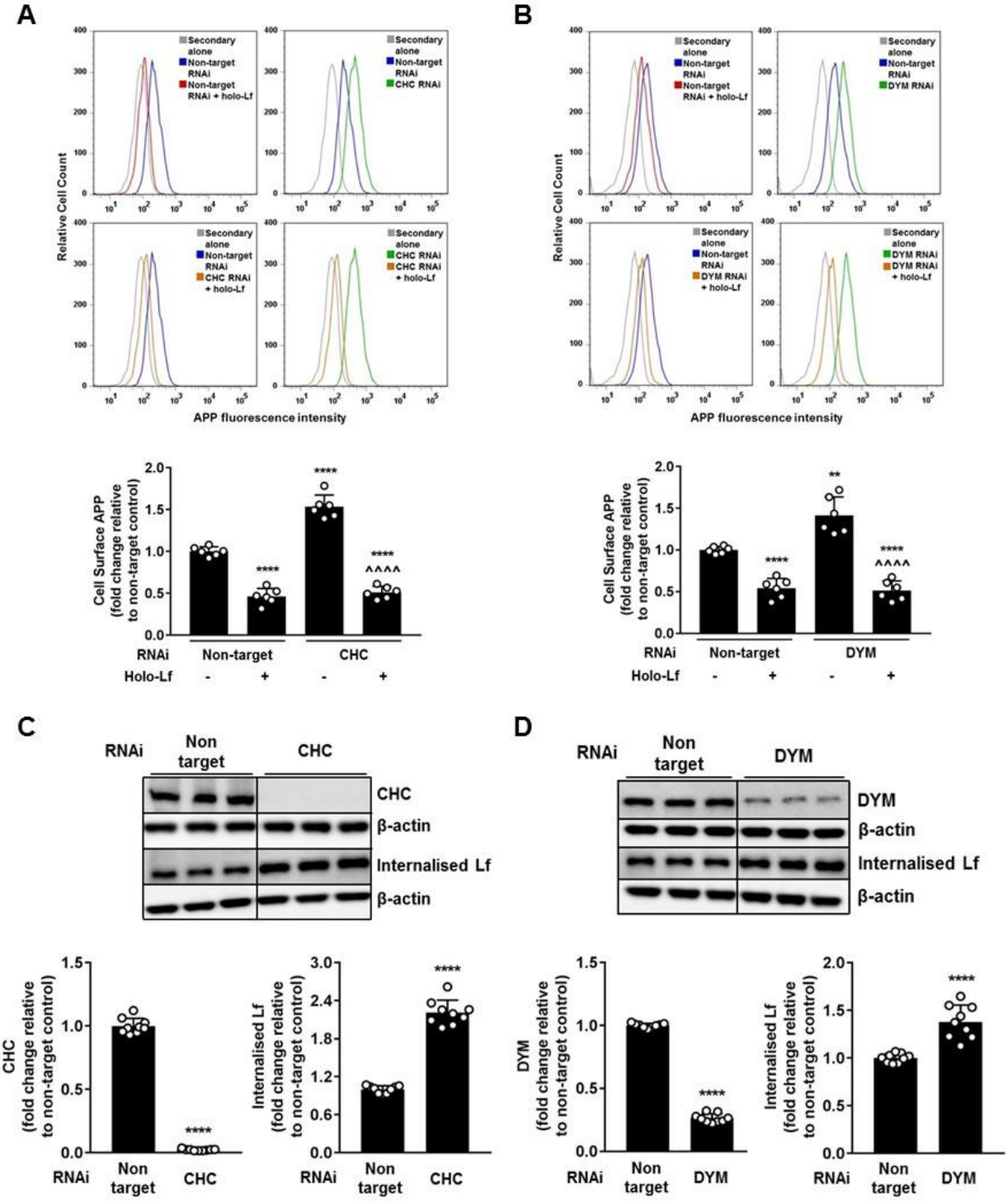
A
Secondary alone
Non-target RNAi
Non-target RNAi + holo-Lf
CHC RNAi
CHC RNAi + holo-Lf
Relative Cell Count
APP fluorescence intensity
Cell Surface APP (fold change relative to non-target control)
RNAi
Non-target
CHC
Holo-Lf
B
DYM RNAi
DYM RNAi + holo-Lf
DYM
C
RNAi
Non target
CHC
β-actin
Internalised Lf
CHC (fold change relative to non-target control)
Internalised Lf (fold change relative to non-target control)
D
DYM
DYM (fold change relative to non-target control)

Figure 4.6. Holo-Lf mediated APP internalisation is clathrin- and dynamin-independent. Quantification of APP levels on the cell surface of non-permeabilised SH-SY5Y cells after being transfected with **(A)** control non-target and CHC RNAi (40 nM) for 72 hours or **(B)** control non-target and DYM RNAi (20 nM) for 48 hours followed by holo-Lf treatment (500 nM; 2 hours). FACS was performed using ab15272 recognising N-terminal extracellular epitopes of APP. SH-SY5Y cells RNAi treated in the same conditions as **(A)** and **(B)** were subjected to the ligand internalisation assay. Surface biotin was stripped with MeSNa to detect internalised biotinylated Lf. **(C)** CHC and **(D)** DYM protein expression, and **(C & D)** internalised holo-Lf were visualised by Western blot normalised to β-actin. Data are means ± SE of 3 experiments performed in **(A & B)** duplicate and **(C & D)** triplicate. ** $p < 0.01$ and **** $p < 0.0001$ compared to non-target control and ^^^^ $p < 0.0001$ compared to **(A)** CHC RNAi and **(B)** DYM RNAi cells.

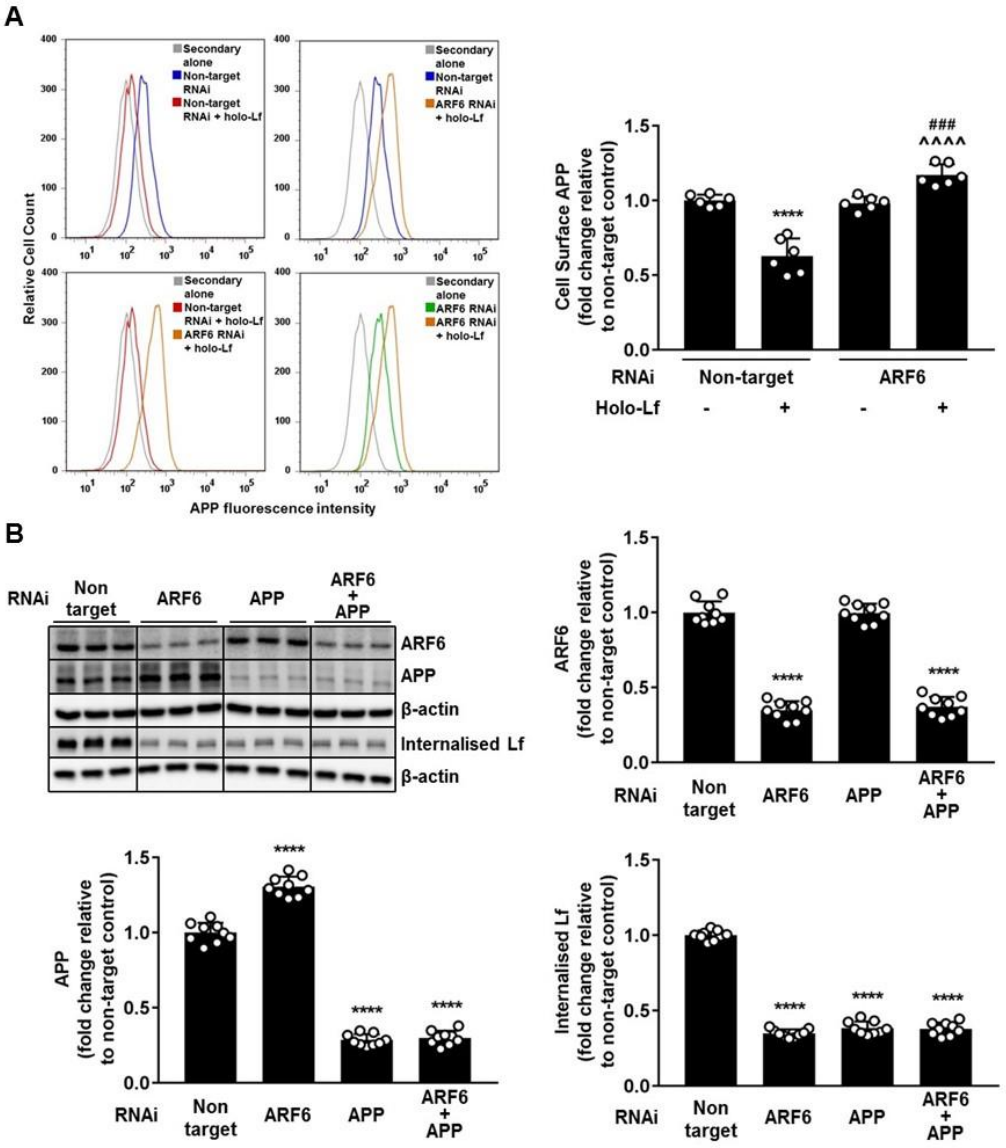

Figure 4.7. Holo-Lf mediated APP internalisation is ARF6-dependent. (A) Quantification of APP levels on the cell surface of non-permeabilised SH-SY5Y cells after being transfected with control non-target and ARF6 RNAi (20 nM) for 48 hours followed by a 2 hour incubation with 500 nM holo-Lf. FACS was performed using ab15272 recognising N-terminal extracellular epitopes of APP. **(B)** SH-SY5Y cells were subjected to the ligand internalisation assay where surface biotin was stripped with MeSNa to detect internalised biotinylated Lf after being transfected with control non-target, APP and/or ARF6 RNAi (20 nM; 48 hours). APP, ARF6 and internalised holo-Lf were visualised by Western blot normalised to β-actin. Data are means ± SE of 3 experiments performed in **(A)** duplicate and **(B)** triplicate. **** $p < 0.0001$ compared to non-target control, **(A)** ^^^^ $p < 0.0001$ compared to holo-Lf treated non-target and ### $p < 0.001$ compared to ARF6 RNAi cells.

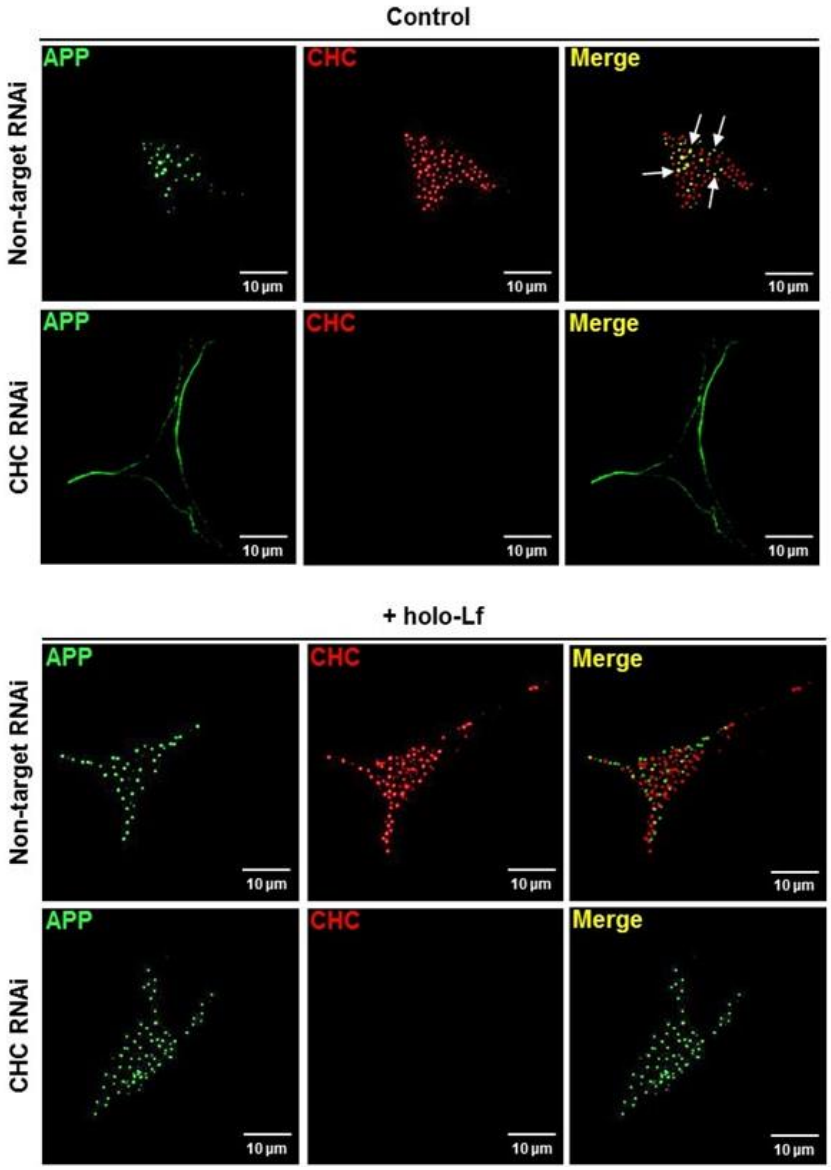

Figure 4.8. APP does not co-localise with clathrin in the presence of holo-Lf. Double immunofluorescence staining was performed on SH-SY5Y-APP695 cells to confirm whether APP internalisation mediated by holo-Lf is clathrin-independent. Deconvoluted confocal microscopy was performed on SH-SY5Y-APP695 cells after being transfected with control non-target and CHC RNAi (40 nM) for 72 hours. After surface labelling with anti-APP antibody, cells were subjected to 1 µM holo-Lf treatment for 1 hour at 37°C. After fixation and permeabilisation, cells were labelled with anti-CHC antibody followed by Alexa Fluor 488 (green) and 568 (red) conjugated secondary antibodies to detect APP and CHC respectively. White arrows denotes co-localisation between APP and CHC in the absence of holo-Lf. Images are representative of an SH-SY5Y-APP695 cell from 2 experiments, performed in duplicate. Scale bar = 10 µm.

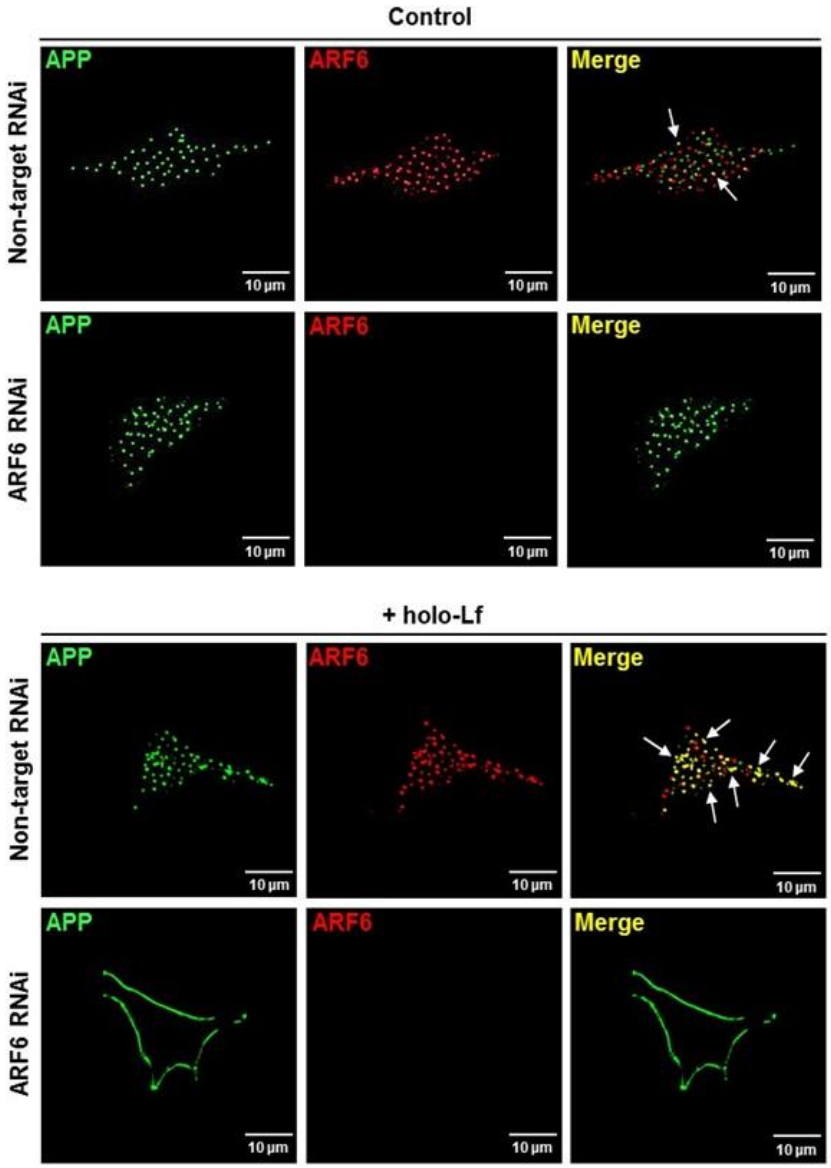

Figure 4.9. Co-localisation of APP and ARF6 increases in the presence of holo-Lf. Double immunofluorescence staining was performed on SH-SY5Y-APP695 cells to test whether APP internalisation mediated by holo-Lf is ARF6-dependent. Deconvoluted confocal microscopy was performed on SH-SY5Y-APP695 cells after being transfected with control non-target and ARF6 RNAi (20 nM) for 48 hours. After surface labelling with anti-APP antibody, cells were subjected to 1 µM holo-Lf treatment for 1 hour at 37°C. After fixation and permeabilisation, cells were labelled with anti-ARF6 antibody followed by Alexa Fluor 488 (green) and 568 (red) conjugated secondary antibodies to detect APP and ARF6 respectively. White arrows denotes co-localisation between APP and ARF6. Images are representative of an SH-SY5Y-APP695 cell from 2 experiments, performed in duplicate. Scale bar = 10 µm.

4.2.6 Internalised APP is diverted to the Rab11 GTPase-positive recycling endosome by holo-Lf

Rab5, Rab7 and Rab11 are major proteins associated with early (Bucci et al., 1992), late (Feng et al., 1995) and recycling (Takahashi et al., 2012) endosomes respectively. All have been associated with the vesicular trafficking of APP. Depleting endogenous Rab5a (20 nM), Rab7a (20 nM) and Rab11a (20 nM) by RNAi altered cell surface presented APP in non-permeabilised SH-SY5Y cells exposed to holo-Lf (500 nM; 2 hours). In cells without holo-Lf but treated with Rab5a and Rab7a RNAi, surface APP significantly increased ($p < 0.0001$) (Figure 4.10A & B), whilst Rab11a RNAi treatment showed a significant decrease ($p < 0.001$) in cell surface presented APP (Figure 4.11A). This was also confirmed by surface biotinylation where Rab11a depleted cells displayed reduced surface APP levels ($p < 0.0001$) (Figure 4.11B). In contrast, cell surface APP levels significantly decreased in Rab5a and Rab7a depleted cells when treated with holo-Lf ($p < 0.0001$) (Figure 4.10A & B) whilst Rab11a RNAi treated cells had an increase in cell surface APP upon holo-Lf exposure ($p < 0.0001$) (Figure 4.11A & B). These findings were investigated further using the ligand internalisation assay as described in Results 4.2.2. Antibodies targeting Rab5, Rab7 and Rab11 were confirmed by knockdown in Rab5a, Rab7a and Rab11a RNAi treated cells, respectively ($p < 0.0001$) (Figure 4.10C & D and Figure 4.11C). In accordance with cell surface APP levels, the ligand internalisation assay showed that cells treated with either Rab5a or Rab7a RNAi had a significant increase in Lf internalisation ($p < 0.0001$) (Figure 4.10C & D), whereas in Rab11a depleted cells Lf internalisation decreased ($p < 0.0001$) (Figure 4.11C).

The accumulation of cell surface APP and decreased levels of Lf internalisation observed with Rab11a RNAi treated cells in the presence of holo-Lf warranted further investigation of the endocytic recycling pathway. Rab4 is one of the major proteins associated with the 'fast' recycling of cargo back to the plasma membrane from the early/sorting endosome (Jovic et al., 2010) and therefore was explored in conjunction with Rab11 using double immunofluorescence confocal microscopy. After depleting Rab4a (20 nM), Rab11a or double Rab4a and Rab11a by RNAi treatment, cell surface APP was labelled in SH-SY5Y-APP695 cells at 4°C with anti-APP (22C11) antibody. Cells were then treated with 1 µM holo-Lf (1 hour) at 37°C before permeabilisation and labelling with anti-Rab4

and/or anti-Rab11 antibody. In the absence of holo-Lf, deconvoluted confocal microscopy revealed APP (green) to co-localise with Rab4 (red) (Figure 4.12A) and Rab11 (red) (Figure 4.12B) positive compartments within the cell. Intracellular staining of APP (green) was evident in cells depleted of Rab4a, Rab11a or double Rab4a and Rab11a (Figure 4.12). In the presence of holo-Lf, co-localisation of APP (green) and Rab4 (red) positive compartments was not apparent (Figure 4.12A), whereas APP co-localisation with Rab11 (red) compartments was still evident (Figure 4.12B) in SH-SY5Y-APP695 cells. Rab4a RNAi treated cells with holo-Lf appeared to have no effect on intracellular staining of APP (green) (Figure 4.12A), but Rab11a RNAi treated cells revealed cell surface APP staining (green) (Figure 4.12B). However, depletion of Rab4a with Rab11a appeared to reverse the effect of Rab11a alone, as intracellular staining of APP was again present upon holo-Lf treatment in these cells (Figure 4.12C). Taken together, these results suggest that holo-Lf directs APP to the Rab11-positive recycling endosome but upon Rab11 depletion, APP is recycled back to the plasma membrane via Rab4-positive endosomes.

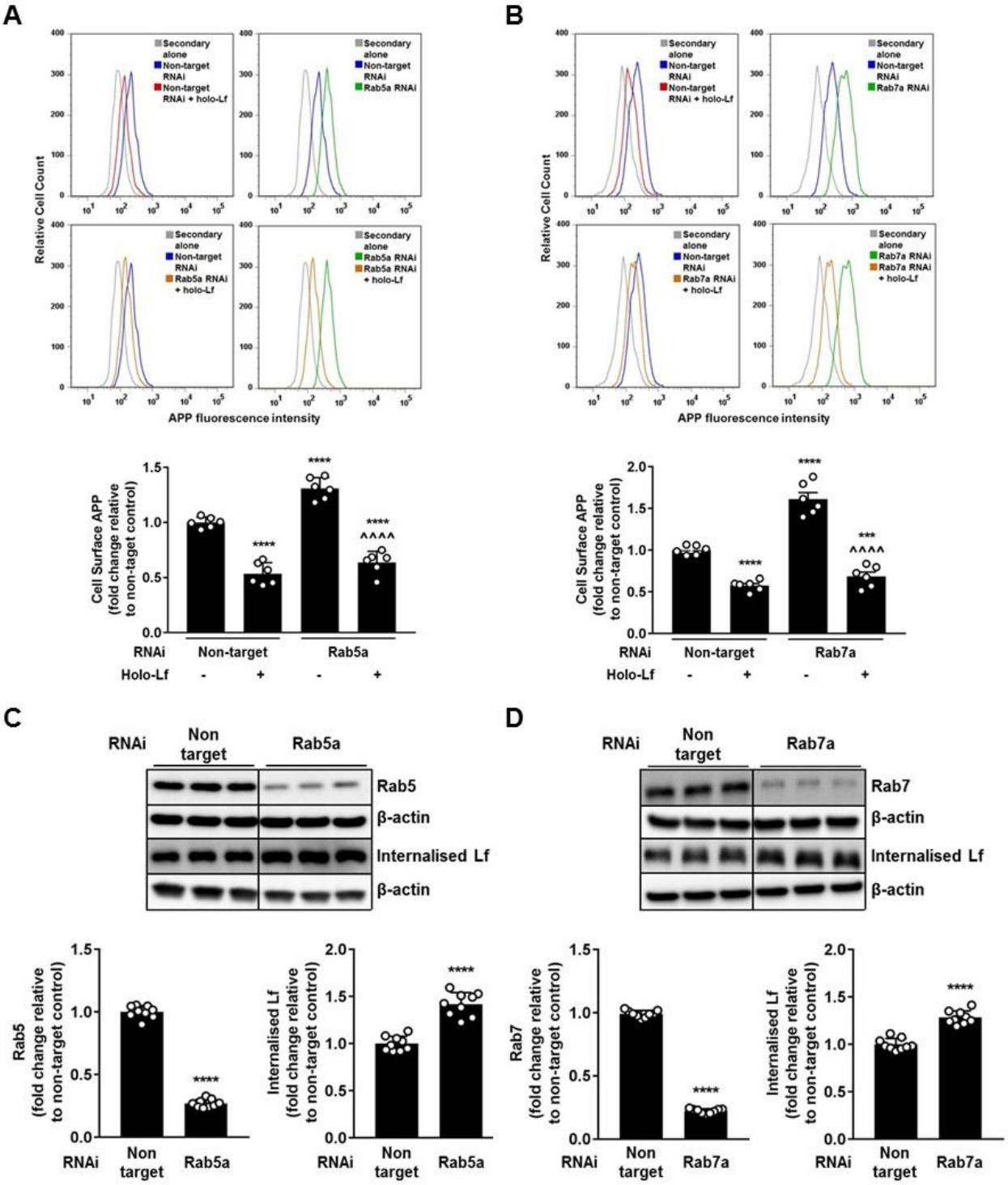
A
Secondary alone
Non-target RNAi
Non-target RNAi + holo-Lf
Rab5a RNAi
Rab5a RNAi + holo-Lf
Relative Cell Count
APP fluorescence intensity
Cell Surface APP (fold change relative to non-taget control)
RNAi
Non-target
Rab5a
Holo-Lf
B
Rab7a RNAi
Rab7a RNAi + holo-Lf
Cell Surface APP (fold change relative to non-target control)
Rab7a
C
RNAi
Non target
Rab5a
Rab5
β-actin
Internalised Lf
Rab5 (fold change relative to non-target control)
Internalised Lf (fold change relative to non-target control)
D
Rab7a
Rab7
Rab7 (fold change relative to non-target control)

Figure 4.10. Rab5 and Rab7-positive endosomes are not involved in the endocytic pathway of holo-Lf and APP. Quantification of APP levels on the cell surface of non-permeabilised SH-SY5Y cells after being transfected with **(A)** control non-target and Rab5a RNAi (20 nM) or **(B)** control non-target and Rab7a RNAi (20 nM) for 48 hours, followed by holo-Lf treatment (500 nM; 2 hours). FACS was performed using ab15272 recognising N-terminal extracellular epitopes of APP. SH-SY5Y cells RNAi treated in the same conditions as **(A)** and **(B)** were subjected to the ligand internalisation assay. Surface biotin was stripped with MeSNa to detect internalised biotinylated Lf. **(C)** Rab5 and **(D)** Rab7 protein expression, and **(C & D)** internalised holo-Lf were visualised by Western blot normalised to β-actin. Data are means ± SE of 3 experiments performed in **(A & B)** duplicate and **(C & D)** triplicate. *** $p < 0.001$ and **** $p < 0.0001$ compared to non-target control and ^^^^ $p < 0.0001$ compared to **(A)** Rab5a RNAi and **(B)** Rab7a RNAi cells.

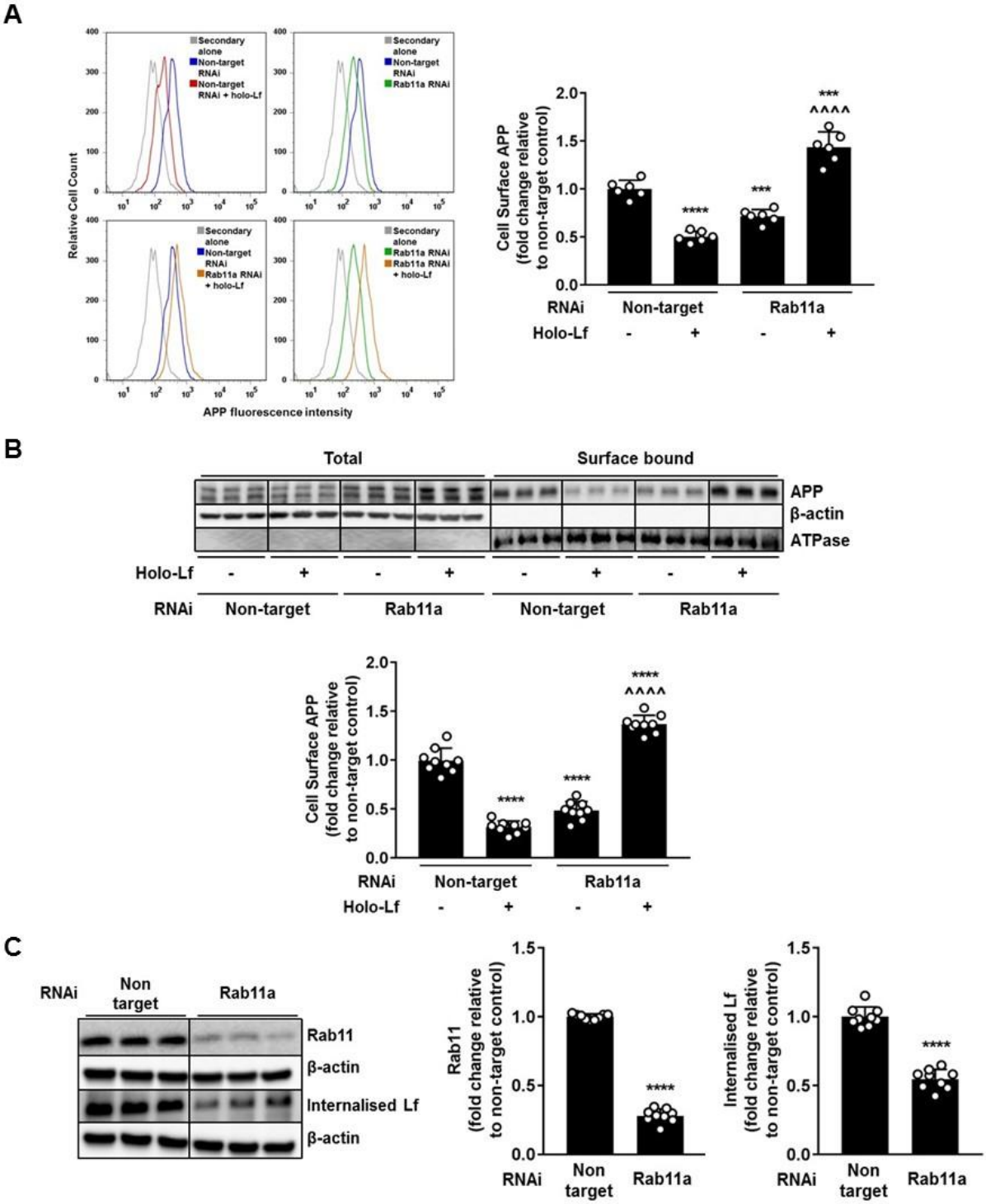
A
Secondary alone
Non-target RNAi
Non-target RNAi + holo-Lf
Rab11a RNAi
Rab11a RNAi + holo-Lf
Relative Cell Count
APP fluorescence intensity
Cell Surface APP (fold change relative to non-target control)
RNAi
Non-target
Rab11a
Holo-Lf
B
Total
Surface bound
APP
β-actin
ATPase
C
Rab11
Internalised Lf
Rab11 (fold change relative to non-target control)
Internalised Lf (fold change relative to non-target control)

Figure 4.11. Holo-Lf directs APP to Rab11-positive recycling endosomes. **(A)** Quantification of APP levels on the cell surface of non-permeabilised SH-SY5Y cells after being transfected with control non-target and Rab11a RNAi (20 nM) for 48 hours followed by a 2 hour incubation with 500 nM holo-Lf. FACS was performed using ab15272 recognising N-terminal extracellular epitopes of APP. **(B)** Cell surface proteins of SH-SY5Y cells RNAi treated in the same conditions as **(A)** followed by holo-Lf treatment (500 nM; 2 hours) were biotinylated to identify changes to APP expression on the cell surface. **(C)** SH-SY5Y cells RNAi treated in the same conditions as **(A)** were subjected to the ligand internalisation assay. Surface biotin was stripped with MeSNa to detect internalised biotinylated Lf. **(B)** Total and cell surface APP, **(C)** Rab11 and internalised holo-Lf were visualised by Western blot and normalised to **(B)** Na^+/K^+ ATPase surface protein and **(C)** β-actin. Data are means ± SE of 3 experiments performed in **(A)** duplicate and **(B & C)** triplicate. *** $p < 0.001$ and **** $p < 0.0001$ compared to non-target control and **(A & B)** ^^^^ $p < 0.0001$ compared to Rab11a RNAi cells.

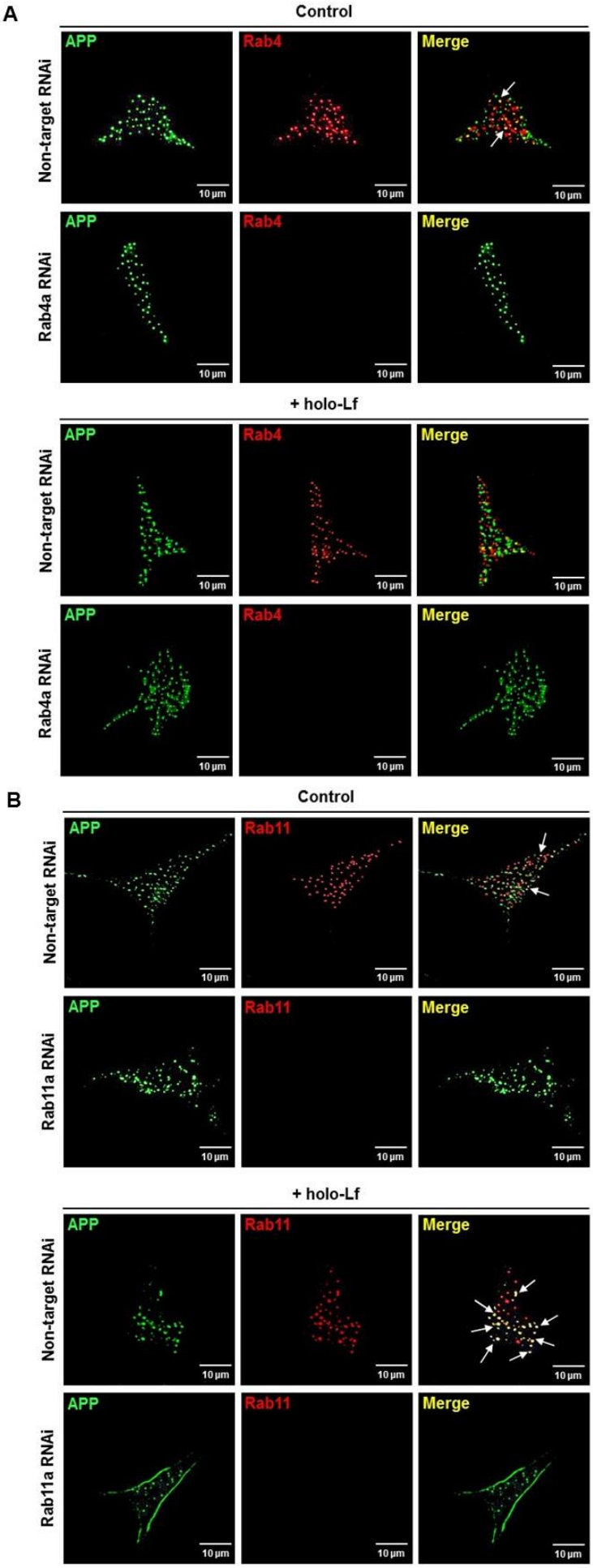
A
Control
APP
Rab4
Merge
Non-target RNAi
Rab4a RNAi
+ holo-Lf
B
Rab11
Rab11a RNAi
10 µm

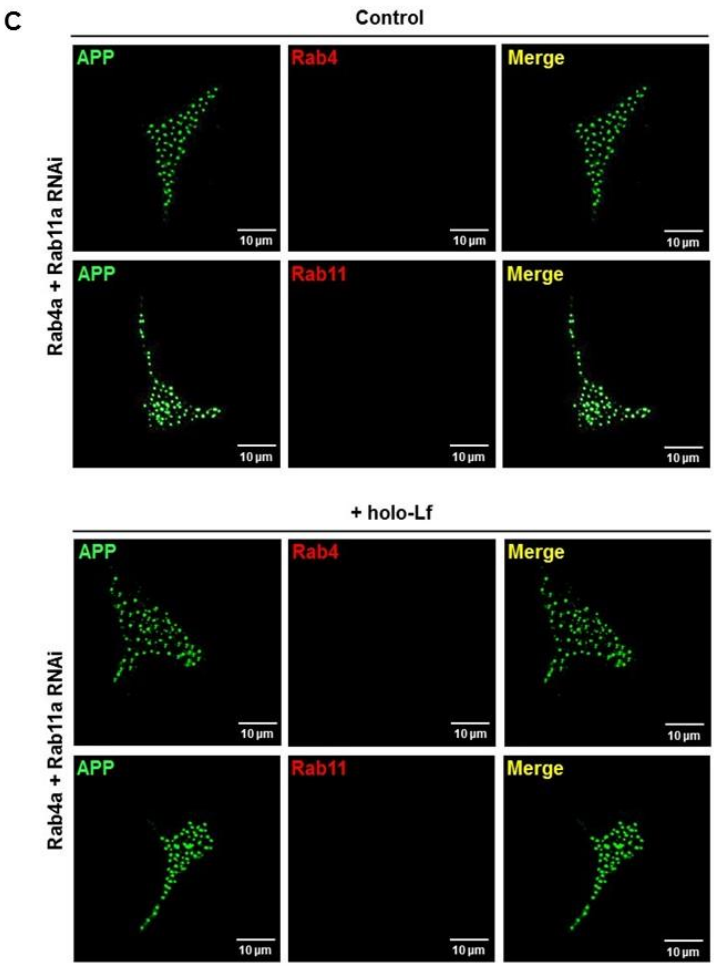

Figure 4.12. APP co-localises with Rab11-positive endosomes in the presence of holo-Lf and is rapidly recycled back to the plasma membrane by Rab4-positive endosomes upon Rab11 knockdown. The endocytic recycling pathway involving Rab4 and Rab11-positive endosomes were investigated in conjunction with holo-Lf directed APP trafficking by double immunofluorescence confocal microscopy. Deconvoluted confocal microscopy was performed on SH-SY5Y-APP695 cells after being transfected with control non-target, **(A)** Rab4a, **(B)** Rab11a, and **(C)** Rab4a and Rab11a RNAi (20 nM; 48 hours). After surface labelling with anti-APP antibody, cells were subjected to 1 µM holo-Lf for 1 hour at 37°C. After fixation and permeabilisation, cells were labelled with either **(A & C)** anti-Rab4 or **(B & C)** anti-Rab11 antibody. Alexa Fluor 488 (green) conjugated secondary antibody was used to detect APP while Alexa Fluor 568 (red) conjugated secondary antibody was used to detect **(A & C)** Rab4 or **(B & C)** Rab11. White arrows denotes co-localisation between **(A)** APP and Rab4, and **(B)** APP and Rab11. Images are representative of an SH-SY5Y-APP695 cell from 2 experiments, performed in duplicate. Scale bar = 10 µm.

4.3 Discussion

Holo-Lf was found to internalise APP from the cell surface in a receptor mediated pathway. Therefore, by using RNAi directed against the major proteins required for clathrin-dependent and independent internalisation pathways, we report here that holo-Lf deviates APP from the previously published clathrin-dependent internalisation route to a clathrin-independent pathway requiring the endocytic trafficking regulator ARF6. Impeding the cholesterol mediated internalisation route also altered holo-Lf dependent APP endocytosis. LRP1 was shown to influence cell surface density levels of APP but was not involved in holo-Lf mediated APP internalisation, confirming earlier results that demonstrated Lf to preferentially bind APP over LRP1 (Chapter 3.2.5). By manipulating the Rab GTPases involved in the various APP trafficking routes, holo-Lf was found to direct APP to Rab11-positive recycling endosomes. When Rab11 activity was disrupted, this led to the recycling of APP back to the plasma membrane via Rab4-positive vesicles. The study of the endocytosis and intracellular trafficking of APP directed by holo-Lf helps define a mode of action for holo-Lf at the cellular level.

The ability of holo-Lf to significantly decrease surface presented APP in SH-SY5Y neuroblastoma cultures (Figure 4.1A & 4.2A) was subsequently confirmed in mouse primary neurons (Figure 4.2B). The inability of apo-Lf to elicit a change in cell surface APP levels (Figure 4.1A) confirmed previous results specifying a lack of interaction between apo-Lf and APP (Chapter 3.2.1), possibly attributed to the large conformational differences observed between apo-Lf and holo-Lf (Jameson et al., 1998; Querinjean et al., 1971). Dropping the temperature down to 4°C reduced enzymatic and metabolic activity, rendering the cell inactive (Peterson et al., 2007), providing a reference for the absence of endocytosis which resulted in unchanged APP cell surface levels (Figure 4.1B).

There was a moderate increase in cell surface APP with holo-Tf in SH-SY5Y cells when examined by surface biotinylation (Figure 4.2A). Transport of iron is largely mediated by internalisation through the Tf/TfR1 complex (Crichton et al., 2011; Moos et al., 2007). Once internalised, iron is released from Tf in the lysosome and proceeds to be either utilised by the cell, stored in the iron storage protein Ft or effluxed via FPN (Ganz, 2005). When cellular homeostatic regulation requires

iron to be exported, all brain cell types use FPN (Song et al., 2010) and the stabilisation of FPN for iron export at the cellular membrane is provided by APP in neurons (Duce et al., 2010; Wong et al., 2014b). Therefore, a Tf promoted increase in iron internalisation via the Tf/TfR1 pathway is likely to promote APP expression on the cell surface so that the iron can be effluxed through FPN.

The reduction of cell surface APP levels in the presence of holo-Lf were complemented by holo-Lf internalisation being significantly reduced upon APP depletion (Figure 4.3). This suggests that holo-Lf may partially be dependent on APP for internalisation. However, earlier results have demonstrated holo-Lf binds LRP1 in the absence of APP (Chapter 3.2.5). Therefore, additional studies examining cell surface APP levels in LRP1 depleted SH-SY5Y cells with and without the presence of holo-Lf, and holo-Lf uptake in SH-SY5Y cells co-transfected with APP and LRP1 RNAi were performed to not only confirm that LRP1 is not involved in the interaction between holo-Lf and APP, but to also determine whether holo-Lf internalisation can be facilitated by LRP1 in the absence of APP. Cells depleted of LRP1 showed an increase in cell surface APP (Figure 4.4A) which correlated with an increase in holo-Lf internalisation (Figure 4.4B). LRP1 is known to endocytose APP via a clathrin-mediated pathway and promote the amyloidogenic pathway thereby reducing APP cell surface levels (Herr et al., 2017). In contrast, depleting cells of LRP1 has shown APP to accumulate on the cell surface (Cam and Bu, 2006; Herr et al., 2017). This could also explain why there is more holo-Lf uptake in LRP1 depleted cells (Figure 4.4B). In the presence of holo-Lf, LRP1 depleted cells showed a significant decrease in cell surface presented APP (Figure 4.4A) and in cells depleted of APP and LRP1, a similar decrease in holo-Lf internalisation was evident compared to APP depleted cells (Figure 4.4B). Taken together, these results confirm that LRP1 is not involved in the internalisation of APP facilitated by holo-Lf. The question still remains as to why LRP1 is not facilitating the internalisation of holo-Lf in APP depleted cells (Figure 4.4B). Several reports have shown Lf can bind cell surface ligands to exert its numerous biological functions without the need for internalisation (Brock et al., 1994; Ismail and Brock, 1993; Roiron-Lagroux and Figarella, 1990; Zhang et al., 2014). This has also been shown with LRP1 which can act as both an endocytic receptor and a cell surface signalling receptor (Herz et al., 2000; Li et al., 2001; Strickland et al., 2002). For instance,

Grey *et al* showed Lf to interact with LRP1 in primary rat osteoblasts to activate cell signalling in conditions where endocytosis was blocked by pharmacological inhibitor treatment, decreasing the temperature to 4°C or by incubating cells in a hypertonic solution (Grey et al., 2004), indicating that the endocytic and signalling properties of LRP1 are independent to each other. This could possibly explain why there was no LRP1 mediated Lf uptake in APP depleted SH-SY5Y cells. Whether Lf was involved in cell signalling through LRP1 that didn't warrant ligand endocytosis in APP depleted SH-SY5Y cells would need further investigation.

Various studies have documented APP endocytosis to be strongly influenced by cholesterol levels (Cossec et al., 2010; Ehehalt et al., 2003; Kojro et al., 2001). Whilst APP and BACE1 may be present at separate regions of the lipid raft domain, endocytosis brings APP and BACE1 together enabling β-secretase processing of APP within endosomes (Cataldo et al., 2004; Chow et al., 2010; Zheng and Koo, 2011). By manipulating cholesterol membrane levels, we examined how this influenced the cellular distribution of APP and what affect this had on holo-Lf mediated APP endocytosis. In the absence of holo-Lf, our data supports previous reports that demonstrate lowering membrane cholesterol in cells (Figure 4.5A) prevents APP endocytosis and results in an accumulation of APP on the cell surface (Figure 4.5B) (Cossec et al., 2010; Kojro et al., 2001). Concomitantly, reducing cell membrane cholesterol levels (Figure 4.5A) also decreases holo-Lf internalisation (Figure 4.5C), indicating a cholesterol-dependent holo-Lf mediated APP internalisation route.

Countless reports have shown APP endocytosis to be dependent on clathrin-coated vesicles (Ehehalt et al., 2003; von Arnim et al., 2008; Yap and Winckler, 2015), whereas BACE1 undergoes clathrin-independent endocytosis and is sorted to the early endosome via the endocytic trafficking regulator ARF6 (Sannerud et al., 2011; Tang et al., 2015). By modifying the specific early regulators of APP and BACE1 endocytosis through depletion of the CHC or ARF6 expression respectively, we may now begin to understand the mechanism by which holo-Lf facilitates the internalisation of APP. Without the presence of holo-Lf, our data supports previous evidence in which silencing the CHC prevents APP endocytosis and increases APP cell surface levels (Figure 4.6A) (Cossec et al., 2010; Motley et al., 2003), which was also observed when silencing DYM (Figure 4.6B), one of the major proteins involved in the budding and scission of clathrin-

coated vesicles from the cell membrane (Carey et al., 2005). However, these surface levels of APP decreased in the presence of holo-Lf (Figure 4.6A & B), indicating that holo-Lf internalises APP via a clathrin and dynamin-independent pathway. Concomitant with this internalisation of APP, holo-Lf endocytosis was also elevated (Figure 4.6C & D). In support of these findings, APP stained on the cell surface was shown to co-localise with clathrin inside SH-SY5Y-APP695 cells in the absence of holo-Lf (Figure 4.8), signifying APP is internalised into the cell via a clathrin-dependent pathway (Cossec et al., 2010; Motley et al., 2003). This was further validated when APP accumulated on the cell surface in CHC depleted cells (Figure 4.8). However, surface presented APP that internalised into the cell in the presence of holo-Lf did not co-localise with CHC, and depleting cells of CHC still resulted in intracellular APP in the presence of holo-Lf (Figure 4.8).

Silencing ARF6 revealed no changes to cell surface APP levels (Figure 4.7A), indicating ARF6 is not directly involved in APP endocytosis (Sannerud et al., 2011; Zhang and Song, 2013b). However, cell surface APP increased in ARF6 depleted cells when holo-Lf was added (Figure 4.7A). A reduction of Lf uptake in cells depleted of ARF6 and APP resulted in a comparable level to that of APP or ARF6 alone (Figure 4.7B). This demonstrates that Lf shares a common internalisation pathway with APP and ARF6 and that the presence of each protein is required to gain entry into the cell. Surface presented APP staining which internalised into the cell co-localised with ARF6 in the absence of holo-Lf (Figure 4.9). A possible explanation as to why APP would co-localise with ARF6 could be the result of ARF6 directed trafficking of BACE1 to the same endocytic compartment as APP to initiate cleavage (Ehehalt et al., 2003; Sannerud et al., 2011). In ARF6 depleted SH-SY5Y-APP695 cells, intracellular staining of APP was evident (Figure 4.9). This confirmed previous findings suggesting APP internalisation is not dependent on ARF6 (Sannerud et al., 2011; Zhang and Song, 2013b). Furthermore, cell surface staining of APP internalised into the cell in the presence of holo-Lf which co-localised with ARF6 (Figure 4.9). Depleting cells of ARF6 resulted in an accumulation of APP on the cell surface in the presence of holo-Lf (Figure 4.9), suggesting that holo-Lf mediated APP endocytosis requires ARF6 to gain entry into the cell. In certain cellular conditions, ARF6 has previously been reported to influence APP internalisation via macropinocytosis, avoiding delivery to the early endosome and transporting

APP to the lysosome for β-processing (Tang et al., 2015). Here, we propose that in the presence of holo-Lf, APP endocytosis could follow a similar pathway that is dependent on ARF6.

Next, we investigated the intracellular trafficking route of holo-Lf mediated APP endocytosis by examining the various intracellular endocytic compartments involved in the trafficking of APP. The Rab5 and Rab11 GTPases are predominantly associated with the early endocytic pathway (Trischler et al., 1999), whereas Rab7 is more linked to the late endocytic pathway (Vitelli et al., 1997). SH-SY5Y cells treated with Rab5a or Rab7a RNAi resulted in an accumulation of cell surface APP (Figure 4.10A & B). Rab5 is the major GTPase involved in endocytosis, trafficking, and sorting of internalised APP to the different membrane compartments (Bucci et al., 1992; Gorvel et al., 1991; Grbovic et al., 2003). Therefore, silencing Rab5a impedes APP internalisation and sorting at the early endosome, explaining the accumulation of cell surface APP. The Rab7 GTPase is associated mainly with late endosomes and lysosomes (Guerra and Bucci, 2016), involved in the degradation of APP and/or its cleaved products (Koo et al., 1996; Yamazaki et al., 1996). Depleting Rab7 therefore can impede the late endocytic degradation pathway, forcing APP to be recycled back to the plasma membrane (Koo et al., 1996). However, increased APP cell surface levels observed with Rab5a and Rab7a RNAi treatment decreased in the presence of holo-Lf (Figure 4.10A & B), correlating with an increase in holo-Lf internalisation (Figure 4.10C & D). In the absence of holo-Lf, co-localisation was observed between APP and Rab11 (Figure 4.12B), indicating a slow recycling process of internalised APP mediated by Rab11-positive vesicles (Ullrich et al., 1996; Urbe et al., 1993). While in cells depleted of Rab11a, there was a decrease in surface presented APP (Figure 4.11A & B) with apparent APP intracellular staining (Figure 4.12B), indicating a lack of APP recycling to the cell surface (Ullrich et al., 1996; Urbe et al., 1993). However, there was co-localisation between APP and Rab11-positive compartments in the presence of holo-Lf (Figure 4.12B), suggesting APP internalised by holo-Lf is trafficked to Rab11-positive endosomes. Furthermore, in cells depleted of Rab11a, APP was found both on the cell surface and intracellularly in the presence of holo-Lf (Figure 4.12B). The accumulation of cell surface APP observed with Rab11a RNAi treated cells in the presence of holo-Lf (Figure 4.11A & B) in addition to the decreased levels of Lf

internalisation (Figure 4.11C) revealed a discrepancy regarding the functional role of Rab11-positive endosomes and therefore warranted further investigation of the endocytic recycling pathway in the presence of holo-Lf. Rab4 and Rab11 GTPases both regulate the recycling of intracellular cargo back to the plasma membrane (Hsu and Prekeris, 2010; Li and DiFiglia, 2012). Rab4 facilitates a 'fast' recycling process and is predominantly localised with Rab5 on the early/sorting endosome in addition to being associated with Rab11-positive compartments which are involved in 'slow' recycling of cargo and are typically perinuclear (Sonnichsen et al., 2000; Ward et al., 2005a). Using double immunofluorescence confocal microscopy, in the absence of holo-Lf, co-localisation was observed between APP and Rab4, and in Rab4a RNAi treated cells intracellular staining of APP was evident (Figure 4.12A). The co-localisation of APP with Rab4 could be explained by the rapid recycling of APP in Rab4-positive vesicles after internalisation (Zhang and Song, 2013a). In the presence of holo-Lf, there was no co-localisation between APP and Rab4-positive compartments (Figure 4.12A), indicating holo-Lf does not direct APP through the rapid recycling route. Whilst in Rab4a RNAi treated cells, there was apparent intracellular staining of APP (Figure 4.12A). Double RNAi treatment of Rab4a and Rab11a to SH-SY5Y-APP695 cells also showed apparent intracellular APP staining both in the absence and presence of holo-Lf (Figure 4.12C). Taken together, we identify a Rab11-dependent pathway as the major trafficking route for APP directed by holo-Lf, and disrupting this pathway leads to the recycling of APP back to the plasma membrane via Rab4-positive vesicles.

Whether holo-Lf is rapidly recycled or dissociates from APP and remains inside the cell after Rab11 disruption requires further investigation. Co-localisation experiments performed within this chapter also posed a limitation. For further validity, a triple stain including holo-Lf would be of benefit to monitor co-localisation of APP and Lf with the associated regulators of endocytosis and trafficking. Also, it is essential that the cellular mechanism of ARF6-dependent holo-Lf mediated APP internalisation and trafficking to Rab11-positive recycling compartments would need to be validated in a primary mammalian neuronal cell line which is more likely to reiterate the properties of neuronal cells *in vivo*. Finally, what impact holo-Lf mediated APP internalisation and trafficking has on the cell fate of APP will be further explored.

CHAPTER 5.0 HOLO-LF PROMOTES TRAFFICKING OF APP TO RAB11 RECYCLING ENDOSOMES TO EXACERBATE Aβ PRODUCTION

5.1 Introduction

The processing of APP is an important determining factor in the development of AD. The ubiquitously expressed APP is predominantly processed by amyloidogenic and non-amyloidogenic pathways (Chow et al., 2010; Zheng and Koo, 2011). In AD, amyloidogenic processing of APP dominates leading to the accumulation of Aβ in the brain. Full-length APP is endocytosed before being cleaved by the β-secretase enzyme BACE1 to release sAPPβ and the amino terminus of Aβ (Seubert et al., 1993). The γ-secretase complex cleaves out the carboxyl end of Aβ (Chow et al., 2010). Physiologically, non-amyloidogenic processing is predominant, requiring ADAM10 α-secretase cleavage within the Aβ domain at the cell surface (Koo et al., 1996), yielding neuroprotective sAPPα (Roberts et al., 1994). The endocytotic shift for amyloidogenic processing of APP depends on cholesterol-enriched lipid rafts (Ehehalt et al., 2003; Simons et al., 1998). The ARF6 endocytic trafficking regulator is required for BACE1 sorting to the early endosome, where it encounters APP for β-secretase processing (Sannerud et al., 2011; Tang et al., 2015).

According to the literature, evidence suggesting a direct interaction between Lf and APP has not been documented. However, one study performed by Guo *et al* has demonstrated the ability of Lf to indirectly alter APP metabolism (Guo et al., 2017). Treatment of Lf to the mouse neuroblastoma N2a cell line overexpressing a FAD causing mutant of APP (APP Swedish mutation; APPsw) and in the APP/presenilin I AD mouse model resulted in a decrease in total APP levels, an upregulation of ADAM10 protein expression and an increase in sAPPα (Guo et al., 2017). These findings indicate that Lf can promote ADAM10 activation to induce non-amyloidogenic α-secretase processing of APP.

In the previous chapter (Chapter 4.0), the cellular mechanism and components required for holo-Lf mediated APP internalisation and trafficking were identified. Using a similar approach, we investigated what impact holo-Lf had of the main amyloidogenic and non-amyloidogenic processing pathways of wild-type APP.

We examined what affect Lf had on the α-secretase enzyme ADAM10 as well as the enzymatic activity of BACE1 associated with the amyloidogenic pathway of APP. Whether the interaction between APP and Lf could possibly be considered as a therapeutic target was also explored.

5.2 Results

5.2.1 Holo-Lf promotes the amyloidogenic pathway of APP

To investigate the effects of holo-Lf on APP processing via the amyloidogenic pathway, dose and time-dependent experiments were carried out to determine the physiological parameters of holo-Lf exposure. To confirm the optimal concentration of holo-Lf treatment, SH-SY5Y cells were treated 0-1000 nM for 2 hours. To confirm the optimal exposure time of holo-Lf, cells were treated for 0.5, 1, 2, and 4 hours with 500 nM holo-Lf. Conditioned media samples from SH-SY5Y cells were concentrated and analysed by Western blot. Total sAPP, generated through either the non-amyloidogenic (α-cleaved) or the amyloidogenic (β-cleaved) pathway was detected by 22C11 (Cater et al., 2008), whilst sAPPβ and Aβ were detected by 1A9 and 6E10 respectively. In the absence of holo-Lf, changes in sAPP expression were observed to steadily increase up to 4 hours (Figure 5.1B) and increasing the concentration and exposure time of holo-Lf significantly increased sAPP, sAPPβ and Aβ levels (Figure 5.1A & B). These findings suggest that holo-Lf exacerbates the amyloidogenic pathway of APP in a dose and time-dependent manner, resulting in an accumulation of sAPPβ and Aβ. The optimal concentration and exposure time of holo-Lf treatment was confirmed at 500 nM for 2 hours. This avoided over-saturation of holo-Lf and achieved a desirable detectable output in the most efficient time.

The exacerbation of APP amyloidogenic fragments observed with holo-Lf treatment was also demonstrated in SH-SY5Y-APP695 cells. Media samples from cells treated with holo-Lf and holo-Tf (500 nM; 2 hours) were concentrated and analysed by Western blot. In the presence of holo-Lf, there was a significant increase in sAPP with subsequent sAPPβ and sAβ production ($p < 0.0001$) whereas treatment with holo-Tf resulted in no amyloidogenic fragment formation (Figure 5.2A). The increase in APP amyloidogenic processing in the presence of holo-Lf was detected and confirmed in primary murine neurons by Western blot. In the presence of holo-Lf, there was a significant increase in both sAPP and sAPPβ ($p < 0.0001$) in the neuronal media when compared to non-treated control cells (Figure 5.2B). In contrast, incubation with holo-Tf had no effect on generating APP amyloidogenic products (Figure 5.2B). Aβ levels within the media and cell lysate was also measured via double-antibody capture ELISA in SH-

SY5Y cells endogenously expressing APP incubated with holo-Lf and apo-Lf (500 nM; 2 hours) (Figure 5.2C). In the presence of holo-Lf, there was a significant increase in Aβ levels detected in both the media and cell lysate ($p < 0.01$) (Figure 5.2C) whereas incubation with apo-Lf had no effect on promoting Aβ production in SH-SY5Y cells.

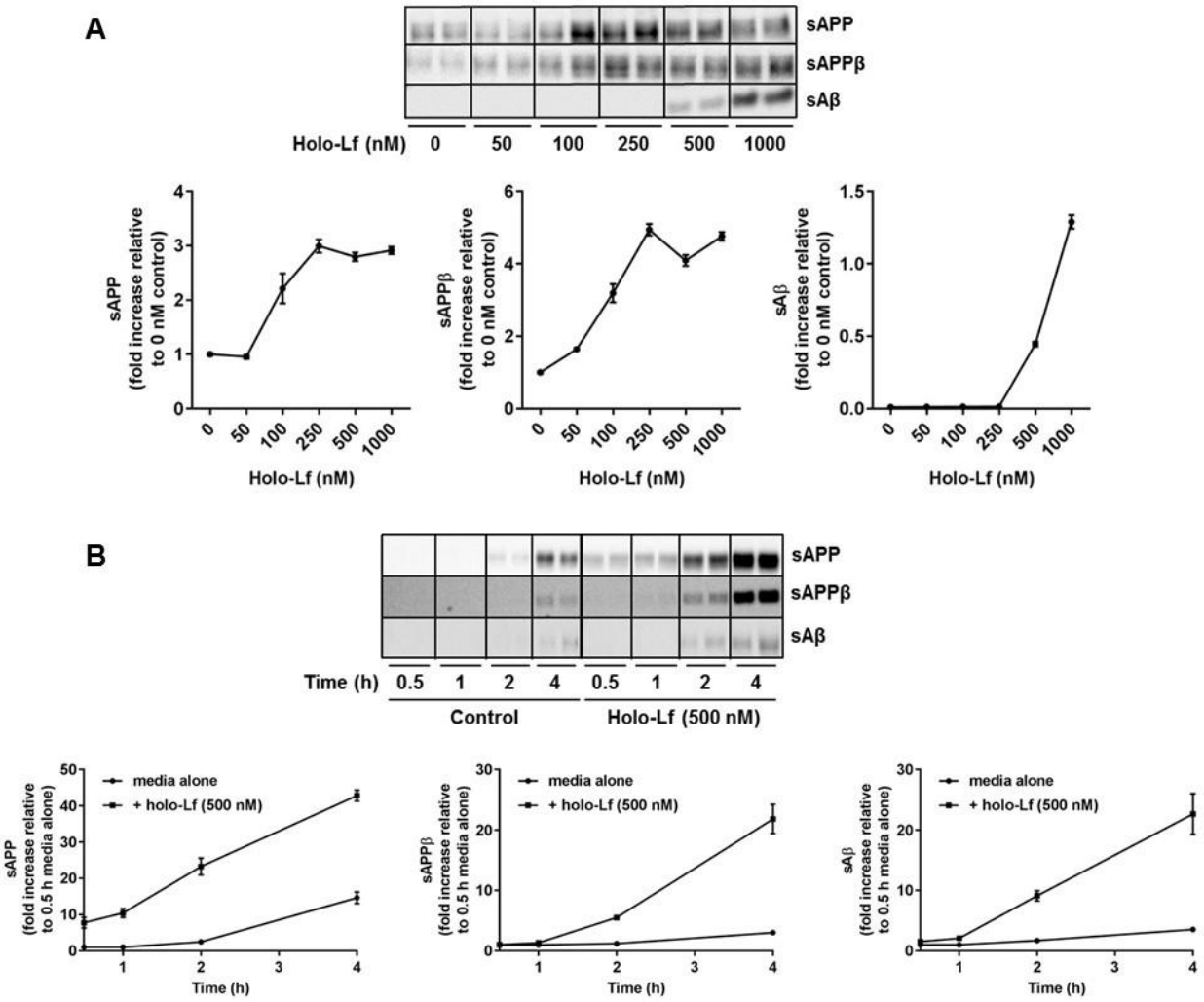

Figure 5.1. Holo-Lf dose and time-dependently promotes the amyloidogenic processing of APP. (A) SH-SY5Y cells were exposed to increasing amounts of holo-Lf (0-1000 nM) for 2 hours to determine optimal concentration. **(B)** SH-SY5Y cells were treated with 500 nM holo-Lf for 0.5, 1, 2, and 4 hours to determine optimal exposure time. Extracellular sAPP, sAPPβ and sAβ protein expression in the media were visualised by Western blot. Data are means ± SE of 3 experiments performed in duplicate. Quantified data depict fold increase relative to **(A)** non-treated control cells (0 nM) and the **(B)** 0.5 hour media alone treatment time.

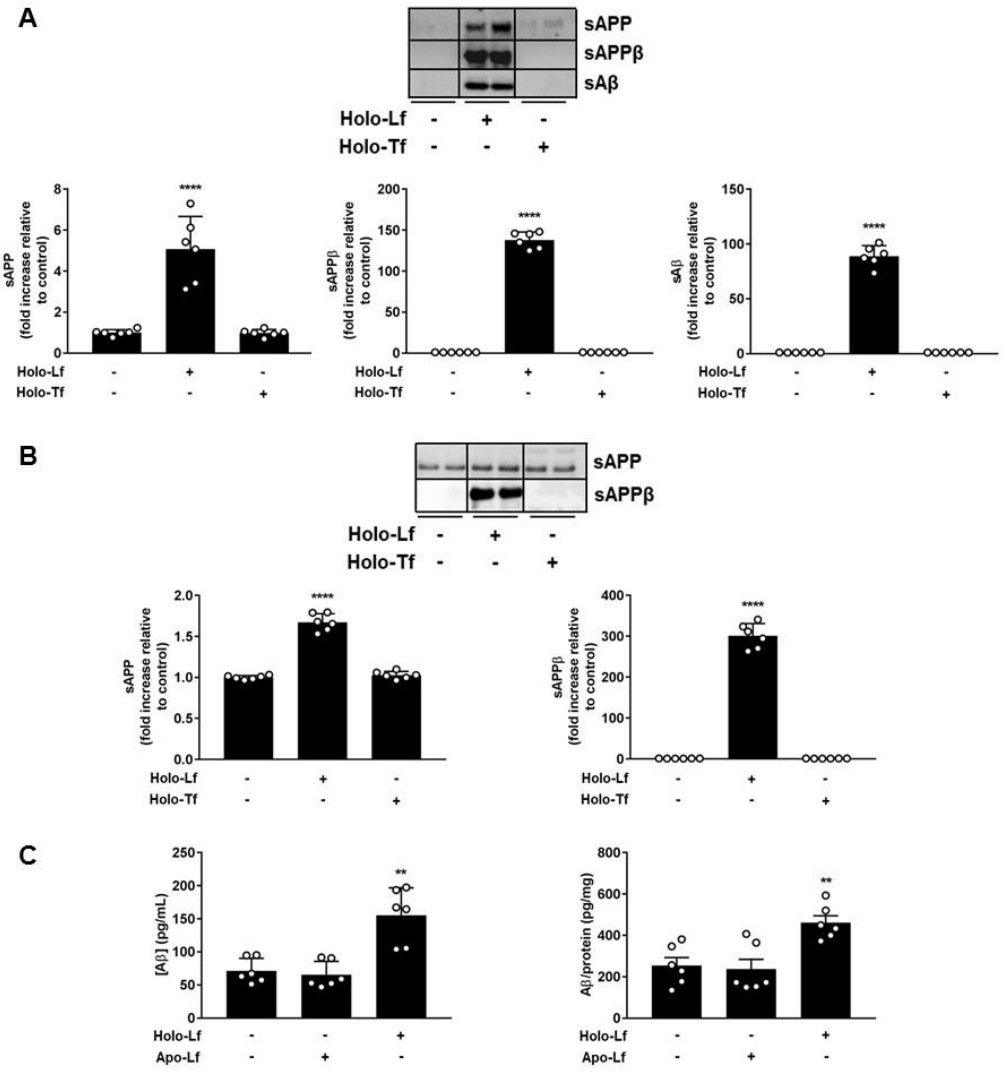

Figure 5.2. Holo-Lf promotes the amyloidogenic processing of APP. (A) SH-SY5Y-APP695 cells and **(B)** primary murine neuronal cultures were treated with holo-Lf and holo-Tf (500 nM; 2 hours) where levels of **(A & B)** sAPP and subsequent amyloidogenic sAPPβ and **(A)** sAβ production were measured in the media and visualised by Western blot. **(C)** Aβ production in the media and cell lysate from SH-SY5Y cells incubated with apo- and holo-forms of Lf (500 nM; 2 hours) were measured by double-antibody capture ELISA. Aβ levels were calculated by comparison to the values obtained from the synthetic $A\beta_{1-42}$ standards. Data are means ± SE of 3 experiments performed in duplicate. Quantified data depict fold increase compared to non-treated control cells, ** $p < 0.01$, **** $p < 0.0001$. **Preparation and isolation of mouse primary neuronal cultures with subsequent Western analysis of sAPP and sAPPβ (Figure 5.2B) was performed by Dr Bruce Wong (The University of Melbourne, Australia).**

5.2.2 Experimental conditions vary holo-Lf response to ADAM10 expression

ADAM10 is the main α-secretase enzyme that cleaves cell surface APP through the non-amyloidogenic pathway (Chow et al., 2010). Lf has been shown to promote non-amyloidogenic processing of APP resulting in an increase in ADAM10 protein expression in N2a cells overexpressing Swedish mutant human APP (N2a-APPSw) (Guo et al., 2017). We examined ADAM10 expression levels in SH-SY5Y and N2a cells overexpressing wild-type APP695 exposed to holo-Lf in treatment conditions comparable to those used by Guo *et al* (Guo et al., 2017). In the experimental parameters obtained from Figure 5.1, SH-SY5Y-APP695 cells subjected to 500 nM holo-Lf for 2 hours revealed a decrease in APP ($p < 0.001$) but no change in ADAM10 protein expression in the cell lysate (Figure 5.3A) when analysed by Western blot. Total APP was detected by an antibody recognising an epitope in the N-terminal of APP (22C11). N2a-APP695 cells that received the same treatment of holo-Lf showed unaltered levels of APP and ADAM10 when compared to non-treated control cells (Figure 5.3B). Following the treatment conditions by Guo *et al* (Guo et al., 2017), SH-SY5Y-APP695 cells that received 0.1 mg/ml holo-Lf for 24 hours revealed a decrease in both APP ($p < 0.0001$) and ADAM10 ($p < 0.01$) protein expression in the cell lysate (Figure 5.3C). N2a-APP695 cells that received the same treatment of holo-Lf also showed reduced levels of APP and ADAM10 when compared to non-treated control cells (Figure 5.3D). These results indicate that holo-Lf does not activate ADAM10 protein expression.

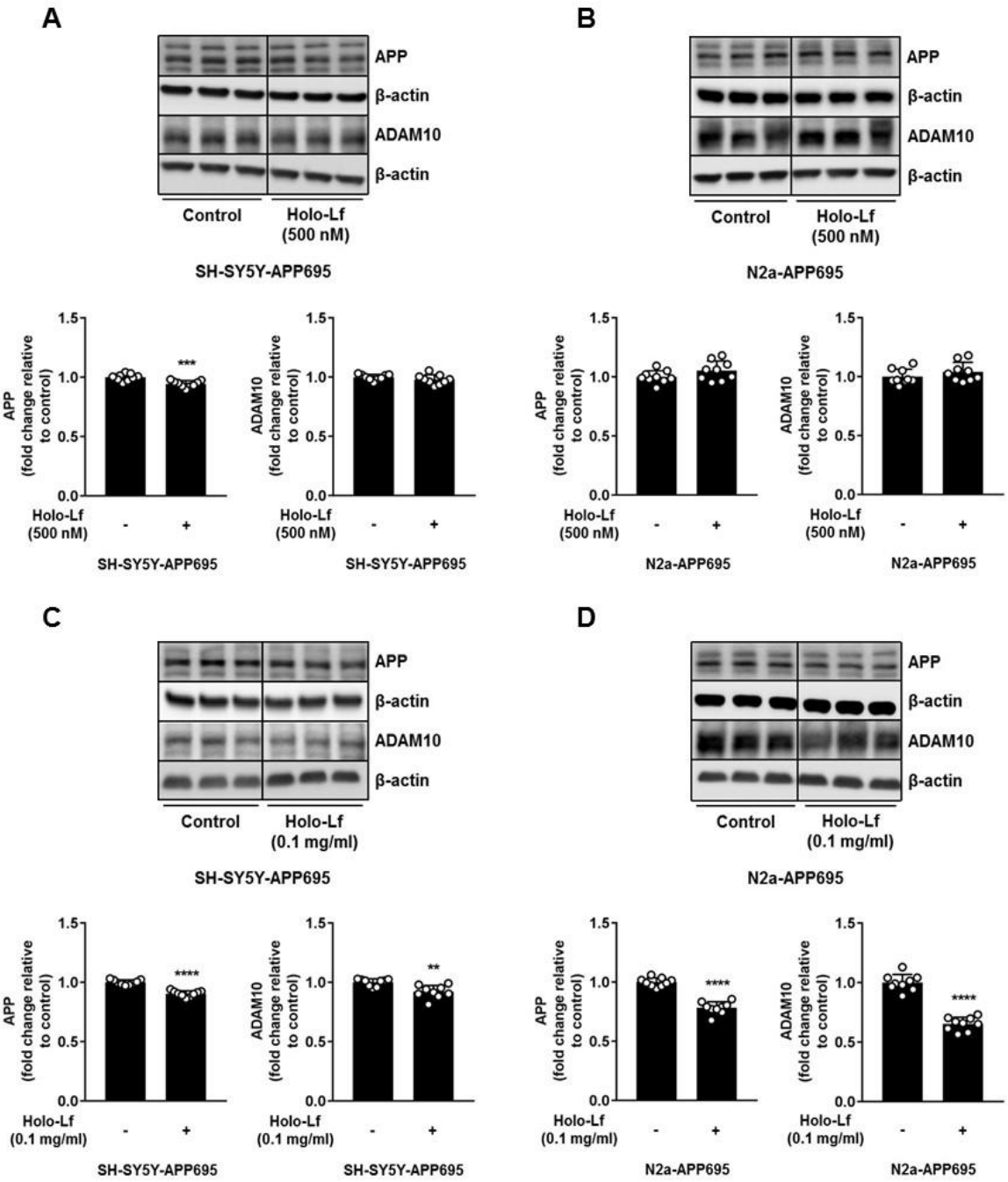

Figure 5.3. Experimental parameters vary holo-Lf effects on ADAM10 protein expression. (A) SH-SY5Y-APP695 and **(B)** N2a-APP695 cells were treated with holo-Lf (500 nM; 2 hours) while **(C)** SH-SY5Y-APP695 and **(D)** N2a-APP695 cells were serum starved for 24 hours followed by holo-Lf treatment (0.1 mg/ml) for an additional 24 hours. APP and ADAM10 protein expression in the cell lysate were analysed by Western blot and normalised against β-actin content. Data are means ± SE of 3 experiments performed in triplicate. Quantified data depict fold change compared to non-treated control cells, ** $p < 0.01$, *** $p < 0.001$, **** $p < 0.0001$.

5.2.3 Lf does not affect BACE1 enzyme activity

To account for the increased amyloidogenic processing of APP observed in the presence of holo-Lf, total BACE1 activity using a recombinant BACE1 enzyme (10 µM/reaction) in the presence of apo- and holo-Lf (20 µM) was examined. Upon adding the substrate (200 nM), measurements were recorded every 2 minutes for a total time of 90 minutes. Neither apo- nor holo-Lf influenced the activity of BACE1 (Figure 5.4). These results suggest that BACE1 activity is not affected by the presence of Lf.

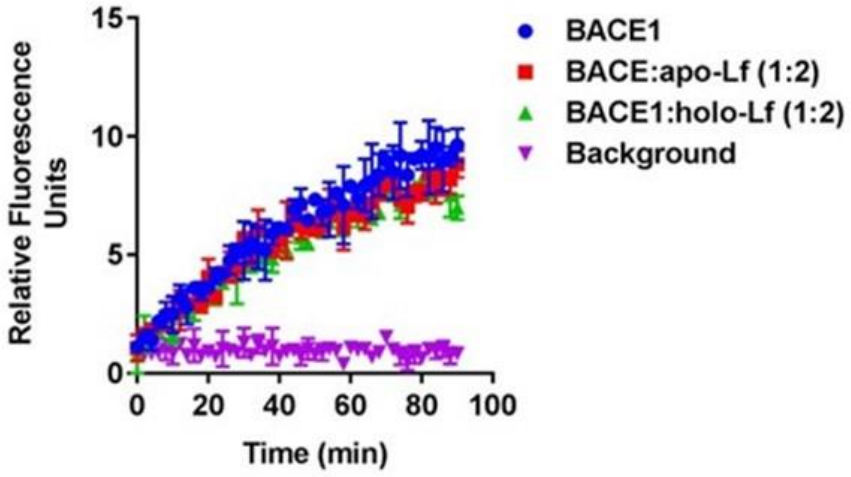

Figure 5.4. Lf does not affect BACE1 activity. Total BACE1 activity using human recombinant BACE1 in the absence (blue) and presence of apo-Lf (20 μM; red) and holo-Lf (20 μM; green). Activity was measured using the TruPoint™ β-Secretase Assay kit. Controls were prepared without the BACE1 enzyme (background; purple). Measurements were started immediately and taken every 2 minutes for a total time of 90 minutes. Data are means ± SE of 2 experiments performed in duplicate.

5.2.4 Depletion of cholesterol by MβCD reduces holo-Lf mediated amyloidogenic processing of APP

Earlier results have demonstrated that the internalisation of APP directed by holo-Lf is dependent upon membrane cholesterol (Chapter 4.2.4). To further substantiate these findings, the cholesterol content in the SH-SY5Y-APP695 plasma membrane was disrupted by MβCD treatment and the effect on holo-Lf directed APP amyloidogenic processing was investigated. SHSY5Y-APP695 cells treated with holo-Lf (500 nM) confirmed an increase of sAPPβ and sAβ ($p < 0.0001$) formation in the media (Figure 5.5A) and Aβ ($p < 0.0001$) production in the cell lysate (Figure 5.5B). In the absence of holo-Lf, cholesterol depletion with MβCD (1 mM; 3 hours) resulted in reduced levels of Aβ ($p < 0.0001$) in both the media (Figure 5.5A) and cell lysate (Figure 5.5B). Cholesterol depletion followed by holo-Lf treatment revealed a decrease in sAPPβ and Aβ formation in the media (Figure 5.5A) as well as reduced levels of Aβ in the lysate (Figure 5.5B). These findings demonstrate that holo-Lf mediated APP amyloidogenic processing can be diminished by reducing membrane cholesterol.

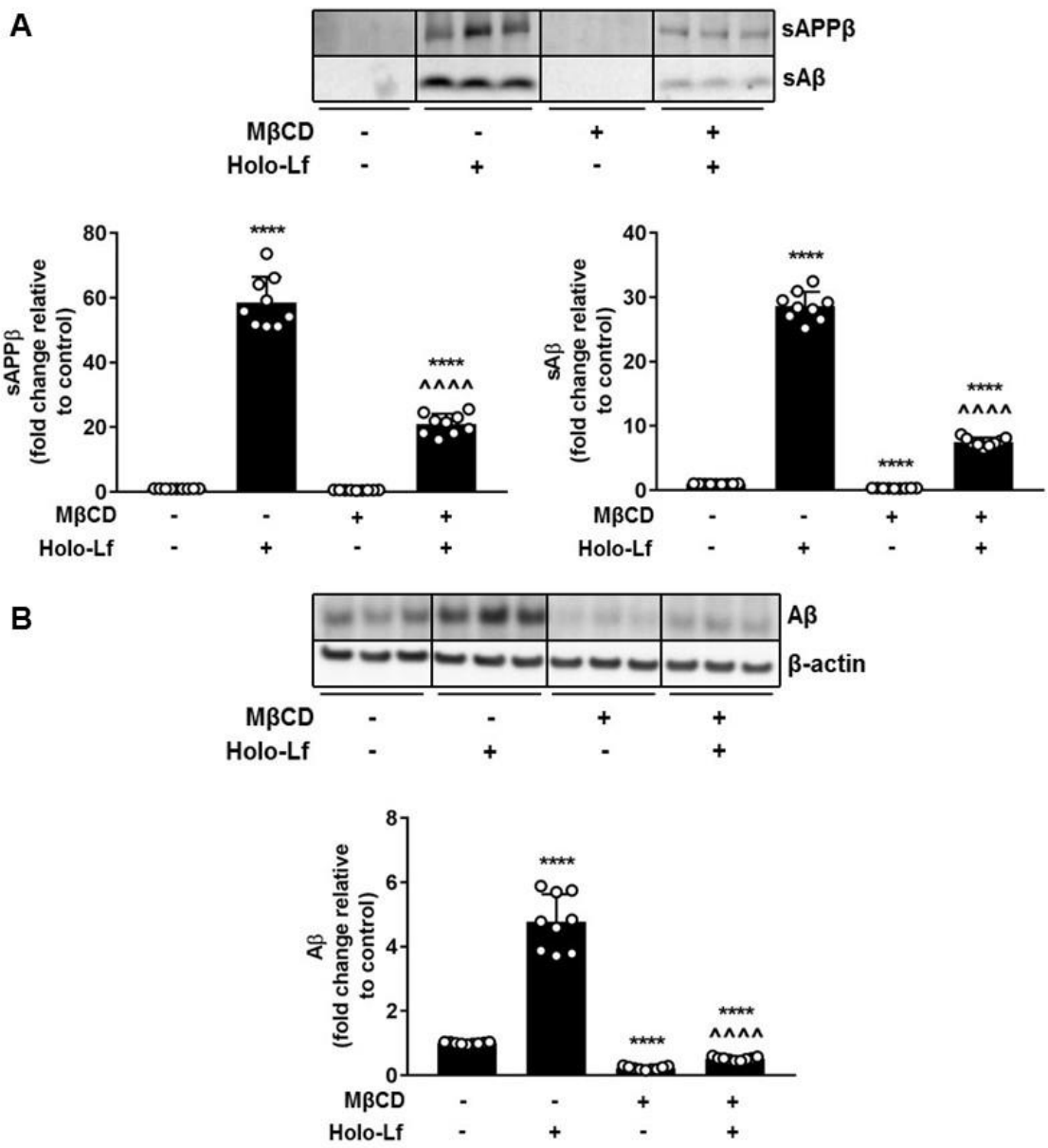

Figure 5.5. Depletion of cholesterol disrupts holo-Lf directed APP amyloidogenic processing. SH-SY5Y-APP695 cells were treated with MβCD (1 mM; 3 hours) followed by holo-Lf (500 nM; 2 hours) where levels of **(A)** sAPPβ and sAβ in the media and **(B)** Aβ in the cell lysate were visualised by Western blot. Data are means ± SE of 3 experiments performed in triplicate normalised to **(A)** total protein or **(B)** β-actin. **** $p < 0.0001$ compared to non-treated control and ^^^^ $p < 0.0001$ compared to holo-Lf only treated cells.

5.2.5 APP is diverted to the Rab11 GTPase-positive recycling endosome by holo-Lf to accelerate the amyloidogenic processing of APP

To examine the effects and intracellular location of holo-Lf directed APP amyloidogenic processing, the formation of APP amyloidogenic fragments sAPPβ and Aβ upon exposure to holo-Lf (500 nM; 2 hours) was investigated in SH-SY5Y-APP695 cells after treatment with RNAi to either CHC (40 nM), DYM (20 nM), ARF6 (20 nM), Rab4a (20 nM), Rab5a (20 nM), Rab7a (20 nM) or Rab11a (20 nM). In the absence of holo-Lf, the depletion of CHC, DYM (Figure 5.6), ARF6 (Figure 5.7), Rab5a, Rab7a (Figure 5.8), or Rab11a (Figure 5.9) by RNAi treatment reduced Aβ ($p < 0.0001$) formation within the media and cell lysate. However, Rab4a RNAi treatment reduced Aβ ($p < 0.0001$) in the media (Figure 5.9A) but increased Aβ ($p < 0.0001$) formation in the cell lysate (Figure 5.9B). This was also evident with cells co-transfected with Rab4a and Rab11a RNAi ($p < 0.0001$) (Figure 5.9). Upon addition of holo-Lf, CHC, DYM (Figure 5.6), Rab5a or Rab7a (Figure 5.8) depleted cells increased both sAPPβ production in the media and Aβ production in the media and cell lysate ($p < 0.0001$), whereas with Rab4a depleted cells, sAPPβ and sAβ in the media, and Aβ in the cell lysate remained unchanged compared to non-targeted treated cells (Figure 5.9). Reducing ARF6 or Rab11 by RNAi with subsequent holo-Lf treatment resulted in a significant decrease in sAPPβ detected within the media and Aβ formation detected in both the media (Figure 5.7A & Figure 5.9A respectively) and cell lysate (Figure 5.7B & Figure 5.9B respectively) ($p < 0.0001$). This also occurred in cells co-transfected with Rab4a and Rab11a RNAi ($p < 0.0001$) (Figure 5.9). Taken together, these results indicate that the intracellular endocytic location of Aβ production exacerbated by holo-Lf is predominantly within the Rab11 GTPase-positive recycling endosome.

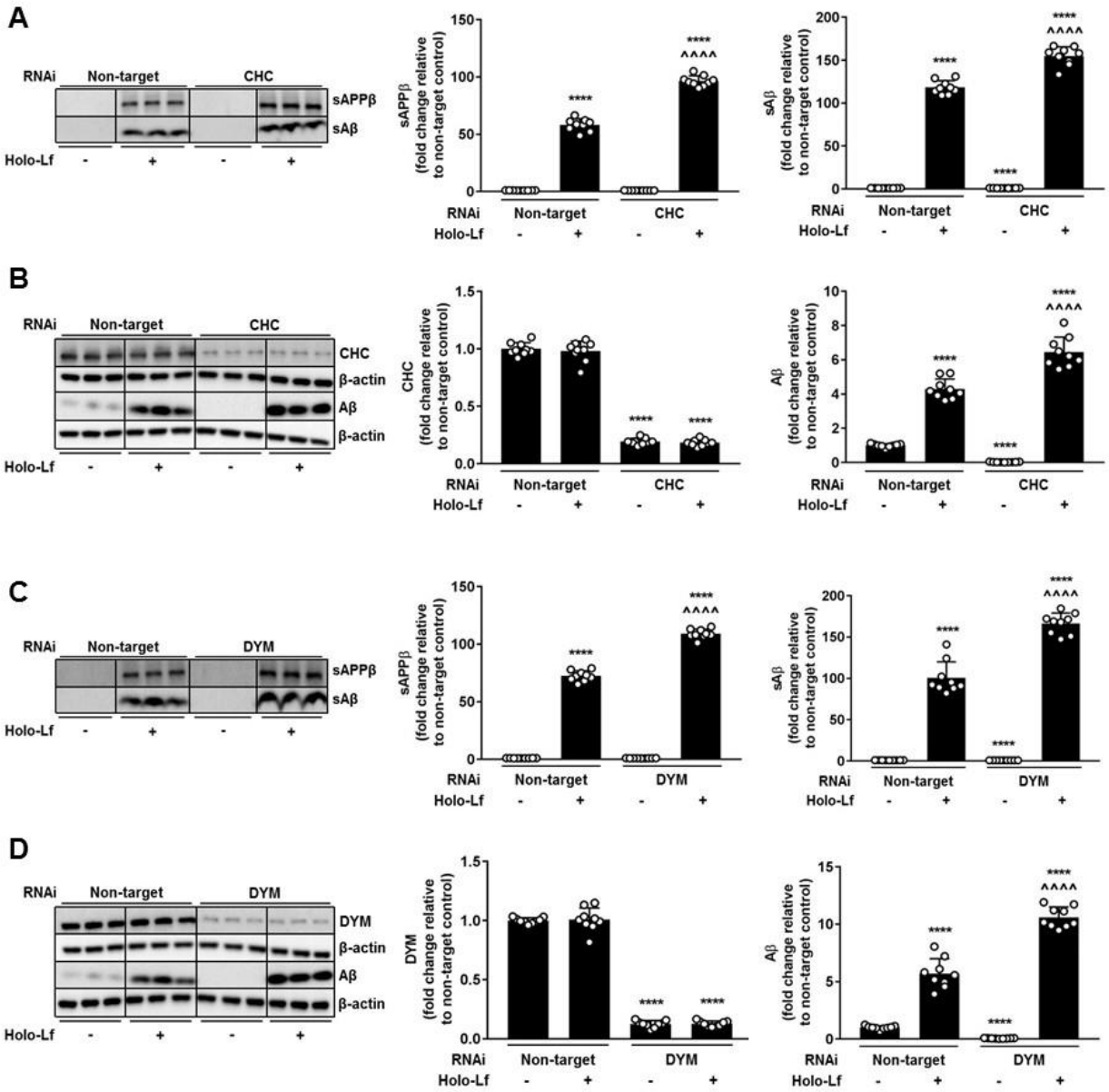

Figure 5.6. Holo-Lf mediated APP endocytosis does not require clathrin or dynamin for the amyloidogenic processing of APP. SH-SY5Y-APP695 cells were treated with holo-Lf (500 nM; 2 hours) after being transfected with **(A & B)** control non-target and CHC RNAi (40 nM) for 72 hours or **(C & D)** control non-target and DYM RNAi (20 nM) for 48 hours. **(A & C)** Extracellular sAPPβ and sAβ in the media, **(B)** CHC, **(D)** DYM and **(B & D)** Aβ protein expression in the cell lysate were visualised by Western blot. Data are means ± SE of 3 experiments performed in triplicate normalised to **(A & C)** total protein or **(B & D)** β-actin. **** $p < 0.0001$ compared to non-target control and ^^^^ $p < 0.0001$ compared to holo-Lf treated non-target cells.

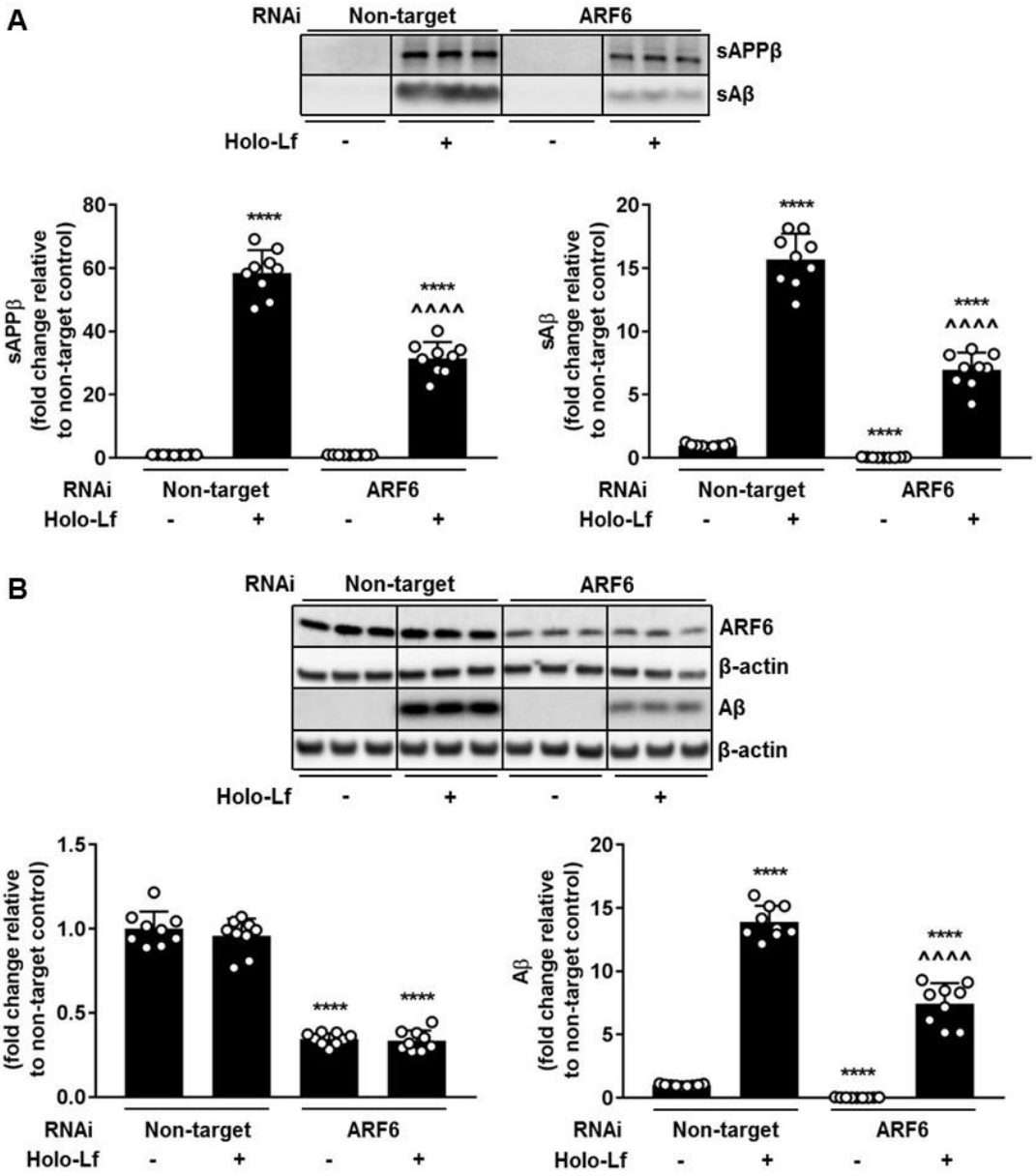

Figure 5.7. Reducing ARF6 associated endocytosis of holo-Lf and APP alleviates APP amyloidogenic processing. SH-SY5Y-APP695 cells were treated with holo-Lf (500 nM; 2 hours) after being transfected with control non-target and ARF6 RNAi (20 nM) for 48 hours. **(A)** Extracellular sAPPβ and sAβ in the media, and **(B)** ARF6 and Aβ protein expression in the cell lysate were visualised by Western blot. Data are means ± SE of 3 experiments performed in triplicate normalised to **(A)** total protein or **(B)** β-actin. **** $p < 0.0001$ compared to non-target control and ^^^^ $p < 0.0001$ compared to holo-Lf treated non-target cells.

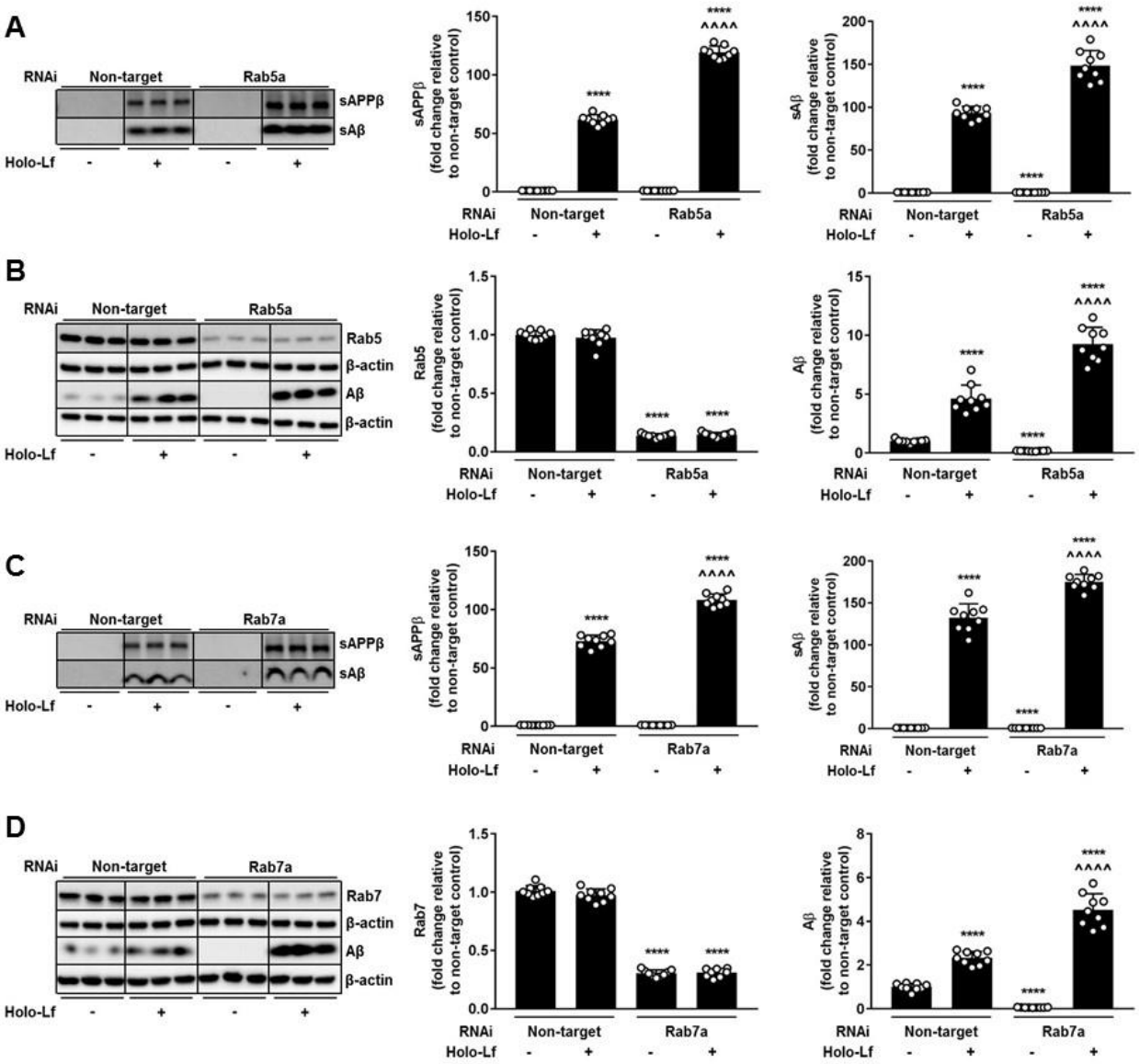

Figure 5.8. Rab5 and Rab7-positive endocytic compartments are not sites for holo-Lf mediated APP amyloidogenic processing. SH-SY5Y-APP695 cells were treated with holo-Lf (500 nM; 2 hours) after being transfected with **(A & B)** control non-target and Rab5a RNAi (20 nM) or **(C & D)** control non-target and Rab7a RNAi (20 nM) for 48 hours. **(A & C)** Extracellular sAPPβ and sAβ in the media, **(B)** Rab5, **(D)** Rab7 and **(B & D)** Aβ protein expression in the cell lysate were visualised by Western blot. Data are means ± SE of 3 experiments performed in triplicate normalised to **(A & C)** total protein or **(B & D)** β-actin. **** $p < 0.0001$ compared to non-target control and ^^^^ $p < 0.0001$ compared to holo-Lf treated non-target cells.

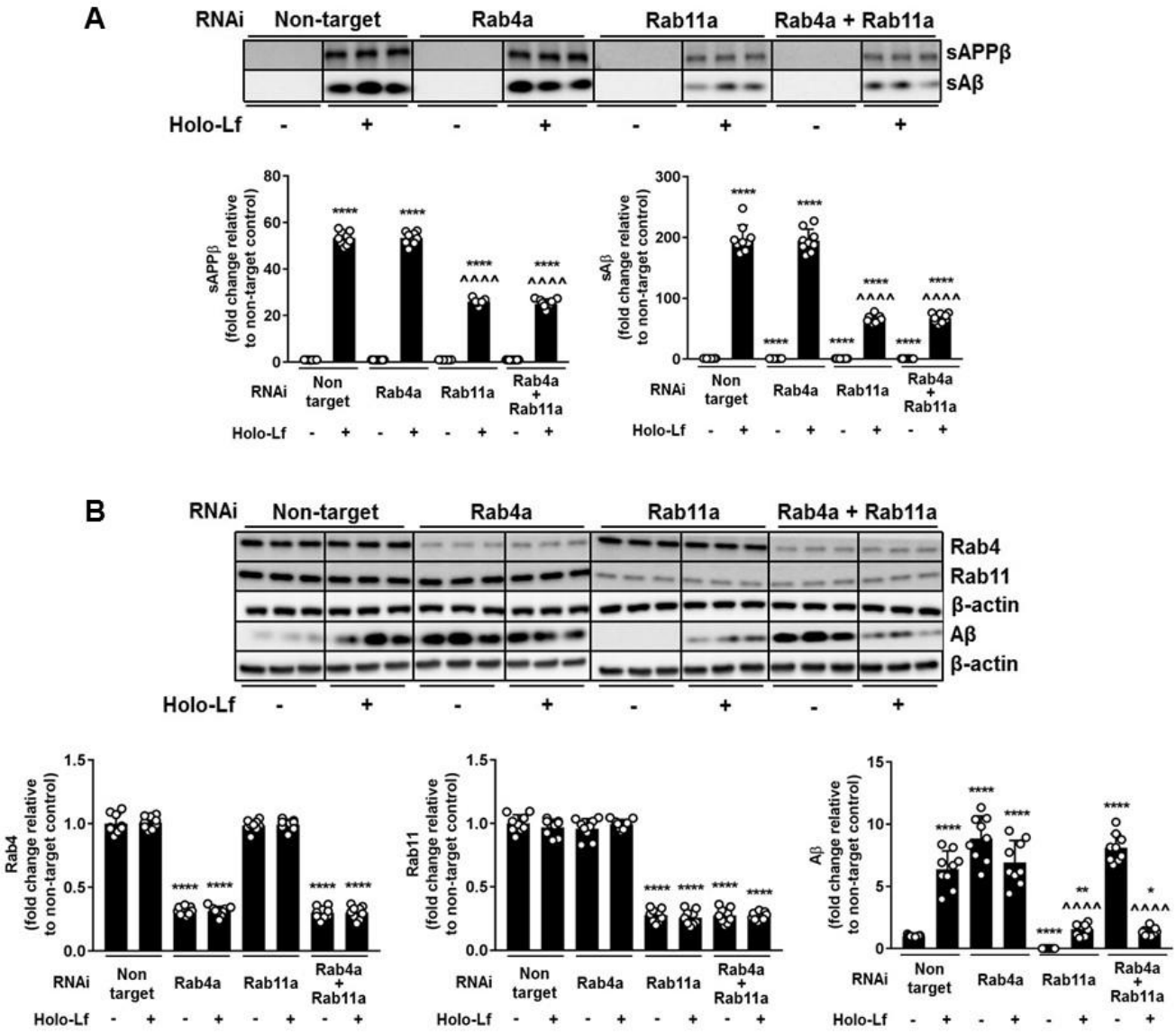

Figure 5.9. Holo-Lf directs APP to the Rab11-positive recycling endosome for the amyloidogenic processing of APP. SH-SY5Y-APP695 cells were treated with holo-Lf (500 nM; 2 hours) after being transfected with control non-target, Rab4a and/or Rab11a RNAi (20 nM; 48 hours). **(A)** Extracellular sAPPβ and sAβ in the media, and **(B)** Rab4, Rab11 and Aβ protein expression in the cell lysate were visualised by Western blot. Data are means ± SE of 3 experiments performed in triplicate normalised to **(A)** total protein or **(B)** β-actin. * $p < 0.05$, ** $p < 0.01$ and **** $p < 0.0001$ compared to non-target control and ^^^^ $p < 0.0001$ compared to holo-Lf treated non-target cells.

5.2.6 APP blocking peptides disrupts the interaction between Lf and APP and dose-dependently decreases amyloidogenic sAPPβ and sAβ production

To hinder the binding of holo-Lf to APP and assess amyloidogenic protein formation, 15-mer APP peptides known to specifically bind to holo-Lf via the APP peptide array (Chapter 3.2.3) were custom synthesised. APP peptides 40, 48, 49, 50 and 55 dissolved in DMSO were pre-incubated at varying concentrations with holo-Lf (500 nM) for 2 hours. Incubated holo-Lf and peptide was added to the media of SH-SY5Y-APP695 cells for 2 hours and dose-responses to sAPPβ formation was measured by Western blot. Each peptide incubated with holo-Lf dose-dependently decreased APP amyloidogenic sAPPβ production in SH-SY5Y-APP695 cells compared to holo-Lf treated control cells (Figure 5.10). IC_{50} values of each peptide to reduce amyloidogenic sAPPβ formation are listed in Table 5.1. APP peptide alone in each respective concentration exposed to SH-SY5Y-APP695 cells did not result in any sAPPβ formation (data not shown).

Peptide 49 proved to be one of the most effective blocking peptides in impeding the binding of holo-Lf to APP and was therefore further investigated in combination with peptides 40 and 55. Holo-Lf (500 nM) was pre-incubated with peptide 49 (5 μM and 10 μM) combined with either peptide 40 or 55 at a 1:1 ratio for 2 hours, then added to the media of SH-SY5Y-APP695 cells for a further 2 hours. Amyloidogenic fragments released into the media were measured by Western blot. Peptide 49 combined with either 40 or 55 at 5 μM masked the binding sites of holo-Lf which significantly decreased APP amyloidogenic sAPPβ and sAβ production in SH-SY5Y-APP695 cells compared to holo-Lf alone treated cells ($p < 0.0001$) (Figure 5.11). 10 μM of 49 compared to 5 μM of 49 with 5 μM of 40 or 55 had no additional effect on inhibiting sAPPβ and sAβ production, whilst 20 μM of total peptide, that is, 10 μM of 49 with 10 μM of 40 or 55 resulted in total inhibition of sAPPβ and sAβ production ($p < 0.0001$) (Figure 5.11). Taken together, the APP peptide sequence of 49 combined with 40 or 55 blocks the ability of APP to bind holo-Lf and that masking these sites diminishes amyloidogenic sAPPβ and sAβ production caused by holo-Lf in SH-SY5Y-APP695 cells.

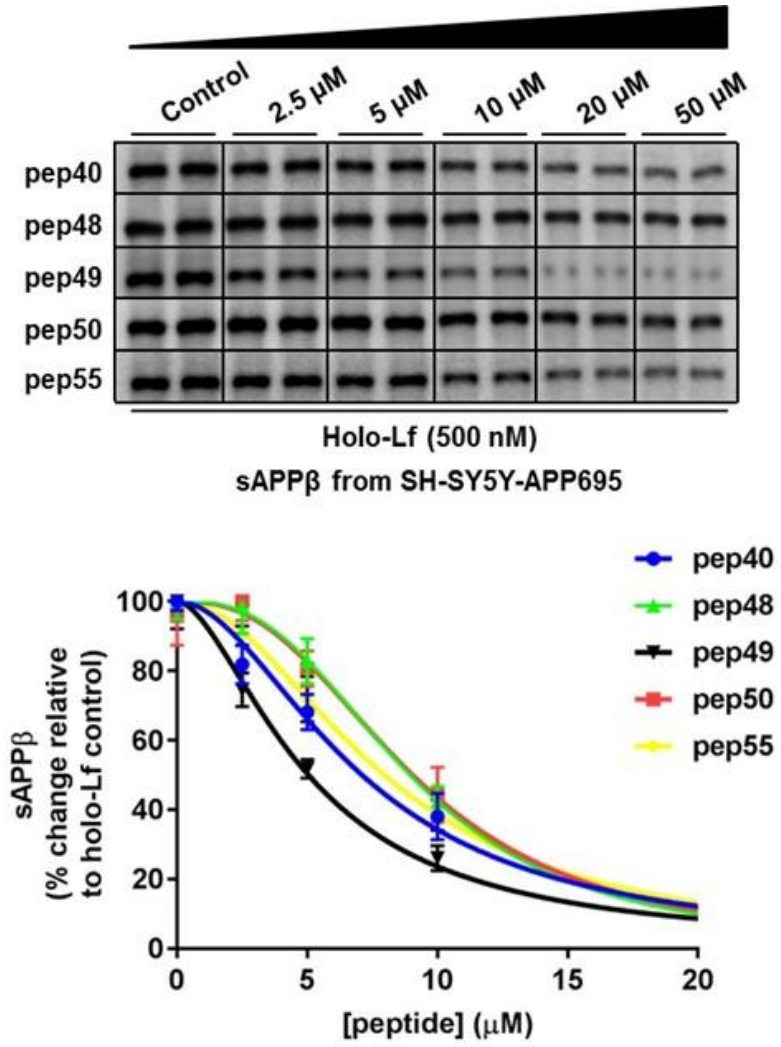

Figure 5.10. APP blocking peptides disrupts the interaction between Lf and APP and dose-dependently decreases amyloidogenic sAPPβ production. APP peptides 40, 48, 49, 50 and 55 were each pre-incubated with holo-Lf (500 nM) in x5 (2500 nM), x10 (5000 nM), x20 (10,000 nM), x50 (25,000 nM) and x100 (50,000 nM) excess for 2 hours, then added to the media of SH-SY5Y-APP695 cells for a further 2 hours. Amyloidogenic sAPPβ in the media was visualised by Western blot. Data are means ± SE of 2 experiments performed in duplicate normalised to total protein. Quantified data depict % change relative to holo-Lf only treated cells.

Table 5.1. Peptide IC_{50} values determined by Western blot for amyloidogenic sAPPβ reduction

Peptide	sAPPβ reduction IC_{50} (μM)
40	7.10 ± 0.38
48	8.95 ± 0.31
49	5.05 ± 0.19
50	9.04 ± 0.36
55	7.96 ± 0.36

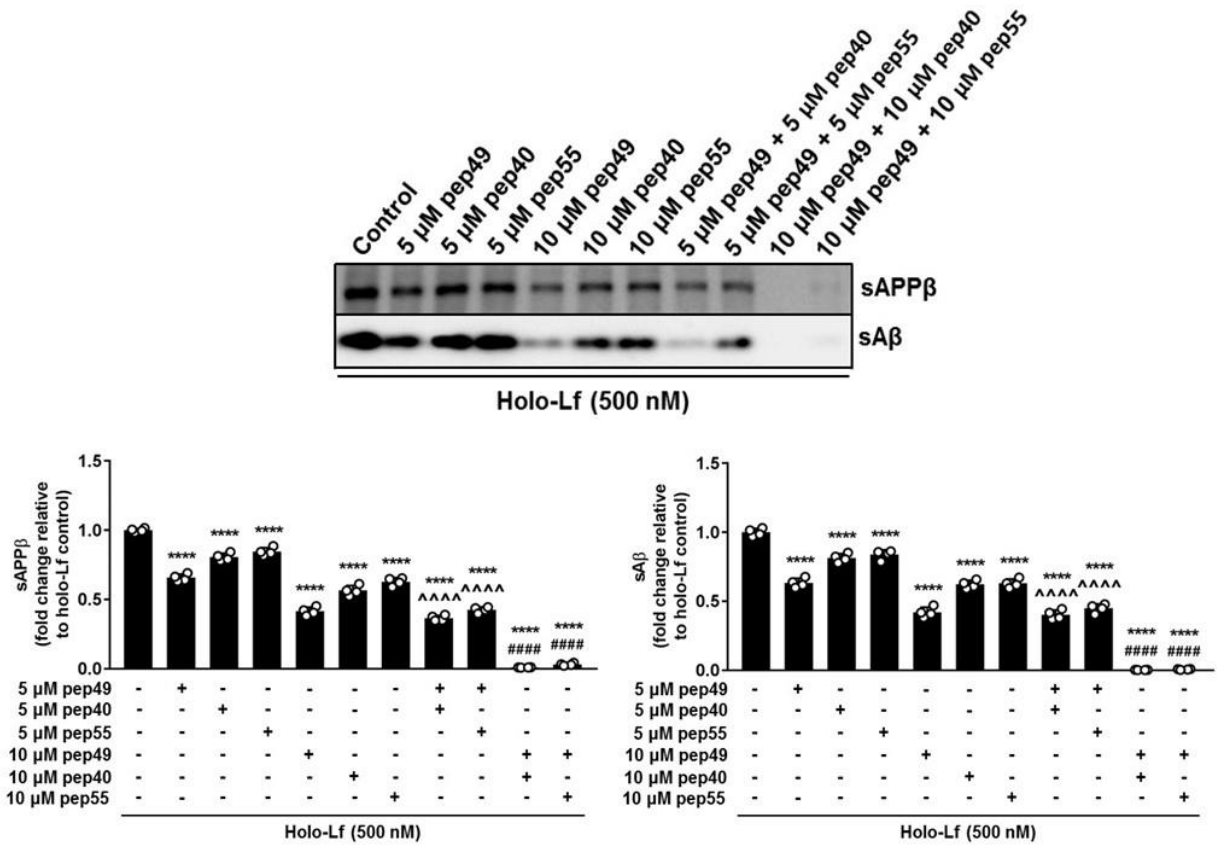

Figure 5.11. Combinations of APP peptides 49, 40 and 55 alleviates APP amyloidogenic processing mediated by holo-Lf. Holo-Lf (500 nM) was pre-incubated with either 5 µM or 10 µM of APP peptide 49 combined with 5 µM or 10 µM of APP peptide 40 or 55 respectively for 2 hours, then applied to the media of SH-SY5Y-APP695 cells and incubated for a further 2 hours. Extracellular sAPPβ and sAβ in the media were visualised by Western blot. Data are means ± SE of 2 experiments performed in duplicate normalised to total protein. **** $p < 0.0001$ compared to holo-Lf only treated, ^^^^ $p < 0.0001$ compared to 5 µM peptide 49, and #### $p < 0.0001$ compared to 10 µM peptide 49 treated cells.

5.3 Discussion

In this chapter, we explored what impact holo-Lf directed APP internalisation and trafficking had on the main processing pathways of APP. Through various techniques to monitor APP and Lf trafficking through the cell, holo-Lf increased the amyloidogenic cleavage of APP within Rab11-positive recycling endosomes, resulting in the exacerbation of Aβ production. By masking the contact sites on holo-Lf for APP, we were able to dose-dependently alleviate holo-Lf mediated APP amyloidogenic processing, signifying holo-Lf as a potential therapeutic target.

We first investigated what impact holo-Lf had on the amyloidogenic pathway of APP. We determined the necessary concentration and exposure time of holo-Lf to exacerbate the amyloidogenic pathway of APP and found increasing levels of sAPP, sAPPβ and sAβ in a time and dose-dependent manner in SH-SY5Y cells (Figure 5.1). An increase in Aβ production in the media and cell lysate from SH-SY5Y cells with holo-Lf treatment was also detected via double-antibody capture ELISA (Figure 5.2C). Through an alternative mechanism to that associated with Tf, holo-Lf exacerbated the amyloidogenic processing of APP in SH-SY5Y-APP695 cells (Figure 5.2A) which was also demonstrated in primary murine neurons (Figure 5.2B). There was a correlation between sAPPβ and Aβ formation, suggesting that BACE1 β-cleavage is either the rate limiting step and therefore determines total Aβ levels or that the intracellular sites that harbour β-cleavage are also involved in γ-secretase cleavage of APP to produce Aβ (Chow et al., 2010; Koo et al., 1996; Udayar et al., 2013). BACE1 and APP on the plasma membrane are found in separate regions and only co-localise via receptor mediated endocytosis, upon which BACE1 cleaves APP to produce sAPPβ. The remaining fragment is subsequently cleaved by the γ-secretase complex to produce Aβ (Chow et al., 2010; Zheng and Koo, 2011).

The main emphasis of the study performed by Guo *et al* was the ability of Lf to promote the non-amyloidogenic pathway of APP in N2a-APPSw cells, resulting in an increase in ADAM10 protein expression (Guo et al., 2017). Therefore, we investigated ADAM10 expression levels in the presence of holo-Lf by replicating the experimental parameters specified by Guo *et al* (0.1 mg/ml holo-Lf; 24 hours) (Guo et al., 2017) in addition to our own (500 nM holo-Lf; 2 hours) in human SH-

SY5Y and mouse N2a neuroblastomas overexpressing wild-type APP695. In the experimental parameters used within this study, there was a decrease in total APP levels with unaltered ADAM10 protein expression in SH-SY5Y-APP695 cells (Figure 5.3A) with unchanged total APP and ADAM10 protein levels in N2a-APP695 cells (Figure 5.3B). Using the experimental parameters specified by Guo *et al*, a decrease in total APP levels (Guo et al., 2017) in the presence of holo-Lf was evident in both SH-SY5Y and N2a overexpressing APP695 cells (Figure 5.3C & D). The decrease in total APP levels with holo-Lf can be explained by earlier findings that indicate holo-Lf to facilitate APP amyloidogenic processing, resulting in an increase in soluble APP fragments released into the media (Figure 5.1). However, holo-Lf failed to upregulate ADAM10 and in contrast caused a decrease in ADAM10 protein expression in both cell lines (Figure 5.3C & D). Studies have shown an increase in β-processing reduces α-secretase cleavage of APP and vice versa (Skovronsky et al., 2000; Vassar, 2013). Therefore, the predominant amyloidogenic APP processing mediated by holo-Lf could induce a negative feedback regulatory mechanism resulting in the loss of ADAM10. It is also possible that the downregulation of ADAM10 caused by holo-Lf could subsequently force APP to shift towards the amyloidogenic pathway for β-secretase processing. These results indicate that holo-Lf does not activate ADAM10 expression and therefore does not promote the non-amyloidogenic pathway of APP.

The inconsistencies between groups may be explained by a number of associated reasons. Firstly, the iron-binding status of Lf could be a defining factor where multiple studies have shown Lf to possess varying functions according to its iron saturation state (Rosa et al., 2017). In accordance with this notion, we have previously shown the iron-binding status of Lf to affect the interaction with APP (Chapter 3.0). Only when Lf is bound to iron (holo-Lf) can it directly bind and interact with APP, whereas in its iron-unsaturated form (apo-Lf) it cannot. The large conformational differences observed between apo-Lf and holo-Lf (Grossmann et al., 1992; Jameson et al., 1998; Querinjean et al., 1971) can lead to the exposure of different binding sites and may cause alternative binding partners to interact with the different Lf forms (Grossmann et al., 1992; Jameson et al., 1998; Lopez et al., 2008). Whether Lf was in its apo or holo form was not addressed by Guo *et al*. Secondly, to examine sAPPα secretion levels in the

presence of Lf *in vitro*, the authors failed to detect secreted APPα in cell supernatant samples and instead were prompted to perform Western analysis on cell lysate samples (Guo et al., 2017). The predominant cellular location of APP cleavage by ADAM10 through the non-amyloidogenic pathway is on the cell surface where APPα is released into the extracellular medium (Culvenor et al., 1995; Koo et al., 1996). Lastly, Guo *et al* examined the effects of Lf on both the non-amyloidogenic and amyloidogenic pathways of APP in cell culture and AD mouse models transgenetically overexpressing a mutant form of APP that already selectively processes APP through the amyloidogenic pathway (i.e. familial Swedish APP) (Citron et al., 1992; Sasaguri et al., 2017; Thinakaran et al., 1996b). AD models harbouring the familial Swedish APP mutation have shown the cellular location of β-secretase cleavage of this mutant form of APP to preferentially occur in the Golgi apparatus, consequently diminishing levels of cell surface APP (Thinakaran et al., 1996b). Therefore, this increase in programmed amyloidogenic APP processing could indeed mask the effects that we have shown with Lf accelerating the amyloidogenic pathway of APP. In addition, without the presence of APP on the cell surface, extracellular (holo) Lf would not be able to bind and internalise APP destined for amyloidogenic processing by β- and γ-secretases in the endocytic compartments. Perhaps a more suitable AD mouse model would be I5 (Line B6.Cg-Tg (PDGFB-APP) 5Lms/J) mice that overexpress human wild-type APP, under the control of the human platelet derived growth factor, β polypeptide (PDGFB) promoter. While mice exhibit minimal levels of Aβ deposition in a normal environment (Borchelt et al., 1996; Guo et al., 1999; Kitazawa et al., 2012; Mucke et al., 2000), they may be a more suitable transgenic mouse line for monitoring the processing pathways of wild-type APP in sporadic AD or under conditions where there is an elevated presence of Lf.

The β-secretase enzyme in the brain that contributes to AD neuropathology has been identified as BACE1 (Evin and Weidemann, 2002; Vassar et al., 1999). Furthermore, BACE1 expression and activity are both elevated in the AD brain (Holsinger et al., 2002; Yang et al., 2003). We therefore explored whether holo-Lf increased the enzymatic activity of BACE1, attributing to the accelerated amyloidogenic processing of APP. Holo-Lf failed to alter the fluorescence of BACE1 enzymatic activity (Figure 5.4), indicating that Lf does not directly affect

BACE1 cleavage. Of note, the substrate used to measure BACE1 enzymatic activity was a small peptide containing the cleavage site for BACE1 and not APP itself. Whilst APP and BACE1 may be present at separate regions of the lipid raft domain, endocytosis brings APP and BACE1 together enabling β-secretase processing of APP within endosomes (Cataldo et al., 2004; Chow et al., 2010; Daugherty and Green, 2001). Whether holo-Lf indirectly affects BACE1 by shifting APP from non-lipid raft to lipid raft regions of the plasma membrane coinciding with BACE1, thereby increasing the proximity and co-localisation of APP and BACE1 for increased APP amyloidogenic processing is also a possibility and warrants further investigation.

To understand the mechanism by which holo-Lf facilitates the production of Aβ via the APP amyloidogenic pathway, we modified the same specific components and early regulators of APP endocytosis as we did in Chapter 4.0. In the absence of holo-Lf, our data supports previous studies that indicate lowering cell membrane cholesterol levels results in a decrease in total Aβ production (Figure 5.5) (Ehehalt et al., 2003; Kojro et al., 2001). In the presence of holo-Lf, an accumulation of sAPPβ and total Aβ (Figure 5.5) confirmed earlier findings that holo-Lf induces the amyloidogenic pathway of APP (Chapter 5.2.1). However, when membrane cholesterol levels were depleted in cells, sAPPβ and total Aβ production decreased (Figure 5.5) which correlated with reduced levels of holo-Lf mediated APP internalisation (Chapter 4.2.4). Whilst APP and BACE1 may be present at separate regions of the lipid raft domain, endocytosis brings APP and BACE1 together enabling β-secretase processing of APP within endosomes (Chow et al., 2010; Zheng and Koo, 2011). Therefore, reducing the cholesterol level in cells limits APP and BACE1 internalisation, reducing amyloidogenic cleavage of APP and Aβ formation (Cossec et al., 2010; Ehehalt et al., 2003). Data presented here not only supports that holo-Lf mediated APP internalisation is cholesterol-dependent but also confirms that endocytosis of APP (facilitated by holo-Lf) is required for APP amyloidogenic processing and the generation of Aβ.

APP internalisation is via a clathrin and DYM-dependent pathway (Cossec et al., 2010; Motley et al., 2003) whereas BACE1 is internalised into the cell via an ARF6-dependent mechanism (Sannerud et al., 2011; Tang et al., 2015). When both are present within the early endosome, then the environment within the vesicle is conducive for the pH-dependent BACE1 activity to optimally cleave

APP where subsequent APP fragments including Aβ are then secreted (Udayar et al., 2013). In the absence of holo-Lf, our data supports previous evidence in which silencing the CHC and DYM prevents APP endocytosis (Chapter 4.2.5) which coincides with a reduction in the amyloidogenic processing of APP (Figure 5.6) (Carey et al., 2005; Cossec et al., 2010; Motley et al., 2003). However, in the presence of holo-Lf, APP internalisation was via a clathrin and dynamin-independent pathway (Chapter 4.2.5), resulting in a concomitant increase in sAPPβ and Aβ (Figure 5.6). This can be explained by the associated increase in both cell surface APP and holo-Lf internalisation in CHC and DYM depleted cells (Chapter 4.2.5). Silencing ARF6 in cells also interrupted the amyloidogenic processing of APP (Figure 5.7) since ARF6 is required by BACE1 to gain entry into the cell to cleave APP within endosomes (Sannerud et al., 2011). Given that our previous findings elucidated holo-Lf to internalise APP via an ARF6-dependent pathway (Chapter 4.2.5), silencing ARF6 in the presence of holo-Lf also reduced levels of sAPPβ and Aβ (Figure 5.7) not only by limiting BACE1 internalisation but also preventing holo-Lf mediated APP endocytosis (Chapter 4.2.5). Intriguingly, the ARF6 expression profile is altered in AD brains, and this accordingly correlates with neurotoxic Aβ formation in the hippocampus of AD brains (Braak et al., 2006; Tang et al., 2015), suggesting that ARF6 may have a key role in AD pathology.

Previous findings have stipulated that holo-Lf directs APP to Rab11-positive endosomes (Chapter 4.2.6). Whether this was the primary site for holo-Lf mediated APP amyloidogenic processing was investigated. The Rab4, Rab5 and Rab11 GTPases are predominantly associated with the early endocytic pathway (McCaffrey et al., 2001; Trischler et al., 1999), whereas Rab7 is more linked to the late endocytic pathway (Vitelli et al., 1997). Rab4 and Rab11 GTPases both regulate the recycling of intracellular cargo back to the plasma membrane (Hsu and Prekeris, 2010; Li and DiFiglia, 2012). Despite Rab5, Rab7 and Rab11 compartments reported to be the sites of β-, and γ-secretase cleavage of APP (Ginsberg et al., 2010b; Grbovic et al., 2003; Udayar et al., 2013), the primary route for APP processing involves Rab5 (Xu et al., 2018) and Rab7 (Feng et al., 1995) dependent vesicles. Data presented here confirms Aβ production associated with all three endocytic compartments, with a significant decrease in Aβ levels when cells were treated with Rab5a, Rab7a (Figure 5.8) or Rab11a

(Figure 5.9) RNAi. However, silencing Rab4a decreased Aβ secretion but accumulated Aβ in the cell lysate which was comparable to total Aβ levels in cells depleted of both Rab4a and Rab11a (Figure 5.9), indicating β-, and γ-secretase cleavage of APP within Rab5-positive endosomes requires Rab4-positive vesicles to secrete the generated Aβ (Arriagada et al., 2007; Udayar et al., 2013). In the presence of holo-Lf, an accumulation of sAPPβ and Aβ levels were observed with Rab5a and Rab7a RNAi treatment (Figure 5.8), concomitant to the increase in both cell surface APP and holo-Lf internalisation in Rab5a and Rab7a depleted cells (Chapter 4.2.6). In contrast, Rab11a depletion revealed a decrease in sAPPβ and Aβ production while Rab4a depletion caused no change in sAPPβ and Aβ in the media and cell lysate (Figure 5.9). When cells were depleted of both Rab4a and Rab11a, sAPPβ and total Aβ levels were akin to sAPPβ and total Aβ levels obtained from only Rab11a depleted cells (Figure 5.9), suggesting that unlike Rab4, Rab11 regulates Aβ production rather than secretion (Udayar et al., 2013). Data presented here indicate that the primary site of Aβ generation facilitated by holo-Lf directed APP amyloidogenic processing is in Rab11-positive endosomes. Refer to Figure 5.12 for a schematic overview of Aβ production and secretion in the absence and presence of holo-Lf in cells depleted of Rab4a, Rab11a and double Rab4a/Rab11a.

Studies have indicated silencing Rab11 *in vitro* leads to a decrease in Aβ production (Udayar et al., 2013), suggesting BACE1 and the γ-secretase complex to be present in Rab11-positive recycling compartments. Furthermore, Rab11 has been shown to directly traffic BACE1 to recycling compartments in the axons of primary neurons (Buggia-Prevot et al., 2014) as well as interact with PSEN1 of the γ-secretase complex in recycling compartments (Dumanchin et al., 1999). Intriguingly, exome sequencing performed by Udayar *et al* revealed a genetic link between Rab11 and sporadic AD, and a network analysis of GWAS genes associated with sporadic AD identified Rab11 as an interacting component (Udayar et al., 2013). In conjunction, these findings strengthen our data that demonstrates holo-Lf to mediate the intracellular vesicular route of APP by directing it to Rab11-positive endosomes, then leading to increased amyloidogenic processing and exacerbation of Aβ. In addition to holo-Lf directing APP to Rab11 endosomes, whether holo-Lf could be a contributing factor involved in the increased amyloidogenic processing of APP by directly affecting

the activity of the γ-secretase complex is a possibility and therefore warrants future investigation.

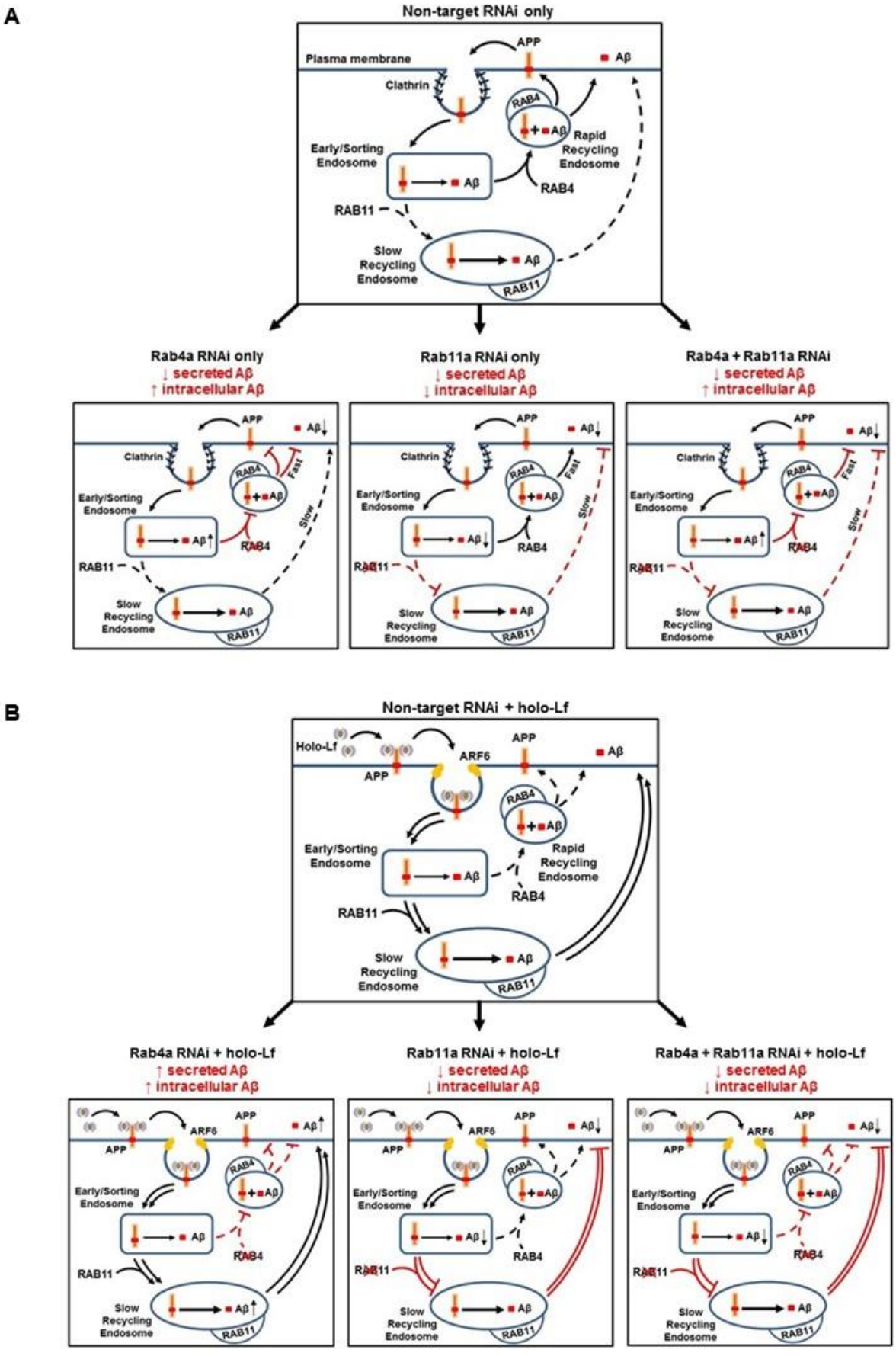
A
Non-target RNAi only
Plasma membrane
APP
Aβ
Clathrin
RAB4
Rapid Recycling Endosome
Early/Sorting Endosome
RAB4
RAB11
Slow Recycling Endosome
RAB11
Rab4a RNAi only
↓ secreted Aβ
↑ intracellular Aβ
Rab11a RNAi only
↓ secreted Aβ
↓ intracellular Aβ
Rab4a + Rab11a RNAi
↓ secreted Aβ
↑ intracellular Aβ
Fast
Slow
B
Non-target RNAi + holo-Lf
Holo-Lf
ARF6
Rab4a RNAi + holo-Lf
↑ secreted Aβ
↑ intracellular Aβ
Rab11a RNAi + holo-Lf
↓ secreted Aβ
↓ intracellular Aβ
Rab4a + Rab11a RNAi + holo-Lf
↓ secreted Aβ
↓ intracellular Aβ

Figure 5.12. Schematic representation of Aβ production and secretion in the absence and presence of holo-Lf in cells depleted of Rab4a, Rab11a and double Rab4a/Rab11a. (A) In the absence of holo-Lf, APP on the cell surface can be internalised into the cell via a clathrin-mediated process that enters the endosomal system. Amyloidogenic processing of APP may occur in the early/sorting endosome or the slow recycling endosome to generate Aβ which can be secreted by Rab4-positive or Rab11-positive compartments respectively. Whereas non-cleaved APP may be rapidly recycled back to the cell surface via Rab4-positive endosomes (Chapter 4.2.6). Silencing Rab4a decreases Aβ secretion but increases intracellular Aβ whilst silencing Rab11a results in a decrease of both intracellular and secreted Aβ. Cells depleted of both Rab4a and Rab11a exhibit an increase in intracellular Aβ and a decrease of Aβ secretion. **(B)** In the presence of holo-Lf, APP internalisation (directed by holo-Lf) is via an ARF6-dependent process. Aβ generation facilitated by holo-Lf mediated APP amyloidogenic processing occurs in the slow recycling endosome and is secreted by Rab11-positive compartments. Depleting Rab4a in cells does not alter the production or secretion of Aβ, whereas depleting Rab11a reduces the amyloidogenic processing of APP and results in a decrease of Aβ secretion and the rapid recycling of non-cleaved APP to the cell surface (Chapter 4.2.6). Depleting cells of both Rab4a/Rab11a reduces Aβ production and secretion.

Despite extensive empirical data implicating Aβ in AD pathogenesis, its utility as a drug target has yet to be established. Several therapeutic approaches aimed at lowering Aβ have proven not effective in multiple large-scale clinical trials (Karran and Hardy, 2014). Whether Lf modulation of APP could possibly be considered as a therapeutic target was explored. Peptides containing the amino acid sequences of APP that were found to be the contact sites for holo-Lf (Chapter 3.2.3) were synthesised. Pre-incubating each of these peptides with holo-Lf before exposure to SH-SY5Y-APP695 cells resulted in a dose-dependent reduction of sAPPβ formation (Figure 5.10), indicating that APP amyloidogenic processing could be alleviated by hindering the interaction between APP and holo-Lf. From this, the half maximal inhibitory concentration (IC_{50}) value of each peptide was determined (Table 5.1). The amino acid sequence of peptide 49 served as the dominant binding site on APP for holo-Lf, requiring ~ 5 μM of peptide to inhibit sAPPβ production by 50 % (Table 5.1). In addition, the efficacy of each peptide to mask the binding site of holo-Lf and reduce amyloidogenic processing of APP was observed to correlate with the affinity of holo-Lf binding to each associated peptide within the APP peptide array (Chapter 3.2.3). There was no complementary effect when comparing 10 μM of peptide 49 to 5 μM of peptide 49 combined with 5 μM of peptide 40 or 55 (Figure 5.11), validating the amino acid sequence of peptide 49 as the dominant binding site on APP for holo-Lf. However, 20 μM of peptide, that is, 10 μM of peptide 49 combined with 10 μM of peptide 40 or 55 totally abolished holo-Lf mediated APP amyloidogenic sAPPβ and sAβ production (Figure 5.11). This revealed that the individual APP binding sites for holo-Lf were independent from each other. Our *in vitro* biophysical data indicate holo-Lf to interact with APP at a 2:1 ratio (Chapter 3.0) with high ($Kd_{1:1}$ ~ 0.6 μM) and low ($Kd_{1:2}$ ~ 8.2 μM) (Chapter 3.0; Table 3.1) binding affinity. We speculate that the predominant high affinity binding site on APP for holo-Lf comprises of the amino acids from peptide 49 (together with the flanking 48 and 50 amino acid peptide regions), while the second lower affinity interacting site corresponds to the amino acid sequence of peptide 40 or 55. Future experiments evaluating the changes in binding affinity between mutant and wildtype protein complexes will help determine which peptide amino acid sequence is responsible for the high and low binding affinity observed between holo-Lf and APP.

Determination of the structure of the APP and holo-Lf complex is critical to not only validate the interacting regions of APP to holo-Lf but to also determine the binding sites on holo-Lf for APP. This structural information will validate and improve the rational design of high affinity peptides to impede the APP and holo-Lf interaction. Complementary studies would involve determining the structure of the holo-Lf and APP peptide complex and conversely, the APP interacting domain and holo-Lf peptide complex. Furthermore, *in vitro* peptide inhibition studies monitoring endocytic transport of APP, Aβ and sAPPβ production, and cell surface location of APP will strengthen the validity for the interaction between APP and holo-Lf being a therapeutic target in neurodegeneration and will facilitate rational drug design.

CHAPTER 6.0 INFLAMMATION-INDUCED LF SECRETION EXACERBATES Aβ PRODUCTION

6.1 Introduction

Activation of the innate immune system in the brain protects against infectious insult but persistent neuroinflammation, as seen in AD, can exacerbate underlying chronic pathology (Hensley, 2010). AD is characterised by reactive gliosis around plaques and tangle-bearing neurons (Serrano-Pozo et al., 2011b). Once activated, these cells produce a range of inflammatory mediators including acute phase proteins, cytokines, prostanoids, chemokines and COX-2 (Heneka and O'Banion, 2007).

Largely due to discoveries made with transcriptomics (including GWAS), data from sporadic AD has implicated an inflammatory and immune response as being a critical pathway (Malik et al., 2015; Pasqualetti et al., 2015). Lf is involved in cellular iron management in neuroinflammation and the immune response (Grossmann et al., 1992; Jameson et al., 1998; Sanchez et al., 1992). It is an acute phase protein that is synthesised and secreted by activated microglia (Fillebeen et al., 2001; Wang et al., 2015) and is highly expressed during iron loading, infection and inflammation (Levay and Viljoen, 1995). This response is partly due to a host's immune response requiring Lf to isolate bacteria from its essential growth nutrient iron (Grossmann et al., 1992; Jameson et al., 1998; Levay and Viljoen, 1995). Lf is elevated in the brain in AD, found in neurons, glia and around lesions of neuronal damage, including plaques and tangle-bearing neurons (Kawamata et al., 1993; Leveugle et al., 1994; Qian and Wang, 1998), signifying an association between Lf and AD pathology. However, the role of Lf within AD remains elusive, and it is yet to be determined whether Lf is protective by sequestering free iron or deleterious by signalling inflammation.

We have previously shown that the addition of exogenous holo-Lf to human neuroblastomas and murine primary neuronal cultures alters the cellular location of APP and exacerbates the amyloidogenic pathway, leading to an increase in sAPPβ and Aβ production (Chapter 4.0 & 5.0). In order to confirm these findings in a more *in vivo*-like cellular environment, we adopted the transwell co-culture device and used HMC3 microglial cells co-cultured with SH-SY5Y-APP695 cells

to determine whether Lf secreted by stimulated microglia promotes the APP amyloidogenic pathway in SH-SY5Y-APP695 cells. Whether the mechanistic effects Lf had on the amyloidogenic processing of APP could be alleviated by either hindering Lf secretion from stimulated microglia or masking the binding sites of Lf for APP was also investigated.

6.2 Results

6.2.1 Activated microglia secrete Lf which decreases cell surface APP and exacerbates APP amyloidogenic processing in co-cultured SH-SY5Y-APP695 cells

Since previous reports have shown Lf to be synthesised by activated microglia (Fillebeen et al., 2001; Wang et al., 2015), we used a transwell co-culture of HMC3 microglial and SH-SY5Y-APP695 cells to examine and confirm the effects observed in the APP amyloidogenic pathway caused by Lf. HMC3 cells were cultured in the upper chamber insert and SH-SY5Y-APP695 cells were cultured in the lower plate compartment of the co-culture device. To activate resting HMC3 microglial cells, IFN-γ (10 ng/ml) was added to the upper chamber insert and incubated for 24 hours. HMC3 activation was confirmed by an increase of the activation marker MHC class II via Western blot (Figure 6.1B). Significant levels of Lf ($p < 0.0001$) were detected within the media of the lower plate compartment containing SH-SY5Y-APP695 cells by Western blot (Figure 6.1A), indicating the permeability and pore size of the membrane insert was sufficient for the free passage of secreted Lf from activated HMC3 cells. To determine the source of Lf production, HMC3 and SH-SY5Y-APP695 cells were cultured separately and treated with and without IFN-γ (10 ng/ml) for 24 hours. Only HMC3 cells showed Lf secretion after being activated for 24 hours ($p < 0.0001$) (Figure 6.1A). Furthermore, only after HMC3 activation and subsequent Lf secretion were co-cultured SH-SY5Y-APP695 cells able to exhibit decreased levels of surface presented APP as measured by surface biotinylation ($p < 0.0001$) (Figure 6.2) and increased production of the APP amyloidogenic products sAPPβ (in the media) (Figure 6.1A) and Aβ (in the media and cell lysate) (Figure 6.1A & B respectively) ($p < 0.0001$).

To confirm that activated HMC3 Lf secretion was responsible for the mislocalisation of APP and therefore subsequent APP amyloidogenic fragment formation, Lf was immunoprecipitated and detected from the media of activated (IFN-γ; 10 ng/ml; 24 hours) HMC3 cells (Figure 6.3A). Unbound and bound Lf fractions were then applied to cultured SH-SY5Y-APP695 cells, incubated for 2 hours and secreted amyloidogenic fragments in the media were analysed by Western blot. SH-SY5Y-APP695 cells treated with bound Lf fractions revealed

significant increased levels of sAPPβ and sAβ ($p < 0.0001$) (Figure 6.3B), compared to non-treated control, cells treated with unbound fractions or when using β-actin as the capture antibody, all confirming specificity of Lf interaction (Figure 6.3B). Taken together, secreted Lf from activated microglia is able to alter cell surface APP location in SH-SY5Y-APP695 cells and induces the amyloidogenic processing of APP to produce sAPPβ and sAβ.

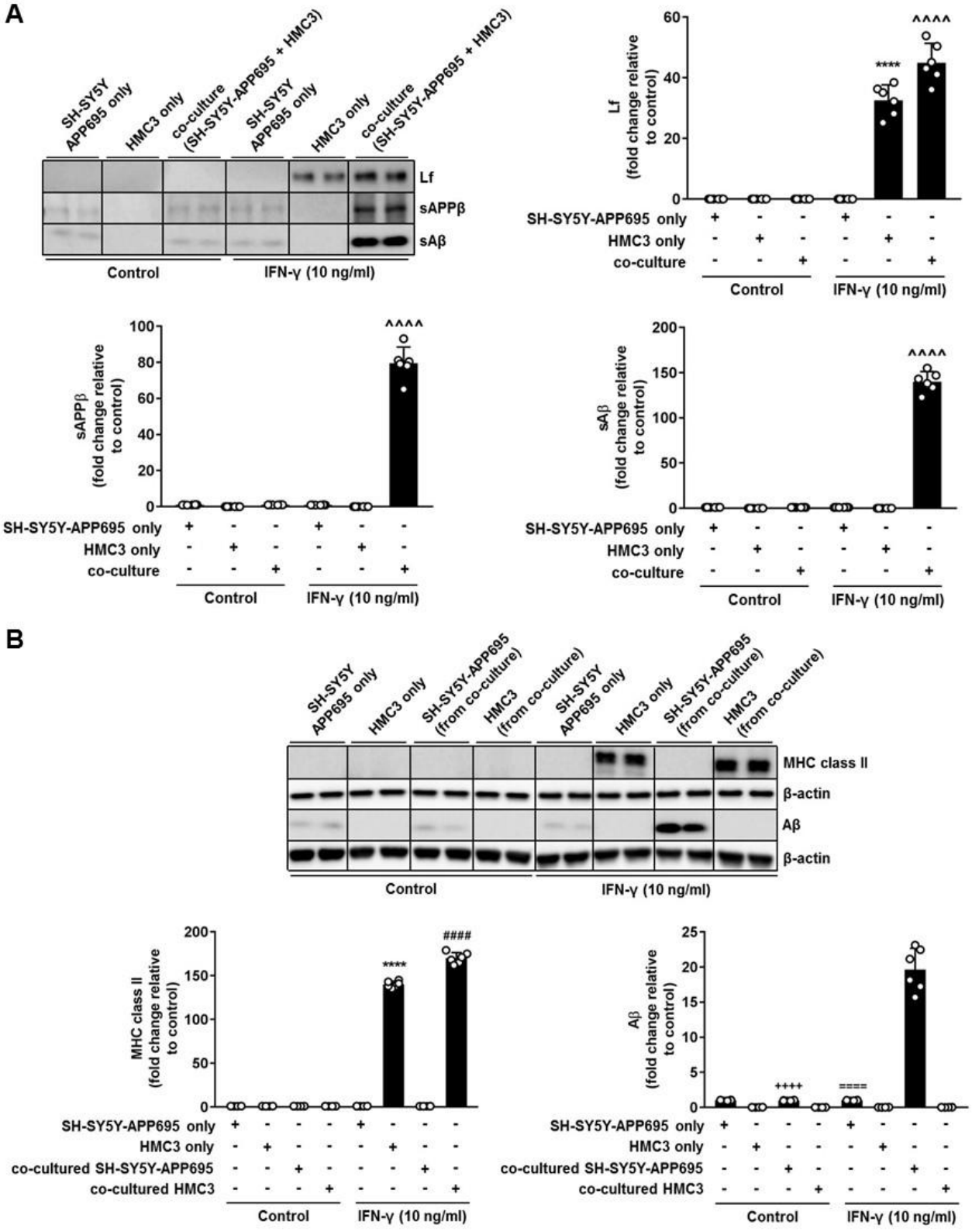
A
SH-SY5Y APP695 only
HMC3 only
co-culture (SH-SY5Y-APP695 + HMC3)
Lf
sAPPβ
sAβ
Control
IFN-γ (10 ng/ml)
Lf (fold change relative to control)
sAPPβ (fold change relative to control)
sAβ (fold change relative to control)
SH-SY5Y-APP695 only
HMC3 only
co-culture
****
^^^^
B
SH-SY5Y-APP695 (from co-culture)
HMC3 (from co-culture)
MHC class II
β-actin
Aβ
MHC class II (fold change relative to control)
Aβ (fold change relative to control)
co-cultured SH-SY5Y-APP695
co-cultured HMC3
####
++++
====

Figure 6.1. Secreted Lf from activated microglia increases APP amyloidogenic processing. In the co-culture device, HMC3 microglial cells were cultured in the upper inserts, while SH-SY5Y-APP695 cells were cultured in the lower plate wells. Human recombinant IFN-γ (10 ng/ml; 24 hours) was added to the upper inserts in serum-free EMEM to activate HMC3 cells. **(A)** Secreted Lf, sAPPβ and Aβ in the media of the lower chamber containing SH-SY5Y-APP695 cells, and the activation marker for induced HMC3 cells, **(B)** MHC class II and Aβ protein expression in the cell lysate were visualised by western blot. Data are means ± SE of 3 experiments performed in duplicate normalised to **(A)** total protein or **(B)** β-actin. **** $p < 0.0001$ compared to non-treated HMC3 only control, **(A)** ^^^^ $p < 0.0001$ compared to non-treated co-culture control, **(B)** #### $p < 0.0001$ compared to non-treated co-cultured HMC3 control, ++++ $p < 0.0001$ and ==== $p < 0.0001$ compared to IFN-γ treated co-cultured SH-SY5Y-APP695 cells.

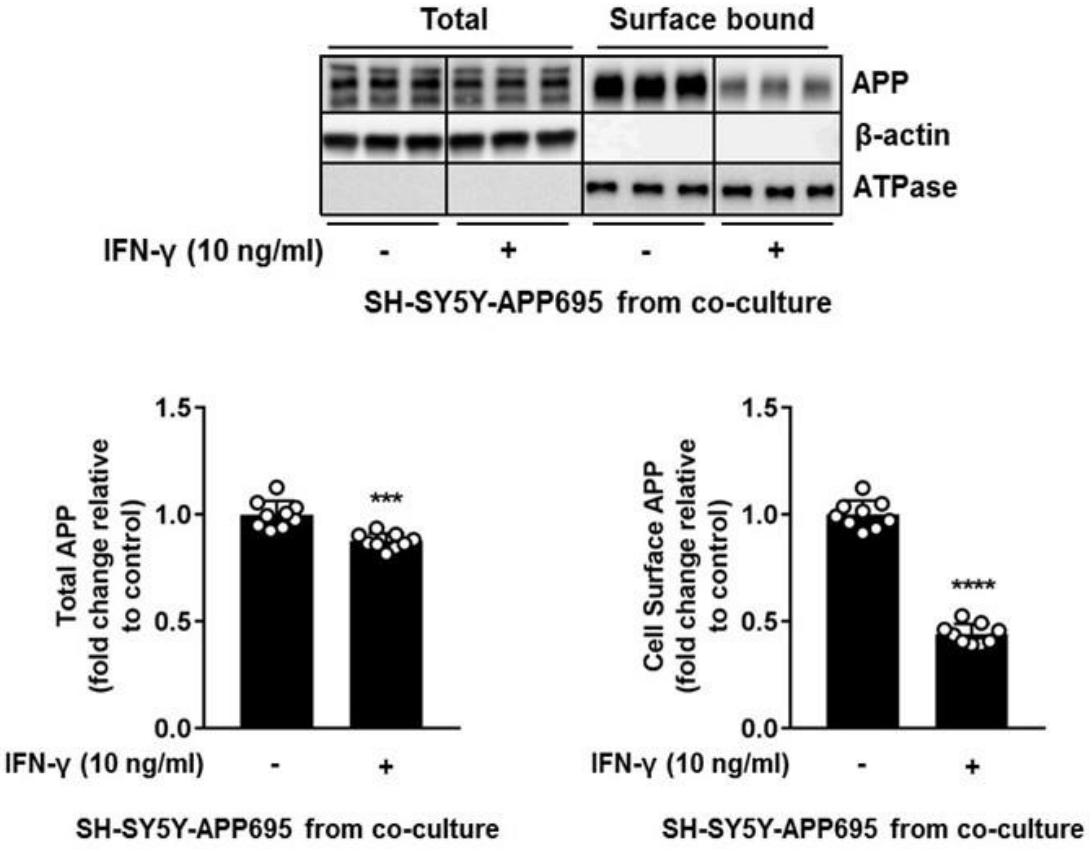

Figure 6.2. Secreted Lf from activated microglia reduces surface presented APP. In the co-culture device, HMC3 microglial cells were cultured in the upper inserts, while SH-SY5Y-APP695 cells were cultured in the lower plate wells. Human recombinant IFN-γ (10 ng/ml; 24 hours) was added to the upper inserts in serum-free EMEM to activate HMC3 cells. Cell surface proteins on SH-SY5Y-APP695 cells were biotinylated after microglial activation to identify changes to APP expression on the cell surface. Total and cell surface APP levels were visualised by Western blot. Data was normalised against β-actin for total APP levels and Na^+/K^+ ATPase for surface protein content, and depict fold change compared to non-treated co-cultured SH-SY5Y-APP695 control cells, presented as means ± SE of 3 experiments performed in triplicate, *** $p < 0.001$ and **** $p < 0.0001$.

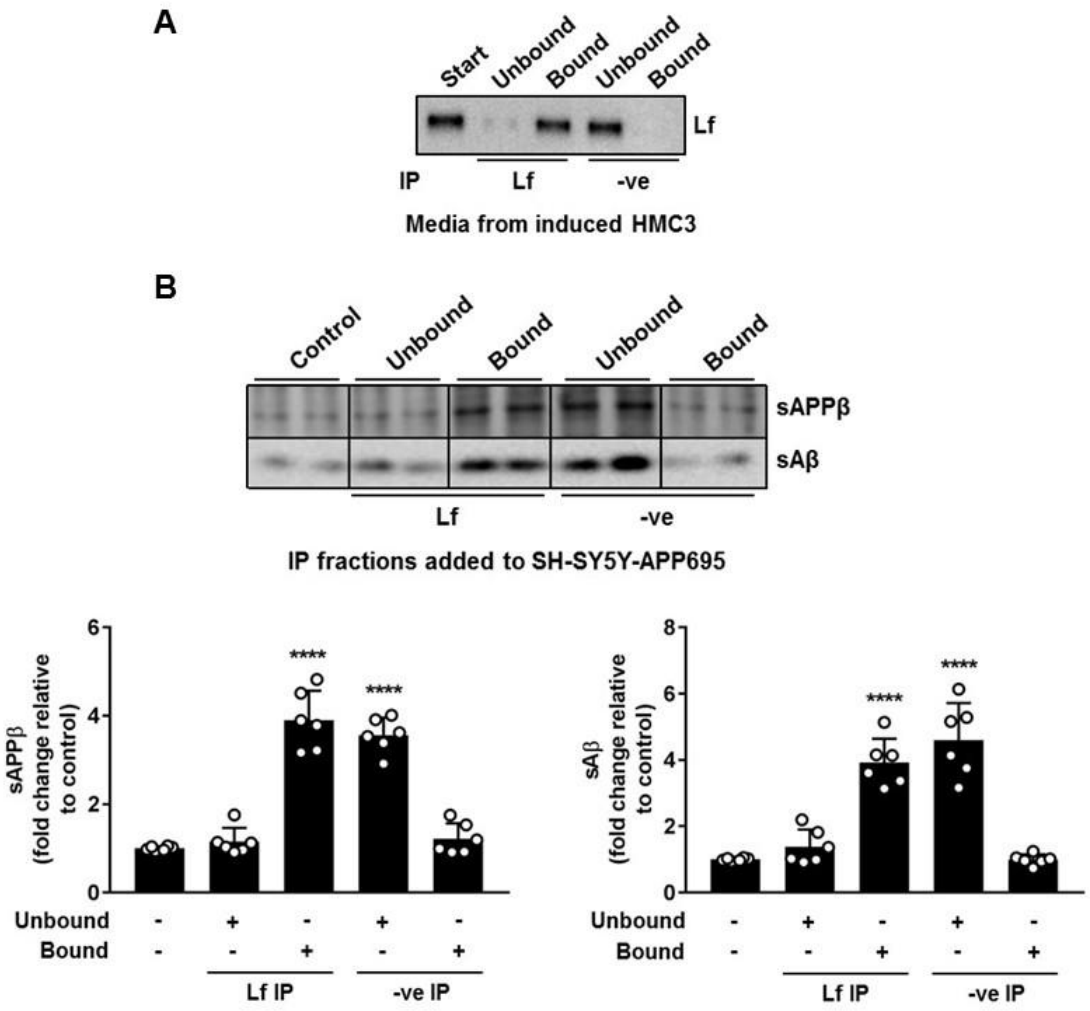

Figure 6.3. Confirmation that Lf produced from activated microglia increases APP amyloidogenic processing. To further validate whether Lf secretion from stimulated microglia induce the amyloidogenic processing of APP, **(A)** anti-Lf (LifeSpan BioSciences) was used to immunoprecipitate while anti-Lf (Bioss) was used to detect Lf in the media (analysed by Western blot) of HMC3 cells activated with IFN-γ (10 ng/ml; 24 hours). No detection of Lf when using anti-β-actin as the capture antibody confirmed specificity of interaction. The 'unbound' refers to the starting material ('start') remaining after separation from the protein G Dynabeads, and the 'bound' fraction refers to the eluted protein. Immunoprecipitation experiments were performed in duplicate on three separate occasions. **(B)** Immunoprecipitated bound and unbound Lf fractions from **(A)** were applied to SH-SY5Y-APP695 cells and incubated for 2 hours. The APP amyloidogenic protein fragments (sAPPβ & sAβ) in the media were visualised by Western blot. Data are means ± SE of 3 experiments performed in duplicate and depict fold change compared to non-treated control cells, **** $p < 0.0001$.

6.2.2 Hindering the interaction between Lf from induced microglia and APP from SH-SY5Y-APP695 cells alleviates amyloidogenic fragment production

To determine whether Lf depletion could alleviate APP from being processed through the amyloidogenic pathway and therefore lessen sAPPβ and sAβ production, HMC3 cells were transfected with Lf RNAi (20 nM) and re-plated into the upper chamber inserts, while SH-SY5Y-APP695 cells were cultured in the lower plate wells of the co-culture device. HMC3 cells depleted of Lf were then incubated with IFN-γ (10 ng/ml) for 24 hours and the media in the lower compartment analysed by Western blot for Lf, sAPPβ and sAβ protein expression. Compared to non-targeting control HMC3 cells induced with IFN-γ, Lf expression detected within the media significantly decreased ($p < 0.0001$), resulting in reduced levels of sAPPβ and sAβ production ($p < 0.0001$) from co-cultured SH-SY5Y-APP695 cells (Figure 6.4).

We then investigated whether we could impede the interaction between Lf and APP by means of a neutralising polyclonal Lf antibody to rescue APP from being processed into sAPPβ and sAβ. Anti-Lf IgG antibody (20 µg/ml) or isotype control IgG (20 µg/ml) was added to the media of the lower chamber of the co-culture device containing SH-SY5Y-APP695 cells whilst IFN-γ (10 ng/ml) was added to the media in the upper chamber inserts containing HMC3 cells. After 24 hours, secreted Lf and the APP amyloidogenic proteins sAPPβ and sAβ were measured by Western blot. Compared to isotype control IgG treated cells, anti-Lf IgG was able to significantly block the interaction between Lf and APP which led to reduced levels of sAPPβ and sAβ formation ($p < 0.0001$) (Figure 6.5). Taken together, impeding microglial induced Lf secretion or disrupting Lf binding to APP reduces the APP amyloidogenic pathway, alleviating sAPPβ and sAβ formation.

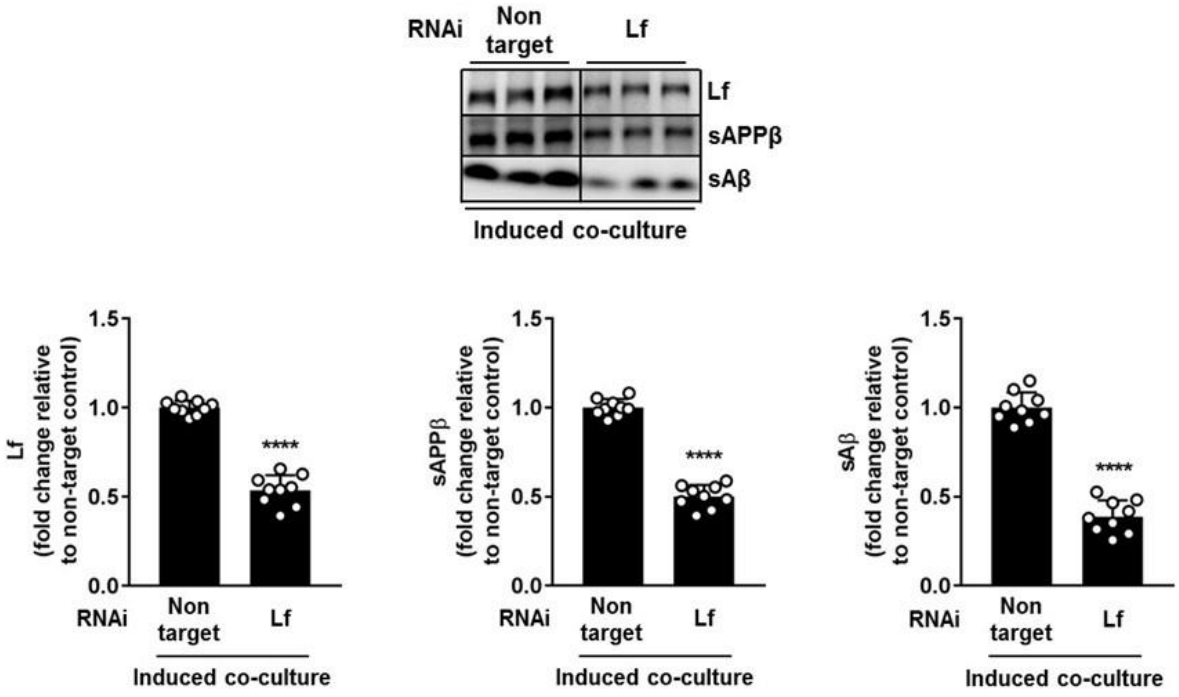

Figure 6.4. Reducing Lf secretion from activated microglia decreases the APP amyloidogenic pathway. HMC3 cells were transfected with control non-target and Lf RNAi (20 nM) for 48 hours, and re-plated into the upper inserts of the co-culture device, while SH-SY5Y-APP695 cells were cultured in the lower plate wells. Human recombinant IFN-γ (10 ng/ml; 24 hours) was added to the upper inserts in serum-free EMEM to activate transfected HMC3 cells. Secreted Lf and the APP amyloidogenic protein fragments (sAPPβ & sAβ) in the media were visualised by Western blot. Data are means ± SE of 3 experiments performed in triplicate and depict fold change compared to non-target control cells, **** $p < 0.0001$.

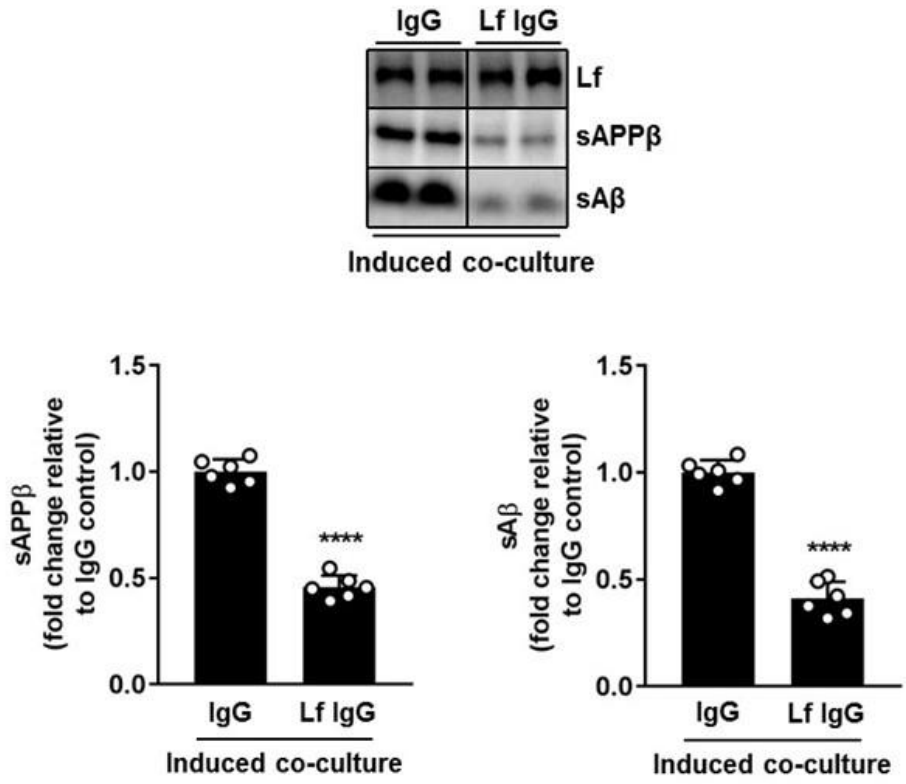

Figure 6.5. Neutralising antibody blocks the interaction of Lf with APP, reducing APP amyloidogenic processing. HMC3 microglial cells were cultured in the upper inserts of the co-culture device, while SH-SY5Y-APP695 cells were cultured in the lower plate wells. Human recombinant IFN-γ (10 ng/ml) was added to the upper inserts in serum-free EMEM to activate HMC3 cells while anti-Lf IgG antibody (20 µg/ml) or isotype control IgG (20 µg/ml) were added to serum-free DMEM of the lower plate wells containing SH-SY5Y-APP695 cells and incubated for 24 hours. Secreted Lf and the APP amyloidogenic protein fragments (sAPPβ & sAβ) in the media were visualised by Western blot. Data are means ± SE of 3 experiments performed in duplicate and depict fold change compared to isotype IgG treated control cells, **** $p < 0.0001$.

6.3 Discussion

Various studies have demonstrated that activated microglia, triggered to elicit an inflammatory response, synthesise and secrete Lf in response to persistent inflammation (Fillebeen et al., 2001; Wang et al., 2015). We therefore adopted the transwell co-culture device which is an effective model for analysing the cross-talk between different cell populations (Lin et al., 2007). Here, we were able to closely resemble physiological conditions and obtain data with stronger biological significance. We measured the inflammatory effects of Lf secreted by IFN-γ-induced HMC3 microglia on SH-SY5Y-APP695 neuroblastomas in a shared co-cultured environment and found Lf secreted by activated microglia to decrease surface presented APP and exacerbate APP amyloidogenic processing in SH-SY5Y-APP695 cells. Hindering Lf secretion from induced microglia or preventing the binding of secreted Lf to APP alleviated Lf mediated APP amyloidogenic processing, further validating Lf as an attractive therapeutic target.

Microglia are the resident immune cells of the brain that become activated in response to infectious insult or unwanted stimuli (Crain et al., 2013; Mammana et al., 2018; Orihuela et al., 2016). IFN-γ was used to activate resting HMC3 microglial cells which was confirmed by an increase in MHC class II expression (Figure 6.1B) (Colonna and Butovsky, 2017; Dello Russo et al., 2018; Sarlus and Heneka, 2017). MHC class II has been linked to the neuroinflammatory response in neurodegenerative diseases, including AD (Perlmutter et al., 1992; Schetters et al., 2017; Tooyama et al., 1990) and is considered as a neuroinflammatory M1 marker that is consistently expressed and upregulated by activated microglia in the AD brain (Colonna and Butovsky, 2017; Lambert et al., 2013; Perlmutter et al., 1992; Tooyama et al., 1990).

HMC3 cells were cultured in the upper chamber while SH-SY5Y-APP695 cells were cultured in the lower plate compartment of the co-culture device. Lf secretion was detected specifically from IFN-γ-stimulated microglia (Figure 6.1A), confirming previous reports that have shown an upregulation of Lf expression within microglia upon pro-inflammatory stimuli such as 1-methyl-4-phenylpyridinium (MPP^+) and ferric ammonium citrate (FAC) (Fillebeen et al., 2001; Wang et al., 2015). In turn, this led to reduced levels of cell surface APP (Figure 6.2) and increased production of amyloidogenic sAPPβ and Aβ fragments

in SH-SY5Y-APP695 cells (Figure 6.1), confirming our previous findings that holo-Lf acutely decreases cell surface APP through amyloidogenic processing (Chapter 4.0 & 5.0). This was further confirmed by applying Lf immunoprecipitated from activated microglia supernatants (Figure 6.3A) onto a culture of SH-SY5Y-APP695 cells, which resulted in an increase in both sAPPβ and Aβ (Figure 6.3B). Our data is also supported by other studies that have shown pro-inflammatory induction of neuroinflammation *in vivo* increases the amyloidogenic pathway of APP, resulting in an accumulation of Aβ (Sheng et al., 2003). The fact that Lf could be detected upon IFN-γ-induced microglial activation confirms Lf is generated through the M1 activated phenotype, acting as a pro-inflammatory mediator (Fillebeen et al., 2001; Hu et al., 2017; Kruzel et al., 2017) that increases the amyloidogenic pathway of APP and resulting in an accumulation of Aβ.

Either hindering Lf secretion from stimulated microglia (Figure 6.4) or masking the binding sites of Lf for APP (Figure 6.5) reduced the mechanistic effects Lf had on the amyloidogenic processing of APP, further emphasising Lf as a potential therapeutic target to alleviate Aβ load. This reveals an unprecedented fundamental insight into how Lf, as an acute phase protein involved in neuroinflammation (Levay and Viljoen, 1995; Sanchez et al., 1992), could have a direct control of Aβ production within neurons. Studies have documented M2 microglial dysfunction in AD mouse models, correlating with Aβ plaque formation (Jimenez et al., 2008; Krabbe et al., 2013), whereby lowering Aβ load restored microglial phagocytic capabilities (Krabbe et al., 2013). Therefore, further experiments are required to evaluate whether reducing sustained Lf signalling shifts microglia more to an M2 activated phenotype that can elicit an anti-inflammatory phagocytic response in sporadic AD.

Earlier results have indicated that only iron-bound holo-Lf is able to interact with APP to exert its effects whereas iron-unbound apo-Lf cannot (Chapter 3.0 & 4.0). Culture media was not supplemented with iron to convert the apo form of Lf to the holo form after microglial activation since Lf has the ability to chelate iron from Tf (Aisen and Leibman, 1972; Baker and Baker, 2004; Metz-Boutigue et al., 1984) in addition to Lf's high binding affinity to the iron originally contained within the media (Aisen and Leibman, 1972; Chung and Raymond, 1993; Yang and Xiong, 2012).

Even though the microglial cell line within this study was purely used as a source of Lf, in the absence of SH-SY5Y-APP695 cells, we expected secreted Lf to induce APP amyloidogenic processing in stimulated microglia since earlier results have indicated the ability of holo-Lf to interact with all three major APP isoforms (Chapter 3.2.1). Despite microglia expressing all three major isoforms of APP (Haass et al., 1991; LeBlanc et al., 1991), we were unable to detect levels of either sAPPβ or Aβ from activated microglia (Figure 6.1). This could be due to the level of surface APP expression in HMC3 cells, since it is far more difficult to detect sAPPβ and Aβ processed from endogenously expressing APP cells as opposed to cells overexpressing APP (Guo et al., 2012; Teich et al., 2013). Whether microglia themselves are actually capable of producing sufficient amounts of Aβ through the APP amyloidogenic pathway is another point that requires further evaluation since multiple studies have indicated neurons to be the main source of Aβ production within the brain (Haass et al., 1991; LeBlanc et al., 1991; LeBlanc et al., 1996). Microglia themselves are more involved in secreting pro-inflammatory mediators via an M1 activated phenotype that can regulate APP expression and processing in neurons (Blasko et al., 1999; Buxbaum et al., 1992; Del Bo et al., 1995; Fassbender et al., 2000; Hirose et al., 1994; Simon et al., 2018). For instance, LeBlanc *et al* investigated APP expression and metabolism in primary rat neurons compared to microglia by pulse-chase analysis using metabolically labeled APP and revealed the rate of APP synthesis to be 10-times higher in neurons than in microglia whereas APP turn over in microglia was 5-fold higher than in neurons, limiting microglial-derived Aβ generation (LeBlanc et al., 1996). In support, immunocytochemically detected APP in primary murine microglial cells revealed diminished surface presented APP levels along with an increase in intracellular full-length APP compared to other cell types (Haass et al., 1991). This led to insignificant levels of sAPPβ and Aβ production (Haass et al., 1991), indicating APP could possibly function intracellularly in microglial cells via an alternative trafficking pathway. In relation to these studies, the APP expression profile in activated HMC3 microglial cells should be evaluated since APP localisation affects Lf induced Aβ production.

While Aβ is implicated in AD pathogenesis, the physiological function of the APP amyloidogenic processing pathway and subsequent generation of Aβ remains uncertain. Increasing attention has been on the antimicrobial properties of Aβ and

its potential role in innate immunity (Bourgade et al., 2016; Kumar et al., 2016; Soscia et al., 2010). Our data suggests that Lf could be protective against neuroinflammation and extracellular pathogen infection in acute conditions through rapidly shedding cell surface APP to secrete Aβ as an antimicrobial. However, in relation to AD, future experiments are required to determine whether chronic Lf signalling leads to sustained Aβ-related neuropathology. To ascertain whether cellular toxicity is a cause of chronic Lf binding to APP, similar experimental procedures will also need to be carried out in cellular models depleted of APP.

CHAPTER 7.0 HOLO-LF ALTERS IRON HOMEOSTASIS THROUGH A DIRECT ASSOCIATION WITH APP

7.1 Introduction

Iron is essential for cell survival, normal development and optimal function of the brain. The brain is particularly vulnerable to damage caused by an imbalance of iron. Iron homeostasis, including storage, transport and metabolism are tightly regulated by iron uptake, transport, storage and enzymatic proteins that are themselves regulated by iron (Hare et al., 2013; Zecca et al., 2004). The ability of iron to freely receive and donate electrons is critical for neurotransmitter regulation as well as oxidative phosphorylation, nitric oxide metabolism and oxygen transport (Zecca et al., 2004). An iron imbalance can lead to metabolic stress on these processes. High levels of unbound iron also detrimentally catalyse the production of toxic ROS (Conrad and Umbreit, 2000; Sharpe et al., 2003). Iron imbalance plays a major role in the pathogenesis of AD. Furthermore, higher brain iron levels are associated with faster disease progression (Ayton et al., 2015a, 2017a; Ayton et al., 2017b), and recent work has implicated ferroptosis, a type of regulated cell death dependent on iron, as a neurodegenerative disease mechanism (Stockwell et al., 2017). This has created significant interest in the possibility that disturbances of brain iron levels may occur through a failure to balance iron inside the cell.

Indicators of an inflammatory response and iron retention are both early hallmarks of AD (Rogers et al., 1996; Smith et al., 1997). For example, in the apo form, Lf safely binds and withholds iron away from regions of infection and by doing so stifles pathogen growth (Grossmann et al., 1992; Jameson et al., 1998; Levay and Viljoen, 1995). Whilst iron bound holo-Lf may provide iron that can catalyse the production of free radicals to eliminate intracellular pathogens within the phagolysosome of phagocytic cells (Anand et al., 2015; Weiss and Schaible, 2015). Another example comes from studies demonstrating neurons to depend upon APP to regulate iron export. APPKO or knockdown causes FPN destabilisation and consequent iron retention, while extracellular supplementation with sAPPα stabilises surface FPN and stimulates iron export (Ayton et al., 2015b; Duce et al., 2010; Wong et al., 2014b). However, the sequence of events that lead to APP mediated iron retention in AD are currently

unknown. Furthermore, whether amyloidogenic APP processing has any impact on iron efflux is not yet known. However, unpublished data from our group has shown that altering the proteolytic processing of APP at the cell surface causes consequential changes in neuronal iron homeostasis. Changing the expression and activity of endogenous secretases to enhance the amyloidogenic pathway of APP processing, or overexpressing APP carrying familial AD mutations, leads to intracellular iron accumulation via cell surface FPN changes.

In the present chapter, the ability of Lf to alter iron homeostasis was investigated by examining the major iron regulatory proteins involved in iron export, uptake and storage in the presence of Lf. Whether Lf altered intracellular iron levels was also assessed. Similar to the previous aims that use an acute dose, a more chronic administration of Lf at varying doses was used to determine whether the persistent presence of Lf altered susceptibility toward iron-associated oxidative stress and cell death.

7.2 Results

7.2.1 Holo-Lf indirectly destabilises ferroportin on the cell surface and alters iron homeostasis

APP is important in maintaining iron homeostasis by stabilising the iron efflux pore protein FPN on the cell surface (Duce et al., 2010; Wong et al., 2014b). Since our earlier results have demonstrated a reduction of APP on the cell surface in the presence of holo-Lf (Chapter 4.2.1 & 6.2.1), FACS was performed to investigate changes in FPN protein expression on the cell surface of non-permeabilised SH-SY5Y cells in the presence of holo-Lf, apo-Lf, holo-Tf, and apo-Tf (500 nM; 2 hours). Treatment with holo-Lf decreased surface levels of FPN ($p < 0.0001$) while holo-Tf increased levels ($p < 0.01$) and there was no evidence of a change in FPN cell surface levels with the addition of either apo-Lf or apo-Tf (Figure 7.1).

In addition to FPN, the other major iron regulatory proteins involved in iron import (TfR) (Zhang et al., 2012) and storage (Ft) (Arosio et al., 2009) were also investigated in the presence and absence of endogenous APP in SH-SY5Y cells exposed to Lf. SH-SY5Y cells were used as a means to examine endogenous iron regulatory protein expression under basal iron conditions (Rogers et al., 2008; Rogers et al., 2002). SH-SY5Y cells were transfected with APP RNAi (20 nM), followed by apo- or holo-Lf treatment (500 nM; 2 hours) where APP, TfR and Ft protein expression were analysed by Western blot. Silencing endogenous APP by RNAi ($p < 0.0001$) led to a reduction in TfR and an increase in Ft ($p < 0.0001$) as expected (Duce et al., 2010; Zhou and Tan, 2017) when compared to RNAi treated non-target control cells. In the presence of holo-Lf, there was also less TfR expression in addition to less APP, and increased levels of Ft ($p < 0.0001$) in non-target RNAi treated cells (Figure 7.2). In APP RNAi treated cells, TfR and Ft protein levels remained unchanged with the addition of holo-Lf. Intriguingly, holo-Lf was more efficient in decreasing TfR and increasing Ft than APP RNAi treatment. There was no change in either APP, TfR or Ft levels upon apo-Lf exposure compared to either APP or non-target RNAi treated cells (Figure 7.2). Taken together, through an APP-dependent pathway, holo-Lf indirectly destabilises cell surface FPN and alters iron homeostasis by affecting iron regulatory proteins responsible for cellular iron import and storage.

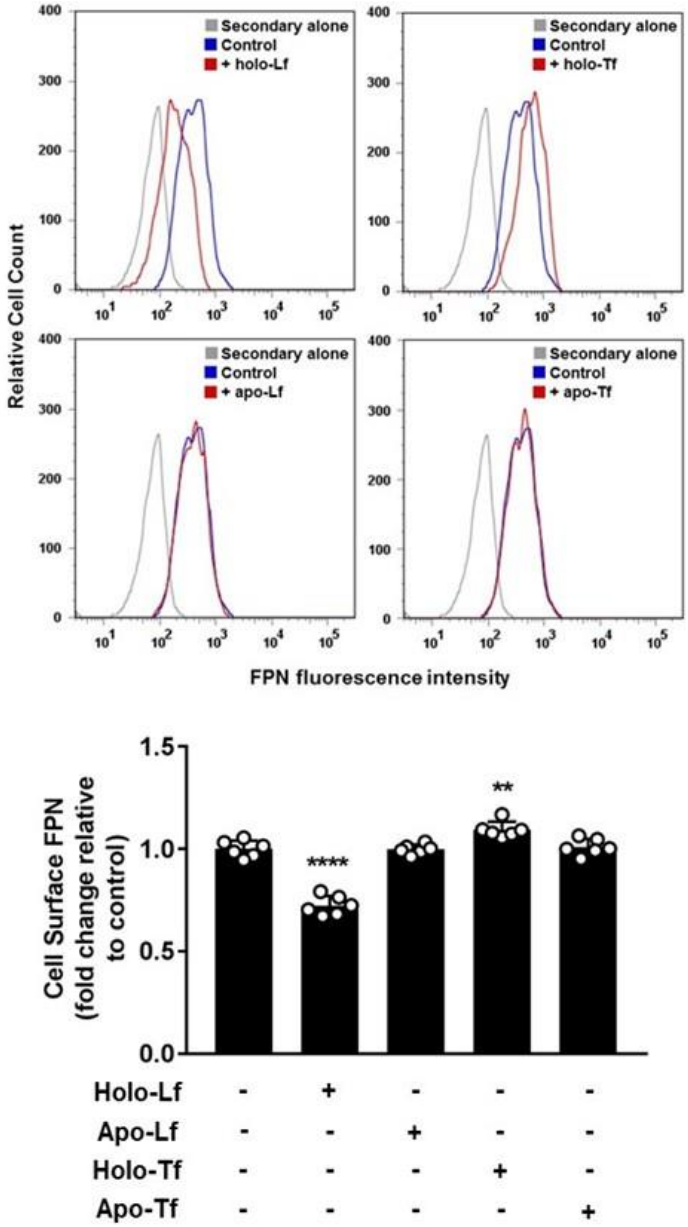

Figure 7.1. Holo-Lf indirectly destabilises ferroportin on the cell surface. FACS was performed to measure FPN levels on the cell surface of non-permeabilised SH-SY5Y cells after a 2 hour incubation with 500 nM holo-Lf, apo-Lf, holo-Tf and apo-Tf at 37°C. The FPN antibody used was raised to epitopes on the extracellular domain. Data are means ± SE of 3 experiments performed in duplicate. Quantified histogram data depict fold change compared to non-treated control cells, ** $p < 0.01$ and **** $p < 0.0001$.

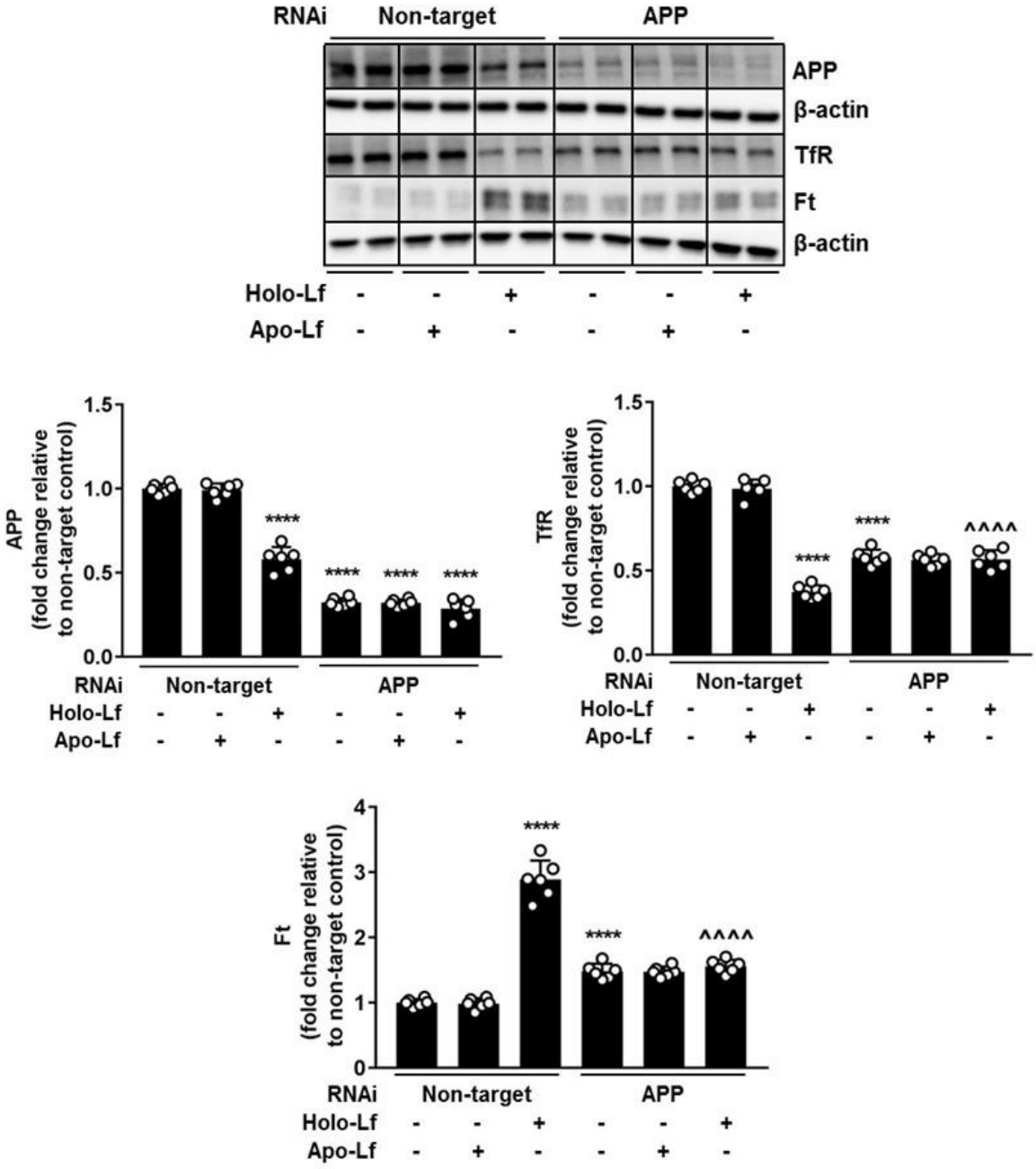

Figure 7.2. Iron homeostasis is dysregulated in the presence of holo-Lf. SH-SY5Y cells were treated with either apo- or holo-Lf (500 nM; 2 hours) after being transfected with control non-target and APP RNAi (20 nM) for 48 hours. Iron regulatory proteins APP, TfR and Ft expression in the cell lysate were visualised by Western blot. Data are means ± SE of 3 experiments performed in duplicate normalised to β-actin. Quantified data depict fold change compared to non-targeting control cells, **** $p < 0.0001$ compared to non-target control and ^^^^ $p < 0.0001$ compared to holo-Lf treated non-target cells.

7.2.2 Holo-Lf causes an accumulation of intracellular iron

To determine whether APP is involved in the ability of Lf to alter intracellular iron levels, iron content in SH-SY5Y cells in the presence and absence of APP exposed to Lf was investigated. SH-SY5Y cells were transfected with APP RNAi (20 nM) followed by apo- or holo-Lf treatment (500 nM; 2 hours) where calcein-AM was used to measure the cytoplasmic LIP. Depleting APP by RNAi treatment resulted in an increase in the cytoplasmic LIP ($p < 0.0001$) which remained unchanged with the addition of holo-Lf (Figure 7.3). Treatment with holo-Lf in non-targeting RNAi cells revealed increased levels of intracellular iron ($p < 0.0001$), more so than in APP depleted cells, and there was no change in intracellular iron levels upon apo-Lf exposure compared to either APP or non-target RNAi treated cells (Figure 7.3).

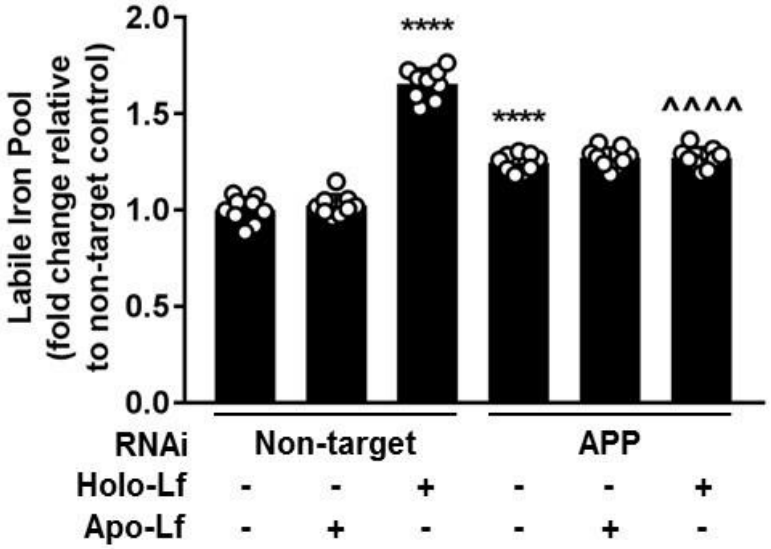

Figure 7.3. Intracellular iron levels are increased in the presence of holo-Lf. SH-SY5Y cells were treated with either apo- or holo-Lf (500 nM; 2 hours) after being transfected with control non-target and APP RNAi (20 nM) for 48 hours. Intracellular iron levels were determined by the direct measurement of cytosolic labile iron using a modified Calcein-AM assay. Data are means ± SE of 3 experiments performed in triplicate. **** $p < 0.0001$ compared to non-target control and ^^^^ $p < 0.0001$ compared to holo-Lf treated non-target cells.

7.2.3 Prolonged exposure of Holo-Lf leads to iron-associated lipid peroxidation and cell death

To further investigate whether increased intracellular iron levels caused by holo-Lf led to cellular toxicity, oxidative stress and cell death were measured in SH-SY5Y cells after a short and sustained exposure of holo-Lf. SH-SY5Y cells were treated with increasing concentrations of holo-Lf (0-10 µM) and incubated for either 2 or 72 hours where oxidative stress and cell death were measured in tandem by FACS using the lipid peroxidation sensor BODIPY-C11 and the cell death marker DAPI. Lipid peroxidation and cell death levels gradually increased with increasing doses of holo-Lf up to 2 hours (Figure 7.4A) whereas increasing the incubation time to 72 hours intensified lipid peroxidation with concomitant cell death (Figure 7.4B). These results indicate that holo-Lf has the ability to alter intracellular iron levels, inducing susceptibility to iron associated lipid peroxidation and cell death.

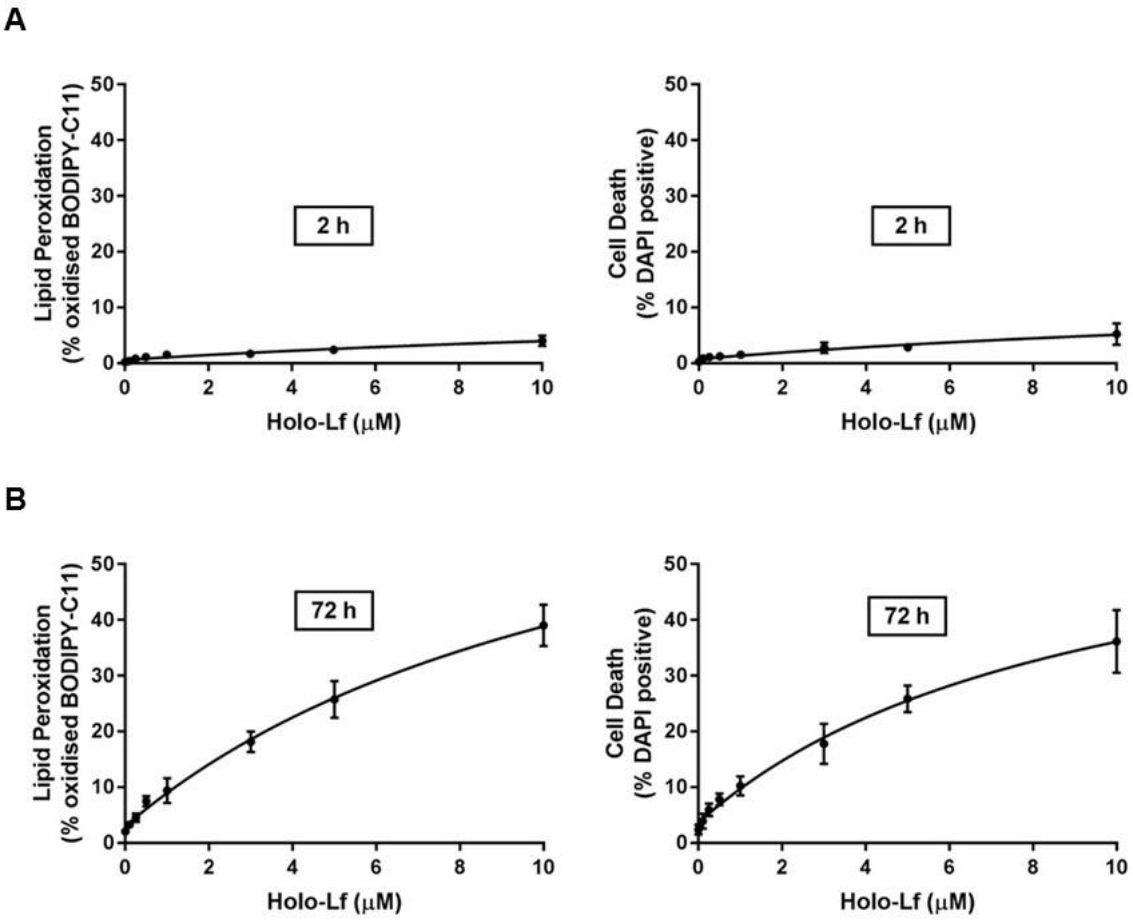

Figure 7.4. Iron dysregulation by holo-Lf induces lipid peroxidation and cell death. SH-SY5Y cells were exposed to increasing concentrations of holo-Lf (0-10 μM) for either **(A)** 2 or **(B)** 72 hours. Oxidative stress and cell death were measured in tandem by FACS using the lipid peroxidation sensor BODIPY-C11 and the cell death marker DAPI. Data are means ± SE of 3 experiments performed in duplicate. Data depict % increase relative to non-treated control cells.

7.3 Discussion

A careful balance of iron within cells is required as it is altered in response to inflammation (for example, through infection) and implicated in AD (Rogers et al., 1996; Smith et al., 1997; Urrutia et al., 2013). We now uncover that APP may be central to iron changes during inflammation by virtue of its ability to bind Lf. Holo-Lf consequently altered iron homeostasis through a direct association with APP in human neuroblastomas. Holo-Lf indirectly destabilised cell surface FPN and caused an accumulation of intracellular iron levels which led to changes in the expression of the major iron regulatory proteins involved in iron uptake and storage. Persistent exposure of holo-Lf triggered iron associated lipid peroxidation and cell death in a dose-dependent manner. Our data suggest that holo-Lf, through a direct association with APP, could be a contributing factor in iron accumulation in AD.

Holo-Lf significantly reduced surface presented FPN levels in human SH-SY5Y neuroblastoma cultures (Figure 7.1) when analysed by flow cytometry. We have previously shown holo-Lf to internalise surface presented APP in a receptor mediated pathway (Chapter 4.0). Therefore, the ability of holo-Lf to remove APP from the cell surface indirectly destabilises surface presented FPN, resulting in reduced surface expression. Whilst the apo form of Lf and Tf failed to elicit a similar change, holo-Tf increased surface presented FPN levels (Figure 7.1). This was in accordance with the ability of holo-Tf to increase cell surface APP levels in neuroblastomas (Chapter 4.2.1). Transport of iron is largely mediated by internalisation through the Tf/TfR1 complex (Moos et al., 2007; Zhang et al., 2012). Therefore, increased internalisation of iron via the Tf/TfR1 pathway promotes APP and concomitantly FPN expression on the cell surface in order to facilitate iron efflux (Duce et al., 2010; Wong et al., 2014b).

The indirect destabilisation of surface presented FPN caused by holo-Lf led us to investigate the other major iron regulatory proteins involved in iron uptake (TfR) (Zhang et al., 2012) and storage (Ft) (Arosio et al., 2009) as well as the intracellular cytoplasmic LIP. To ascertain whether Lf altered LIP levels and TfR and Ft expression through an APP dependent pathway, we exposed Lf to SH-SY5Y cells with and without the presence of APP. In the absence of holo-Lf, APP depleted cells exhibited a decrease in TfR, an increase in Ft protein expression

(Figure 7.2) and intracellular labile iron (Figure 7.3) compared to non-target control cells. This was in accordance with findings published by others where ablation of APP impeded iron export and in response limited further iron uptake by translationally downregulating TfR whilst increasing Ft translation to accommodate intracellular iron levels in APPKO primary murine neuronal cultures (Duce et al., 2010; Wong et al., 2014b). The presence of holo-Lf did not result in any further change in TfR and Ft protein expression (Figure 7.2) or iron accumulation (Figure 7.3) in APP depleted cells, indicating holo-Lf indirectly alters iron homeostasis through an association with APP. However, there was a decrease in total APP and TfR, an increase in Ft expression (Figure 7.2) as well as intracellular LIP (Figure 7.3) with holo-Lf exposure compared to non-target control cells. The decrease in total APP levels with holo-Lf can be explained by previous findings that demonstrate holo-Lf to facilitate APP amyloidogenic processing, resulting in reduced levels of total cellular APP (Chapter 5.0). The changes detected in TfR and Ft expression are likely to be in response to the increased level of free iron within the LIP which prevents IRPs from binding to IREs located in the UTR of TfR and Ft mRNA, governing an increase and decrease in Ft and TfR translation respectively (Duce et al., 2010; Rogers et al., 2002). The rise in intracellular iron levels (Figure 7.3) which further affected the expression levels of TfR and Ft in non-target cells (Figure 7.2) were more significant in the presence of holo-Lf than in cells depleted of APP. This could possibly be a potential mechanism by the cell to retain intracellular iron in the presence of Lf since Lf's main role is to withhold extracellular iron that cannot be sequestered by the invading pathogen (Grossmann et al., 1992; Jameson et al., 1998). In addition, Lf could be releasing its bound iron intracellularly to maintain homeostasis and promote cell survival. This is supported by evidence indicating Lf to activate autophagy *in vitro* to increase cell survival during nutrient deficiency and promote cellular homeostasis (Aizawa et al., 2017). However, there are inconsistencies within the literature on whether the effects of Lf has any impact on any of the associated iron regulatory proteins involved in iron homeostasis. For example, Cutone *et al* demonstrated no change in FPN, TfR or Ft levels with exogenous Lf treatment to THP-1 differentiated macrophages when analysed by Western blot (Cutone et al., 2017). These variations in results could be due to the type of cell used in the study and therefore we cannot exclude the possibility that Lf might possess differing roles in iron homeostasis which might vary among

different cell types (Levay and Viljoen, 1995; Suzuki et al., 2005; Ward et al., 2005b). However, further experimentation to determine the APP expression profile in addition to cellular location in THP-1 differentiated macrophages used by Cutone *et al* is essential since results within our study indicate holo-Lf to be dependent upon the presence of cell surface APP for its indirect role in altering the expression of the major iron regulatory proteins. Furthermore, whether Lf was in its apo or holo form was not addressed by Cutone *et al* since several studies have shown Lf to possess varying functions according to its iron saturation state (Grossmann et al., 1992; Jameson et al., 1998). Further investigation on whether Lf affects any of the other iron regulatory proteins is also warranted since multiple studies have shown DMT1 and the iron export regulator hepcidin to be altered in neurons exposed to a pro-inflammatory environment (Salazar et al., 2008; Urrutia et al., 2013; Vela, 2018).

The presence of apo-Lf did not affect any of the iron regulatory proteins and had no impact on intracellular iron levels in either APP depleted or non-target cells (Figure 7.2 and Figure 7.3). A study conducted by Wang *et al* demonstrated apo-Lf endocytosis mediated by the LfR to chelate intracellular iron and reduce cytoplasmic iron levels in primary murine neurons which ceased when apo-Lf uptake was halted by LfR RNAi treatment (Wang et al., 2015). Even though the authors showed holo-Lf to gain cellular entry by the same mechanism as apo-Lf, holo-Lf did not have any effect on intracellular iron levels (Wang et al., 2015), indicating that the iron saturation state of Lf does not seem to play any role in cellular uptake via the LfR (Florian et al., 2012; Jiang et al., 2011; Suzuki et al., 2005). However, our data suggests an APP dependent mechanism for holo-Lf to accumulate iron within the cell which is supported by earlier findings indicating holo-Lf may be dependent on the presence of APP to gain cellular entry (Chapter 4.2.2) and therefore could explain the disparities in results.

The ability of iron to accept and donate electrons with molecular oxygen generates ROS through Fenton and Haber-Weiss chemistry. An overproduction of ROS may lead to severe cell damage and eventual death (Conrad and Umbreit, 2000; Sharpe et al., 2003). Increased cellular susceptibility to oxidative stress associated with iron accumulation leads to neurodegeneration within patients and animal models of dementia related disorders (Connor et al., 1992b; Jack et al., 2005; LeVine, 1997). A loss of APP *in vitro* leads to iron dependent

oxidative stress (Ayton et al., 2015b; Duce et al., 2010) and dietary iron exposure in APPKO mice results in marked oxidative stress in cortical neurons (Duce et al., 2010). Ferroptosis is a recently described form of iron-dependent non-apoptotic programmed cell death (Dixon et al., 2012) that results in toxic lipid peroxidation products, mitochondrial fragmentation, loss of plasma membrane integrity, and several other changes, which are all features of AD (Park et al., 2015; Sanchez Campos et al., 2015). *Post mortem* evidence that demonstrates increased lipid peroxidation and iron elevation (Connor et al., 1992b; Jack et al., 2005; LeVine, 1997; Montine et al., 2002) also suggests a role for ferroptosis in AD. A sustained exposure of holo-Lf led to a dose-dependent increase in lipid peroxidation and cell death (Figure 7.4). There has been other studies indicating holo-Lf to generate ROS production *in vitro* via increasing iron levels inside the cell (Ambruso and Johnston, 1981; Fillebeen et al., 1999). Anand *et al* demonstrated a dose dependent increase in ROS production with holo-Lf in peripheral human macrophages, enhancing phagocytic activity to eliminate intracellular pathogens (Anand et al., 2015). However, the mechanism of how holo-Lf gains entry into the cell to raise intracellular iron levels was not elucidated but authors assumed it was via the LfR (Anand et al., 2015). Taken together, these studies suggest different cell types seem to express their own receptors for Lf with varying functional characteristics (Suzuki and Lonnerdal, 2002; Suzuki et al., 2005). However, whether the LfR could play a role in the interaction between APP and holo-Lf requires further investigation.

Ferroptosis is triggered by loss of Gpx4 activity (Dixon et al., 2012). Therefore, further experimentation to determine whether holo-Lf causes a reduction in Gpx4 and whether agents that enable the restoration of iron efflux to reduce iron induced lipid peroxidation mediated by holo-Lf and protect against ferroptosis, such as the known ferroptosis inhibitors liproxstatin-1 (Friedmann Angeli et al., 2014), ferrostatin-1 (Cao and Dixon, 2016) and DFP (Stockwell et al., 2017) are warranted to confirm a holo-Lf mediated ferroptosis route.

CHAPTER 8.0 DISCUSSION

A careful balance of iron in cells is required as it is altered in response to inflammation (for example, through infection) and implicated in AD (Rogers et al., 1996; Smith et al., 1997; Urrutia et al., 2013). Lf is an acute phase protein that is upregulated in response to infection and inflammation (Levay and Viljoen, 1995) and is involved in cellular iron management in neuroinflammation and the immune response (Grossmann et al., 1992; Jameson et al., 1998; Sanchez et al., 1992). It is secreted by activated microglia (Fillebeen et al., 2001; Wang et al., 2015) where its primary role is to sequester iron away from invading pathogens, limiting their growth and spread of infection (Actor et al., 2009; Jameson et al., 1998; Levay and Viljoen, 1995). Lf is elevated in the AD brain and studies have documented its presence in neurons, microglia and around lesions of neuronal damage, including plaques (Kawamata et al., 1993; Leveugle et al., 1994; Qian and Wang, 1998) but it is unknown at present whether this has a neuroprotective role by sequestering free iron, or is deleterious through signalling inflammation.

Data within this study uncovers a possible role for APP that links both iron imbalance and Aβ accumulation with neuroinflammation, through an ability to interact with Lf. The relationship between Lf and APP was explored where iron bound holo-Lf was found to directly bind APP and facilitate internalisation into the cell to increase the production of Aβ. Through various techniques to monitor APP and Lf trafficking through the cell, the cellular mechanism of how Lf (together with APP) enters the cell along with the precise location of Aβ production were identified. By altering the cellular location of APP (through APP internalisation), holo-Lf was shown to alter the regulation of iron, causing entrapment of iron inside the cell where after a sustained presence, led to the build-up of lipid peroxidation and induction of cell death.

The conformational modification to Lf caused when iron is bound (holo-Lf) (Grossmann et al., 1992; Jameson et al., 1998) led to a high affinity interaction with cell surface APP. Physiologically, APP is internalised into the cell through a receptor mediated event typically through a clathrin dependent pathway (Figure 8.1) (Cossec et al., 2010; Motley et al., 2003; Nordstedt et al., 1993). Most of the APP is either recycled via Rab4-positive vesicles (fast recycling) from the early endosome, Rab11-positive vesicles from the perinuclear recycling compartment

(slow recycling) or degraded in Rab7-positive late endosomes and lysosomes (Figure 8.1) (Caporaso et al., 1992a; Lai et al., 1995; Yamazaki et al., 1996). Although studies have indicated Rab7 and Rab11 compartments to be possible sites for APP amyloidogenic processing (Ginsberg et al., 2010b; Udayar et al., 2013), the primary site of Aβ production lies within the Rab5-positive early endosome (Figure 8.1) (Ginsberg et al., 2010a; Grbovic et al., 2003; Xu et al., 2018). Amyloidogenic processing to produce Aβ primarily requires receptor mediated endocytosis of full-length APP before cleavage by BACE1 and the γ-secretase complex (Chow et al., 2010; Ehehalt et al., 2003). However, holo-Lf promotes APP trafficking from the cell surface down the same endocytic pathway that regulates BACE1 internalisation through an ARF6-dependent mechanism (Sannerud et al., 2011; Tang et al., 2015) that prevents APP from being recycled or degraded. This increased trafficking of APP to (Rab11-positive) compartments in which APP is amyloidogenically processed leads to increased Aβ formation (Figure 8.1). The recent data reveals an important insight into how Lf, as an acute phase protein of the brain's innate immune system, has direct control of Aβ production within cells. Intriguingly, a network analysis of GWAS genes associated with sporadic AD identifies Rab11 as an interacting component (Udayar et al., 2013). Furthermore, the ARF6 expression profile is increased in AD brains, and this accordingly correlates with neurotoxic Aβ formation in the hippocampus of AD brains (Braak et al., 2006; Tang et al., 2015), indicating a causal link between ARF6 and Rab11 with AD. Therefore, Lf directed APP internalisation (involving ARF6) and trafficking (involving Rab11) may have key roles in AD pathology.

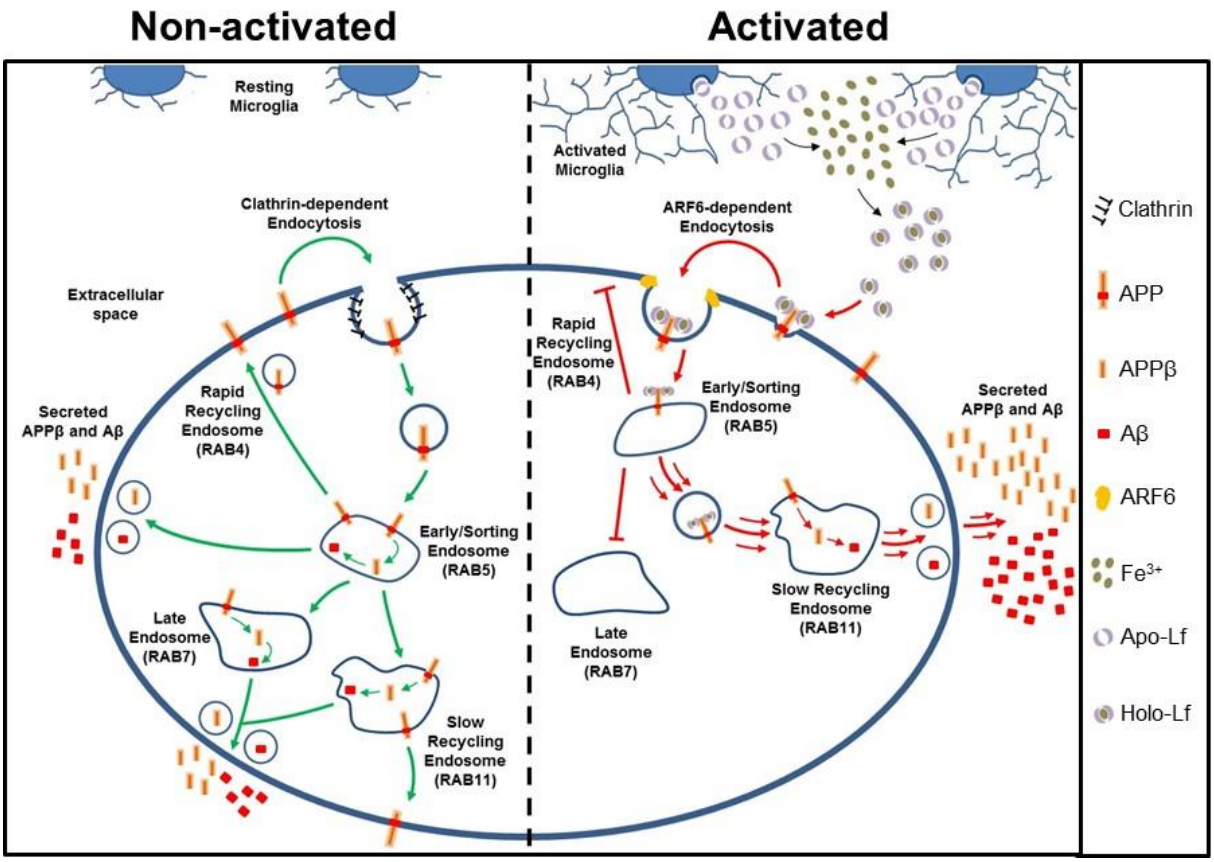

Figure 8.1. Schematic representation of APP endocytosis and amyloidogenic processing in the absence (non-activated) and presence (activated) of Lf. In the non-activated state, APP on the cell surface can be internalised back into the cell via a clathrin-mediated process that enters the endosomal system. Amyloidogenic processing of APP may occur in either the Rab5-positive early, Rab7-positive late or Rab11-positive recycling endosomes to generate sAPPβ and Aβ which are both secreted. Some of the APP can also be sorted either into Rab4 or Rab11-positive compartments for rapid or slow recycling, respectively, or into Rab7-positive compartments destined for degradation. In the activated state, induced microglia secrete iron-free apo-Lf which binds iron to form holo-Lf. Holo-Lf directly binds APP and internalises into the cell via a clathrin-independent, ARF6-dependent mechanism. Holo-Lf directed APP internalisation is directed to the Rab11-positive recycling endosome to exacerbate the amyloidogenic processing of APP, increasing sAPPβ and Aβ production, which are both secreted. Abbreviations: APP, amyloid-β precursor protein; Lf, lactoferrin; ARF6, ADP ribosylation factor 6; Aβ, amyloid-β.

To confirm findings in a more physiological cellular environment, we developed a transwell co-culture model to interrogate the signalling cross-talk between different populations of cells found in the brain. Here, we were able to more closely resemble physiological conditions and obtain data with stronger biological significance. When co-cultured with neuroblastomas, the ability of stimulated microglia to secrete Lf in an inflammatory environment provided physiological relevance and in turn confirmed Lf to induce Aβ production in neuroblastomas through an ability to bind APP on the cell surface. Studies have documented the expression of Lf and the LfR in endothelial cells within the brain, indicating the BBB as a possible point of entry into the brain for peripheral Lf through receptor mediated endocytosis. For instance, Fillebeen *et al* developed an *in vitro* co-culture model of the BBB consisting of differentiated bovine brain capillary endothelial cells (BBCECs) in the upper chamber, representing the capillary wall of the BBB and astrocytes in the lower compartment (Fillebeen et al., 1999). Exogenous addition of radiolabelled holo-Lf to the upper chamber was detected in the lower compartment as well as LfR expression on the surface of BBCECs (Fillebeen et al., 1999). Furthermore, radiolabelled holo-Lf added to the lower chamber could not be detected within the upper compartment containing BBCECs, indicating the transport of holo-Lf to be unidirectional, from the apical to the abluminal membrane (Fillebeen et al., 1999). These findings suggest that the presence of Lf within the brain may come from a source within the periphery. Results presented in this thesis demonstrating an increase in Lf expression from activated microglia suggests Lf may originate from within the brain. The presence of Lf transcripts in human brain tissue is also in favour of an *in situ* synthesis of Lf (An et al., 2009; Wang et al., 2015). Therefore, the accumulation of Lf within the AD brain (Kawamata et al., 1993; Leveugle et al., 1994) is likely to originate from a mixture of sources from within the brain and periphery.

Taken together, our findings suggest that APP can ‘switch’ the cell into a form that protects against inflammation. Holo-Lf may be required when neuronal iron levels are sufficiently low to promote normal metabolic function or as an innate defence mechanism (Actor et al., 2009; Legrand et al., 2005). Shedding APP from the cell surface by holo-Lf could provide an acute neuroinflammatory response aimed at preventing iron availability to invading pathogens outside the cell and a concomitant utilisation of the amyloidogenic processing pathway of

APP. Intriguing new research has revealed that Aβ shares many features with known antimicrobial peptides that have key protective roles in innate immunity (Bourgade et al., 2016; Kumar et al., 2016; Soscia et al., 2010; Spitzer et al., 2016). Therefore, the amyloidogenic processing of APP may not only have a role in stifling invading pathogens by withholding iron but also producing Aβ to eradicate invading pathogens. While this may provide a protective role for Lf in acute conditions, whereby it removes iron required for extracellular pathogen survival (Jameson et al., 1998; Sanchez et al., 1992), more persistent presence of such a potent modulator of inflammation and immunity may become detrimental to the brain over time. Chronic processing of APP through the amyloidogenic pathway may lead to Aβ production within the local extracellular environment and retention of neurotoxic iron, both harmful components commonly observed in AD (Cras et al., 1991; Liu et al., 2018). Furthermore, persistent induction of the pathway by Lf could lead to increased susceptibility to a novel form of cell death called ferroptosis that involves both elevated iron and lipid peroxidation (Dixon et al., 2012; Maiorino et al., 2018).

The amyloid cascade hypothesis clearly states that Aβ deposition is the initiating trigger that drives AD pathology (Hardy, 2006; Hardy and Allsop, 1991). The classification of Aβ as an antimicrobial peptide (Soscia et al., 2010) does not necessarily refute the amyloid cascade hypothesis but does attempt to update and expand the existing hypothesis to include an explanation for sporadic AD. Also, it shifts the focus of Aβ from being a harmful toxic by-product that aggregates to form plaques, to a protective role as an innate immune response peptide that becomes dysregulated under a chronic inflammatory environment (Moir et al., 2018). Nevertheless, instead of being regarded as a repercussion of Aβ production, it does elude to neuroinflammation as having a more causative role and is what might drive Aβ deposition to counterbalance immunochallenge (Li et al., 2018; Moir et al., 2018). Perhaps the existing amyloid cascade hypothesis is more applicable to early onset FAD that involves a pure genetic predisposition to the disease while the theory related to the antimicrobial activity of Aβ is more appropriate for late onset sporadic AD. Whether the triggering mechanism that elicits neuroinflammation with subsequent Aβ production is from an infectious or non-infectious insult to the brain remains unclear and warrants further investigation. Either way, the amyloidogenic processing of APP that leads

to the generation of Aβ is through receptor mediated APP endocytosis (Cirrito et al., 2008; Cossec et al., 2010) and the existence of a currently unknown cognate functional ligand. Data presented here identifies Lf as a potential ligand prominently expressed during inflammation (Kruzel et al., 2017; Levay and Viljoen, 1995), that promotes the amyloidogenic pathway of APP and give rise to Aβ known to have antimicrobial properties (Gosztyla et al., 2018). This also supports that microglial activation, leading to the production and secretion of Lf, is an underlying factor in the development of AD rather than a consequence of AD pathology.

Multiple studies have shown several pro-inflammatory cytokines produced from activated microglia to affect the amyloidogenic pathway of APP, thereby promoting Aβ peptide production (Atwood et al., 2003; Del Bo et al., 1995; Fassbender et al., 2000; Ringheim et al., 1998). The ability to attenuate the majority of Aβ production by masking the holo-Lf binding sites of APP using either an antibody recognising Lf or peptides from APP that recognise the binding site to holo-Lf suggests that the source of Aβ production could predominantly originate from the interaction between holo-Lf and APP. This also proposes that Lf may possibly regulate cytokine production by activated microglia that act downstream to further exacerbate Aβ formation. Since Aβ itself can further activate microglia to secrete pro-inflammatory cytokines (Fassbender et al., 2000; Meda et al., 1995), this would lead to a viscous cycle resulting in chronic neuroinflammation, further accelerating the development of AD (Griffin et al., 1998; Lindberg et al., 2005). The effects of Lf on cytokine secretion remain unclear. However, Lf has been shown to interact with members of the pattern recognition receptor (PRR) family such as the receptor for advanced glycation end products (RAGE) where binding leads to NF-κB stimulation and subsequent gene transcription of pro-inflammatory cytokines and chemokines including IL-1, IL-6, TNF-α, COX-2 and NO formation (Huang et al., 2001; Kruzel et al., 2017; Schmidt et al., 1994; Vallabhapurapu and Karin, 2009; Zemankova et al., 2016). This suggests that cytokine release by activated microglia could occur secondary to Lf, demonstrating Lf as one of the first lines of host defence by activated microglia (Actor et al., 2009; Kruzel et al., 2007; Kruzel et al., 2017) and that the presence of Lf contributes to pro-inflammatory cytokine induced Aβ production. Therefore, further experiments proposed for this study would be to examine

cytokine levels in Lf knockdown activated microglia to confirm whether cytokine release is affected by the presence of Lf.

Data presented within this study provides the framework for potential progression into a more translational and pre-clinical setting. Future longer-term supporting studies will need to be carried out to validate and confirm results *in vivo*. Whether persistent Lf signalling leads to sustained Aβ-related neuropathology would also need to be established *in vivo*. However, one major limitation is that none of the existing mouse models available fully reproduce the complete spectrum of AD, and therefore investigation is limited to an in-depth analysis of one or two components of the disease (Esquerda-Canals et al., 2017). Choosing a suitable mouse model to study the effects of Lf on APP amyloidogenic processing for therapeutic intervention could present certain difficulties. For example, mice carrying the familial Swedish APP mutation, such as the Tg2576 and J20 models, among many others, tend to accumulate high levels of Aβ and develop amyloid pathology (Kitazawa et al., 2012; Lee and Han, 2013). One might assume that the administration of Lf in a model that always develops amyloid would help determine whether Lf can accelerate neuropathology associated with AD. However, these transgenic mouse models that rely on the utilisation of genetic mutations are mostly associated with FAD and therefore do not accurately represent the sporadic, late onset form of AD (Lee and Han, 2013). Furthermore, AD mouse models harbouring the familial Swedish APP mutation have shown β-secretase processing of APP to predominantly occur at the Golgi apparatus, resulting in decreasing levels of cell surface APP (Thinakaran et al., 1996a). This increase in programmed amyloidogenic APP processing could mimic the effects that we have shown Lf to have on promoting the APP amyloidogenic pathway. In addition, without the presence of APP on the cell surface, extracellular (holo) Lf would not be able to bind and internalise APP destined for amyloidogenic processing by β- and γ-secretases in the endocytic compartments. Also, using transgenic mouse models overexpressing APP to study Aβ amyloidosis non-physiologically overexpress APP which often results in the overproduction of various APP fragments in addition to Aβ, making it difficult to distinguish the neuropathological phenotype specifically caused by Aβ (Gidyk et al., 2015; Rice et al., 2019; Sasaguri et al., 2017). Perhaps a more suitable alternative mouse model to study the effects of Lf on APP would be the APP knock-in model carrying

a humanised Aβ sequence that is capable of endogenously overproducing Aβ without non-physiologically overexpressing APP (Saito et al., 2014; Sasaguri et al., 2017). The APP knock-in model administered with a pro-inflammatory stimulus known to induce microglial derived Lf production (Fillebeen et al., 2001; Wang et al., 2015) will identify whether Lf can induce APP amyloidogenic processing, leading to pathological deficits associated with sporadic AD. The use of the LfKO mouse model would also be advantageous which under normal physiological conditions show no obvious phenotypic abnormalities (Ward et al., 2003). An APP knock-in model crossed with a LfKO mouse line challenged with the same pro-inflammatory stimulus would help determine whether Lf ablation has any correlation with APP processing, Aβ production and iron homeostasis.

Currently there are no effective treatments for AD and with a greater understanding of the APP processing machinery, continuing studies should be supported in designing drugs that can alleviate Aβ production in an AD pathological environment. While small inhibitor compounds can be designed to achieve highly specific binding to inhibit complex formation, precise identification of the binding motif involved in the interaction between Lf and APP is critical to maximise specificity and affinity while keeping the compound size reasonable. Other approaches such as antibody based therapy and inhibitor peptides must also be able to cross the BBB for efficient delivery into the brain as well as the ability to compete with the interaction (Dong, 2018; Paul, 2011) between Lf and APP. The type of therapy used must also avoid disrupting the physiological role of APP, since APP has been shown to interact with multiple ligands to exert numerous functions (Muller et al., 2017; van der Kant and Goldstein, 2015). Perhaps the most suitable approach in blocking the interaction between Lf and APP would be via allosteric modulation (Abdel-Magid, 2015), inhibiting the conformational change that occurs when Lf binds iron, since data within this thesis has shown Lf to interact with APP only in its iron bound holo-form.

8.1 Conclusion

How neuroinflammation and iron dysregulation contributes to AD pathogenesis is not entirely understood. Taken together, information presented within this thesis describes iron bound Lf, a pro-inflammatory mediator as a novel extracellular ligand to APP. The binding of Lf to APP promotes APP

internalisation through an ARF6-dependent pathway that increases trafficking to Rab11-positive compartments resulting in an increase in Aβ formation. Shedding APP off the cell surface by Lf indirectly destabilises cell surface FPN, increasing iron retention and under a sustained exposure facilitates iron-associated toxicity and cell death. Therefore, current observations indicate Lf to be a key player connecting neuroinflammation, iron accumulation, APP processing, and Aβ secretion, displaying a unified mechanism responsible for the neurodegeneration prevalent in AD. Lf serves as a promising therapeutic target for reducing intraneuronal iron accumulation and Aβ production, especially under chronic inflammatory conditions. Where a strong persistent inflammatory response may not be required, such as in patients living with AD, the blocking of the interaction between APP and Lf could restore the flow of iron out of cells and reduce the production of Aβ. However, if the production of Aβ is indeed warranted due to a microbial presence then the blocking of the interaction between Lf and APP may prove to be detrimental. To address this issue, comprehensive screening of patients for a microbial presence will be required. This could lead to the hope for providing a new potential therapy in a population of people that have no pre-existing family history of the disease.

REFERENCES

Abdel-Magid, A.F. (2015). Allosteric modulators: an emerging concept in drug discovery. ACS medicinal chemistry letters *6*, 104-107.

Actor, J.K., Hwang, S.A., and Kruzel, M.L. (2009). Lactoferrin as a natural immune modulator. Current pharmaceutical design *15*, 1956-1973.

Aisen, P., Enns, C., and Wessling-Resnick, M. (2001). Chemistry and biology of eukaryotic iron metabolism. The international journal of biochemistry & cell biology *33*, 940-959.

Aisen, P., and Leibman, A. (1972). Lactoferrin and transferrin: a comparative study. Biochimica et biophysica acta *257*, 314-323.

Aizawa, S., Hoki, M., and Yamamuro, Y. (2017). Lactoferrin promotes autophagy via AMP-activated protein kinase activation through low-density lipoprotein receptor-related protein 1. Biochemical and biophysical research communications *493*, 509-513.

Allison, R., Lumb, J.H., Fassier, C., Connell, J.W., Ten Martin, D., Seaman, M.N., Hazan, J., and Reid, E. (2013). An ESCRT-spastin interaction promotes fission of recycling tubules from the endosome. The Journal of cell biology *202*, 527-543.

Alory, C., and Balch, W.E. (2001). Organization of the Rab-GDI/CHM superfamily: the functional basis for choroideremia disease. Traffic *2*, 532-543.

Ambruso, D.R., and Johnston, R.B., Jr. (1981). Lactoferrin enhances hydroxyl radical production by human neutrophils, neutrophil particulate fractions, and an enzymatic generating system. The Journal of clinical investigation *67*, 352-360.

An, L., Sato, H., Konishi, Y., Walker, D.G., Beach, T.G., Rogers, J., and Tooyama, I. (2009). Expression and localization of lactotransferrin messenger RNA in the cortex of Alzheimer's disease. Neuroscience letters *452*, 277-280.

Anand, N., Kanwar, R.K., Dubey, M.L., Vahishta, R.K., Sehgal, R., Verma, A.K., and Kanwar, J.R. (2015). Effect of lactoferrin protein on red blood cells and macrophages: mechanism of parasite-host interaction. Drug design, development and therapy *9*, 3821-3835.

Andersen, O.M., Reiche, J., Schmidt, V., Gotthardt, M., Spoelgen, R., Behlke, J., von Arnim, C.A., Breiderhoff, T., Jansen, P., Wu, X., Bales, K.R., Cappai, R., Masters, C.L., Gliemann, J., Mufson, E.J., Hyman, B.T., Paul, S.M., Nykjaer, A., and Willnow, T.E. (2005). Neuronal sorting protein-related receptor sorLA/LR11 regulates processing of the amyloid precursor protein. Proceedings of the National Academy of Sciences of the United States of America *102*, 13461-13466.

Anderson, B.F., Baker, H.M., Dodson, E.J., Norris, G.E., Rumball, S.V., Waters, J.M., and Baker, E.N. (1987). Structure of human lactoferrin at 3.2-A resolution. Proceedings of the National Academy of Sciences of the United States of America *84*, 1769-1773.

Anderson, B.F., Baker, H.M., Norris, G.E., Rice, D.W., and Baker, E.N. (1989). Structure of human lactoferrin: crystallographic structure analysis and refinement at 2.8 A resolution. Journal of molecular biology *209*, 711-734.

Anderson, C.P., Shen, M., Eisenstein, R.S., and Leibold, E.A. (2012). Mammalian iron metabolism and its control by iron regulatory proteins. Biochimica et biophysica acta *1823*, 1468-1483.

Anderson, G.J., Frazer, D.M., and McLaren, G.D. (2009). Iron absorption and metabolism. Current opinion in gastroenterology *25*, 129-135.

Armstrong, R.A. (2009). The molecular biology of senile plaques and neurofibrillary tangles in Alzheimer's disease. Folia neuropathologica / Association of Polish Neuropathologists and Medical Research Centre, Polish Academy of Sciences *47*, 289-299.

Armstrong, R.A. (2011). The pathogenesis of Alzheimer's disease: a reevaluation of the "amyloid cascade hypothesis". International journal of Alzheimer's disease *2011*, 630865.

Arosio, P., Ingrassia, R., and Cavadini, P. (2009). Ferritins: a family of molecules for iron storage, antioxidation and more. Biochimica et biophysica acta *1790*, 589-599.

Arriagada, C., Astorga, C., Atwater, I., Rojas, E., Mears, D., Caviedes, R., and Caviedes, P. (2007). Endosomal abnormalities related to amyloid precursor protein in cholesterol treated cerebral cortex neuronal cells derived from trisomy 16 mice, an animal model of Down syndrome. Neuroscience letters *423*, 172-177.

Arriagada, C., Bustamante, M., Atwater, I., Rojas, E., Caviedes, R., and Caviedes, P. (2010). Apoptosis is directly related to intracellular amyloid accumulation in a cell line derived from the cerebral cortex of a trisomy 16 mouse, an animal model of Down syndrome. Neuroscience letters *470*, 81-85.

Arriagada, P.V., Marzloff, K., and Hyman, B.T. (1992). Distribution of Alzheimer-type pathologic changes in nondemented elderly individuals matches the pattern in Alzheimer's disease. Neurology *42*, 1681-1688.

Atwood, C.S., Obrenovich, M.E., Liu, T., Chan, H., Perry, G., Smith, M.A., and Martins, R.N. (2003). Amyloid-beta: a chameleon walking in two worlds: a review of the trophic and toxic properties of amyloid-beta. Brain research Brain research reviews *43*, 1-16.

Austin, S.A., Santhanam, A.V., and Katusic, Z.S. (2010). Endothelial nitric oxide modulates expression and processing of amyloid precursor protein. Circulation research *107*, 1498-1502.

Ayton, S., Faux, N.G., and Bush, A.I. (2015a). Ferritin levels in the cerebrospinal fluid predict Alzheimer's disease outcomes and are regulated by APOE. Nature communications *6*, 6760.

Ayton, S., Faux, N.G., and Bush, A.I. (2017a). Association of Cerebrospinal Fluid Ferritin Level With Preclinical Cognitive Decline in APOE-epsilon4 Carriers. JAMA neurology *74*, 122-125.

Ayton, S., Fazlollahi, A., Bourgeat, P., Raniga, P., Ng, A., Lim, Y.Y., Diouf, I., Farquharson, S., Fripp, J., Ames, D., Doecke, J., Desmond, P., Ordidge, R., Masters, C.L., Rowe, C.C., Maruff, P., Villemagne, V.L., Salvado, O., and Bush, A.I. (2017b). Cerebral quantitative susceptibility mapping predicts amyloid-beta-related cognitive decline. Brain : a journal of neurology *140*, 2112-2119.

Ayton, S., Lei, P., Hare, D.J., Duce, J.A., George, J.L., Adlard, P.A., McLean, C., Rogers, J.T., Cherny, R.A., Finkelstein, D.I., and Bush, A.I. (2015b). Parkinson's disease iron deposition caused by nitric oxide-induced loss of beta-amyloid precursor protein. The Journal of neuroscience : the official journal of the Society for Neuroscience *35*, 3591-3597.

Ayton, S., Zhang, M., Roberts, B.R., Lam, L.Q., Lind, M., McLean, C., Bush, A.I., Frugier, T., Crack, P.J., and Duce, J.A. (2014). Ceruloplasmin and beta-amyloid precursor protein confer neuroprotection in traumatic brain injury and lower neuronal iron. Free radical biology & medicine *69*, 331-337.

Bacskai, B.J., Xia, M.Q., Strickland, D.K., Rebeck, G.W., and Hyman, B.T. (2000). The endocytic receptor protein LRP also mediates neuronal calcium signaling via N-methyl-D-aspartate receptors. Proceedings of the National Academy of Sciences of the United States of America *97*, 11551-11556.

Bai, Y., Markham, K., Chen, F., Weerasekera, R., Watts, J., Horne, P., Wakutani, Y., Bagshaw, R., Mathews, P.M., Fraser, P.E., Westaway, D., St George-Hyslop, P., and Schmitt-Ulms, G. (2008). The in vivo brain interactome of the amyloid precursor protein. Molecular & cellular proteomics : MCP *7*, 15-34.

Bailey, M.F., Van der Schans, E.J.C., and Millar, D.P. (2007). Dimerization of the Klenow Fragment of Escherichia coli DNA Polymerase I Is Linked to Its Mode of DNA Binding. Biochemistry *46*, 8085-8099.

Baker, E.N. (1994). Structure and Reactivity of Transferrins. In Advances in Inorganic Chemistry, A.G. Sykes, ed. (Academic Press), pp. 389-463.

Baker, E.N., and Baker, H.M. (2005). Molecular structure, binding properties and dynamics of lactoferrin. Cellular and molecular life sciences : CMLS *62*, 2531-2539.

Baker, E.N., Baker, H.M., and Kidd, R.D. (2002). Lactoferrin and transferrin: functional variations on a common structural framework. Biochemistry and cell biology = Biochimie et biologie cellulaire *80*, 27-34.

Baker, H.M., and Baker, E.N. (2004). Lactoferrin and iron: structural and dynamic aspects of binding and release. Biometals : an international journal on the role of metal ions in biology, biochemistry, and medicine *17*, 209-216.

Ballatore, C., Lee, V.M., and Trojanowski, J.Q. (2007). Tau-mediated neurodegeneration in Alzheimer's disease and related disorders. Nature reviews Neuroscience *8*, 663-672.

Baranello, R.J., Bharani, K.L., Padmaraju, V., Chopra, N., Lahiri, D.K., Greig, N.H., Pappolla, M.A., and Sambamurti, K. (2015). Amyloid-beta protein clearance and degradation (ABCD) pathways and their role in Alzheimer's disease. Current Alzheimer research *12*, 32-46.

Baranger, K., Marchalant, Y., Bonnet, A.E., Crouzin, N., Carrete, A., Paumier, J.M., Py, N.A., Bernard, A., Bauer, C., Charrat, E., Moschke, K., Seiki, M., Vignes, M., Lichtenthaler, S.F., Checler, F., Khrestchatisky, M., and Rivera, S. (2016). MT5-MMP is a new pro-amyloidogenic proteinase that promotes amyloid pathology and cognitive decline in a transgenic mouse model of Alzheimer's disease. Cellular and molecular life sciences : CMLS *73*, 217-236.

Barbagallo, A.P., Weldon, R., Tamayev, R., Zhou, D., Giliberto, L., Foreman, O., and D'Adamio, L. (2010). Tyr(682) in the intracellular domain of APP regulates amyloidogenic APP processing in vivo. PloS one *5*, e15503.

Barnham, K.J., McKinstry, W.J., Multhaup, G., Galatis, D., Morton, C.J., Curtain, C.C., Williamson, N.A., White, A.R., Hinds, M.G., Norton, R.S., Beyreuther, K., Masters, C.L., Parker, M.W., and Cappai, R. (2003). Structure of the Alzheimer's disease amyloid precursor protein copper binding domain. A regulator of neuronal copper homeostasis. The Journal of biological chemistry *278*, 17401-17407.

Barrett, P.J., Song, Y., Van Horn, W.D., Hustedt, E.J., Schafer, J.M., Hadziselimovic, A., Beel, A.J., and Sanders, C.R. (2012). The amyloid precursor protein has a flexible transmembrane domain and binds cholesterol. Science *336*, 1168-1171.

Beckett, C., Nalivaeva, N.N., Belyaev, N.D., and Turner, A.J. (2012). Nuclear signalling by membrane protein intracellular domains: the AICD enigma. Cellular signalling *24*, 402-409.

Beher, D., Hesse, L., Masters, C.L., and Multhaup, G. (1996). Regulation of amyloid protein precursor (APP) binding to collagen and mapping of the binding sites on APP and collagen type I. The Journal of biological chemistry *271*, 1613-1620.

Belaidi, A.A., Gunn, A.P., Wong, B.X., Ayton, S., Appukuttan, A.T., Roberts, B.R., Duce, J.A., and Bush, A.I. (2018). Marked Age-Related Changes in Brain Iron Homeostasis in Amyloid Protein Precursor Knockout Mice. Neurotherapeutics : the journal of the American Society for Experimental NeuroTherapeutics *15*, 1055-1062.

Belyaev, N.D., Kellett, K.A., Beckett, C., Makova, N.Z., Revett, T.J., Nalivaeva, N.N., Hooper, N.M., and Turner, A.J. (2010). The transcriptionally active amyloid precursor protein (APP) intracellular domain is preferentially produced from the 695 isoform of APP in a {beta}-secretase-dependent pathway. The Journal of biological chemistry *285*, 41443-41454.

Benjannet, S., Elagoz, A., Wickham, L., Mamarbachi, M., Munzer, J.S., Basak, A., Lazure, C., Cromlish, J.A., Sisodia, S., Checler, F., Chretien, M., and Seidah, N.G. (2001). Post-translational processing of beta-secretase (beta-amyloid-converting enzyme) and its ectodomain shedding. The pro- and transmembrane/cytosolic domains affect its cellular activity and amyloid-beta production. The Journal of biological chemistry *276*, 10879-10887.

Bertram, L., Lill, C.M., and Tanzi, R.E. (2010). The genetics of Alzheimer disease: back to the future. Neuron *68*, 270-281.

Bhat, N.R., Feinstein, D.L., Shen, Q., and Bhat, A.N. (2002). p38 MAPK-mediated transcriptional activation of inducible nitric-oxide synthase in glial cells. Roles of nuclear factors, nuclear factor kappa B, cAMP response element-binding protein, CCAAT/enhancer-binding protein-beta, and activating transcription factor-2. The Journal of biological chemistry *277*, 29584-29592.

Bien, J., Jefferson, T., Causevic, M., Jumpertz, T., Munter, L., Multhaup, G., Weggen, S., Becker-Pauly, C., and Pietrzik, C.U. (2012). The metalloprotease meprin beta generates amino terminal-truncated amyloid beta peptide species. The Journal of biological chemistry *287*, 33304-33313.

Bishop, A., and Anderson, J.E. (2005). NO signaling in the CNS: from the physiological to the pathological. Toxicology *208*, 193-205.

Bjorklund, N.L., Reese, L.C., Sadagoparamanujam, V.M., Ghirardi, V., Woltjer, R.L., and Taglialatela, G. (2012). Absence of amyloid beta oligomers at the postsynapse and regulated synaptic Zn2+ in cognitively intact aged individuals with Alzheimer's disease neuropathology. Molecular neurodegeneration *7*, 23.

Blasko, I., Marx, F., Steiner, E., Hartmann, T., and Grubeck-Loebenstein, B. (1999). TNFalpha plus IFNgamma induce the production of Alzheimer beta-amyloid peptides and decrease the secretion of APPs. FASEB journal : official publication of the Federation of American Societies for Experimental Biology *13*, 63-68.

Blennow, K., Brody, D.L., Kochanek, P.M., Levin, H., McKee, A., Ribbers, G.M., Yaffe, K., and Zetterberg, H. (2016). Traumatic brain injuries. Nature reviews Disease primers *2*, 16084.

Bolmont, T., Clavaguera, F., Meyer-Luehmann, M., Herzig, M.C., Radde, R., Staufenbiel, M., Lewis, J., Hutton, M., Tolnay, M., and Jucker, M. (2007). Induction of tau pathology by intracerebral infusion of amyloid-beta -containing brain extract and by amyloid-beta deposition in APP x Tau transgenic mice. The American journal of pathology *171*, 2012-2020.

Bonda, D.J., Lee, H.G., Blair, J.A., Zhu, X., Perry, G., and Smith, M.A. (2011). Role of metal dyshomeostasis in Alzheimer's disease. Metallomics : integrated biometal science *3*, 267-270.

Bonifacino, J.S., and Traub, L.M. (2003). Signals for sorting of transmembrane proteins to endosomes and lysosomes. Annual review of biochemistry *72*, 395-447.

Borchelt, D.R., Thinakaran, G., Eckman, C.B., Lee, M.K., Davenport, F., Ratovitsky, T., Prada, C.M., Kim, G., Seekins, S., Yager, D., Slunt, H.H., Wang, R., Seeger, M., Levey, A.I., Gandy, S.E., Copeland, N.G., Jenkins, N.A., Price, D.L., Younkin, S.G., and Sisodia, S.S. (1996). Familial Alzheimer's disease-linked presenilin 1 variants elevate Abeta1-42/1-40 ratio in vitro and in vivo. Neuron *17*, 1005-1013.

Botelho, M.G., Gralle, M., Oliveira, C.L., Torriani, I., and Ferreira, S.T. (2003). Folding and stability of the extracellular domain of the human amyloid precursor protein. The Journal of biological chemistry *278*, 34259-34267.

Boucher, P., Gotthardt, M., Li, W.P., Anderson, R.G., and Herz, J. (2003). LRP: role in vascular wall integrity and protection from atherosclerosis. Science *300*, 329-332.

Bourgade, K., Garneau, H., Giroux, G., Le Page, A.Y., Bocti, C., Dupuis, G., Frost, E.H., and Fulop, T., Jr. (2015). beta-Amyloid peptides display protective activity against the human Alzheimer's disease-associated herpes simplex virus-1. Biogerontology *16*, 85-98.

Bourgade, K., Le Page, A., Bocti, C., Witkowski, J.M., Dupuis, G., Frost, E.H., and Fulop, T., Jr. (2016). Protective Effect of Amyloid-beta Peptides Against Herpes Simplex Virus-1 Infection in a Neuronal Cell Culture Model. Journal of Alzheimer's disease : JAD *50*, 1227-1241.

Bousejra-ElGarah, F., Bijani, C., Coppel, Y., Faller, P., and Hureau, C. (2011). Iron(II) binding to amyloid-beta, the Alzheimer's peptide. Inorganic chemistry *50*, 9024-9030.

Braak, H., Alafuzoff, I., Arzberger, T., Kretzschmar, H., and Del Tredici, K. (2006). Staging of Alzheimer disease-associated neurofibrillary pathology using paraffin sections and immunocytochemistry. Acta neuropathologica *112*, 389-404.

Braak, H., and Braak, E. (1991). Neuropathological stageing of Alzheimer-related changes. Acta neuropathologica *82*, 239-259.

Brandes, C., Novak, S., Stockinger, W., Herz, J., Schneider, W.J., and Nimpf, J. (1997). Avian and murine LR8B and human apolipoprotein E receptor 2: differentially spliced products from corresponding genes. Genomics *42*, 185-191.

Breuer, W., Ghoti, H., Shattat, A., Goldfarb, A., Koren, A., Levin, C., Rachmilewitz, E., and Cabantchik, Z.I. (2012). Non-transferrin bound iron in Thalassemia: differential detection of redox active forms in children and older patients. American journal of hematology *87*, 55-61.

Breuer, W., Shvartsman, M., and Cabantchik, Z.I. (2008). Intracellular labile iron. The international journal of biochemistry & cell biology *40*, 350-354.

Brifault, C., Gilder, A.S., Laudati, E., Banki, M., and Gonias, S.L. (2017). Shedding of membrane-associated LDL receptor-related protein-1 from microglia amplifies and sustains neuroinflammation. The Journal of biological chemistry *292*, 18699-18712.

Bright, N.A., Gratian, M.J., and Luzio, J.P. (2005). Endocytic delivery to lysosomes mediated by concurrent fusion and kissing events in living cells. Current biology : CB *15*, 360-365.

Brissot, P., Ropert, M., Le Lan, C., and Loreal, O. (2012). Non-transferrin bound iron: a key role in iron overload and iron toxicity. Biochimica et biophysica acta *1820*, 403-410.

Brock, J.H., Ismail, M., and Sanchez, L. (1994). Interaction of lactoferrin with mononuclear and colon carcinoma cells. Advances in experimental medicine and biology *357*, 157-169.

Brodeur, J., Theriault, C., Lessard-Beaudoin, M., Marcil, A., Dahan, S., and Lavoie, C. (2012). LDLR-related protein 10 (LRP10) regulates amyloid precursor protein (APP) trafficking and processing: evidence for a role in Alzheimer's disease. Molecular neurodegeneration *7*, 31.

Brodsky, F.M., Chen, C.Y., Knuehl, C., Towler, M.C., and Wakeham, D.E. (2001). Biological basket weaving: formation and function of clathrin-coated vesicles. Annual review of cell and developmental biology *17*, 517-568.

Bucci, C., Parton, R.G., Mather, I.H., Stunnenberg, H., Simons, K., Hoflack, B., and Zerial, M. (1992). The small GTPase rab5 functions as a regulatory factor in the early endocytic pathway. Cell *70*, 715-728.

Bucci, C., Thomsen, P., Nicoziani, P., McCarthy, J., and van Deurs, B. (2000). Rab7: a key to lysosome biogenesis. Molecular biology of the cell *11*, 467-480.

Buggia-Prevot, V., Fernandez, C.G., Riordan, S., Vetrivel, K.S., Roseman, J., Waters, J., Bindokas, V.P., Vassar, R., and Thinakaran, G. (2014). Axonal BACE1 dynamics and targeting in hippocampal neurons: a role for Rab11 GTPase. Molecular neurodegeneration *9*, 1.

Burdo, J.R., Menzies, S.L., Simpson, I.A., Garrick, L.M., Garrick, M.D., Dolan, K.G., Haile, D.J., Beard, J.L., and Connor, J.R. (2001). Distribution of divalent metal transporter 1 and metal transport protein 1 in the normal and Belgrade rat. Journal of neuroscience research *66*, 1198-1207.

Burns, M., Gaynor, K., Olm, V., Mercken, M., LaFrancois, J., Wang, L., Mathews, P.M., Noble, W., Matsuoka, Y., and Duff, K. (2003). Presenilin redistribution associated with aberrant cholesterol transport enhances beta-amyloid production in vivo. The Journal of neuroscience : the official journal of the Society for Neuroscience *23*, 5645-5649.

Bush, A.I. (2013). The metal theory of Alzheimer's disease. Journal of Alzheimer's disease : JAD *33 Suppl 1*, S277-281.

Buxbaum, J.D., Liu, K.N., Luo, Y., Slack, J.L., Stocking, K.L., Peschon, J.J., Johnson, R.S., Castner, B.J., Cerretti, D.P., and Black, R.A. (1998). Evidence that tumor necrosis factor alpha converting enzyme is involved in regulated alpha-secretase cleavage of the Alzheimer amyloid protein precursor. The Journal of biological chemistry *273*, 27765-27767.

Buxbaum, J.D., Oishi, M., Chen, H.I., Pinkas-Kramarski, R., Jaffe, E.A., Gandy, S.E., and Greengard, P. (1992). Cholinergic agonists and interleukin 1 regulate processing and secretion of the Alzheimer beta/A4 amyloid protein precursor. Proceedings of the National Academy of Sciences of the United States of America *89*, 10075-10078.

Cabantchik, Z.I. (2014). Labile iron in cells and body fluids: physiology, pathology, and pharmacology. Frontiers in pharmacology *5*, 45.

Cabrera, M., and Ungermann, C. (2013). Guanine nucleotide exchange factors (GEFs) have a critical but not exclusive role in organelle localization of Rab GTPases. The Journal of biological chemistry *288*, 28704-28712.

Caille, I., Allinquant, B., Dupont, E., Bouillot, C., Langer, A., Muller, U., and Prochiantz, A. (2004). Soluble form of amyloid precursor protein regulates proliferation of progenitors in the adult subventricular zone. Development *131*, 2173-2181.

Calabrese, V., Mancuso, C., Calvani, M., Rizzarelli, E., Butterfield, D.A., and Stella, A.M. (2007). Nitric oxide in the central nervous system: neuroprotection versus neurotoxicity. Nature reviews Neuroscience *8*, 766-775.

Cam, J.A., and Bu, G. (2006). Modulation of beta-amyloid precursor protein trafficking and processing by the low density lipoprotein receptor family. Molecular neurodegeneration *1*, 8.

Cao, J.Y., and Dixon, S.J. (2016). Mechanisms of ferroptosis. Cellular and molecular life sciences : CMLS *73*, 2195-2209.

Cao, X., and Sudhof, T.C. (2001). A transcriptionally [correction of transcriptively] active complex of APP with Fe65 and histone acetyltransferase Tip60. Science *293*, 115-120.

Caporaso, G.L., Gandy, S.E., Buxbaum, J.D., and Greengard, P. (1992a). Chloroquine inhibits intracellular degradation but not secretion of Alzheimer beta/A4 amyloid precursor protein. Proceedings of the National Academy of Sciences of the United States of America *89*, 2252-2256.

Caporaso, G.L., Gandy, S.E., Buxbaum, J.D., Ramabhadran, T.V., and Greengard, P. (1992b). Protein phosphorylation regulates secretion of Alzheimer beta/A4 amyloid precursor protein. Proceedings of the National Academy of Sciences of the United States of America *89*, 3055-3059.

Caporaso, G.L., Takei, K., Gandy, S.E., Matteoli, M., Mundigl, O., Greengard, P., and De Camilli, P. (1994). Morphologic and biochemical analysis of the intracellular trafficking of the Alzheimer beta/A4 amyloid precursor protein. The

Journal of neuroscience : the official journal of the Society for Neuroscience *14*, 3122-3138.

Cappai, R., Mok, S.S., Galatis, D., Tucker, D.F., Henry, A., Beyreuther, K., Small, D.H., and Masters, C.L. (1999). Recombinant human amyloid precursor-like protein 2 (APLP2) expressed in the yeast Pichia pastoris can stimulate neurite outgrowth. FEBS letters *442*, 95-98.

Carey, R.M., Balcz, B.A., Lopez-Coviella, I., and Slack, B.E. (2005). Inhibition of dynamin-dependent endocytosis increases shedding of the amyloid precursor protein ectodomain and reduces generation of amyloid beta protein. BMC cell biology *6*, 30.

Carrano, A., and Das, P. (2015). Altered Innate Immune and Glial Cell Responses to Inflammatory Stimuli in Amyloid Precursor Protein Knockout Mice. PloS one *10*, e0140210.

Carrillo-Mora, P., Luna, R., and Colin-Barenque, L. (2014). Amyloid beta: multiple mechanisms of toxicity and only some protective effects? Oxidative medicine and cellular longevity *2014*, 795375.

Cataldo, A., Rebeck, G.W., Ghetri, B., Hulette, C., Lippa, C., Van Broeckhoven, C., van Duijn, C., Cras, P., Bogdanovic, N., Bird, T., Peterhoff, C., and Nixon, R. (2001). Endocytic disturbances distinguish among subtypes of Alzheimer's disease and related disorders. Annals of neurology *50*, 661-665.

Cataldo, A.M., Mathews, P.M., Boiteau, A.B., Hassinger, L.C., Peterhoff, C.M., Jiang, Y., Mullaney, K., Neve, R.L., Gruenberg, J., and Nixon, R.A. (2008). Down syndrome fibroblast model of Alzheimer-related endosome pathology: accelerated endocytosis promotes late endocytic defects. The American journal of pathology *173*, 370-384.

Cataldo, A.M., Petanceska, S., Terio, N.B., Peterhoff, C.M., Durham, R., Mercken, M., Mehta, P.D., Buxbaum, J., Haroutunian, V., and Nixon, R.A. (2004). Abeta localization in abnormal endosomes: association with earliest Abeta elevations in AD and Down syndrome. Neurobiology of aging *25*, 1263-1272.

Cataldo, A.M., Peterhoff, C.M., Troncoso, J.C., Gomez-Isla, T., Hyman, B.T., and Nixon, R.A. (2000). Endocytic pathway abnormalities precede amyloid beta deposition in sporadic Alzheimer's disease and Down syndrome: differential effects of APOE genotype and presenilin mutations. The American journal of pathology *157*, 277-286.

Cater, M., T McInnes, K., Li, Q.-X., Volitakis, I., La Fontaine, S., Mercer, J., and Bush, A. (2008). Intracellular copper deficiency increases amyloid-β secretion by diverse mechanisms, Vol 412.

Chan, S.L., Kim, W.S., Kwok, J.B., Hill, A.F., Cappai, R., Rye, K.A., and Garner, B. (2008). ATP-binding cassette transporter A7 regulates processing of amyloid precursor protein in vitro. Journal of neurochemistry *106*, 793-804.

Chaufty, J., Sullivan, S.E., and Ho, A. (2012). Intracellular amyloid precursor protein sorting and amyloid-beta secretion are regulated by Src-mediated phosphorylation of Mint2. The Journal of neuroscience : the official journal of the Society for Neuroscience *32*, 9613-9625.

Chen, A.C., and Selkoe, D.J. (2007). Response to: Pardossi-Piquard et al., "Presenilin-Dependent Transcriptional Control of the Abeta-Degrading Enzyme Neprilysin by Intracellular Domains of betaAPP and APLP." Neuron 46, 541-554. Neuron *53*, 479-483.

Chen, C.H., Zhou, W., Liu, S., Deng, Y., Cai, F., Tone, M., Tone, Y., Tong, Y., and Song, W. (2012). Increased NF-kappaB signalling up-regulates BACE1 expression and its therapeutic potential in Alzheimer's disease. Int J Neuropsychopharmacol *15*, 77-90.

Chen, P.W., Luo, R., Jian, X., and Randazzo, P.A. (2014). The Arf6 GTPase-activating proteins ARAP2 and ACAP1 define distinct endosomal compartments that regulate integrin alpha5beta1 traffic. The Journal of biological chemistry *289*, 30237-30248.

Chen, W., Feng, Y., Chen, D., and Wandinger-Ness, A. (1998). Rab11 is required for trans-golgi network-to-plasma membrane transport and a preferential target for GDP dissociation inhibitor. Molecular biology of the cell *9*, 3241-3257.

Chesneau, L., Dambournet, D., Machicoane, M., Kouranti, I., Fukuda, M., Goud, B., and Echard, A. (2012). An ARF6/Rab35 GTPase cascade for endocytic recycling and successful cytokinesis. Current biology : CB *22*, 147-153.

Cho, J.H., and Johnson, G.V. (2004). Primed phosphorylation of tau at Thr231 by glycogen synthase kinase 3beta (GSK3beta) plays a critical role in regulating tau's ability to bind and stabilize microtubules. Journal of neurochemistry *88*, 349-358.

Choi, S.H., and Bosetti, F. (2009). Cyclooxygenase-1 null mice show reduced neuroinflammation in response to beta-amyloid. Aging *1*, 234-244.

Chow, V.W., Mattson, M.P., Wong, P.C., and Gleichmann, M. (2010). An overview of APP processing enzymes and products. Neuromolecular medicine *12*, 1-12.

Christen, Y. (2000). Oxidative stress and Alzheimer disease. The American journal of clinical nutrition *71*, 621S-629S.

Chung, T.D.Y., and Raymond, K.N. (1993). Lactoferrin: The role of conformational changes in its iron binding and release, Vol 115.

Cirrito, J.R., Kang, J.E., Lee, J., Stewart, F.R., Verges, D.K., Silverio, L.M., Bu, G., Mennerick, S., and Holtzman, D.M. (2008). Endocytosis is required for synaptic activity-dependent release of amyloid-beta in vivo. Neuron *58*.

Citron, M., Oltersdorf, T., Haass, C., McConlogue, L., Hung, A.Y., Seubert, P., Vigo-Pelfrey, C., Lieberburg, I., and Selkoe, D.J. (1992). Mutation of the beta-

amyloid precursor protein in familial Alzheimer's disease increases beta-protein production. Nature *360*, 672-674.

Ciuculescu, E.D., Mekmouche, Y., and Faller, P. (2005). Metal-binding properties of the peptide APP170-188: a model of the ZnII-binding site of amyloid precursor protein (APP). Chemistry *11*, 903-909.

Coburger, I., Dahms, S.O., Roeser, D., Guhrs, K.H., Hortschansky, P., and Than, M.E. (2013). Analysis of the overall structure of the multi-domain amyloid precursor protein (APP). PloS one *8*, e81926.

Coleman, P.D., and Yao, P.J. (2003). Synaptic slaughter in Alzheimer's disease. Neurobiology of aging *24*, 1023-1027.

Colonna, M., and Butovsky, O. (2017). Microglia Function in the Central Nervous System During Health and Neurodegeneration. Annual review of immunology *35*, 441-468.

Colton, C.A., Mott, R.T., Sharpe, H., Xu, Q., Van Nostrand, W.E., and Vitek, M.P. (2006). Expression profiles for macrophage alternative activation genes in AD and in mouse models of AD. Journal of neuroinflammation *3*, 27.

Cong, R., Li, Y., and Biemesderfer, D. (2011). A disintegrin and metalloprotease 10 activity sheds the ectodomain of the amyloid precursor-like protein 2 and regulates protein expression in proximal tubule cells. American journal of physiology Cell physiology *300*, C1366-1374.

Connor, J.R., Menzies, S.L., St Martin, S.M., and Mufson, E.J. (1992a). A histochemical study of iron, transferrin, and ferritin in Alzheimer's diseased brains. Journal of neuroscience research *31*, 75-83.

Connor, J.R., Snyder, B.S., Beard, J.L., Fine, R.E., and Mufson, E.J. (1992b). Regional distribution of iron and iron-regulatory proteins in the brain in aging and Alzheimer's disease. Journal of neuroscience research *31*, 327-335.

Conrad, M.E., and Umbreit, J.N. (2000). Disorders of iron metabolism. The New England journal of medicine *342*, 1293-1294.

Cooper, R.A. (1978). Influence of increased membrane cholesterol on membrane fluidity and cell function in human red blood cells. Journal of supramolecular structure *8*, 413-430.

Cordy, J.M., Hussain, I., Dingwall, C., Hooper, N.M., and Turner, A.J. (2003). Exclusively targeting beta-secretase to lipid rafts by GPI-anchor addition up-regulates beta-site processing of the amyloid precursor protein. Proceedings of the National Academy of Sciences of the United States of America *100*, 11735-11740.

Cossec, J.C., Simon, A., Marquer, C., Moldrich, R.X., Leterrier, C., Rossier, J., Duyckaerts, C., Lenkei, Z., and Potier, M.C. (2010). Clathrin-dependent APP endocytosis and Abeta secretion are highly sensitive to the level of plasma membrane cholesterol. Biochimica et biophysica acta *1801*, 846-852.

Crain, B.J., Hu, W., Sze, C.I., Slunt, H.H., Koo, E.H., Price, D.L., Thinakaran, G., and Sisodia, S.S. (1996). Expression and distribution of amyloid precursor protein-like protein-2 in Alzheimer's disease and in normal brain. The American journal of pathology *149*, 1087-1095.

Crain, J.M., Nikodemova, M., and Watters, J.J. (2013). Microglia express distinct M1 and M2 phenotypic markers in the postnatal and adult central nervous system in male and female mice. Journal of neuroscience research *91*, 1143-1151.

Cras, P., Kawai, M., Lowery, D., Gonzalez-DeWhitt, P., Greenberg, B., and Perry, G. (1991). Senile plaque neurites in Alzheimer disease accumulate amyloid precursor protein. Proceedings of the National Academy of Sciences of the United States of America *88*, 7552-7556.

Crichton, R.R., and Charloteaux-Wauters, M. (1987). Iron transport and storage. European journal of biochemistry *164*, 485-506.

Crichton, R.R., Dexter, D.T., and Ward, R.J. (2011). Brain iron metabolism and its perturbation in neurological diseases. J Neural Transm (Vienna) *118*, 301-314.

Crichton, R.R., and Ward, R.J. (1992). Iron metabolism--new perspectives in view. Biochemistry *31*, 11255-11264.

Culvenor, J.G., Friedhuber, A., Fuller, S.J., Beyreuther, K., and Masters, C.L. (1995). Expression of the amyloid precursor protein of Alzheimer's disease on the surface of transfected HeLa cells. Experimental cell research *220*, 474-481.

Cutler, R.G., Kelly, J., Storie, K., Pedersen, W.A., Tammara, A., Hatanpaa, K., Troncoso, J.C., and Mattson, M.P. (2004). Involvement of oxidative stress-induced abnormalities in ceramide and cholesterol metabolism in brain aging and Alzheimer's disease. Proceedings of the National Academy of Sciences of the United States of America *101*, 2070-2075.

Cutone, A., Rosa, L., Lepanto, M.S., Scotti, M.J., Berlutti, F., Bonaccorsi di Patti, M.C., Musci, G., and Valenti, P. (2017). Lactoferrin Efficiently Counteracts the Inflammation-Induced Changes of the Iron Homeostasis System in Macrophages. Frontiers in immunology *8*, 705.

Dahlgren, K.N., Manelli, A.M., Stine, W.B., Jr., Baker, L.K., Krafft, G.A., and LaDu, M.J. (2002). Oligomeric and fibrillar species of amyloid-beta peptides differentially affect neuronal viability. The Journal of biological chemistry *277*, 32046-32053.

Dahms, S.O., Hoefgen, S., Roeser, D., Schlott, B., Guhrs, K.H., and Than, M.E. (2010). Structure and biochemical analysis of the heparin-induced E1 dimer of the amyloid precursor protein. Proceedings of the National Academy of Sciences of the United States of America *107*, 5381-5386.

Dai, Y.Q., Jin, D.Z., Zhu, X.Z., and Lei, D.L. (2006). Triptolide inhibits COX-2 expression via NF-kappa B pathway in astrocytes. Neuroscience research *55*, 154-160.

Daigle, I., and Li, C. (1993). apl-1, a Caenorhabditis elegans gene encoding a protein related to the human beta-amyloid protein precursor. Proceedings of the National Academy of Sciences of the United States of America *90*, 12045-12049.

Dam, J., Velikovsky, C.A., Mariuzza, R.A., Urbanke, C., and Schuck, P. (2005). Sedimentation Velocity Analysis of Heterogeneous Protein-Protein Interactions: Lamm Equation Modeling and Sedimentation Coefficient Distributions. Biophysical journal *89*, 619-634.

Damke, H., Baba, T., Warnock, D.E., and Schmid, S.L. (1994). Induction of mutant dynamin specifically blocks endocytic coated vesicle formation. The Journal of cell biology *127*, 915-934.

Daro, E., van der Sluijs, P., Galli, T., and Mellman, I. (1996). Rab4 and cellubrevin define different early endosome populations on the pathway of transferrin receptor recycling. Proceedings of the National Academy of Sciences of the United States of America *93*, 9559-9564.

Daugherty, B.L., and Green, S.A. (2001). Endosomal sorting of amyloid precursor protein-P-selectin chimeras influences secretase processing. Traffic *2*, 908-916.

Dautry-Varsat, A., Ciechanover, A., and Lodish, H.F. (1983). pH and the recycling of transferrin during receptor-mediated endocytosis. Proceedings of the National Academy of Sciences of the United States of America *80*, 2258-2262.

Dawson, G.R., Seabrook, G.R., Zheng, H., Smith, D.W., Graham, S., O'Dowd, G., Bowery, B.J., Boyce, S., Trumbauer, M.E., Chen, H.Y., Van der Ploeg, L.H., and Sirinathsinghji, D.J. (1999). Age-related cognitive deficits, impaired long-term potentiation and reduction in synaptic marker density in mice lacking the beta-amyloid precursor protein. Neuroscience *90*, 1-13.

De Domenico, I., Lo, E., Ward, D.M., and Kaplan, J. (2009). Hepcidin-induced internalization of ferroportin requires binding and cooperative interaction with Jak2. Proceedings of the National Academy of Sciences of the United States of America *106*, 3800-3805.

De Domenico, I., McVey Ward, D., and Kaplan, J. (2008). Regulation of iron acquisition and storage: consequences for iron-linked disorders. Nature reviews Molecular cell biology *9*, 72-81.

De Domenico, I., Ward, D.M., and Kaplan, J. (2011). Hepcidin and ferroportin: the new players in iron metabolism. Seminars in liver disease *31*, 272-279.

de Lillo, A., Tejerina, J.M., and Fierro, J.F. (1992). Interaction of calmodulin with lactoferrin. FEBS letters *298*, 195-198.

De Strooper, B. (2003). Aph-1, Pen-2, and Nicastrin with Presenilin generate an active gamma-Secretase complex. Neuron *38*, 9-12.

De Strooper, B., and Annaert, W. (2000). Proteolytic processing and cell biological functions of the amyloid precursor protein. Journal of cell science *113 (Pt 11)*, 1857-1870.

De Strooper, B., Iwatsubo, T., and Wolfe, M.S. (2012). Presenilins and gamma-secretase: structure, function, and role in Alzheimer Disease. Cold Spring Harbor perspectives in medicine *2*, a006304.

Deane, R., Sagare, A., and Zlokovic, B.V. (2008). The role of the cell surface LRP and soluble LRP in blood-brain barrier Abeta clearance in Alzheimer's disease. Current pharmaceutical design *14*, 1601-1605.

Deane, R., Wu, Z., Sagare, A., Davis, J., Du Yan, S., Hamm, K., Xu, F., Parisi, M., LaRue, B., Hu, H.W., Spijkers, P., Guo, H., Song, X., Lenting, P.J., Van Nostrand, W.E., and Zlokovic, B.V. (2004a). LRP/amyloid beta-peptide interaction mediates differential brain efflux of Abeta isoforms. Neuron *43*, 333-344.

Deane, R., Zheng, W., and Zlokovic, B.V. (2004b). Brain capillary endothelium and choroid plexus epithelium regulate transport of transferrin-bound and free iron into the rat brain. Journal of neurochemistry *88*, 813-820.

Del Bo, R., Angeretti, N., Lucca, E., De Simoni, M.G., and Forloni, G. (1995). Reciprocal control of inflammatory cytokines, IL-1 and IL-6, and beta-amyloid production in cultures. Neuroscience letters *188*, 70-74.

Dello Russo, C., Cappoli, N., Coletta, I., Mezzogori, D., Paciello, F., Pozzoli, G., Navarra, P., and Battaglia, A. (2018). The human microglial HMC3 cell line: where do we stand? A systematic literature review. Journal of neuroinflammation *15*, 259.

Diekmann, Y., Seixas, E., Gouw, M., Tavares-Cadete, F., Seabra, M.C., and Pereira-Leal, J.B. (2011). Thousands of rab GTPases for the cell biologist. PLoS computational biology *7*, e1002217.

Dixon, S.J., Lemberg, K.M., Lamprecht, M.R., Skouta, R., Zaitsev, E.M., Gleason, C.E., Patel, D.N., Bauer, A.J., Cantley, A.M., Yang, W.S., Morrison, B., 3rd, and Stockwell, B.R. (2012). Ferroptosis: an iron-dependent form of nonapoptotic cell death. Cell *149*, 1060-1072.

Do Van, B., Gouel, F., Jonneaux, A., Timmerman, K., Gele, P., Petrault, M., Bastide, M., Laloux, C., Moreau, C., Bordet, R., Devos, D., and Devedjian, J.C. (2016). Ferroptosis, a newly characterized form of cell death in Parkinson's disease that is regulated by PKC. Neurobiology of disease *94*, 169-178.

Dolma, S., Lessnick, S.L., Hahn, W.C., and Stockwell, B.R. (2003). Identification of genotype-selective antitumor agents using synthetic lethal chemical screening in engineered human tumor cells. Cancer cell *3*, 285-296.

Dong, H.K., Gim, J.A., Yeo, S.H., and Kim, H.S. (2017). Integrated late onset Alzheimer's disease (LOAD) susceptibility genes: Cholesterol metabolism and trafficking perspectives. Gene *597*, 10-16.

Dong, X. (2018). Current Strategies for Brain Drug Delivery. Theranostics *8*, 1481-1493.

Du, L., Zhao, Z., Cui, A., Zhu, Y., Zhang, L., Liu, J., Shi, S., Fu, C., Han, X., Gao, W., Song, T., Xie, L., Wang, L., Sun, S., Guo, R., and Ma, G. (2018). Increased Iron Deposition on Brain Quantitative Susceptibility Mapping Correlates with Decreased Cognitive Function in Alzheimer's Disease. ACS chemical neuroscience *9*, 1849-1857.

Dubbelaar, M.L., Kracht, L., Eggen, B.J.L., and Boddeke, E. (2018). The Kaleidoscope of Microglial Phenotypes. Frontiers in immunology *9*, 1753.

Duce, J.A., Tsatsanis, A., Cater, M.A., James, S.A., Robb, E., Wikhe, K., Leong, S.L., Perez, K., Johanssen, T., Greenough, M.A., Cho, H.H., Galatis, D., Moir, R.D., Masters, C.L., McLean, C., Tanzi, R.E., Cappai, R., Barnham, K.J., Ciccotosto, G.D., Rogers, J.T., and Bush, A.I. (2010). Iron-export ferroxidase activity of beta-amyloid precursor protein is inhibited by zinc in Alzheimer's disease. Cell *142*, 857-867.

Duit, S., Mayer, H., Blake, S.M., Schneider, W.J., and Nimpf, J. (2010). Differential functions of ApoER2 and very low density lipoprotein receptor in Reelin signaling depend on differential sorting of the receptors. The Journal of biological chemistry *285*, 4896-4908.

Dumanchin, C., Czech, C., Campion, D., Cuif, M.H., Poyot, T., Martin, C., Charbonnier, F., Goud, B., Pradier, L., and Frebourg, T. (1999). Presenilins interact with Rab11, a small GTPase involved in the regulation of vesicular transport. Human molecular genetics *8*, 1263-1269.

Dumurgier, J., Vercruysse, O., Paquet, C., Bombois, S., Chaulet, C., Laplanche, J.L., Peoc'h, K., Schraen, S., Pasquier, F., Touchon, J., Hugon, J., Lehmann, S., and Gabelle, A. (2013). Intersite variability of CSF Alzheimer's disease biomarkers in clinical setting. Alzheimer's & dementia : the journal of the Alzheimer's Association *9*, 406-413.

Dunn, K.W., and Maxfield, F.R. (1992). Delivery of ligands from sorting endosomes to late endosomes occurs by maturation of sorting endosomes. The Journal of cell biology *117*, 301-310.

E Donahue, J., L Flaherty, S., Johanson, C., Duncan, J., D Silverberg, G., Miller, M., Tavares, R., Yang, W., Wu, Q., Sabo, E., Hovanesian, G., and Stopa, E. (2006). RAGE, LRP-1, and amyloid-beta protein in Alzheimer’s disease, Vol 112.

Edbauer, D., Winkler, E., Regula, J.T., Pesold, B., Steiner, H., and Haass, C. (2003). Reconstitution of gamma-secretase activity. Nature cell biology *5*, 486-488.

Eggen, B.J.L., Boddeke, E., and Kooistra, S.M. (2019). Regulation of Microglia Identity from an Epigenetic and Transcriptomic Point of View. Neuroscience *405*, 3-13.

Eggert, S., Paliga, K., Soba, P., Evin, G., Masters, C.L., Weidemann, A., and Beyreuther, K. (2004). The proteolytic processing of the amyloid precursor protein gene family members APLP-1 and APLP-2 involves alpha-, beta-, gamma-, and epsilon-like cleavages: modulation of APLP-1 processing by n-glycosylation. The Journal of biological chemistry *279*, 18146-18156.

Ehehalt, R., Keller, P., Haass, C., Thiele, C., and Simons, K. (2003). Amyloidogenic processing of the Alzheimer beta-amyloid precursor protein depends on lipid rafts. The Journal of cell biology *160*, 113-123.

Eimer, W.A., Vijaya Kumar, D.K., Navalpur Shanmugam, N.K., Rodriguez, A.S., Mitchell, T., Washicosky, K.J., Gyorgy, B., Breakefield, X.O., Tanzi, R.E., and Moir, R.D. (2018). Alzheimer's Disease-Associated beta-Amyloid Is Rapidly Seeded by Herpesviridae to Protect against Brain Infection. Neuron *99*, 56-63 e53.

Ellis, C.R., and Shen, J. (2015). pH-Dependent Population Shift Regulates BACE1 Activity and Inhibition. Journal of the American Chemical Society *137*, 9543-9546.

Endres, K., Postina, R., Schroeder, A., Mueller, U., and Fahrenholz, F. (2005). Shedding of the amyloid precursor protein-like protein APLP2 by disintegrin-metalloproteinases. The FEBS journal *272*, 5808-5820.

Esparza, T.J., Wildburger, N.C., Jiang, H., Gangolli, M., Cairns, N.J., Bateman, R.J., and Brody, D.L. (2016). Soluble Amyloid-beta Aggregates from Human Alzheimer's Disease Brains. Scientific reports *6*, 38187.

Esquerda-Canals, G., Montoliu-Gaya, L., Guell-Bosch, J., and Villegas, S. (2017). Mouse Models of Alzheimer's Disease. Journal of Alzheimer's disease : JAD *57*, 1171-1183.

Evin, G., and Weidemann, A. (2002). Biogenesis and metabolism of Alzheimer's disease Abeta amyloid peptides. Peptides *23*, 1285-1297.

Farber, S.A., Nitsch, R.M., Schulz, J.G., and Wurtman, R.J. (1995). Regulated secretion of beta-amyloid precursor protein in rat brain. The Journal of neuroscience : the official journal of the Society for Neuroscience *15*, 7442-7451.

Fassbender, K., Masters, C., and Beyreuther, K. (2000). Alzheimer's disease: an inflammatory disease? Neurobiology of aging *21*, 433-436; discussion 451-433.

Feng, H., and Stockwell, B.R. (2018). Unsolved mysteries: How does lipid peroxidation cause ferroptosis? PLoS biology *16*, e2006203.

Feng, Y., He, D., Yao, Z., and Klionsky, D.J. (2014). The machinery of macroautophagy. Cell research *24*, 24-41.

Feng, Y., Press, B., and Wandinger-Ness, A. (1995). Rab 7: an important regulator of late endocytic membrane traffic. The Journal of cell biology *131*, 1435-1452.

Fielding, A.B., Schonteich, E., Matheson, J., Wilson, G., Yu, X., Hickson, G.R., Srivastava, S., Baldwin, S.A., Prekeris, R., and Gould, G.W. (2005). Rab11-FIP3 and FIP4 interact with Arf6 and the exocyst to control membrane traffic in cytokinesis. The EMBO journal *24*, 3389-3399.

Fillebeen, C., Descamps, L., Dehouck, M.P., Fenart, L., Benaissa, M., Spik, G., Cecchelli, R., and Pierce, A. (1999). Receptor-mediated transcytosis of lactoferrin through the blood-brain barrier. The Journal of biological chemistry *274*, 7011-7017.

Fillebeen, C., Ruchoux, M.M., Mitchell, V., Vincent, S., Benaissa, M., and Pierce, A. (2001). Lactoferrin is synthesized by activated microglia in the human substantia nigra and its synthesis by the human microglial CHME cell line is upregulated by tumor necrosis factor alpha or 1-methyl-4-phenylpyridinium treatment. Brain research Molecular brain research *96*, 103-113.

Fischer, R., Debbabi, H., Blais, A., Dubarry, M., Rautureau, M., Boyaka, P.N., and Tome, D. (2007). Uptake of ingested bovine lactoferrin and its accumulation in adult mouse tissues. International immunopharmacology *7*, 1387-1393.

Florian, P., Macovei, A., Sima, L., Nichita, N., Mattsby-Baltzer, I., and Roseanu, A. (2012). Endocytosis and trafficking of human lactoferrin in macrophage-like human THP-1 cells (1). Biochemistry and cell biology = Biochimie et biologie cellulaire *90*, 449-455.

Fotin, A., Cheng, Y., Sliz, P., Grigorieff, N., Harrison, S.C., Kirchhausen, T., and Walz, T. (2004). Molecular model for a complete clathrin lattice from electron cryomicroscopy. Nature *432*, 573-579.

Fotinopoulou, A., Tsachaki, M., Vlavaki, M., Poulopoulos, A., Rostagno, A., Frangione, B., Ghiso, J., and Efthimiopoulos, S. (2005). BRI2 interacts with amyloid precursor protein (APP) and regulates amyloid beta (Abeta) production. The Journal of biological chemistry *280*, 30768-30772.

Frautschy, S.A., Yang, F., Irrizarry, M., Hyman, B., Saido, T.C., Hsiao, K., and Cole, G.M. (1998). Microglial response to amyloid plaques in APPsw transgenic mice. The American journal of pathology *152*, 307-317.

Freude, K.K., Penjwini, M., Davis, J.L., LaFerla, F.M., and Blurton-Jones, M. (2011). Soluble amyloid precursor protein induces rapid neural differentiation of human embryonic stem cells. The Journal of biological chemistry *286*, 24264-24274.

Friedmann Angeli, J.P., Schneider, M., Proneth, B., Tyurina, Y.Y., Tyurin, V.A., Hammond, V.J., Herbach, N., Aichler, M., Walch, A., Eggenhofer, E., Basavarajappa, D., Radmark, O., Kobayashi, S., Seibt, T., Beck, H., Neff, F., Esposito, I., Wanke, R., Forster, H., Yefremova, O., Heinrichmeyer, M., Bornkamm, G.W., Geissler, E.K., Thomas, S.B., Stockwell, B.R., O'Donnell, V.B., Kagan, V.E., Schick, J.A., and Conrad, M. (2014). Inactivation of the ferroptosis regulator Gpx4 triggers acute renal failure in mice. Nature cell biology *16*, 1180-1191.

Fuentealba, R.A., Barria, M.I., Lee, J., Cam, J., Araya, C., Escudero, C.A., Inestrosa, N.C., Bronfman, F.C., Bu, G., and Marzolo, M.P. (2007). ApoER2 expression increases Abeta production while decreasing Amyloid Precursor Protein (APP) endocytosis: Possible role in the partitioning of APP into lipid rafts and in the regulation of gamma-secretase activity. Molecular neurodegeneration *2*, 14.

Fuentealba, R.A., Liu, Q., Zhang, J., Kanekiyo, T., Hu, X., Lee, J.M., LaDu, M.J., and Bu, G. (2010). Low-density lipoprotein receptor-related protein 1 (LRP1) mediates neuronal Abeta42 uptake and lysosomal trafficking. PloS one *5*, e11884.

Gakhar-Koppole, N., Hundeshagen, P., Mandl, C., Weyer, S.W., Allinquant, B., Muller, U., and Ciccolini, F. (2008). Activity requires soluble amyloid precursor protein alpha to promote neurite outgrowth in neural stem cell-derived neurons via activation of the MAPK pathway. The European journal of neuroscience *28*, 871-882.

Ganz, T. (2003). Hepcidin, a key regulator of iron metabolism and mediator of anemia of inflammation. Blood *102*, 783-788.

Ganz, T. (2005). Cellular iron: ferroportin is the only way out. Cell metabolism *1*, 155-157.

Ganz, T., and Nemeth, E. (2011). Hepcidin and disorders of iron metabolism. Annual review of medicine *62*, 347-360.

Gao, M., Monian, P., Quadri, N., Ramasamy, R., and Jiang, X. (2015). Glutaminolysis and Transferrin Regulate Ferroptosis. Molecular cell *59*, 298-308.

Gaschet, J., and Hsu, V.W. (1999). Distribution of ARF6 between membrane and cytosol is regulated by its GTPase cycle. The Journal of biological chemistry *274*, 20040-20045.

Gendron, T.F., and Petrucelli, L. (2009). The role of tau in neurodegeneration. Molecular neurodegeneration *4*, 13.

Geng, N., Shi, B.J., Li, S.L., Zhong, Z.Y., Li, Y.C., Xua, W.L., Zhou, H., and Cai, J.H. (2018). Knockdown of ferroportin accelerates erastin-induced ferroptosis in neuroblastoma cells. European review for medical and pharmacological sciences *22*, 3826-3836.

Ghiso, J., Rostagno, A., Gardella, J.E., Liem, L., Gorevic, P.D., and Frangione, B. (1992). A 109-amino-acid C-terminal fragment of Alzheimer's-disease amyloid precursor protein contains a sequence, -RHDS-, that promotes cell adhesion. The Biochemical journal *288 (Pt 3)*, 1053-1059.

Giannone, G., Hosy, E., Levet, F., Constals, A., Schulze, K., Sobolevsky, A.I., Rosconi, M.P., Gouaux, E., Tampe, R., Choquet, D., and Cognet, L. (2010). Dynamic superresolution imaging of endogenous proteins on living cells at ultra-high density. Biophysical journal *99*, 1303-1310.

Gidyk, D.C., Deibel, S.H., Hong, N.S., and McDonald, R.J. (2015). Barriers to developing a valid rodent model of Alzheimer's disease: from behavioral analysis to etiological mechanisms. Frontiers in neuroscience *9*, 245.

Gilbert, A., Paccaud, J.P., and Carpentier, J.L. (1997). Direct measurement of clathrin-coated vesicle formation using a cell-free assay. Journal of cell science *110 (Pt 24)*, 3105-3115.

Ginsberg, S.D., Alldred, M.J., Counts, S.E., Cataldo, A.M., Neve, R.L., Jiang, Y., Wuu, J., Chao, M.V., Mufson, E.J., Nixon, R.A., and Che, S. (2010a). Microarray analysis of hippocampal CA1 neurons implicates early endosomal dysfunction during Alzheimer's disease progression. Biological psychiatry *68*, 885-893.

Ginsberg, S.D., Mufson, E.J., Alldred, M.J., Counts, S.E., Wuu, J., Nixon, R.A., and Che, S. (2011). Upregulation of select rab GTPases in cholinergic basal forebrain neurons in mild cognitive impairment and Alzheimer's disease. Journal of chemical neuroanatomy *42*, 102-110.

Ginsberg, S.D., Mufson, E.J., Counts, S.E., Wuu, J., Alldred, M.J., Nixon, R.A., and Che, S. (2010b). Regional selectivity of rab5 and rab7 protein upregulation in mild cognitive impairment and Alzheimer's disease. Journal of Alzheimer's disease : JAD *22*, 631-639.

Goldenring, J.R. (2015). Recycling endosomes. Current opinion in cell biology *35*, 117-122.

Goldgaber, D., Lerman, M.I., McBride, O.W., Saffiotti, U., and Gajdusek, D.C. (1987). Characterization and chromosomal localization of a cDNA encoding brain amyloid of Alzheimer's disease. Science *235*, 877-880.

Goodger, Z.V., Rajendran, L., Trutzel, A., Kohli, B.M., Nitsch, R.M., and Konietzko, U. (2009). Nuclear signaling by the APP intracellular domain occurs predominantly through the amyloidogenic processing pathway. Journal of cell science *122*, 3703-3714.

Goodman, Y., and Mattson, M.P. (1994). Secreted forms of beta-amyloid precursor protein protect hippocampal neurons against amyloid beta-peptide-induced oxidative injury. Experimental neurology *128*, 1-12.

Gopalakrishnan, S.M., Karvinen, J., Kofron, J.L., Burns, D.J., and Warrior, U. (2002). Application of Micro Arrayed Compound Screening (microARCS) to identify inhibitors of caspase-3. Journal of biomolecular screening *7*, 317-323.

Gorvel, J.P., Chavrier, P., Zerial, M., and Gruenberg, J. (1991). rab5 controls early endosome fusion in vitro. Cell *64*, 915-925.

Gosztyla, M.L., Brothers, H.M., and Robinson, S.R. (2018). Alzheimer's Amyloid-beta is an Antimicrobial Peptide: A Review of the Evidence. Journal of Alzheimer's disease : JAD *62*, 1495-1506.

Gotz, J., and Ittner, L.M. (2008). Animal models of Alzheimer's disease and frontotemporal dementia. Nature reviews Neuroscience *9*, 532-544.

Graebert, K.S., Popp, G.M., Kehle, T., and Herzog, V. (1995). Regulated O-glycosylation of the Alzheimer beta-A4 amyloid precursor protein in thyrocytes. European journal of cell biology *66*, 39-46.

Gralle, M., Botelho, M.M., de Oliveira, C.L., Torriani, I., and Ferreira, S.T. (2002). Solution studies and structural model of the extracellular domain of the human amyloid precursor protein. Biophysical journal *83*, 3513-3524.

Gralle, M., and Ferreira, S.T. (2007). Structure and functions of the human amyloid precursor protein: the whole is more than the sum of its parts. Progress in neurobiology *82*, 11-32.

Grant, B.D., and Donaldson, J.G. (2009). Pathways and mechanisms of endocytic recycling. Nature reviews Molecular cell biology *10*, 597-608.

Grbovic, O.M., Mathews, P.M., Jiang, Y., Schmidt, S.D., Dinakar, R., Summers-Terio, N.B., Ceresa, B.P., Nixon, R.A., and Cataldo, A.M. (2003). Rab5-stimulated up-regulation of the endocytic pathway increases intracellular beta-cleaved amyloid precursor protein carboxyl-terminal fragment levels and Abeta production. The Journal of biological chemistry *278*, 31261-31268.

Greenough, M.A., Camakaris, J., and Bush, A.I. (2013). Metal dyshomeostasis and oxidative stress in Alzheimer's disease. Neurochemistry international *62*, 540-555.

Grey, A., Banovic, T., Zhu, Q., Watson, M., Callon, K., Palmano, K., Ross, J., Naot, D., Reid, I.R., and Cornish, J. (2004). The low-density lipoprotein receptor-related protein 1 is a mitogenic receptor for lactoferrin in osteoblastic cells. Mol Endocrinol *18*, 2268-2278.

Griffin, W.S., Sheng, J.G., Roberts, G.W., and Mrak, R.E. (1995). Interleukin-1 expression in different plaque types in Alzheimer's disease: significance in plaque evolution. Journal of neuropathology and experimental neurology *54*, 276-281.

Griffin, W.S., Sheng, J.G., Royston, M.C., Gentleman, S.M., McKenzie, J.E., Graham, D.I., Roberts, G.W., and Mrak, R.E. (1998). Glial-neuronal interactions in Alzheimer's disease: the potential role of a 'cytokine cycle' in disease progression. Brain Pathol *8*, 65-72.

Griffiths, G., and Gruenberg, J. (1991). The arguments for pre-existing early and late endosomes. Trends in cell biology *1*, 5-9.

Grosshans, B.L., Ortiz, D., and Novick, P. (2006). Rabs and their effectors: achieving specificity in membrane traffic. Proceedings of the National Academy of Sciences of the United States of America *103*, 11821-11827.

Grossmann, J.G., Neu, M., Pantos, E., Schwab, F.J., Evans, R.W., Townes-Andrews, E., Lindley, P.F., Appel, H., Thies, W.G., and Hasnain, S.S. (1992). X-ray solution scattering reveals conformational changes upon iron uptake in lactoferrin, serum and ovo-transferrins. Journal of molecular biology *225*, 811-819.

Gruenberg, J. (2001). The endocytic pathway: a mosaic of domains. Nature reviews Molecular cell biology *2*, 721-730.

Gruenberg, J., Griffiths, G., and Howell, K.E. (1989). Characterization of the early endosome and putative endocytic carrier vesicles in vivo and with an assay of vesicle fusion in vitro. The Journal of cell biology *108*, 1301-1316.

Gruenberg, J., and Stenmark, H. (2004). The biogenesis of multivesicular endosomes. Nature reviews Molecular cell biology *5*, 317-323.

Gu, Y., Misonou, H., Sato, T., Dohmae, N., Takio, K., and Ihara, Y. (2001). Distinct intramembrane cleavage of the beta-amyloid precursor protein family resembling gamma-secretase-like cleavage of Notch. The Journal of biological chemistry *276*, 35235-35238.

Guerra, F., and Bucci, C. (2016). Multiple Roles of the Small GTPase Rab7. Cells *5*.

Guerreiro, R., Wojtas, A., Bras, J., Carrasquillo, M., Rogaeva, E., Majounie, E., Cruchaga, C., Sassi, C., Kauwe, J.S., Younkin, S., Hazrati, L., Collinge, J., Pocock, J., Lashley, T., Williams, J., Lambert, J.C., Amouyel, P., Goate, A., Rademakers, R., Morgan, K., Powell, J., St George-Hyslop, P., Singleton, A., and Hardy, J. (2013). TREM2 variants in Alzheimer's disease. The New England journal of medicine *368*, 117-127.

Guo, C., Yang, Z.H., Zhang, S., Chai, R., Xue, H., Zhang, Y.H., Li, J.Y., and Wang, Z.Y. (2017). Intranasal Lactoferrin Enhances alpha-Secretase-Dependent Amyloid Precursor Protein Processing via the ERK1/2-CREB and HIF-1alpha Pathways in an Alzheimer's Disease Mouse Model. Neuropsychopharmacology : official publication of the American College of Neuropsychopharmacology *42*, 2504-2515.

Guo, Q., Fu, W., Sopher, B.L., Miller, M.W., Ware, C.B., Martin, G.M., and Mattson, M.P. (1999). Increased vulnerability of hippocampal neurons to excitotoxic necrosis in presenilin-1 mutant knock-in mice. Nature medicine *5*, 101-106.

Guo, Q., Li, H., Gaddam, S.S., Justice, N.J., Robertson, C.S., and Zheng, H. (2012). Amyloid precursor protein revisited: neuron-specific expression and highly stable nature of soluble derivatives. The Journal of biological chemistry *287*, 2437-2445.

Gustafsen, C., Glerup, S., Pallesen, L.T., Olsen, D., Andersen, O.M., Nykjaer, A., Madsen, P., and Petersen, C.M. (2013). Sortilin and SorLA display distinct roles in processing and trafficking of amyloid precursor protein. The Journal of neuroscience : the official journal of the Society for Neuroscience *33*, 64-71.

Gutierrez, M.G., Munafo, D.B., Beron, W., and Colombo, M.I. (2004). Rab7 is required for the normal progression of the autophagic pathway in mammalian cells. Journal of cell science *117*, 2687-2697.

H, E.H., Noristani, H.N., and Perrin, F.E. (2017). Microglia Responses in Acute and Chronic Neurological Diseases: What Microglia-Specific Transcriptomic Studies Taught (and did Not Teach) Us. Frontiers in aging neuroscience *9*, 227.

Ha-Duong, N.T., Eid, C., Hemadi, M., and El Hage Chahine, J.M. (2010). In vitro interaction between ceruloplasmin and human serum transferrin. Biochemistry *49*, 10261-10263.

Haass, C., Hung, A.Y., and Selkoe, D.J. (1991). Processing of beta-amyloid precursor protein in microglia and astrocytes favors an internal localization over constitutive secretion. The Journal of neuroscience : the official journal of the Society for Neuroscience *11*, 3783-3793.

Haass, C., Kaether, C., Thinakaran, G., and Sisodia, S. (2012). Trafficking and proteolytic processing of APP. Cold Spring Harbor perspectives in medicine *2*, a006270.

Haass, C., and Selkoe, D.J. (2007). Soluble protein oligomers in neurodegeneration: lessons from the Alzheimer's amyloid beta-peptide. Nature reviews Molecular cell biology *8*, 101-112.

Hafez, D.M., Huang, J.Y., Richardson, J.C., Masliah, E., Peterson, D.A., and Marr, R.A. (2012). F-spondin gene transfer improves memory performance and reduces amyloid-beta levels in mice. Neuroscience *223*, 465-472.

Halliday, G., Robinson, S.R., Shepherd, C., and Kril, J. (2000). Alzheimer's disease and inflammation: a review of cellular and therapeutic mechanisms. Clinical and experimental pharmacology & physiology *27*, 1-8.

Hanninen, M.M., Haapasalo, J., Haapasalo, H., Fleming, R.E., Britton, R.S., Bacon, B.R., and Parkkila, S. (2009). Expression of iron-related genes in human brain and brain tumors. BMC neuroscience *10*, 36.

Hansen, N.E., Malmquist, J., and Thorell, J. (1975). Plasma myeloperoxidase and lactoferrin measured by radioimmunoassay: relations to neutrophil kinetics. Acta medica Scandinavica *198*, 437-443.

Hardy, J. (2006). Alzheimer's disease: the amyloid cascade hypothesis: an update and reappraisal. Journal of Alzheimer's disease : JAD *9*, 151-153.

Hardy, J. (2009). The amyloid hypothesis for Alzheimer's disease: a critical reappraisal. Journal of neurochemistry *110*, 1129-1134.

Hardy, J., and Allsop, D. (1991). Amyloid deposition as the central event in the aetiology of Alzheimer's disease. Trends in pharmacological sciences *12*, 383-388.

Hardy, J., and Selkoe, D.J. (2002). The amyloid hypothesis of Alzheimer's disease: progress and problems on the road to therapeutics. Science *297*, 353-356.

Hardy, J.A., and Higgins, G.A. (1992). Alzheimer's disease: the amyloid cascade hypothesis. Science *256*, 184-185.

Hare, D., Ayton, S., Bush, A., and Lei, P. (2013). A delicate balance: Iron metabolism and diseases of the brain. Frontiers in aging neuroscience *5*, 34.

Haridas, M., Anderson, B.F., and Baker, E.N. (1995). Structure of human diferric lactoferrin refined at 2.2 A resolution. Acta crystallographica Section D, Biological crystallography *51*, 629-646.

Harmsen, M.C., Swart, P.J., de Bethune, M.P., Pauwels, R., De Clercq, E., The, T.H., and Meijer, D.K. (1995). Antiviral effects of plasma and milk proteins: lactoferrin shows potent activity against both human immunodeficiency virus and human cytomegalovirus replication in vitro. The Journal of infectious diseases *172*, 380-388.

Harold, D., Abraham, R., Hollingworth, P., Sims, R., Gerrish, A., Hamshere, M.L., Pahwa, J.S., Moskvina, V., Dowzell, K., Williams, A., Jones, N., Thomas, C., Stretton, A., Morgan, A.R., Lovestone, S., Powell, J., Proitsi, P., Lupton, M.K., Brayne, C., Rubinsztein, D.C., Gill, M., Lawlor, B., Lynch, A., Morgan, K., Brown, K.S., Passmore, P.A., Craig, D., McGuinness, B., Todd, S., Holmes, C., Mann, D., Smith, A.D., Love, S., Kehoe, P.G., Hardy, J., Mead, S., Fox, N., Rossor, M., Collinge, J., Maier, W., Jessen, F., Schurmann, B., Heun, R., van den Bussche, H., Heuser, I., Kornhuber, J., Wiltfang, J., Dichgans, M., Frolich, L., Hampel, H., Hull, M., Rujescu, D., Goate, A.M., Kauwe, J.S., Cruchaga, C., Nowotny, P., Morris, J.C., Mayo, K., Sleegers, K., Bettens, K., Engelborghs, S., De Deyn, P.P., Van Broeckhoven, C., Livingston, G., Bass, N.J., Gurling, H., McQuillin, A., Gwilliam, R., Deloukas, P., Al-Chalabi, A., Shaw, C.E., Tsolaki, M., Singleton, A.B., Guerreiro, R., Muhleisen, T.W., Nothen, M.M., Moebus, S., Jockel, K.H., Klopp, N., Wichmann, H.E., Carrasquillo, M.M., Pankratz, V.S., Younkin, S.G., Holmans, P.A., O'Donovan, M., Owen, M.J., and Williams, J. (2009). Genome-wide association study identifies variants at CLU and PICALM associated with Alzheimer's disease. Nat Genet *41*, 1088-1093.

Hass, M.R., and Yankner, B.A. (2005). A {gamma}-secretase-independent mechanism of signal transduction by the amyloid precursor protein. The Journal of biological chemistry *280*, 36895-36904.

Haugabook, S.J., Yager, D.M., Eckman, E.A., Golde, T.E., Younkin, S.G., and Eckman, C.B. (2001). High throughput screens for the identification of compounds that alter the accumulation of the Alzheimer's amyloid beta peptide (Abeta). Journal of neuroscience methods *108*, 171-179.

Heber, S., Herms, J., Gajic, V., Hainfellner, J., Aguzzi, A., Rulicke, T., von Kretzschmar, H., von Koch, C., Sisodia, S., Tremml, P., Lipp, H.P., Wolfer, D.P., and Muller, U. (2000). Mice with combined gene knock-outs reveal essential and partially redundant functions of amyloid precursor protein family members. The Journal of neuroscience : the official journal of the Society for Neuroscience *20*, 7951-7963.

Hebert, S.S., Serneels, L., Tolia, A., Craessaerts, K., Derks, C., Filippov, M.A., Muller, U., and De Strooper, B. (2006). Regulated intramembrane proteolysis of

amyloid precursor protein and regulation of expression of putative target genes. EMBO reports *7*, 739-745.

Heinrich, R., and Rapoport, T.A. (2005). Generation of nonidentical compartments in vesicular transport systems. The Journal of cell biology *168*, 271-280.

Heneka, M.T., and O'Banion, M.K. (2007). Inflammatory processes in Alzheimer's disease. Journal of neuroimmunology *184*, 69-91.

Henley, J.R., Krueger, E.W., Oswald, B.J., and McNiven, M.A. (1998). Dynamin-mediated internalization of caveolae. The Journal of cell biology *141*, 85-99.

Henry, A., Masters, C.L., Beyreuther, K., and Cappai, R. (1997). Expression of Human Amyloid Precursor Protein Ectodomains inPichia pastoris:Analysis of Culture Conditions, Purification, and Characterization. Protein Expression and Purification *10*, 283-291.

Hensley, K. (2010). Neuroinflammation in Alzheimer's disease: mechanisms, pathologic consequences, and potential for therapeutic manipulation. Journal of Alzheimer's disease : JAD *21*, 1-14.

Hentze, M.W., Muckenthaler, M.U., and Andrews, N.C. (2004). Balancing acts: molecular control of mammalian iron metabolism. Cell *117*, 285-297.

Herr, U.M., Strecker, P., Storck, S.E., Thomas, C., Rabiej, V., Junker, A., Schilling, S., Schmidt, N., Dowds, C.M., Eggert, S., Pietrzik, C.U., and Kins, S. (2017). LRP1 Modulates APP Intraneuronal Transport and Processing in Its Monomeric and Dimeric State. Frontiers in molecular neuroscience *10*, 118.

Herz, J., and Bock, H.H. (2002). Lipoprotein receptors in the nervous system. Annual review of biochemistry *71*, 405-434.

Herz, J., Gotthardt, M., and Willnow, T.E. (2000). Cellular signalling by lipoprotein receptors. Current opinion in lipidology *11*, 161-166.

Hickman, S.E., and El Khoury, J. (2014). TREM2 and the neuroimmunology of Alzheimer's disease. Biochemical pharmacology *88*, 495-498.

Hickson, G.R., Matheson, J., Riggs, B., Maier, V.H., Fielding, A.B., Prekeris, R., Sullivan, W., Barr, F.A., and Gould, G.W. (2003). Arfophilins are dual Arf/Rab 11 binding proteins that regulate recycling endosome distribution and are related to Drosophila nuclear fallout. Molecular biology of the cell *14*, 2908-2920.

Hiltunen, M., van Groen, T., and Jolkkonen, J. (2009). Functional roles of amyloid-beta protein precursor and amyloid-beta peptides: evidence from experimental studies. Journal of Alzheimer's disease : JAD *18*, 401-412.

Hirose, Y., Imai, Y., Nakajima, K., Takemoto, N., Toya, S., and Kohsaka, S. (1994). Glial conditioned medium alters the expression of amyloid precursor protein in SH-SY5Y neuroblastoma cells. Biochemical and biophysical research communications *198*, 504-509.

Ho, A., Liu, X., and Sudhof, T.C. (2008). Deletion of Mint proteins decreases amyloid production in transgenic mouse models of Alzheimer's disease. The Journal of neuroscience : the official journal of the Society for Neuroscience *28*, 14392-14400.

Ho, A., and Sudhof, T.C. (2004). Binding of F-spondin to amyloid-beta precursor protein: a candidate amyloid-beta precursor protein ligand that modulates amyloid-beta precursor protein cleavage. Proceedings of the National Academy of Sciences of the United States of America *101*, 2548-2553.

Hoe, H.S., and Rebeck, G.W. (2005). Regulation of ApoE receptor proteolysis by ligand binding. Brain research Molecular brain research *137*, 31-39.

Hoe, H.S., Tran, T.S., Matsuoka, Y., Howell, B.W., and Rebeck, G.W. (2006). DAB1 and Reelin effects on amyloid precursor protein and ApoE receptor 2 trafficking and processing. The Journal of biological chemistry *281*, 35176-35185.

Hoe, H.S., Wessner, D., Beffert, U., Becker, A.G., Matsuoka, Y., and Rebeck, G.W. (2005). F-spondin interaction with the apolipoprotein E receptor ApoEr2 affects processing of amyloid precursor protein. Molecular and cellular biology *25*, 9259-9268.

Hoefgen, S., Coburger, I., Roeser, D., Schaub, Y., Dahms, S.O., and Than, M.E. (2014). Heparin induced dimerization of APP is primarily mediated by E1 and regulated by its acidic domain. Journal of structural biology *187*, 30-37.

Hogl, S., Kuhn, P.H., Colombo, A., and Lichtenthaler, S.F. (2011). Determination of the proteolytic cleavage sites of the amyloid precursor-like protein 2 by the proteases ADAM10, BACE1 and gamma-secretase. PloS one *6*, e21337.

Hollingworth, P., Harold, D., Jones, L., Owen, M.J., and Williams, J. (2011a). Alzheimer's disease genetics: current knowledge and future challenges. International journal of geriatric psychiatry *26*, 793-802.

Hollingworth, P., Harold, D., Sims, R., Gerrish, A., Lambert, J.C., Carrasquillo, M.M., Abraham, R., Hamshere, M.L., Pahwa, J.S., Moskvina, V., Dowzell, K., Jones, N., Stretton, A., Thomas, C., Richards, A., Ivanov, D., Widdowson, C., Chapman, J., Lovestone, S., Powell, J., Proitsi, P., Lupton, M.K., Brayne, C., Rubinsztein, D.C., Gill, M., Lawlor, B., Lynch, A., Brown, K.S., Passmore, P.A., Craig, D., McGuinness, B., Todd, S., Holmes, C., Mann, D., Smith, A.D., Beaumont, H., Warden, D., Wilcock, G., Love, S., Kehoe, P.G., Hooper, N.M., Vardy, E.R., Hardy, J., Mead, S., Fox, N.C., Rossor, M., Collinge, J., Maier, W., Jessen, F., Ruther, E., Schurmann, B., Heun, R., Kolsch, H., van den Bussche, H., Heuser, I., Kornhuber, J., Wiltfang, J., Dichgans, M., Frolich, L., Hampel, H., Gallacher, J., Hull, M., Rujescu, D., Giegling, I., Goate, A.M., Kauwe, J.S., Cruchaga, C., Nowotny, P., Morris, J.C., Mayo, K., Sleegers, K., Bettens, K., Engelborghs, S., De Deyn, P.P., Van Broeckhoven, C., Livingston, G., Bass, N.J., Gurling, H., McQuillin, A., Gwilliam, R., Deloukas, P., Al-Chalabi, A., Shaw, C.E., Tsolaki, M., Singleton, A.B., Guerreiro, R., Muhleisen, T.W., Nothen, M.M., Moebus, S., Jockel, K.H., Klopp, N., Wichmann, H.E., Pankratz, V.S., Sando, S.B., Aasly, J.O., Barcikowska, M., Wszolek, Z.K., Dickson, D.W., Graff-Radford,

N.R., Petersen, R.C., van Duijn, C.M., Breteler, M.M., Ikram, M.A., DeStefano, A.L., Fitzpatrick, A.L., Lopez, O., Launer, L.J., Seshadri, S., Berr, C., Campion, D., Epelbaum, J., Dartigues, J.F., Tzourio, C., Alperovitch, A., Lathrop, M., Feulner, T.M., Friedrich, P., Riehle, C., Krawczak, M., Schreiber, S., Mayhaus, M., Nicolhaus, S., Wagenpfeil, S., Steinberg, S., Stefansson, H., Stefansson, K., Snaedal, J., Bjornsson, S., Jonsson, P.V., Chouraki, V., Genier-Boley, B., Hiltunen, M., Soininen, H., Combarros, O., Zelenika, D., Delepine, M., Bullido, M.J., Pasquier, F., Mateo, I., Frank-Garcia, A., Porcellini, E., Hanon, O., Coto, E., Alvarez, V., Bosco, P., Siciliano, G., Mancuso, M., Panza, F., Solfrizzi, V., Nacmias, B., Sorbi, S., Bossu, P., Piccardi, P., Arosio, B., Annoni, G., Seripa, D., Pilotto, A., Scarpini, E., Galimberti, D., Brice, A., Hannequin, D., Licastro, F., Jones, L., Holmans, P.A., Jonsson, T., Riemenschneider, M., Morgan, K., Younkin, S.G., Owen, M.J., O'Donovan, M., Amouyel, P., and Williams, J. (2011b). Common variants at ABCA7, MS4A6A/MS4A4E, EPHA1, CD33 and CD2AP are associated with Alzheimer's disease. Nat Genet *43*, 429-435.

Holsinger, R.M., McLean, C.A., Beyreuther, K., Masters, C.L., and Evin, G. (2002). Increased expression of the amyloid precursor beta-secretase in Alzheimer's disease. Annals of neurology *51*, 783-786.

Hsu, V.W., and Prekeris, R. (2010). Transport at the recycling endosome. Current opinion in cell biology *22*, 528-534.

Hu, L., Hu, X., Long, K., Gao, C., Dong, H.-L., Zhong, Q., Gao, X.-M., and Gong, F.-Y. (2017). Extraordinarily potent proinflammatory properties of lactoferrin-containing immunocomplexes against human monocytes and macrophages. Scientific reports *7*, 4230.

Hu, Y.B., Dammer, E.B., Ren, R.J., and Wang, G. (2015). The endosomal-lysosomal system: from acidification and cargo sorting to neurodegeneration. Translational neurodegeneration *4*, 18.

Huang, Q., Liu, D., Majewski, P., Schulte, L.C., Korn, J.M., Young, R.A., Lander, E.S., and Hacohen, N. (2001). The plasticity of dendritic cell responses to pathogens and their components. Science *294*, 870-875.

Hull, M., Fiebich, B.L., Lieb, K., Strauss, S., Berger, S.S., Volk, B., and Bauer, J. (1996). Interleukin-6-associated inflammatory processes in Alzheimer's disease: new therapeutic options. Neurobiology of aging *17*, 795-800.

Humphries, W.H.t., Szymanski, C.J., and Payne, C.K. (2011). Endo-lysosomal vesicles positive for Rab7 and LAMP1 are terminal vesicles for the transport of dextran. PloS one *6*, e26626.

Hung, A.Y., Koo, E.H., Haass, C., and Selkoe, D.J. (1992). Increased expression of beta-amyloid precursor protein during neuronal differentiation is not accompanied by secretory cleavage. Proceedings of the National Academy of Sciences of the United States of America *89*, 9439-9443.

Huotari, J., and Helenius, A. (2011). Endosome maturation. The EMBO journal *30*, 3481-3500.

Huse, J.T., Liu, K., Pijak, D.S., Carlin, D., Lee, V.M., and Doms, R.W. (2002). Beta-secretase processing in the trans-Golgi network preferentially generates truncated amyloid species that accumulate in Alzheimer's disease brain. The Journal of biological chemistry *277*, 16278-16284.

Hyman, B.T., Van Hoesen, G.W., Beyreuther, K., and Masters, C.L. (1989). A4 amyloid protein immunoreactivity is present in Alzheimer's disease neurofibrillary tangles. Neuroscience letters *101*, 352-355.

Hynes, T.R., Randal, M., Kennedy, L.A., Eigenbrot, C., and Kossiakoff, A.A. (1990). X-ray crystal structure of the protease inhibitor domain of Alzheimer's amyloid beta-protein precursor. Biochemistry *29*, 10018-10022.

Hyttinen, J.M., Niittykoski, M., Salminen, A., and Kaarniranta, K. (2013). Maturation of autophagosomes and endosomes: a key role for Rab7. Biochimica et biophysica acta *1833*, 503-510.

Igbavboa, U., Sun, G.Y., Weisman, G.A., He, Y., and Wood, W.G. (2009). Amyloid beta-protein stimulates trafficking of cholesterol and caveolin-1 from the plasma membrane to the Golgi complex in mouse primary astrocytes. Neuroscience *162*, 328-338.

Irvine, G.B., El-Agnaf, O.M., Shankar, G.M., and Walsh, D.M. (2008). Protein aggregation in the brain: the molecular basis for Alzheimer's and Parkinson's diseases. Mol Med *14*, 451-464.

Ismail, M., and Brock, J.H. (1993). Binding of lactoferrin and transferrin to the human promonocytic cell line U937. Effect on iron uptake and release. The Journal of biological chemistry *268*, 21618-21625.

Israel, M.A., Yuan, S.H., Bardy, C., Reyna, S.M., Mu, Y., Herrera, C., Hefferan, M.P., Van Gorp, S., Nazor, K.L., Boscolo, F.S., Carson, C.T., Laurent, L.C., Marsala, M., Gage, F.H., Remes, A.M., Koo, E.H., and Goldstein, L.S. (2012). Probing sporadic and familial Alzheimer's disease using induced pluripotent stem cells. Nature *482*, 216-220.

Jack, C.R., Jr., Wengenack, T.M., Reyes, D.A., Garwood, M., Curran, G.L., Borowski, B.J., Lin, J., Preboske, G.M., Holasek, S.S., Adriany, G., and Poduslo, J.F. (2005). In vivo magnetic resonance microimaging of individual amyloid plaques in Alzheimer's transgenic mice. The Journal of neuroscience : the official journal of the Society for Neuroscience *25*, 10041-10048.

Jacobsen, K.T., and Iverfeldt, K. (2009). Amyloid precursor protein and its homologues: a family of proteolysis-dependent receptors. Cellular and molecular life sciences : CMLS *66*, 2299-2318.

Jager, S., Bucci, C., Tanida, I., Ueno, T., Kominami, E., Saftig, P., and Eskelinen, E.L. (2004). Role for Rab7 in maturation of late autophagic vacuoles. Journal of cell science *117*, 4837-4848.

Jahn, H. (2013). Memory loss in Alzheimer's disease. Dialogues in clinical neuroscience *15*, 445-454.

Jameson, G.B., Anderson, B.F., Norris, G.E., Thomas, D.H., and Baker, E.N. (1998). Structure of human apolactoferrin at 2.0 A resolution. Refinement and analysis of ligand-induced conformational change. Acta crystallographica Section D, Biological crystallography *54*, 1319-1335.

Jana, M., Dasgupta, S., Liu, X., and Pahan, K. (2002). Regulation of tumor necrosis factor-alpha expression by CD40 ligation in BV-2 microglial cells. Journal of neurochemistry *80*, 197-206.

Janelidze, S., Pannee, J., Mikulskis, A., Chiao, P., Zetterberg, H., Blennow, K., and Hansson, O. (2017). Concordance Between Different Amyloid Immunoassays and Visual Amyloid Positron Emission Tomographic Assessment. JAMA neurology *74*, 1492-1501.

Janelidze, S., Zetterberg, H., Mattsson, N., Palmqvist, S., Vanderstichele, H., Lindberg, O., van Westen, D., Stomrud, E., Minthon, L., Blennow, K., and Hansson, O. (2016). CSF Abeta42/Abeta40 and Abeta42/Abeta38 ratios: better diagnostic markers of Alzheimer disease. Annals of clinical and translational neurology *3*, 154-165.

Jefferson, T., Causevic, M., auf dem Keller, U., Schilling, O., Isbert, S., Geyer, R., Maier, W., Tschickardt, S., Jumpertz, T., Weggen, S., Bond, J.S., Overall, C.M., Pietrzik, C.U., and Becker-Pauly, C. (2011). Metalloprotease meprin beta generates nontoxic N-terminal amyloid precursor protein fragments in vivo. The Journal of biological chemistry *286*, 27741-27750.

Jeynes, B., and Provias, J. (2008). Evidence for altered LRP/RAGE expression in Alzheimer lesion pathogenesis. Current Alzheimer research *5*, 432-437.

Ji, C., Steimle, B.L., Bailey, D.K., and Kosman, D.J. (2018). The Ferroxidase Hephaestin But Not Amyloid Precursor Protein is Required for Ferroportin-Supported Iron Efflux in Primary Hippocampal Neurons. Cellular and molecular neurobiology *38*, 941-954.

Ji, M., Arbel, M., Zhang, L., Freudiger, C.W., Hou, S.S., Lin, D., Yang, X., Bacskai, B.J., and Xie, X.S. (2018). Label-free imaging of amyloid plaques in Alzheimer's disease with stimulated Raman scattering microscopy. Science advances *4*, eaat7715.

Jiang, R., Lopez, V., Kelleher, S.L., and Lonnerdal, B. (2011). Apo- and holo-lactoferrin are both internalized by lactoferrin receptor via clathrin-mediated endocytosis but differentially affect ERK-signaling and cell proliferation in Caco-2 cells. Journal of cellular physiology *226*, 3022-3031.

Jimenez, S., Baglietto-Vargas, D., Caballero, C., Moreno-Gonzalez, I., Torres, M., Sanchez-Varo, R., Ruano, D., Vizuete, M., Gutierrez, A., and Vitorica, J. (2008). Inflammatory response in the hippocampus of PS1M146L/APP751SL mouse model of Alzheimer's disease: age-dependent switch in the microglial phenotype from alternative to classic. The Journal of neuroscience : the official journal of the Society for Neuroscience *28*, 11650-11661.

Jin, L.W., Ninomiya, H., Roch, J.M., Schubert, D., Masliah, E., Otero, D.A., and Saitoh, T. (1994). Peptides containing the RERMS sequence of amyloid beta/A4 protein precursor bind cell surface and promote neurite extension. The Journal of neuroscience : the official journal of the Society for Neuroscience *14*, 5461-5470.

Jolly-Tornetta, C., and Wolf, B.A. (2000). Protein kinase C regulation of intracellular and cell surface amyloid precursor protein (APP) cleavage in CHO695 cells. Biochemistry *39*, 15282-15290.

Jones, A.T. (2007). Macropinocytosis: searching for an endocytic identity and role in the uptake of cell penetrating peptides. Journal of cellular and molecular medicine *11*, 670-684.

Jonsson, T., Stefansson, H., Steinberg, S., Jonsdottir, I., Jonsson, P.V., Snaedal, J., Bjornsson, S., Huttenlocher, J., Levey, A.I., Lah, J.J., Rujescu, D., Hampel, H., Giegling, I., Andreassen, O.A., Engedal, K., Ulstein, I., Djurovic, S., Ibrahim-Verbaas, C., Hofman, A., Ikram, M.A., van Duijn, C.M., Thorsteinsdottir, U., Kong, A., and Stefansson, K. (2013). Variant of TREM2 associated with the risk of Alzheimer's disease. The New England journal of medicine *368*, 107-116.

Jovic, M., Sharma, M., Rahajeng, J., and Caplan, S. (2010). The early endosome: a busy sorting station for proteins at the crossroads. Histology and histopathology *25*, 99-112.

Jung, S.S., Nalbantoglu, J., and Cashman, N.R. (1996). Alzheimer's beta-amyloid precursor protein is expressed on the surface of immediately ex vivo brain cells: a flow cytometric study. Journal of neuroscience research *46*, 336-348.

Kadavath, H., Hofele, R.V., Biernat, J., Kumar, S., Tepper, K., Urlaub, H., Mandelkow, E., and Zweckstetter, M. (2015). Tau stabilizes microtubules by binding at the interface between tubulin heterodimers. Proceedings of the National Academy of Sciences of the United States of America *112*, 7501-7506.

Kaddai, V., Le Marchand-Brustel, Y., and Cormont, M. (2008). Rab proteins in endocytosis and Glut4 trafficking. Acta Physiol (Oxf) *192*, 75-88.

Kajiho, H., Saito, K., Tsujita, K., Kontani, K., Araki, Y., Kurosu, H., and Katada, T. (2003). RIN3: a novel Rab5 GEF interacting with amphiphysin II involved in the early endocytic pathway. Journal of cell science *116*, 4159-4168.

Kakhlon, O., and Cabantchik, Z.I. (2002). The labile iron pool: characterization, measurement, and participation in cellular processes(1). Free radical biology & medicine *33*, 1037-1046.

Kanekiyo, T., Cirrito, J.R., Liu, C.C., Shinohara, M., Li, J., Schuler, D.R., Holtzman, D.M., and Bu, G. (2013). Neuronal clearance of amyloid-beta by endocytic receptor LRP1. The Journal of neuroscience : the official journal of the Society for Neuroscience *33*, 19276-19283.

Kang, J., Lemaire, H.G., Unterbeck, A., Salbaum, J.M., Masters, C.L., Grzeschik, K.H., Multhaup, G., Beyreuther, K., and Muller-Hill, B. (1987). The precursor of

Alzheimer's disease amyloid A4 protein resembles a cell-surface receptor. Nature *325*, 733-736.

Kang, J., and Muller-Hill, B. (1990). Differential splicing of Alzheimer's disease amyloid A4 precursor RNA in rat tissues: PreA4(695) mRNA is predominantly produced in rat and human brain. Biochemical and biophysical research communications *166*, 1192-1200.

Karch, C.M., Cruchaga, C., and Goate, A.M. (2014). Alzheimer's disease genetics: from the bench to the clinic. Neuron *83*, 11-26.

Karran, E., and Hardy, J. (2014). A critique of the drug discovery and phase 3 clinical programs targeting the amyloid hypothesis for Alzheimer disease. Annals of neurology *76*, 185-205.

Karran, E., Mercken, M., and De Strooper, B. (2011). The amyloid cascade hypothesis for Alzheimer's disease: an appraisal for the development of therapeutics. Nature reviews Drug discovery *10*, 698-712.

Kawamata, T., Tooyama, I., Yamada, T., Walker, D.G., and McGeer, P.L. (1993). Lactotransferrin immunocytochemistry in Alzheimer and normal human brain. The American journal of pathology *142*, 1574-1585.

Kern, A., and Behl, C. (2009). The unsolved relationship of brain aging and late-onset Alzheimer disease. Biochimica et biophysica acta *1790*, 1124-1132.

Kerr, M.L., and Small, D.H. (2005). Cytoplasmic domain of the beta-amyloid protein precursor of Alzheimer's disease: function, regulation of proteolysis, and implications for drug development. Journal of neuroscience research *80*, 151-159.

Kibbey, M.C., Jucker, M., Weeks, B.S., Neve, R.L., Van Nostrand, W.E., and Kleinman, H.K. (1993). beta-Amyloid precursor protein binds to the neurite-promoting IKVAV site of laminin. Proceedings of the National Academy of Sciences of the United States of America *90*, 10150-10153.

Kim, D.H., Iijima, H., Goto, K., Sakai, J., Ishii, H., Kim, H.J., Suzuki, H., Kondo, H., Saeki, S., and Yamamoto, T. (1996). Human apolipoprotein E receptor 2. A novel lipoprotein receptor of the low density lipoprotein receptor family predominantly expressed in brain. The Journal of biological chemistry *271*, 8373-8380.

Kim, T.W., Wu, K., Xu, J.L., McAuliffe, G., Tanzi, R.E., Wasco, W., and Black, I.B. (1995). Selective localization of amyloid precursor-like protein 1 in the cerebral cortex postsynaptic density. Brain research Molecular brain research *32*, 36-44.

Kiral, F.R., Kohrs, F.E., Jin, E.J., and Hiesinger, P.R. (2018). Rab GTPases and Membrane Trafficking in Neurodegeneration. Current biology : CB *28*, R471-R486.

Kirchhausen, T. (1999). Adaptors for clathrin-mediated traffic. Annual review of cell and developmental biology *15*, 705-732.

Kirfel, G., Borm, B., Rigort, A., and Herzog, V. (2002). The secretory beta-amyloid precursor protein is a motogen for human epidermal keratinocytes. European journal of cell biology *81*, 664-676.

Kitazawa, M., Medeiros, R., and Laferla, F.M. (2012). Transgenic mouse models of Alzheimer disease: developing a better model as a tool for therapeutic interventions. Current pharmaceutical design *18*, 1131-1147.

Klein, A.M., Kowall, N.W., and Ferrante, R.J. (1999). Neurotoxicity and oxidative damage of beta amyloid 1-42 versus beta amyloid 1-40 in the mouse cerebral cortex. Annals of the New York Academy of Sciences *893*, 314-320.

Klein, S., Franco, M., Chardin, P., and Luton, F. (2006). Role of the Arf6 GDP/GTP cycle and Arf6 GTPase-activating proteins in actin remodeling and intracellular transport. The Journal of biological chemistry *281*, 12352-12361.

Knauer, M.F., Orlando, R.A., and Glabe, C.G. (1996). Cell surface APP751 forms complexes with protease nexin 2 ligands and is internalized via the low density lipoprotein receptor-related protein (LRP). Brain research *740*, 6-14.

Knopman, D.S., DeKosky, S.T., Cummings, J.L., Chui, H., Corey-Bloom, J., Relkin, N., Small, G.W., Miller, B., and Stevens, J.C. (2001). Practice parameter: diagnosis of dementia (an evidence-based review). Report of the Quality Standards Subcommittee of the American Academy of Neurology. Neurology *56*, 1143-1153.

Knutson, M.D. (2007). Steap proteins: implications for iron and copper metabolism. Nutrition reviews *65*, 335-340.

Koffie, R.M., Hyman, B.T., and Spires-Jones, T.L. (2011). Alzheimer's disease: synapses gone cold. Molecular neurodegeneration *6*, 63.

Kojro, E., Gimpl, G., Lammich, S., Marz, W., and Fahrenholz, F. (2001). Low cholesterol stimulates the nonamyloidogenic pathway by its effect on the alpha - secretase ADAM 10. Proceedings of the National Academy of Sciences of the United States of America *98*, 5815-5820.

Kong, G.K., Adams, J.J., Harris, H.H., Boas, J.F., Curtain, C.C., Galatis, D., Masters, C.L., Barnham, K.J., McKinstry, W.J., Cappai, R., and Parker, M.W. (2007). Structural studies of the Alzheimer's amyloid precursor protein copper-binding domain reveal how it binds copper ions. Journal of molecular biology *367*, 148-161.

Konietzko, U., Goodger, Z.V., Meyer, M., Kohli, B.M., Bosset, J., Lahiri, D.K., and Nitsch, R.M. (2010). Co-localization of the amyloid precursor protein and Notch intracellular domains in nuclear transcription factories. Neurobiology of aging *31*, 58-73.

Kontoghiorghe, C.N., and Kontoghiorghes, G.J. (2016). Efficacy and safety of iron-chelation therapy with deferoxamine, deferiprone, and deferasirox for the treatment of iron-loaded patients with non-transfusion-dependent thalassemia syndromes. Drug design, development and therapy *10*, 465-481.

Koo, E.H., and Squazzo, S.L. (1994). Evidence that production and release of amyloid beta-protein involves the endocytic pathway. The Journal of biological chemistry *269*.

Koo, E.H., Squazzo, S.L., Selkoe, D.J., and Koo, C.H. (1996). Trafficking of cell-surface amyloid beta-protein precursor. I. Secretion, endocytosis and recycling as detected by labeled monoclonal antibody. Journal of cell science *109 (Pt 5)*, 991-998.

Koo, J.W., Russo, S.J., Ferguson, D., Nestler, E.J., and Duman, R.S. (2010). Nuclear factor-kappaB is a critical mediator of stress-impaired neurogenesis and depressive behavior. Proceedings of the National Academy of Sciences of the United States of America *107*, 2669-2674.

Koudinov, A.R., and Koudinova, N.V. (2001). Essential role for cholesterol in synaptic plasticity and neuronal degeneration. FASEB journal : official publication of the Federation of American Societies for Experimental Biology *15*, 1858-1860.

Krabbe, G., Halle, A., Matyash, V., Rinnenthal, J.L., Eom, G.D., Bernhardt, U., Miller, K.R., Prokop, S., Kettenmann, H., and Heppner, F.L. (2013). Functional impairment of microglia coincides with Beta-amyloid deposition in mice with Alzheimer-like pathology. PloS one *8*, e60921.

Kruzel, M.L., Actor, J.K., Boldogh, I., and Zimecki, M. (2007). Lactoferrin in health and disease. Postepy Hig Med Dosw (Online) *61*, 261-267.

Kruzel, M.L., Zimecki, M., and Actor, J.K. (2017). Lactoferrin in a Context of Inflammation-Induced Pathology. Frontiers in immunology *8*, 1438.

Kuhn, P.H., Wang, H., Dislich, B., Colombo, A., Zeitschel, U., Ellwart, J.W., Kremmer, E., Rossner, S., and Lichtenthaler, S.F. (2010). ADAM10 is the physiologically relevant, constitutive alpha-secretase of the amyloid precursor protein in primary neurons. The EMBO journal *29*, 3020-3032.

Kukull, W.A., Higdon, R., Bowen, J.D., McCormick, W.C., Teri, L., Schellenberg, G.D., van Belle, G., Jolley, L., and Larson, E.B. (2002). Dementia and Alzheimer disease incidence: a prospective cohort study. Archives of neurology *59*, 1737-1746.

Kumar, D.K., Choi, S.H., Washicosky, K.J., Eimer, W.A., Tucker, S., Ghofrani, J., Lefkowitz, A., McColl, G., Goldstein, L.E., Tanzi, R.E., and Moir, R.D. (2016). Amyloid-beta peptide protects against microbial infection in mouse and worm models of Alzheimer's disease. Science translational medicine *8*, 340ra372.

Lai, A., Sisodia, S.S., and Trowbridge, I.S. (1995). Characterization of sorting signals in the beta-amyloid precursor protein cytoplasmic domain. The Journal of biological chemistry *270*, 3565-3573.

Laifenfeld, D., Patzek, L.J., McPhie, D.L., Chen, Y., Levites, Y., Cataldo, A.M., and Neve, R.L. (2007). Rab5 mediates an amyloid precursor protein signaling pathway that leads to apoptosis. The Journal of neuroscience : the official journal of the Society for Neuroscience *27*, 7141-7153.

Lakshmana, M.K., Chen, E., Yoon, I.S., and Kang, D.E. (2008). C-terminal 37 residues of LRP promote the amyloidogenic processing of APP independent of FE65. Journal of cellular and molecular medicine *12*, 2665-2674.

Lambert, J.C., Heath, S., Even, G., Campion, D., Sleegers, K., Hiltunen, M., Combarros, O., Zelenika, D., Bullido, M.J., Tavernier, B., Letenneur, L., Bettens, K., Berr, C., Pasquier, F., Fievet, N., Barberger-Gateau, P., Engelborghs, S., De Deyn, P., Mateo, I., Franck, A., Helisalmi, S., Porcellini, E., Hanon, O., de Pancorbo, M.M., Lendon, C., Dufouil, C., Jaillard, C., Leveillard, T., Alvarez, V., Bosco, P., Mancuso, M., Panza, F., Nacmias, B., Bossu, P., Piccardi, P., Annoni, G., Seripa, D., Galimberti, D., Hannequin, D., Licastro, F., Soininen, H., Ritchie, K., Blanche, H., Dartigues, J.F., Tzourio, C., Gut, I., Van Broeckhoven, C., Alperovitch, A., Lathrop, M., and Amouyel, P. (2009). Genome-wide association study identifies variants at CLU and CR1 associated with Alzheimer's disease. Nat Genet *41*, 1094-1099.

Lambert, J.C., Ibrahim-Verbaas, C.A., Harold, D., Naj, A.C., Sims, R., Bellenguez, C., DeStafano, A.L., Bis, J.C., Beecham, G.W., Grenier-Boley, B., Russo, G., Thorton-Wells, T.A., Jones, N., Smith, A.V., Chouraki, V., Thomas, C., Ikram, M.A., Zelenika, D., Vardarajan, B.N., Kamatani, Y., Lin, C.F., Gerrish, A., Schmidt, H., Kunkle, B., Dunstan, M.L., Ruiz, A., Bihoreau, M.T., Choi, S.H., Reitz, C., Pasquier, F., Cruchaga, C., Craig, D., Amin, N., Berr, C., Lopez, O.L., De Jager, P.L., Deramecourt, V., Johnston, J.A., Evans, D., Lovestone, S., Letenneur, L., Moron, F.J., Rubinsztein, D.C., Eiriksdottir, G., Sleegers, K., Goate, A.M., Fievet, N., Huentelman, M.W., Gill, M., Brown, K., Kamboh, M.I., Keller, L., Barberger-Gateau, P., McGuiness, B., Larson, E.B., Green, R., Myers, A.J., Dufouil, C., Todd, S., Wallon, D., Love, S., Rogaeva, E., Gallacher, J., St George-Hyslop, P., Clarimon, J., Lleo, A., Bayer, A., Tsuang, D.W., Yu, L., Tsolaki, M., Bossu, P., Spalletta, G., Proitsi, P., Collinge, J., Sorbi, S., Sanchez-Garcia, F., Fox, N.C., Hardy, J., Deniz Naranjo, M.C., Bosco, P., Clarke, R., Brayne, C., Galimberti, D., Mancuso, M., Matthews, F., Moebus, S., Mecocci, P., Del Zompo, M., Maier, W., Hampel, H., Pilotto, A., Bullido, M., Panza, F., Caffarra, P., Nacmias, B., Gilbert, J.R., Mayhaus, M., Lannefelt, L., Hakonarson, H., Pichler, S., Carrasquillo, M.M., Ingelsson, M., Beekly, D., Alvarez, V., Zou, F., Valladares, O., Younkin, S.G., Coto, E., Hamilton-Nelson, K.L., Gu, W., Razquin, C., Pastor, P., Mateo, I., Owen, M.J., Faber, K.M., Jonsson, P.V., Combarros, O., O'Donovan, M.C., Cantwell, L.B., Soininen, H., Blacker, D., Mead, S., Mosley, T.H., Jr., Bennett, D.A., Harris, T.B., Fratiglioni, L., Holmes, C., de Bruijn, R.F., Passmore, P., Montine, T.J., Bettens, K., Rotter, J.I., Brice, A., Morgan, K., Foroud, T.M., Kukull, W.A., Hannequin, D., Powell, J.F., Nalls, M.A., Ritchie, K., Lunetta, K.L., Kauwe, J.S., Boerwinkle, E., Riemenschneider, M., Boada, M., Hiltuenen, M., Martin, E.R., Schmidt, R., Rujescu, D., Wang, L.S., Dartigues, J.F., Mayeux, R., Tzourio, C., Hofman, A., Nothen, M.M., Graff, C., Psaty, B.M., Jones, L., Haines, J.L., Holmans, P.A., Lathrop, M., Pericak-Vance, M.A., Launer, L.J., Farrer, L.A., van Duijn, C.M., Van Broeckhoven, C., Moskvina, V., Seshadri, S., Williams, J., Schellenberg, G.D., and Amouyel, P. (2013). Meta-analysis of

74,046 individuals identifies 11 new susceptibility loci for Alzheimer's disease. Nat Genet *45*, 1452-1458.

Lampreave, F., Pineiro, A., Brock, J.H., Castillo, H., Sanchez, L., and Calvo, M. (1990). Interaction of bovine lactoferrin with other proteins of milk whey. International journal of biological macromolecules *12*, 2-5.

Laporte, V., Lombard, Y., Levy-Benezra, R., Tranchant, C., Poindron, P., and Warter, J.-M. (2004). Uptake of Aβ 1-40- and Aβ 1-42-coated yeast by microglial cells: A role for LRP, Vol 76.

Lassek, M., Weingarten, J., Einsfelder, U., Brendel, P., Muller, U., and Volknandt, W. (2013). Amyloid precursor proteins are constituents of the presynaptic active zone. Journal of neurochemistry *127*, 48-56.

Le Page, A., Dupuis, G., Frost, E.H., Larbi, A., Pawelec, G., Witkowski, J.M., and Fulop, T. (2018). Role of the peripheral innate immune system in the development of Alzheimer's disease. Experimental gerontology *107*, 59-66.

LeBlanc, A.C., Chen, H.Y., Autilio-Gambetti, L., and Gambetti, P. (1991). Differential APP gene expression in rat cerebral cortex, meninges, and primary astroglial, microglial and neuronal cultures. FEBS letters *292*, 171-178.

LeBlanc, A.C., and Goodyer, C.G. (1999). Role of endoplasmic reticulum, endosomal-lysosomal compartments, and microtubules in amyloid precursor protein metabolism of human neurons. Journal of neurochemistry *72*, 1832-1842.

LeBlanc, A.C., Xue, R., and Gambetti, P. (1996). Amyloid precursor protein metabolism in primary cell cultures of neurons, astrocytes, and microglia. Journal of neurochemistry *66*, 2300-2310.

Lee, J.E., and Han, P.L. (2013). An update of animal models of Alzheimer disease with a reevaluation of plaque depositions. Experimental neurobiology *22*, 84-95.

Lee, S., Sato, Y., and Nixon, R.A. (2011a). Lysosomal proteolysis inhibition selectively disrupts axonal transport of degradative organelles and causes an Alzheimer's-like axonal dystrophy. The Journal of neuroscience : the official journal of the Society for Neuroscience *31*, 7817-7830.

Lee, S., Xue, Y., Hu, J., Wang, Y., Liu, X., Demeler, B., and Ha, Y. (2011b). The E2 domains of APP and APLP1 share a conserved mode of dimerization. Biochemistry *50*, 5453-5464.

Legrand, D., Elass, E., Carpentier, M., and Mazurier, J. (2005). Lactoferrin: a modulator of immune and inflammatory responses. Cellular and molecular life sciences : CMLS *62*, 2549-2559.

Levay, P.F., and Viljoen, M. (1995). Lactoferrin: a general review. Haematologica *80*, 252-267.

Leveugle, B., Spik, G., Perl, D.P., Bouras, C., Fillit, H.M., and Hof, P.R. (1994). The iron-binding protein lactotransferrin is present in pathologic lesions in a

variety of neurodegenerative disorders: a comparative immunohistochemical analysis. Brain research *650*, 20-31.

LeVine, S.M. (1997). Iron deposits in multiple sclerosis and Alzheimer's disease brains. Brain research *760*, 298-303.

Lewczuk, P., Matzen, A., Blennow, K., Parnetti, L., Molinuevo, J.L., Eusebi, P., Kornhuber, J., Morris, J.C., and Fagan, A.M. (2017). Cerebrospinal Fluid Abeta42/40 Corresponds Better than Abeta42 to Amyloid PET in Alzheimer's Disease. Journal of Alzheimer's disease : JAD *55*, 813-822.

Leyssen, M., Ayaz, D., Hebert, S.S., Reeve, S., De Strooper, B., and Hassan, B.A. (2005). Amyloid precursor protein promotes post-developmental neurite arborization in the Drosophila brain. The EMBO journal *24*, 2944-2955.

Li, G. (2011). Rab GTPases, membrane trafficking and diseases. Current drug targets *12*, 1188-1193.

Li, G., and Stahl, P.D. (1993). Structure-function relationship of the small GTPase rab5. The Journal of biological chemistry *268*, 24475-24480.

Li, H., Liu, C.-C., Zheng, H., and Huang, T.Y. (2018). Amyloid, tau, pathogen infection and antimicrobial protection in Alzheimer's disease –conformist, nonconformist, and realistic prospects for AD pathogenesis. Translational neurodegeneration *7*, 34.

Li, H.L., Roch, J.M., Sundsmo, M., Otero, D., Sisodia, S., Thomas, R., and Saitoh, T. (1997). Defective neurite extension is caused by a mutation in amyloid beta/A4 (A beta) protein precursor found in familial Alzheimer's disease. Journal of neurobiology *32*, 469-480.

Li, J., Kanekiyo, T., Shinohara, M., Zhang, Y., LaDu, M.J., Xu, H., and Bu, G. (2012). Differential regulation of amyloid-beta endocytic trafficking and lysosomal degradation by apolipoprotein E isoforms. The Journal of biological chemistry *287*, 44593-44601.

Li, Q., and Sudhof, T.C. (2004). Cleavage of amyloid-beta precursor protein and amyloid-beta precursor-like protein by BACE 1. The Journal of biological chemistry *279*, 10542-10550.

Li, X., and DiFiglia, M. (2012). The recycling endosome and its role in neurological disorders. Progress in neurobiology *97*, 127-141.

Li, Y., Cam, J., and Bu, G. (2001). Low-density lipoprotein receptor family: endocytosis and signal transduction. Molecular neurobiology *23*, 53-67.

Li, Y., Jiao, Q., Xu, H., Du, X., Shi, L., Jia, F., and Jiang, H. (2017). Biometal Dyshomeostasis and Toxic Metal Accumulations in the Development of Alzheimer's Disease. Frontiers in molecular neuroscience *10*, 339.

Li, Z.W., Stark, G., Gotz, J., Rulicke, T., Gschwind, M., Huber, G., Muller, U., and Weissmann, C. (1996). Generation of mice with a 200-kb amyloid precursor

protein gene deletion by Cre recombinase-mediated site-specific recombination in embryonic stem cells. Proceedings of the National Academy of Sciences of the United States of America *93*, 6158-6162.

Lin, Y.C., Uang, H.W., Lin, R.J., Chen, I.J., and Lo, Y.C. (2007). Neuroprotective effects of glyceryl nonivamide against microglia-like cells and 6-hydroxydopamine-induced neurotoxicity in SH-SY5Y human dopaminergic neuroblastoma cells. The Journal of pharmacology and experimental therapeutics *323*, 877-887.

Lindberg, C., Hjorth, E., Post, C., Winblad, B., and Schultzberg, M. (2005). Cytokine production by a human microglial cell line: effects of beta-amyloid and alpha-melanocyte-stimulating hormone. Neurotoxicity research *8*, 267-276.

Lingwood, D., and Simons, K. (2010). Lipid rafts as a membrane-organizing principle. Science *327*, 46-50.

Liu, B., Gao, H.M., Wang, J.Y., Jeohn, G.H., Cooper, C.L., and Hong, J.S. (2002). Role of nitric oxide in inflammation-mediated neurodegeneration. Annals of the New York Academy of Sciences *962*, 318-331.

Liu, B., Moloney, A., Meehan, S., Morris, K., Thomas, S.E., Serpell, L.C., Hider, R., Marciniak, S.J., Lomas, D.A., and Crowther, D.C. (2011). Iron promotes the toxicity of amyloid beta peptide by impeding its ordered aggregation. The Journal of biological chemistry *286*, 4248-4256.

Liu, C.C., Hu, J., Zhao, N., Wang, J., Wang, N., Cirrito, J.R., Kanekiyo, T., Holtzman, D.M., and Bu, G. (2017). Astrocytic LRP1 Mediates Brain Abeta Clearance and Impacts Amyloid Deposition. The Journal of neuroscience : the official journal of the Society for Neuroscience *37*, 4023-4031.

Liu, J.L., Fan, Y.G., Yang, Z.S., Wang, Z.Y., and Guo, C. (2018). Iron and Alzheimer's Disease: From Pathogenesis to Therapeutic Implications. Frontiers in neuroscience *12*, 632.

Liu, Q., Zhang, J., Tran, H., Verbeek, M.M., Reiss, K., Estus, S., and Bu, G. (2009). LRP1 shedding in human brain: roles of ADAM10 and ADAM17. Molecular neurodegeneration *4*, 17.

Liu, R.Q., Zhou, Q.H., Ji, S.R., Zhou, Q., Feng, D., Wu, Y., and Sui, S.F. (2010). Membrane localization of beta-amyloid 1-42 in lysosomes: a possible mechanism for lysosome labilization. The Journal of biological chemistry *285*, 19986-19996.

Loane, D.J., and Byrnes, K.R. (2010). Role of microglia in neurotrauma. Neurotherapeutics : the journal of the American Society for Experimental NeuroTherapeutics *7*, 366-377.

Lobo, A., Launer, L.J., Fratiglioni, L., Andersen, K., Di Carlo, A., Breteler, M.M., Copeland, J.R., Dartigues, J.F., Jagger, C., Martinez-Lage, J., Soininen, H., and Hofman, A. (2000). Prevalence of dementia and major subtypes in Europe: A collaborative study of population-based cohorts. Neurologic Diseases in the Elderly Research Group. Neurology *54*, S4-9.

Lopez, V., Kelleher, S.L., and Lonnerdal, B. (2008). Lactoferrin receptor mediates apo- but not holo-lactoferrin internalization via clathrin-mediated endocytosis in trophoblasts. The Biochemical journal *411*, 271-278.

Lu, L.N., Qian, Z.M., Wu, K.C., Yung, W.H., and Ke, Y. (2017). Expression of Iron Transporters and Pathological Hallmarks of Parkinson's and Alzheimer's Diseases in the Brain of Young, Adult, and Aged Rats. Molecular neurobiology *54*, 5213-5224.

Luhrs, T., Ritter, C., Adrian, M., Riek-Loher, D., Bohrmann, B., Dobeli, H., Schubert, D., and Riek, R. (2005). 3D structure of Alzheimer's amyloid-beta(1-42) fibrils. Proceedings of the National Academy of Sciences of the United States of America *102*, 17342-17347.

Lukiw, W.J., Cui, J.G., Yuan, L.Y., Bhattacharjee, P.S., Corkern, M., Clement, C., Kammerman, E.M., Ball, M.J., Zhao, Y., Sullivan, P.M., and Hill, J.M. (2010). Acyclovir or Abeta42 peptides attenuate HSV-1-induced miRNA-146a levels in human primary brain cells. Neuroreport *21*, 922-927.

Luo, L. (2000). Rho GTPases in neuronal morphogenesis. Nature reviews Neuroscience *1*, 173-180.

Luo, L.Q., Martin-Morris, L.E., and White, K. (1990). Identification, secretion, and neural expression of APPL, a Drosophila protein similar to human amyloid protein precursor. The Journal of neuroscience : the official journal of the Society for Neuroscience *10*, 3849-3861.

Luo, Y., Bolon, B., Damore, M.A., Fitzpatrick, D., Liu, H., Zhang, J., Yan, Q., Vassar, R., and Citron, M. (2003). BACE1 (beta-secretase) knockout mice do not acquire compensatory gene expression changes or develop neural lesions over time. Neurobiology of disease *14*, 81-88.

Lyckman, A.W., Confaloni, A.M., Thinakaran, G., Sisodia, S.S., and Moya, K.L. (1998). Post-translational processing and turnover kinetics of presynaptically targeted amyloid precursor superfamily proteins in the central nervous system. The Journal of biological chemistry *273*, 11100-11106.

Ma, Q.H., Bagnard, D., Xiao, Z.C., and Dawe, G.S. (2008). A TAG on to the neurogenic functions of APP. Cell adhesion & migration *2*, 2-8.

Macia, E., Luton, F., Partisani, M., Cherfils, J., Chardin, P., and Franco, M. (2004). The GDP-bound form of Arf6 is located at the plasma membrane. Journal of cell science *117*, 2389-2398.

Magara, F., Muller, U., Li, Z.W., Lipp, H.P., Weissmann, C., Stagljar, M., and Wolfer, D.P. (1999). Genetic background changes the pattern of forebrain commissure defects in transgenic mice underexpressing the beta-amyloid-precursor protein. Proceedings of the National Academy of Sciences of the United States of America *96*, 4656-4661.

Maiorino, M., Conrad, M., and Ursini, F. (2018). GPx4, Lipid Peroxidation, and Cell Death: Discoveries, Rediscoveries, and Open Issues. Antioxidants & redox signaling *29*, 61-74.

Majka, G., Śpiewak, K., Kurpiewska, K., Heczko, P., Stochel, G., Strus, M., & Brindell, M. (2013). A high-throughput method for the quantification of iron saturation in lactoferrin preparations. Analytical and bioanalytical chemistry *405*, 5191–5200.

Maldonado-Baez, L., Cole, N.B., Kramer, H., and Donaldson, J.G. (2013). Microtubule-dependent endosomal sorting of clathrin-independent cargo by Hook1. The Journal of cell biology *201*, 233-247.

Malik, M., Parikh, I., Vasquez, J.B., Smith, C., Tai, L., Bu, G., LaDu, M.J., Fardo, D.W., Rebeck, G.W., and Estus, S. (2015). Genetics ignite focus on microglial inflammation in Alzheimer's disease. Molecular neurodegeneration *10*, 52.

Mammana, S., Fagone, P., Cavalli, E., Basile, M.S., Petralia, M.C., Nicoletti, F., Bramanti, P., and Mazzon, E. (2018). The Role of Macrophages in Neuroinflammatory and Neurodegenerative Pathways of Alzheimer's Disease, Amyotrophic Lateral Sclerosis, and Multiple Sclerosis: Pathogenetic Cellular Effectors and Potential Therapeutic Targets. International journal of molecular sciences *19*.

Mandelkow, E.M., and Mandelkow, E. (1998). Tau in Alzheimer's disease. Trends in cell biology *8*, 425-427.

Mandrekar-Colucci, S., and Landreth, G.E. (2010). Microglia and inflammation in Alzheimer's disease. CNS & neurological disorders drug targets *9*, 156-167.

Manolov, V., Hadjidekova, S., Petrova, J., Maria, P., Traykov, L., Tzatchev, K., Borislav, M., Grozdanova, R., and Ivo, B. (2017). The Role of Iron Homeostasis in Alzheimer’s Disease, Vol 3.

Mantuano, E., Brifault, C., Lam, M.S., Azmoon, P., Gilder, A.S., and Gonias, S.L. (2016). LDL receptor-related protein-1 regulates NFkappaB and microRNA-155 in macrophages to control the inflammatory response. Proceedings of the National Academy of Sciences of the United States of America *113*, 1369-1374.

Mantuano, E., Lam, M.S., and Gonias, S.L. (2013). LRP1 assembles unique co-receptor systems to initiate cell signaling in response to tissue-type plasminogen activator and myelin-associated glycoprotein. The Journal of biological chemistry *288*, 34009-34018.

Mantuano, E., Mukandala, G., Li, X., Campana, W.M., and Gonias, S.L. (2008). Molecular dissection of the human alpha2-macroglobulin subunit reveals domains with antagonistic activities in cell signaling. The Journal of biological chemistry *283*, 19904-19911.

Mantyh, P.W., Ghilardi, J.R., Rogers, S., DeMaster, E., Allen, C.J., Stimson, E.R., and Maggio, J.E. (1993). Aluminum, iron, and zinc ions promote aggregation of

physiological concentrations of beta-amyloid peptide. Journal of neurochemistry *61*, 1171-1174.

Markgraf, D.F., Peplowska, K., and Ungermann, C. (2007). Rab cascades and tethering factors in the endomembrane system. FEBS letters *581*, 2125-2130.

Marquer, C., Devauges, V., Cossec, J.C., Liot, G., Lecart, S., Saudou, F., Duyckaerts, C., Leveque-Fort, S., and Potier, M.C. (2011). Local cholesterol increase triggers amyloid precursor protein-Bace1 clustering in lipid rafts and rapid endocytosis. FASEB journal : official publication of the Federation of American Societies for Experimental Biology *25*, 1295-1305.

Marquez-Sterling, N.R., Lo, A.C., Sisodia, S.S., and Koo, E.H. (1997). Trafficking of cell-surface beta-amyloid precursor protein: evidence that a sorting intermediate participates in synaptic vesicle recycling. The Journal of neuroscience : the official journal of the Society for Neuroscience *17*, 140-151.

Marzolo, M.P., and Bu, G. (2009). Lipoprotein receptors and cholesterol in APP trafficking and proteolytic processing, implications for Alzheimer's disease. Seminars in cell & developmental biology *20*, 191-200.

Masiulis, I., Quill, T.A., Burk, R.F., and Herz, J. (2009). Differential functions of the Apoer2 intracellular domain in selenium uptake and cell signaling. Biological chemistry *390*, 67-73.

Masters, C.L., Simms, G., Weinman, N.A., Multhaup, G., McDonald, B.L., and Beyreuther, K. (1985). Amyloid plaque core protein in Alzheimer disease and Down syndrome. Proceedings of the National Academy of Sciences of the United States of America *82*, 4245-4249.

Matsuda, S., Giliberto, L., Matsuda, Y., Davies, P., McGowan, E., Pickford, F., Ghiso, J., Frangione, B., and D'Adamio, L. (2005). The familial dementia BRI2 gene binds the Alzheimer gene amyloid-beta precursor protein and inhibits amyloid-beta production. The Journal of biological chemistry *280*, 28912-28916.

Matsuda, S., Matsuda, Y., Snapp, E.L., and D'Adamio, L. (2011). Maturation of BRI2 generates a specific inhibitor that reduces APP processing at the plasma membrane and in endocytic vesicles. Neurobiology of aging *32*, 1400-1408.

Mattson, M.P., Barger, S.W., Furukawa, K., Bruce, A.J., Wyss-Coray, T., Mark, R.J., and Mucke, L. (1997). Cellular signaling roles of TGF beta, TNF alpha and beta APP in brain injury responses and Alzheimer's disease. Brain research Brain research reviews *23*, 47-61.

Maxfield, F.R., and McGraw, T.E. (2004). Endocytic recycling. Nature reviews Molecular cell biology *5*, 121-132.

May, P., Rohlmann, A., Bock, H.H., Zurhove, K., Marth, J.D., Schomburg, E.D., Noebels, J.L., Beffert, U., Sweatt, J.D., Weeber, E.J., and Herz, J. (2004). Neuronal LRP1 functionally associates with postsynaptic proteins and is required for normal motor function in mice. Molecular and cellular biology *24*, 8872-8883.

Maynard, C.J., Cappai, R., Volitakis, I., Cherny, R.A., White, A.R., Beyreuther, K., Masters, C.L., Bush, A.I., and Li, Q.X. (2002). Overexpression of Alzheimer's disease amyloid-beta opposes the age-dependent elevations of brain copper and iron. The Journal of biological chemistry *277*, 44670-44676.

McAbee, D.D., and Ling, Y.Y. (1997). Iron-loading of cultured adult rat hepatocytes reversibly enhances lactoferrin binding and endocytosis. Journal of cellular physiology *171*, 75-86.

McCaffrey, M.W., Bielli, A., Cantalupo, G., Mora, S., Roberti, V., Santillo, M., Drummond, F., and Bucci, C. (2001). Rab4 affects both recycling and degradative endosomal trafficking. FEBS letters *495*, 21-30.

McCarthy, R.C., and Kosman, D.J. (2013). Ferroportin and exocytoplasmic ferroxidase activity are required for brain microvascular endothelial cell iron efflux. The Journal of biological chemistry *288*, 17932-17940.

McCarthy, R.C., Park, Y.H., and Kosman, D.J. (2014). sAPP modulates iron efflux from brain microvascular endothelial cells by stabilizing the ferrous iron exporter ferroportin. EMBO reports *15*, 809-815.

McGeer, E.G., and McGeer, P.L. (2010). Neuroinflammation in Alzheimer's disease and mild cognitive impairment: a field in its infancy. Journal of Alzheimer's disease : JAD *19*, 355-361.

McGowan, E., Eriksen, J., and Hutton, M. (2006). A decade of modeling Alzheimer's disease in transgenic mice. Trends in genetics : TIG *22*, 281-289.

McNamara, M.J., Ruff, C.T., Wasco, W., Tanzi, R.E., Thinakaran, G., and Hyman, B.T. (1998). Immunohistochemical and in situ analysis of amyloid precursor-like protein-1 and amyloid precursor-like protein-2 expression in Alzheimer disease and aged control brains. Brain research *804*, 45-51.

McNiven, M.A., and Thompson, H.M. (2006). Vesicle formation at the plasma membrane and trans-Golgi network: the same but different. Science *313*, 1591-1594.

Meadowcroft, M.D., Connor, J.R., Smith, M.B., and Yang, Q.X. (2009). MRI and histological analysis of beta-amyloid plaques in both human Alzheimer's disease and APP/PS1 transgenic mice. Journal of magnetic resonance imaging : JMRI *29*, 997-1007.

Mecca, C., Giambanco, I., Donato, R., and Arcuri, C. (2018). Microglia and Aging: The Role of the TREM2-DAP12 and CX3CL1-CX3CR1 Axes. International journal of molecular sciences *19*.

Meda, L., Cassatella, M.A., Szendrei, G.I., Otvos, L., Jr., Baron, P., Villalba, M., Ferrari, D., and Rossi, F. (1995). Activation of microglial cells by beta-amyloid protein and interferon-gamma. Nature *374*, 647-650.

Mendez, M.F. (2017). What is the Relationship of Traumatic Brain Injury to Dementia? Journal of Alzheimer's disease : JAD *57*, 667-681.

Menendez-Gonzalez, M., Padilla-Zambrano, H.S., Alvarez, G., Capetillo-Zarate, E., Tomas-Zapico, C., and Costa, A. (2018). Targeting Beta-Amyloid at the CSF: A New Therapeutic Strategy in Alzheimer's Disease. Frontiers in aging neuroscience *10*, 100.

Meraz-Rios, M.A., Toral-Rios, D., Franco-Bocanegra, D., Villeda-Hernandez, J., and Campos-Pena, V. (2013). Inflammatory process in Alzheimer's Disease. Frontiers in integrative neuroscience *7*, 59.

Meresse, S., Gorvel, J.P., and Chavrier, P. (1995). The rab7 GTPase resides on a vesicular compartment connected to lysosomes. Journal of cell science *108 (Pt 11)*, 3349-3358.

Metaxas, A., and Kempf, S.J. (2016). Neurofibrillary tangles in Alzheimer's disease: elucidation of the molecular mechanism by immunohistochemistry and tau protein phospho-proteomics. Neural regeneration research *11*, 1579-1581.

Metz-Boutigue, M.H., Jolles, J., Mazurier, J., Schoentgen, F., Legrand, D., Spik, G., Montreuil, J., and Jolles, P. (1984). Human lactotransferrin: amino acid sequence and structural comparisons with other transferrins. European journal of biochemistry *145*, 659-676.

Michell-Robinson, M.A., Touil, H., Healy, L.M., Owen, D.R., Durafourt, B.A., Bar-Or, A., Antel, J.P., and Moore, C.S. (2015). Roles of microglia in brain development, tissue maintenance and repair. Brain : a journal of neurology *138*, 1138-1159.

Mietelska-Porowska, A., Wasik, U., Goras, M., Filipek, A., and Niewiadomska, G. (2014). Tau protein modifications and interactions: their role in function and dysfunction. International journal of molecular sciences *15*, 4671-4713.

Minogue, A.M., Stubbs, A.K., Frigerio, C.S., Boland, B., Fadeeva, J.V., Tang, J., Selkoe, D.J., and Walsh, D.M. (2009). gamma-secretase processing of APLP1 leads to the production of a p3-like peptide that does not aggregate and is not toxic to neurons. Brain research *1262*, 89-99.

Mir, M., Tolosa, L., Asensio, V.J., Llado, J., and Olmos, G. (2008). Complementary roles of tumor necrosis factor alpha and interferon gamma in inducible microglial nitric oxide generation. Journal of neuroimmunology *204*, 101-109.

Misonou, H., Morishima-Kawashima, M., and Ihara, Y. (2000). Oxidative stress induces intracellular accumulation of amyloid beta-protein (Abeta) in human neuroblastoma cells. Biochemistry *39*, 6951-6959.

Mitra, S., Cheng, K.W., and Mills, G.B. (2011). Rab GTPases implicated in inherited and acquired disorders. Seminars in cell & developmental biology *22*, 57-68.

Moir, R.D., Lathe, R., and Tanzi, R.E. (2018). The antimicrobial protection hypothesis of Alzheimer's disease. Alzheimer's & dementia : the journal of the Alzheimer's Association *14*, 1602-1614.

Montine, T.J., Neely, M.D., Quinn, J.F., Beal, M.F., Markesbery, W.R., Roberts, L.J., and Morrow, J.D. (2002). Lipid peroxidation in aging brain and Alzheimer's disease. Free radical biology & medicine *33*, 620-626.

Moos, T., Rosengren Nielsen, T., Skjorringe, T., and Morgan, E.H. (2007). Iron trafficking inside the brain. Journal of neurochemistry *103*, 1730-1740.

Morgan, K. (2011). The three new pathways leading to Alzheimer's disease. Neuropathology and applied neurobiology *37*, 353-357.

Morris, G.P., Clark, I.A., and Vissel, B. (2014). Inconsistencies and controversies surrounding the amyloid hypothesis of Alzheimer's disease. Acta neuropathologica communications *2*, 135.

Morris, S.M., and Cooper, J.A. (2001). Disabled-2 colocalizes with the LDLR in clathrin-coated pits and interacts with AP-2. Traffic *2*, 111-123.

Morrison, J.H., and Hof, P.R. (1997). Life and death of neurons in the aging brain. Science *278*, 412-419.

Motley, A., Bright, N.A., Seaman, M.N., and Robinson, M.S. (2003). Clathrin-mediated endocytosis in AP-2-depleted cells. The Journal of cell biology *162*, 909-918.

Motter, R., Vigo-Pelfrey, C., Kholodenko, D., Barbour, R., Johnson-Wood, K., Galasko, D., Chang, L., Miller, B., Clark, C., Green, R., and et al. (1995). Reduction of beta-amyloid peptide42 in the cerebrospinal fluid of patients with Alzheimer's disease. Annals of neurology *38*, 643-648.

Mrak, R.E., and Griffin, W.S. (2001). Interleukin-1, neuroinflammation, and Alzheimer's disease. Neurobiology of aging *22*, 903-908.

Mucke, L., Masliah, E., Yu, G.Q., Mallory, M., Rockenstein, E.M., Tatsuno, G., Hu, K., Kholodenko, D., Johnson-Wood, K., and McConlogue, L. (2000). High-level neuronal expression of abeta 1-42 in wild-type human amyloid protein precursor transgenic mice: synaptotoxicity without plaque formation. The Journal of neuroscience : the official journal of the Society for Neuroscience *20*, 4050-4058.

Muckenthaler, M.U., Galy, B., and Hentze, M.W. (2008). Systemic iron homeostasis and the iron-responsive element/iron-regulatory protein (IRE/IRP) regulatory network. Annual review of nutrition *28*, 197-213.

Muller, U., Cristina, N., Li, Z.W., Wolfer, D.P., Lipp, H.P., Rulicke, T., Brandner, S., Aguzzi, A., and Weissmann, C. (1994). Behavioral and anatomical deficits in mice homozygous for a modified beta-amyloid precursor protein gene. Cell *79*, 755-765.

Muller, U.C., Deller, T., and Korte, M. (2017). Not just amyloid: physiological functions of the amyloid precursor protein family. Nature reviews Neuroscience *18*, 281-298.

Multhaup, G. (1994). Identification and regulation of the high affinity binding site of the Alzheimer's disease amyloid protein precursor (APP) to glycosaminoglycans. Biochimie *76*, 304-311.

Munter, L.M., Voigt, P., Harmeier, A., Kaden, D., Gottschalk, K.E., Weise, C., Pipkorn, R., Schaefer, M., Langosch, D., and Multhaup, G. (2007). GxxxG motifs within the amyloid precursor protein transmembrane sequence are critical for the etiology of Abeta42. The EMBO journal *26*, 1702-1712.

Muresan, Z., and Muresan, V. (2006). Neuritic deposits of amyloid-beta peptide in a subpopulation of central nervous system-derived neuronal cells. Molecular and cellular biology *26*, 4982-4997.

Murphy, M.P., and LeVine, H., 3rd (2010). Alzheimer's disease and the amyloid-beta peptide. Journal of Alzheimer's disease : JAD *19*, 311-323.

Murrell, J., Farlow, M., Ghetti, B., and Benson, M.D. (1991). A mutation in the amyloid precursor protein associated with hereditary Alzheimer's disease. Science *254*, 97-99.

Myhre, O., Utkilen, H., Duale, N., Brunborg, G., and Hofer, T. (2013). Metal dyshomeostasis and inflammation in Alzheimer's and Parkinson's diseases: possible impact of environmental exposures. Oxidative medicine and cellular longevity *2013*, 726954.

Nadezhdin, K.D., Bocharova, O.V., Bocharov, E.V., and Arseniev, A.S. (2011). Structural and dynamic study of the transmembrane domain of the amyloid precursor protein. Acta naturae *3*, 69-76.

Naj, A.C., Jun, G., Beecham, G.W., Wang, L.S., Vardarajan, B.N., Buros, J., Gallins, P.J., Buxbaum, J.D., Jarvik, G.P., Crane, P.K., Larson, E.B., Bird, T.D., Boeve, B.F., Graff-Radford, N.R., De Jager, P.L., Evans, D., Schneider, J.A., Carrasquillo, M.M., Ertekin-Taner, N., Younkin, S.G., Cruchaga, C., Kauwe, J.S., Nowotny, P., Kramer, P., Hardy, J., Huentelman, M.J., Myers, A.J., Barmada, M.M., Demirci, F.Y., Baldwin, C.T., Green, R.C., Rogaeva, E., St George-Hyslop, P., Arnold, S.E., Barber, R., Beach, T., Bigio, E.H., Bowen, J.D., Boxer, A., Burke, J.R., Cairns, N.J., Carlson, C.S., Carney, R.M., Carroll, S.L., Chui, H.C., Clark, D.G., Corneveaux, J., Cotman, C.W., Cummings, J.L., DeCarli, C., DeKosky, S.T., Diaz-Arrastia, R., Dick, M., Dickson, D.W., Ellis, W.G., Faber, K.M., Fallon, K.B., Farlow, M.R., Ferris, S., Frosch, M.P., Galasko, D.R., Ganguli, M., Gearing, M., Geschwind, D.H., Ghetti, B., Gilbert, J.R., Gilman, S., Giordani, B., Glass, J.D., Growdon, J.H., Hamilton, R.L., Harrell, L.E., Head, E., Honig, L.S., Hulette, C.M., Hyman, B.T., Jicha, G.A., Jin, L.W., Johnson, N., Karlawish, J., Karydas, A., Kaye, J.A., Kim, R., Koo, E.H., Kowall, N.W., Lah, J.J., Levey, A.I., Lieberman, A.P., Lopez, O.L., Mack, W.J., Marson, D.C., Martiniuk, F., Mash, D.C., Masliah, E., McCormick, W.C., McCurry, S.M., McDavid, A.N., McKee, A.C., Mesulam, M., Miller, B.L., Miller, C.A., Miller, J.W., Parisi, J.E., Perl, D.P., Peskind, E., Petersen, R.C., Poon, W.W., Quinn, J.F., Rajbhandary, R.A., Raskind, M.,

Reisberg, B., Ringman, J.M., Roberson, E.D., Rosenberg, R.N., Sano, M., Schneider, L.S., Seeley, W., Shelanski, M.L., Slifer, M.A., Smith, C.D., Sonnen, J.A., Spina, S., Stern, R.A., Tanzi, R.E., Trojanowski, J.Q., Troncoso, J.C., Van Deerlin, V.M., Vinters, H.V., Vonsattel, J.P., Weintraub, S., Welsh-Bohmer, K.A., Williamson, J., Woltjer, R.L., Cantwell, L.B., Dombroski, B.A., Beekly, D., Lunetta, K.L., Martin, E.R., Kamboh, M.I., Saykin, A.J., Reiman, E.M., Bennett, D.A., Morris, J.C., Montine, T.J., Goate, A.M., Blacker, D., Tsuang, D.W., Hakonarson, H., Kukull, W.A., Foroud, T.M., Haines, J.L., Mayeux, R., Pericak-Vance, M.A., Farrer, L.A., and Schellenberg, G.D. (2011). Common variants at MS4A4/MS4A6E, CD2AP, CD33 and EPHA1 are associated with late-onset Alzheimer's disease. Nat Genet *43*, 436-441.

Nakajima, K., Matsushita, Y., Tohyama, Y., Kohsaka, S., and Kurihara, T. (2006). Differential suppression of endotoxin-inducible inflammatory cytokines by nuclear factor kappa B (NFkappaB) inhibitor in rat microglia. Neuroscience letters *401*, 199-202.

Naot, D., Grey, A., Reid, I.R., and Cornish, J. (2005). Lactoferrin--a novel bone growth factor. Clinical medicine & research *3*, 93-101.

Needham, B.E., Ciccotosto, G.D., and Cappai, R. (2014). Combined deletions of amyloid precursor protein and amyloid precursor-like protein 2 reveal different effects on mouse brain metal homeostasis. Metallomics : integrated biometal science *6*, 598-603.

Neta, R., Sayers, T.J., and Oppenheim, J.J. (1992). Relationship of TNF to interleukins. Immunology series *56*, 499-566.

Neumann, H., and Takahashi, K. (2007). Essential role of the microglial triggering receptor expressed on myeloid cells-2 (TREM2) for central nervous tissue immune homeostasis. Journal of neuroimmunology *184*, 92-99.

Niemantsverdriet, E., Ottoy, J., Somers, C., De Roeck, E., Struyfs, H., Soetewey, F., Verhaeghe, J., Van den Bossche, T., Van Mossevelde, S., Goeman, J., De Deyn, P.P., Marien, P., Versijpt, J., Sleegers, K., Van Broeckhoven, C., Wyffels, L., Albert, A., Ceyssens, S., Stroobants, S., Staelens, S., Bjerke, M., and Engelborghs, S. (2017). The Cerebrospinal Fluid Abeta1-42/Abeta1-40 Ratio Improves Concordance with Amyloid-PET for Diagnosing Alzheimer's Disease in a Clinical Setting. Journal of Alzheimer's disease : JAD *60*, 561-576.

Nieuwenhuis, B., and Eva, R. (2018). ARF6 and Rab11 as intrinsic regulators of axon regeneration. Small GTPases, 1-10.

Nikolaev, A., McLaughlin, T., O'Leary, D.D., and Tessier-Lavigne, M. (2009). APP binds DR6 to trigger axon pruning and neuron death via distinct caspases. Nature *457*, 981-989.

Ninomiya, H., Roch, J.M., Sundsmo, M.P., Otero, D.A., and Saitoh, T. (1993). Amino acid sequence RERMS represents the active domain of amyloid beta/A4 protein precursor that promotes fibroblast growth. The Journal of cell biology *121*, 879-886.

Nisbet, R.M., Polanco, J.C., Ittner, L.M., and Gotz, J. (2015). Tau aggregation and its interplay with amyloid-beta. Acta neuropathologica *129*, 207-220.

Nitsch, R.M., Slack, B.E., Wurtman, R.J., and Growdon, J.H. (1992). Release of Alzheimer amyloid precursor derivatives stimulated by activation of muscarinic acetylcholine receptors. Science *258*, 304-307.

Nixon, R.A. (2005). Endosome function and dysfunction in Alzheimer's disease and other neurodegenerative diseases. Neurobiology of aging *26*, 373-382.

Nixon, R.A. (2007). Autophagy, amyloidogenesis and Alzheimer disease. Journal of cell science *120*, 4081-4091.

Nixon, R.A., Wegiel, J., Kumar, A., Yu, W.H., Peterhoff, C., Cataldo, A., and Cuervo, A.M. (2005). Extensive involvement of autophagy in Alzheimer disease: an immuno-electron microscopy study. Journal of neuropathology and experimental neurology *64*, 113-122.

Nordstedt, C., Caporaso, G.L., Thyberg, J., Gandy, S.E., and Greengard, P. (1993). Identification of the Alzheimer beta/A4 amyloid precursor protein in clathrin-coated vesicles purified from PC12 cells. The Journal of biological chemistry *268*.

O'Connor, T., Sadleir, K.R., Maus, E., Velliquette, R.A., Zhao, J., Cole, S.L., Eimer, W.A., Hitt, B., Bembinster, L.A., Lammich, S., Lichtenthaler, S.F., Hebert, S.S., De Strooper, B., Haass, C., Bennett, D.A., and Vassar, R. (2008). Phosphorylation of the translation initiation factor eIF2alpha increases BACE1 levels and promotes amyloidogenesis. Neuron *60*, 988-1009.

Oddo, S., Caccamo, A., Kitazawa, M., Tseng, B.P., and LaFerla, F.M. (2003). Amyloid deposition precedes tangle formation in a triple transgenic model of Alzheimer's disease. Neurobiology of aging *24*, 1063-1070.

Ohkawara, T., Nagase, H., Koh, C.S., and Nakayama, K. (2011). The amyloid precursor protein intracellular domain alters gene expression and induces neuron-specific apoptosis. Gene *475*, 1-9.

Ohm, T.G., Muller, H., Braak, H., and Bohl, J. (1995). Close-meshed prevalence rates of different stages as a tool to uncover the rate of Alzheimer's disease-related neurofibrillary changes. Neuroscience *64*, 209-217.

Olmos, G., and Llado, J. (2014). Tumor necrosis factor alpha: a link between neuroinflammation and excitotoxicity. Mediators of inflammation *2014*, 861231.

Orihuela, R., McPherson, C.A., and Harry, G.J. (2016). Microglial M1/M2 polarization and metabolic states. British journal of pharmacology *173*, 649-665.

Osenkowski, P., Ye, W., Wang, R., Wolfe, M.S., and Selkoe, D.J. (2008). Direct and potent regulation of gamma-secretase by its lipid microenvironment. The Journal of biological chemistry *283*, 22529-22540.

Padayachee, E.R., Zetterberg, H., Portelius, E., Boren, J., Molinuevo, J.L., Andreasen, N., Cukalevski, R., Linse, S., Blennow, K., and Andreasson, U. (2016). Cerebrospinal fluid-induced retardation of amyloid beta aggregation correlates with Alzheimer's disease and the APOE epsilon4 allele. Brain research *1651*, 11-16.

Pantopoulos, K. (2004). Iron metabolism and the IRE/IRP regulatory system: an update. Annals of the New York Academy of Sciences *1012*, 1-13.

Pardossi-Piquard, R., Petit, A., Kawarai, T., Sunyach, C., Alves da Costa, C., Vincent, B., Ring, S., D'Adamio, L., Shen, J., Muller, U., St George Hyslop, P., and Checler, F. (2005). Presenilin-dependent transcriptional control of the Abeta-degrading enzyme neprilysin by intracellular domains of betaAPP and APLP. Neuron *46*, 541-554.

Park, J., Lee, D.G., Kim, B., Park, S.J., Kim, J.H., Lee, S.R., Chang, K.T., Lee, H.S., and Lee, D.S. (2015). Iron overload triggers mitochondrial fragmentation via calcineurin-sensitive signals in HT-22 hippocampal neuron cells. Toxicology *337*, 39-46.

Park, J.H., Gimbel, D.A., GrandPre, T., Lee, J.K., Kim, J.E., Li, W., Lee, D.H., and Strittmatter, S.M. (2006). Alzheimer precursor protein interaction with the Nogo-66 receptor reduces amyloid-beta plaque deposition. The Journal of neuroscience : the official journal of the Society for Neuroscience *26*, 1386-1395.

Park, J.H., and Strittmatter, S.M. (2007). Nogo receptor interacts with brain APP and Abeta to reduce pathologic changes in Alzheimer's transgenic mice. Current Alzheimer research *4*, 568-570.

Parkin, E.T., Watt, N.T., Hussain, I., Eckman, E.A., Eckman, C.B., Manson, J.C., Baybutt, H.N., Turner, A.J., and Hooper, N.M. (2007). Cellular prion protein regulates beta-secretase cleavage of the Alzheimer's amyloid precursor protein. Proceedings of the National Academy of Sciences of the United States of America *104*, 11062-11067.

Parvathy, S., Hussain, I., Karran, E.H., Turner, A.J., and Hooper, N.M. (1999). Cleavage of Alzheimer's amyloid precursor protein by alpha-secretase occurs at the surface of neuronal cells. Biochemistry *38*.

Pasqualato, S., Menetrey, J., Franco, M., and Cherfils, J. (2001). The structural GDP/GTP cycle of human Arf6. EMBO reports *2*, 234-238.

Pasqualetti, G., Brooks, D.J., and Edison, P. (2015). The role of neuroinflammation in dementias. Current neurology and neuroscience reports *15*, 17.

Patel, B.N., Dunn, R.J., Jeong, S.Y., Zhu, Q., Julien, J.P., and David, S. (2002). Ceruloplasmin regulates iron levels in the CNS and prevents free radical injury. The Journal of neuroscience : the official journal of the Society for Neuroscience *22*, 6578-6586.

Paul, S.M. (2011). Therapeutic antibodies for brain disorders. Science translational medicine *3*, 84ps20.

Perl, D.P. (2010). Neuropathology of Alzheimer's disease. The Mount Sinai journal of medicine, New York *77*, 32-42.

Perlmutter, L.S., Scott, S.A., Barron, E., and Chui, H.C. (1992). MHC class II-positive microglia in human brain: association with Alzheimer lesions. Journal of neuroscience research *33*, 549-558.

Perreau, V.M., Orchard, S., Adlard, P.A., Bellingham, S.A., Cappai, R., Ciccotosto, G.D., Cowie, T.F., Crouch, P.J., Duce, J.A., Evin, G., Faux, N.G., Hill, A.F., Hung, Y.H., James, S.A., Li, Q.X., Mok, S.S., Tew, D.J., White, A.R., Bush, A.I., Hermjakob, H., and Masters, C.L. (2010). A domain level interaction network of amyloid precursor protein and Abeta of Alzheimer's disease. Proteomics *10*, 2377-2395.

Perrin, R.J., Fagan, A.M., and Holtzman, D.M. (2009). Multimodal techniques for diagnosis and prognosis of Alzheimer's disease. Nature *461*, 916-922.

Perry, G., Friedman, R., Shaw, G., and Chau, V. (1987). Ubiquitin is detected in neurofibrillary tangles and senile plaque neurites of Alzheimer disease brains. Proceedings of the National Academy of Sciences of the United States of America *84*, 3033-3036.

Peterson, M.E., Daniel, R.M., Danson, M.J., and Eisenthal, R. (2007). The dependence of enzyme activity on temperature: determination and validation of parameters. The Biochemical journal *402*, 331-337.

Pietrangelo, A. (2011). Hepcidin in human iron disorders: therapeutic implications. Journal of hepatology *54*, 173-181.

Pietrzik, C.U., Busse, T., Merriam, D.E., Weggen, S., and Koo, E.H. (2002). The cytoplasmic domain of the LDL receptor-related protein regulates multiple steps in APP processing. The EMBO journal *21*, 5691-5700.

Pigeon, C., Ilyin, G., Courselaud, B., Leroyer, P., Turlin, B., Brissot, P., and Loreal, O. (2001). A new mouse liver-specific gene, encoding a protein homologous to human antimicrobial peptide hepcidin, is overexpressed during iron overload. The Journal of biological chemistry *276*, 7811-7819.

Pike, C.J., Overman, M.J., and Cotman, C.W. (1995). Amino-terminal deletions enhance aggregation of beta-amyloid peptides in vitro. The Journal of biological chemistry *270*, 23895-23898.

Pimplikar, S.W. (2009). Reassessing the amyloid cascade hypothesis of Alzheimer's disease. The international journal of biochemistry & cell biology *41*, 1261-1268.

Plant, L.D., Webster, N.J., Boyle, J.P., Ramsden, M., Freir, D.B., Peers, C., and Pearson, H.A. (2006). Amyloid beta peptide as a physiological modulator of neuronal 'A'-type K+ current. Neurobiology of aging *27*, 1673-1683.

Ponte, P., Gonzalez-DeWhitt, P., Schilling, J., Miller, J., Hsu, D., Greenberg, B., Davis, K., Wallace, W., Lieberburg, I., and Fuller, F. (1988). A new A4 amyloid mRNA contains a domain homologous to serine proteinase inhibitors. Nature *331*, 525-527.

Postina, R., Schroeder, A., Dewachter, I., Bohl, J., Schmitt, U., Kojro, E., Prinzen, C., Endres, K., Hiemke, C., Blessing, M., Flamez, P., Dequenne, A., Godaux, E., van Leuven, F., and Fahrenholz, F. (2004). A disintegrin-metalloproteinase prevents amyloid plaque formation and hippocampal defects in an Alzheimer disease mouse model. The Journal of clinical investigation *113*, 1456-1464.

Poteryaev, D., Datta, S., Ackema, K., Zerial, M., and Spang, A. (2010). Identification of the switch in early-to-late endosome transition. Cell *141*, 497-508.

Prabhu, Y., Burgos, P.V., Schindler, C., Farias, G.G., Magadan, J.G., and Bonifacino, J.S. (2012). Adaptor protein 2-mediated endocytosis of the beta-secretase BACE1 is dispensable for amyloid precursor protein processing. Molecular biology of the cell *23*, 2339-2351.

Prasad, H., and Rao, R. (2015). The Na+/H+ exchanger NHE6 modulates endosomal pH to control processing of amyloid precursor protein in a cell culture model of Alzheimer disease. The Journal of biological chemistry *290*, 5311-5327.

Prasad, J.M., Migliorini, M., Galisteo, R., and Strickland, D.K. (2015). Generation of a Potent Low Density Lipoprotein Receptor-related Protein 1 (LRP1) Antagonist by Engineering a Stable Form of the Receptor-associated Protein (RAP) D3 Domain. The Journal of biological chemistry *290*, 17262-17268.

Price, J.L., Davis, P.B., Morris, J.C., and White, D.L. (1991). The distribution of tangles, plaques and related immunohistochemical markers in healthy aging and Alzheimer's disease. Neurobiology of aging *12*, 295-312.

Prince, M., Knapp, M., Guerchet, M., McCrone, P., Prina, M., Comas-Herrera, A., Wittenberg, R., Adelaja, B., Hu, B., King, D., Rehill, A., and Salimkumar, D. (2014). Dementia UK: Update (Second edition). In Alzheimer's Society (Alzheimer's Society).

Prince, M., Wimo, A., Guerchet, M., Ali, G.-C., Wu, Y.-T., and Prina, M. (2015). World Alzheimer Report 2015. The Global Impact of Dementia: An analysis of prevalence, incidence, cost and trends. In Alzheimer's Disease International (London).

Puig, K.L., Swigost, A.J., Zhou, X., Sens, M.A., and Combs, C.K. (2012). Amyloid precursor protein expression modulates intestine immune phenotype. Journal of neuroimmune pharmacology : the official journal of the Society on NeuroImmune Pharmacology *7*, 215-230.

Pulina, M.O., Zakharova, E.T., Sokolov, A.V., Shavlovski, M.M., Bass, M.G., Solovyov, K.V., Kokryakov, V.N., and Vasilyev, V.B. (2002). Studies of the ceruloplasmin-lactoferrin complex. Biochemistry and cell biology = Biochimie et biologie cellulaire *80*, 35-39.

Qian, Z.M., and Wang, Q. (1998). Expression of iron transport proteins and excessive iron accumulation in the brain in neurodegenerative disorders. Brain research Brain research reviews *27*, 257-267.

Qiu, C., Kivipelto, M., and von Strauss, E. (2009). Epidemiology of Alzheimer's disease: occurrence, determinants, and strategies toward intervention. Dialogues in clinical neuroscience *11*, 111-128.

Qiu, W.Q., Walsh, D.M., Ye, Z., Vekrellis, K., Zhang, J., Podlisny, M.B., Rosner, M.R., Safavi, A., Hersh, L.B., and Selkoe, D.J. (1998). Insulin-degrading enzyme regulates extracellular levels of amyloid beta-protein by degradation. The Journal of biological chemistry *273*, 32730-32738.

Qiu, Z., Hyman, B.T., and Rebeck, G.W. (2004). Apolipoprotein E receptors mediate neurite outgrowth through activation of p44/42 mitogen-activated protein kinase in primary neurons. The Journal of biological chemistry *279*, 34948-34956.

Querinjean, P., Masson, P.L., and Heremans, J.F. (1971). Molecular weight, single-chain structure and amino acid composition of human lactoferrin. European journal of biochemistry *20*, 420-425.

Quinn, K.A., Grimsley, P.G., Dai, Y.P., Tapner, M., Chesterman, C.N., and Owensby, D.A. (1997). Soluble low density lipoprotein receptor-related protein (LRP) circulates in human plasma. The Journal of biological chemistry *272*, 23946-23951.

Racoosin, E.L., and Swanson, J.A. (1993). Macropinosome maturation and fusion with tubular lysosomes in macrophages. The Journal of cell biology *121*, 1011-1020.

Radhakrishna, H., and Donaldson, J.G. (1997). ADP-ribosylation factor 6 regulates a novel plasma membrane recycling pathway. The Journal of cell biology *139*, 49-61.

Raha-Chowdhury, R., Raha, A.A., Forostyak, S., Zhao, J.W., Stott, S.R., and Bomford, A. (2015). Expression and cellular localization of hepcidin mRNA and protein in normal rat brain. BMC neuroscience *16*, 24.

Raha, A.A., Vaishnav, R.A., Friedland, R.P., Bomford, A., and Raha-Chowdhury, R. (2013). The systemic iron-regulatory proteins hepcidin and ferroportin are reduced in the brain in Alzheimer's disease. Acta neuropathologica communications *1*, 55.

Rao, J.S., Kellom, M., Kim, H.W., Rapoport, S.I., and Reese, E.A. (2012). Neuroinflammation and synaptic loss. Neurochemical research *37*, 903-910.

Rebelo, S., Vieira, S.I., da Cruz, E.S.E.F., and da Cruz, E.S.O.A. (2008). Monitoring "De Novo"APP synthesis by taking advantage of the reversible effect of cycloheximide. American journal of Alzheimer's disease and other dementias *23*, 602-608.

Rebelo, S., Vieira, S.I., Esselmann, H., Wiltfang, J., da Cruz e Silva, E.F., and da Cruz e Silva, O.A. (2007). Tyr687 dependent APP endocytosis and Abeta production. Journal of molecular neuroscience : MN *32*, 1-8.

Reddy, S.S., Connor, T.E., Weeber, E.J., and Rebeck, W. (2011). Similarities and differences in structure, expression, and functions of VLDLR and ApoER2. Molecular neurodegeneration *6*, 30.

Reinhard, C., Hebert, S.S., and De Strooper, B. (2005). The amyloid-beta precursor protein: integrating structure with biological function. The EMBO journal *24*, 3996-4006.

Rice, H.C., de Malmazet, D., Schreurs, A., Frere, S., Van Molle, I., Volkov, A.N., Creemers, E., Vertkin, I., Nys, J., Ranaivoson, F.M., Comoletti, D., Savas, J.N., Remaut, H., Balschun, D., Wierda, K.D., Slutsky, I., Farrow, K., De Strooper, B., and de Wit, J. (2019). Secreted amyloid-beta precursor protein functions as a GABABR1a ligand to modulate synaptic transmission. Science *363*.

Ring, S., Weyer, S.W., Kilian, S.B., Waldron, E., Pietrzik, C.U., Filippov, M.A., Herms, J., Buchholz, C., Eckman, C.B., Korte, M., Wolfer, D.P., and Muller, U.C. (2007). The secreted beta-amyloid precursor protein ectodomain APPs alpha is sufficient to rescue the anatomical, behavioral, and electrophysiological abnormalities of APP-deficient mice. The Journal of neuroscience : the official journal of the Society for Neuroscience *27*, 7817-7826.

Ringheim, G.E., Szczepanik, A.M., Petko, W., Burgher, K.L., Zhu, S.Z., and Chao, C.C. (1998). Enhancement of beta-amyloid precursor protein transcription and expression by the soluble interleukin-6 receptor/interleukin-6 complex. Brain research Molecular brain research *55*, 35-44.

Rink, J., Ghigo, E., Kalaidzidis, Y., and Zerial, M. (2005). Rab conversion as a mechanism of progression from early to late endosomes. Cell *122*, 735-749.

Rishi, G., Wallace, D.F., and Subramaniam, V.N. (2015). Hepcidin: regulation of the master iron regulator. Bioscience reports *35*.

Rival, T., Page, R.M., Chandraratna, D.S., Sendall, T.J., Ryder, E., Liu, B., Lewis, H., Rosahl, T., Hider, R., Camargo, L.M., Shearman, M.S., Crowther, D.C., and Lomas, D.A. (2009). Fenton chemistry and oxidative stress mediate the toxicity of the beta-amyloid peptide in a Drosophila model of Alzheimer's disease. The European journal of neuroscience *29*, 1335-1347.

Robakis, N.K., Ramakrishna, N., Wolfe, G., and Wisniewski, H.M. (1987a). Molecular cloning and characterization of a cDNA encoding the cerebrovascular and the neuritic plaque amyloid peptides. Proceedings of the National Academy of Sciences of the United States of America *84*.

Robakis, N.K., Wisniewski, H.M., Jenkins, E.C., Devine-Gage, E.A., Houck, G.E., Yao, X.L., Ramakrishna, N., Wolfe, G., Silverman, W.P., and Brown, W.T. (1987b). Chromosome 21q21 sublocalisation of gene encoding beta-amyloid peptide in cerebral vessels and neuritic (senile) plaques of people with Alzheimer disease and Down syndrome. Lancet *1*, 384-385.

Roberts, S.B., Ripellino, J.A., Ingalls, K.M., Robakis, N.K., and Felsenstein, K.M. (1994). Non-amyloidogenic cleavage of the beta-amyloid precursor protein by an integral membrane metalloendopeptidase. The Journal of biological chemistry *269*, 3111-3116.

Rog, T., Pasenkiewicz-Gierula, M., Vattulainen, I., and Karttunen, M. (2009). Ordering effects of cholesterol and its analogues. Biochimica et biophysica acta *1788*, 97-121.

Rogers, J., Webster, S., Lue, L.-F., Brachova, L., Harold Civin, W., Emmerling, M., Shivers, B., Walker, D., and McGeer, P. (1996). Inflammation and Alzheimer's disease pathogenesis. Neurobiology of aging *17*, 681-686.

Rogers, J.T., Bush, A.I., Cho, H.H., Smith, D.H., Thomson, A.M., Friedlich, A.L., Lahiri, D.K., Leedman, P.J., Huang, X., and Cahill, C.M. (2008). Iron and the translation of the amyloid precursor protein (APP) and ferritin mRNAs: riboregulation against neural oxidative damage in Alzheimer's disease. Biochemical Society transactions *36*, 1282-1287.

Rogers, J.T., Randall, J.D., Cahill, C.M., Eder, P.S., Huang, X., Gunshin, H., Leiter, L., McPhee, J., Sarang, S.S., Utsuki, T., Greig, N.H., Lahiri, D.K., Tanzi, R.E., Bush, A.I., Giordano, T., and Gullans, S.R. (2002). An iron-responsive element type II in the 5'-untranslated region of the Alzheimer's amyloid precursor protein transcript. The Journal of biological chemistry *277*, 45518-45528.

Roiron-Lagroux, D., and Figarella, C. (1990). Evidence for a different mechanism of lactoferrin and transferrin translocation on HT 29-D4 cells, Vol 170.

Rosa, L., Cutone, A., Lepanto, M.S., Paesano, R., and Valenti, P. (2017). Lactoferrin: A Natural Glycoprotein Involved in Iron and Inflammatory Homeostasis. International journal of molecular sciences *18*.

Rosen, C., Hansson, O., Blennow, K., and Zetterberg, H. (2013). Fluid biomarkers in Alzheimer's disease - current concepts. Molecular neurodegeneration *8*, 20.

Rosen, D.R., Martin-Morris, L., Luo, L.Q., and White, K. (1989). A Drosophila gene encoding a protein resembling the human beta-amyloid protein precursor. Proceedings of the National Academy of Sciences of the United States of America *86*, 2478-2482.

Rosenthal, S.L., and Kamboh, M.I. (2014). Late-Onset Alzheimer's Disease Genes and the Potentially Implicated Pathways. Current genetic medicine reports *2*, 85-101.

Rossjohn, J., Cappai, R., Feil, S.C., Henry, A., McKinstry, W.J., Galatis, D., Hesse, L., Multhaup, G., Beyreuther, K., Masters, C.L., and Parker, M.W. (1999). Crystal structure of the N-terminal, growth factor-like domain of Alzheimer amyloid precursor protein. Nature structural biology *6*, 327-331.

Rossner, S., Apelt, J., Schliebs, R., Perez-Polo, J.R., and Bigl, V. (2001). Neuronal and glial beta-secretase (BACE) protein expression in transgenic Tg2576 mice with amyloid plaque pathology. Journal of neuroscience research *64*, 437-446.

Rossner, S., Lange-Dohna, C., Zeitschel, U., and Perez-Polo, J.R. (2005). Alzheimer's disease beta-secretase BACE1 is not a neuron-specific enzyme. Journal of neurochemistry *92*, 226-234.

Rottkamp, C.A., Raina, A.K., Zhu, X., Gaier, E., Bush, A.I., Atwood, C.S., Chevion, M., Perry, G., and Smith, M.A. (2001). Redox-active iron mediates amyloid-beta toxicity. Free radical biology & medicine *30*, 447-450.

Rouault, T.A., Zhang, D.L., and Jeong, S.Y. (2009). Brain iron homeostasis, the choroid plexus, and localization of iron transport proteins. Metabolic brain disease *24*, 673-684.

Rubio-Perez, J.M., and Morillas-Ruiz, J.M. (2012). A review: inflammatory process in Alzheimer's disease, role of cytokines. TheScientificWorldJournal *2012*, 756357.

Rushworth, J.V., Griffiths, H.H., Watt, N.T., and Hooper, N.M. (2013). Prion protein-mediated toxicity of amyloid-beta oligomers requires lipid rafts and the transmembrane LRP1. The Journal of biological chemistry *288*, 8935-8951.

Russo, C., Venezia, V., Repetto, E., Nizzari, M., Violani, E., Carlo, P., and Schettini, G. (2005). The amyloid precursor protein and its network of interacting proteins: physiological and pathological implications. Brain research Brain research reviews *48*, 257-264.

Ruvinsky, A.M., Kirys, T., Tuzikov, A.V., and Vakser, I.A. (2012). Structure fluctuations and conformational changes in protein binding. Journal of bioinformatics and computational biology *10*, 1241002.

Sabatucci, A., Vachette, P., Vasilyev, V.B., Beltramini, M., Sokolov, A., Pulina, M., Salvato, B., Angelucci, C.B., Maccarrone, M., Cozzani, I., and Dainese, E. (2007). Structural characterization of the ceruloplasmin: lactoferrin complex in solution. Journal of molecular biology *371*, 1038-1046.

Sabuncu, M.R., Desikan, R.S., Sepulcre, J., Yeo, B.T., Liu, H., Schmansky, N.J., Reuter, M., Weiner, M.W., Buckner, R.L., Sperling, R.A., and Fischl, B. (2011). The dynamics of cortical and hippocampal atrophy in Alzheimer disease. Archives of neurology *68*, 1040-1048.

Sagare, A., Deane, R., Bell, R.D., Johnson, B., Hamm, K., Pendu, R., Marky, A., Lenting, P.J., Wu, Z., Zarcone, T., Goate, A., Mayo, K., Perlmutter, D., Coma, M., Zhong, Z., and Zlokovic, B.V. (2007). Clearance of amyloid-beta by circulating lipoprotein receptors. Nature medicine *13*, 1029-1031.

Sagare, A.P., Deane, R., Zetterberg, H., Wallin, A., Blennow, K., and Zlokovic, B.V. (2011). Impaired lipoprotein receptor-mediated peripheral binding of plasma

amyloid-beta is an early biomarker for mild cognitive impairment preceding Alzheimer's disease. Journal of Alzheimer's disease : JAD *24*, 25-34.

Saido, T., and Leissring, M.A. (2012). Proteolytic degradation of amyloid beta-protein. Cold Spring Harbor perspectives in medicine *2*, a006379.

Saito, T., Matsuba, Y., Mihira, N., Takano, J., Nilsson, P., Itohara, S., Iwata, N., and Saido, T.C. (2014). Single App knock-in mouse models of Alzheimer's disease. Nature neuroscience *17*, 661-663.

Sakamoto, K., Ito, Y., Mori, T., and Sugimura, K. (2006). Interaction of human lactoferrin with cell adhesion molecules through RGD motif elucidated by lactoferrin-binding epitopes. The Journal of biological chemistry *281*, 24472-24478.

Salazar, J., Mena, N., Hunot, S., Prigent, A., Alvarez-Fischer, D., Arredondo, M., Duyckaerts, C., Sazdovitch, V., Zhao, L., Garrick, L.M., Nuñez, M.T., Garrick, M.D., Raisman-Vozari, R., and Hirsch, E.C. (2008). Divalent metal transporter 1 (DMT1) contributes to neurodegeneration in animal models of Parkinson's disease. Proceedings of the National Academy of Sciences *105*, 18578-18583.

Sanchez Campos, S., Rodriguez Diez, G., Oresti, G.M., and Salvador, G.A. (2015). Dopaminergic Neurons Respond to Iron-Induced Oxidative Stress by Modulating Lipid Acylation and Deacylation Cycles. PloS one *10*, e0130726.

Sanchez, L., Calvo, M., and Brock, J.H. (1992). Biological role of lactoferrin. Archives of disease in childhood *67*, 657-661.

Sandbrink, R., Masters, C.L., and Beyreuther, K. (1994). Similar alternative splicing of a non-homologous domain in beta A4-amyloid protein precursor-like proteins. The Journal of biological chemistry *269*, 14227-14234.

Sangkhae, V., and Nemeth, E. (2017). Regulation of the Iron Homeostatic Hormone Hepcidin. Adv Nutr *8*, 126-136.

Sannerud, R., Declerck, I., Peric, A., Raemaekers, T., Menendez, G., Zhou, L., Veerle, B., Coen, K., Munck, S., De Strooper, B., Schiavo, G., and Annaert, W. (2011). ADP ribosylation factor 6 (ARF6) controls amyloid precursor protein (APP) processing by mediating the endosomal sorting of BACE1. Proceedings of the National Academy of Sciences of the United States of America *108*, E559-568.

Sarlus, H., and Heneka, M.T. (2017). Microglia in Alzheimer’s disease. The Journal of clinical investigation *127*, 3240-3249.

Sasaguri, H., Nilsson, P., Hashimoto, S., Nagata, K., Saito, T., De Strooper, B., Hardy, J., Vassar, R., Winblad, B., and Saido, T.C. (2017). APP mouse models for Alzheimer's disease preclinical studies. The EMBO journal *36*, 2473-2487.

Scheinfeld, M.H., Ghersi, E., Laky, K., Fowlkes, B.J., and D'Adamio, L. (2002). Processing of beta-amyloid precursor-like protein-1 and -2 by gamma-secretase regulates transcription. The Journal of biological chemistry *277*, 44195-44201.

Schetters, S.T.T., Gomez-Nicola, D., Garcia-Vallejo, J.J., and Van Kooyk, Y. (2017). Neuroinflammation: Microglia and T Cells Get Ready to Tango. Frontiers in immunology *8*, 1905.

Schmid, S.L. (1997). Clathrin-coated vesicle formation and protein sorting: an integrated process. Annual review of biochemistry *66*, 511-548.

Schmidt, A.M., Mora, R., Cao, R., Yan, S.D., Brett, J., Ramakrishnan, R., Tsang, T.C., Simionescu, M., and Stern, D. (1994). The endothelial cell binding site for advanced glycation end products consists of a complex: an integral membrane protein and a lactoferrin-like polypeptide. The Journal of biological chemistry *269*, 9882-9888.

Schneider, A., Rajendran, L., Honsho, M., Gralle, M., Donnert, G., Wouters, F., Hell, S.W., and Simons, M. (2008). Flotillin-dependent clustering of the amyloid precursor protein regulates its endocytosis and amyloidogenic processing in neurons. The Journal of neuroscience : the official journal of the Society for Neuroscience *28*, 2874-2882.

Schobel, S., Neumann, S., Hertweck, M., Dislich, B., Kuhn, P.H., Kremmer, E., Seed, B., Baumeister, R., Haass, C., and Lichtenthaler, S.F. (2008). A novel sorting nexin modulates endocytic trafficking and alpha-secretase cleavage of the amyloid precursor protein. The Journal of biological chemistry *283*, 14257-14268.

Schonteich, E., Pilli, M., Simon, G.C., Matern, H.T., Junutula, J.R., Sentz, D., Holmes, R.K., and Prekeris, R. (2007). Molecular characterization of Rab11-FIP3 binding to ARF GTPases. European journal of cell biology *86*, 417-431.

Schrader-Fischer, G., and Paganetti, P.A. (1996). Effect of alkalizing agents on the processing of the beta-amyloid precursor protein. Brain research *716*, 91-100.

Schryvers, A.B., Bonnah, R., Yu, R.H., Wong, H., and Retzer, M. (1998). Bacterial lactoferrin receptors. Advances in experimental medicine and biology *443*, 123-133.

Schuck, P. (2000). Size-Distribution Analysis of Macromolecules by Sedimentation Velocity Ultracentrifugation and Lamm Equation Modeling. Biophysical journal *78*, 1606-1619.

Seabra, M.C., Mules, E.H., and Hume, A.N. (2002). Rab GTPases, intracellular traffic and disease. Trends in molecular medicine *8*, 23-30.

Seabrook, G.R., Smith, D.W., Bowery, B.J., Easter, A., Reynolds, T., Fitzjohn, S.M., Morton, R.A., Zheng, H., Dawson, G.R., Sirinathsinghji, D.J., Davies, C.H., Collingridge, G.L., and Hill, R.G. (1999). Mechanisms contributing to the deficits in hippocampal synaptic plasticity in mice lacking amyloid precursor protein. Neuropharmacology *38*, 349-359.

Selvais, C., D'Auria, L., Tyteca, D., Perrot, G., Lemoine, P., Troeberg, L., Dedieu, S., Noel, A., Nagase, H., Henriet, P., Courtoy, P.J., Marbaix, E., and Emonard, H. (2011). Cell cholesterol modulates metalloproteinase-dependent shedding of

low-density lipoprotein receptor-related protein-1 (LRP-1) and clearance function. FASEB journal : official publication of the Federation of American Societies for Experimental Biology *25*, 2770-2781.

Serrano-Pozo, A., Frosch, M.P., Masliah, E., and Hyman, B.T. (2011a). Neuropathological alterations in Alzheimer disease. Cold Spring Harbor perspectives in medicine *1*, a006189.

Serrano-Pozo, A., Mielke, M.L., Gomez-Isla, T., Betensky, R.A., Growdon, J.H., Frosch, M.P., and Hyman, B.T. (2011b). Reactive glia not only associates with plaques but also parallels tangles in Alzheimer's disease. The American journal of pathology *179*, 1373-1384.

Seshadri, S., Fitzpatrick, A.L., Ikram, M.A., DeStefano, A.L., Gudnason, V., Boada, M., Bis, J.C., Smith, A.V., Carassquillo, M.M., Lambert, J.C., Harold, D., Schrijvers, E.M., Ramirez-Lorca, R., Debette, S., Longstreth, W.T., Jr., Janssens, A.C., Pankratz, V.S., Dartigues, J.F., Hollingworth, P., Aspelund, T., Hernandez, I., Beiser, A., Kuller, L.H., Koudstaal, P.J., Dickson, D.W., Tzourio, C., Abraham, R., Antunez, C., Du, Y., Rotter, J.I., Aulchenko, Y.S., Harris, T.B., Petersen, R.C., Berr, C., Owen, M.J., Lopez-Arrieta, J., Varadarajan, B.N., Becker, J.T., Rivadeneira, F., Nalls, M.A., Graff-Radford, N.R., Campion, D., Auerbach, S., Rice, K., Hofman, A., Jonsson, P.V., Schmidt, H., Lathrop, M., Mosley, T.H., Au, R., Psaty, B.M., Uitterlinden, A.G., Farrer, L.A., Lumley, T., Ruiz, A., Williams, J., Amouyel, P., Younkin, S.G., Wolf, P.A., Launer, L.J., Lopez, O.L., van Duijn, C.M., and Breteler, M.M. (2010). Genome-wide analysis of genetic loci associated with Alzheimer disease. Jama *303*, 1832-1840.

Seubert, P., Oltersdorf, T., Lee, M.G., Barbour, R., Blomquist, C., Davis, D.L., Bryant, K., Fritz, L.C., Galasko, D., Thal, L.J., and et al. (1993). Secretion of beta-amyloid precursor protein cleaved at the amino terminus of the beta-amyloid peptide. Nature *361*, 260-263.

Shahani, N., Seshadri, S., Jaaro-Peled, H., Ishizuka, K., Hirota-Tsuyada, Y., Wang, Q., Koga, M., Sedlak, T.W., Korth, C., Brandon, N.J., Kamiya, A., Subramaniam, S., Tomoda, T., and Sawa, A. (2015). DISC1 regulates trafficking and processing of APP and Abeta generation. Molecular psychiatry *20*, 874-879.

Shankar, G.M., and Walsh, D.M. (2009). Alzheimer's disease: synaptic dysfunction and Abeta. Molecular neurodegeneration *4*, 48.

Sharpe, M.A., Robb, S.J., and Clark, J.B. (2003). Nitric oxide and Fenton/Haber-Weiss chemistry: nitric oxide is a potent antioxidant at physiological concentrations. Journal of neurochemistry *87*, 386-394.

Shaw, L.M., Vanderstichele, H., Knapik-Czajka, M., Clark, C.M., Aisen, P.S., Petersen, R.C., Blennow, K., Soares, H., Simon, A., Lewczuk, P., Dean, R., Siemers, E., Potter, W., Lee, V.M., and Trojanowski, J.Q. (2009). Cerebrospinal fluid biomarker signature in Alzheimer's disease neuroimaging initiative subjects. Annals of neurology *65*, 403-413.

Sheff, D.R., Daro, E.A., Hull, M., and Mellman, I. (1999). The receptor recycling pathway contains two distinct populations of early endosomes with different sorting functions. The Journal of cell biology *145*, 123-139.

Sheng, J.G., Bora, S.H., Xu, G., Borchelt, D.R., Price, D.L., and Koliatsos, V.E. (2003). Lipopolysaccharide-induced-neuroinflammation increases intracellular accumulation of amyloid precursor protein and amyloid beta peptide in APPswe transgenic mice. Neurobiology of disease *14*, 133-145.

Shi, Y., Mantuano, E., Inoue, G., Campana, W.M., and Gonias, S.L. (2009). Ligand binding to LRP1 transactivates Trk receptors by a Src family kinase-dependent pathway. Science signaling *2*, ra18.

Shibata, M., Yamada, S., Kumar, S.R., Calero, M., Bading, J., Frangione, B., Holtzman, D.M., Miller, C.A., Strickland, D.K., Ghiso, J., and Zlokovic, B.V. (2000). Clearance of Alzheimer's amyloid-ss(1-40) peptide from brain by LDL receptor-related protein-1 at the blood-brain barrier. The Journal of clinical investigation *106*, 1489-1499.

Shin, R.W., Lee, V.M., and Trojanowski, J.Q. (1994). Aluminum modifies the properties of Alzheimer's disease PHF tau proteins in vivo and in vitro. The Journal of neuroscience : the official journal of the Society for Neuroscience *14*, 7221-7233.

Shinohara, M., Tachibana, M., Kanekiyo, T., and Bu, G. (2017). Role of LRP1 in the pathogenesis of Alzheimer's disease: evidence from clinical and preclinical studies. Journal of lipid research *58*, 1267-1281.

Siebert, P.D., and Huang, B.C. (1997). Identification of an alternative form of human lactoferrin mRNA that is expressed differentially in normal tissues and tumor-derived cell lines. Proceedings of the National Academy of Sciences of the United States of America *94*, 2198-2203.

Simic, G., Babic Leko, M., Wray, S., Harrington, C., Delalle, I., Jovanov-Milosevic, N., Bazadona, D., Buee, L., de Silva, R., Di Giovanni, G., Wischik, C., and Hof, P.R. (2016). Tau Protein Hyperphosphorylation and Aggregation in Alzheimer's Disease and Other Tauopathies, and Possible Neuroprotective Strategies. Biomolecules *6*, 6.

Simon, E., Obst, J., and Gomez-Nicola, D. (2018). The Evolving Dialogue of Microglia and Neurons in Alzheimer's Disease: Microglia as Necessary Transducers of Pathology. Neuroscience.

Simons, K., and Gerl, M.J. (2010). Revitalizing membrane rafts: new tools and insights. Nature reviews Molecular cell biology *11*, 688-699.

Simons, M., de Strooper, B., Multhaup, G., Tienari, P.J., Dotti, C.G., and Beyreuther, K. (1996). Amyloidogenic processing of the human amyloid precursor protein in primary cultures of rat hippocampal neurons. The Journal of neuroscience : the official journal of the Society for Neuroscience *16*, 899-908.

Simons, M., Keller, P., De Strooper, B., Beyreuther, K., Dotti, C.G., and Simons, K. (1998). Cholesterol depletion inhibits the generation of beta-amyloid in hippocampal neurons. Proceedings of the National Academy of Sciences of the United States of America *95*, 6460-6464.

Simons, M., Tienari, P.J., Dotti, C.G., and Beyreuther, K. (1995). Two-dimensional gel mapping of the processing of the human amyloid precursor protein in rat hippocampal neurons. FEBS letters *368*, 363-366.

Sinha, M., Kaushik, S., Kaur, P., Sharma, S., and Singh, T.P. (2013). Antimicrobial lactoferrin peptides: the hidden players in the protective function of a multifunctional protein. International journal of peptides *2013*, 390230.

Sinha, S., Dovey, H.F., Seubert, P., Ward, P.J., Blacher, R.W., Blaber, M., Bradshaw, R.A., Arici, M., Mobley, W.C., and Lieberburg, I. (1990). The protease inhibitory properties of the Alzheimer's beta-amyloid precursor protein. The Journal of biological chemistry *265*, 8983-8985.

Sisodia, S.S., Koo, E.H., Beyreuther, K., Unterbeck, A., and Price, D.L. (1990). Evidence that beta-amyloid protein in Alzheimer's disease is not derived by normal processing. Science *248*, 492-495.

Skovronsky, D.M., Moore, D.B., Milla, M.E., Doms, R.W., and Lee, V.M. (2000). Protein kinase C-dependent alpha-secretase competes with beta-secretase for cleavage of amyloid-beta precursor protein in the trans-golgi network. The Journal of biological chemistry *275*, 2568-2575.

Slunt, H.H., Thinakaran, G., Von Koch, C., Lo, A.C., Tanzi, R.E., and Sisodia, S.S. (1994). Expression of a ubiquitous, cross-reactive homologue of the mouse beta-amyloid precursor protein (APP). The Journal of biological chemistry *269*, 2637-2644.

Smith, M.A., Harris, P.L., Sayre, L.M., and Perry, G. (1997). Iron accumulation in Alzheimer disease is a source of redox-generated free radicals. Proceedings of the National Academy of Sciences of the United States of America *94*, 9866-9868.

Smith, R.P., Higuchi, D.A., and Broze, G.J., Jr. (1990). Platelet coagulation factor XIa-inhibitor, a form of Alzheimer amyloid precursor protein. Science *248*, 1126-1128.

Soba, P., Eggert, S., Wagner, K., Zentgraf, H., Siehl, K., Kreger, S., Lower, A., Langer, A., Merdes, G., Paro, R., Masters, C.L., Muller, U., Kins, S., and Beyreuther, K. (2005). Homo- and heterodimerization of APP family members promotes intercellular adhesion. The EMBO journal *24*, 3624-3634.

Sokolov, A.V., Pulina, M.O., Zakharova, E.T., Shavlovski, M.M., and Vasilyev, V.B. (2005). Effect of lactoferrin on the ferroxidase activity of ceruloplasmin. Biochemistry Biokhimiia *70*, 1015-1019.

Sokolov, A.V., Pulina, M.O., Zakharova, E.T., Susorova, A.S., Runova, O.L., Kolodkin, N.I., and Vasilyev, V.B. (2006). Identification and isolation from breast milk of ceruloplasmin-lactoferrin complex. Biochemistry Biokhimiia *71*, 160-166.

Somsel Rodman, J., and Wandinger-Ness, A. (2000). Rab GTPases coordinate endocytosis. Journal of cell science *113 Pt 2*, 183-192.

Song, N., Wang, J., Jiang, H., and Xie, J. (2010). Ferroportin 1 but not hephaestin contributes to iron accumulation in a cell model of Parkinson's disease. Free radical biology & medicine *48*, 332-341.

Sonnichsen, B., De Renzis, S., Nielsen, E., Rietdorf, J., and Zerial, M. (2000). Distinct membrane domains on endosomes in the recycling pathway visualized by multicolor imaging of Rab4, Rab5, and Rab11. The Journal of cell biology *149*, 901-914.

Soscia, S.J., Kirby, J.E., Washicosky, K.J., Tucker, S.M., Ingelsson, M., Hyman, B., Burton, M.A., Goldstein, L.E., Duong, S., Tanzi, R.E., and Moir, R.D. (2010). The Alzheimer's disease-associated amyloid beta-protein is an antimicrobial peptide. PloS one *5*, e9505.

Spitzer, P., Condic, M., Herrmann, M., Oberstein, T.J., Scharin-Mehlmann, M., Gilbert, D.F., Friedrich, O., Gromer, T., Kornhuber, J., Lang, R., and Maler, J.M. (2016). Amyloidogenic amyloid-beta-peptide variants induce microbial agglutination and exert antimicrobial activity. Scientific reports *6*, 32228.

Spoelgen, R., von Arnim, C.A., Thomas, A.V., Peltan, I.D., Koker, M., Deng, A., Irizarry, M.C., Andersen, O.M., Willnow, T.E., and Hyman, B.T. (2006). Interaction of the cytosolic domains of sorLA/LR11 with the amyloid precursor protein (APP) and beta-secretase beta-site APP-cleaving enzyme. The Journal of neuroscience : the official journal of the Society for Neuroscience *26*, 418-428.

Spooren, A., Kolmus, K., Laureys, G., Clinckers, R., De Keyser, J., Haegeman, G., and Gerlo, S. (2011). Interleukin-6, a mental cytokine. Brain research reviews *67*, 157-183.

Spuch, C., Ortolano, S., and Navarro, C. (2012). LRP-1 and LRP-2 receptors function in the membrane neuron. Trafficking mechanisms and proteolytic processing in Alzheimer's disease. Frontiers in Physiology *3*.

Sriram, V., Krishnan, K.S., and Mayor, S. (2003). deep-orange and carnation define distinct stages in late endosomal biogenesis in Drosophila melanogaster. The Journal of cell biology *161*, 593-607.

Sriram, V., Krishnan, K.S., and Mayor, S. (2006). Biogenesis and Function of Late Endosomes and Lysosomes, Vol 72.

Stahl, R., Schilling, S., Soba, P., Rupp, C., Hartmann, T., Wagner, K., Merdes, G., Eggert, S., and Kins, S. (2014). Shedding of APP limits its synaptogenic activity and cell adhesion properties. Frontiers in cellular neuroscience *8*, 410.

Stenmark, H., and Olkkonen, V.M. (2001). The Rab GTPase family. Genome biology *2*, REVIEWS3007.

Stiles, T.L., Dickendesher, T.L., Gaultier, A., Fernandez-Castaneda, A., Mantuano, E., Giger, R.J., and Gonias, S.L. (2013). LDL receptor-related protein-1 is a sialic-acid-independent receptor for myelin-associated glycoprotein that functions in neurite outgrowth inhibition by MAG and CNS myelin. Journal of cell science *126*, 209-220.

Stockwell, B.R., Friedmann Angeli, J.P., Bayir, H., Bush, A.I., Conrad, M., Dixon, S.J., Fulda, S., Gascon, S., Hatzios, S.K., Kagan, V.E., Noel, K., Jiang, X., Linkermann, A., Murphy, M.E., Overholtzer, M., Oyagi, A., Pagnussat, G.C., Park, J., Ran, Q., Rosenfeld, C.S., Salnikow, K., Tang, D., Torti, F.M., Torti, S.V., Toyokuni, S., Woerpel, K.A., and Zhang, D.D. (2017). Ferroptosis: A Regulated Cell Death Nexus Linking Metabolism, Redox Biology, and Disease. Cell *171*, 273-285.

Stoorvogel, W., Strous, G.J., Geuze, H.J., Oorschot, V., and Schwartz, A.L. (1991). Late endosomes derive from early endosomes by maturation. Cell *65*, 417-427.

Storck, S.E., Meister, S., Nahrath, J., Meissner, J.N., Schubert, N., Di Spiezio, A., Baches, S., Vandenbroucke, R.E., Bouter, Y., Prikulis, I., Korth, C., Weggen, S., Heimann, A., Schwaninger, M., Bayer, T.A., and Pietrzik, C.U. (2016). Endothelial LRP1 transports amyloid-beta(1-42) across the blood-brain barrier. The Journal of clinical investigation *126*, 123-136.

Storey, E., Beyreuther, K., and Masters, C.L. (1996). Alzheimer's disease amyloid precursor protein on the surface of cortical neurons in primary culture co-localizes with adhesion patch components. Brain research *735*, 217-231.

Storrie, B., and Desjardins, M. (1996). The biogenesis of lysosomes: is it a kiss and run, continuous fusion and fission process? BioEssays : news and reviews in molecular, cellular and developmental biology *18*, 895-903.

Strickland, D.K., Gonias, S.L., and Argraves, W.S. (2002). Diverse roles for the LDL receptor family. Trends in endocrinology and metabolism: TEM *13*, 66-74.

Strittmatter, W.J., Saunders, A.M., Schmechel, D., Pericak-Vance, M., Enghild, J., Salvesen, G.S., and Roses, A.D. (1993). Apolipoprotein E: high-avidity binding to beta-amyloid and increased frequency of type 4 allele in late-onset familial Alzheimer disease. Proceedings of the National Academy of Sciences of the United States of America *90*, 1977-1981.

Struble, R.G., Ala, T., Patrylo, P.R., Brewer, G.J., and Yan, X.X. (2010). Is brain amyloid production a cause or a result of dementia of the Alzheimer's type? Journal of Alzheimer's disease : JAD *22*, 393-399.

Sun, C., Song, N., Xie, A., Xie, J., and Jiang, H. (2012). High hepcidin level accounts for the nigral iron accumulation in acute peripheral iron intoxication rats. Toxicology letters *212*, 276-281.

Sun, P., Yamamoto, H., Suetsugu, S., Miki, H., Takenawa, T., and Endo, T. (2003). Small GTPase Rah/Rab34 is associated with membrane ruffles and macropinosomes and promotes macropinosome formation. The Journal of biological chemistry *278*, 4063-4071.

Suzuki, T., Ando, K., Isohara, T., Oishi, M., Lim, G.S., Satoh, Y., Wasco, W., Tanzi, R.E., Nairn, A.C., Greengard, P., Gandy, S.E., and Kirino, Y. (1997). Phosphorylation of Alzheimer beta-amyloid precursor-like proteins. Biochemistry *36*, 4643-4649.

Suzuki, Y.A., and Lonnerdal, B. (2002). Characterization of mammalian receptors for lactoferrin. Biochemistry and cell biology = Biochimie et biologie cellulaire *80*, 75-80.

Suzuki, Y.A., Lopez, V., and Lonnerdal, B. (2005). Mammalian lactoferrin receptors: structure and function. Cellular and molecular life sciences : CMLS *62*, 2560-2575.

Szczepanik, A.M., Funes, S., Petko, W., and Ringheim, G.E. (2001). IL-4, IL-10 and IL-13 modulate A beta(1--42)-induced cytokine and chemokine production in primary murine microglia and a human monocyte cell line. Journal of neuroimmunology *113*, 49-62.

Szodorai, A., Kuan, Y.H., Hunzelmann, S., Engel, U., Sakane, A., Sasaki, T., Takai, Y., Kirsch, J., Muller, U., Beyreuther, K., Brady, S., Morfini, G., and Kins, S. (2009). APP anterograde transport requires Rab3A GTPase activity for assembly of the transport vesicle. The Journal of neuroscience : the official journal of the Society for Neuroscience *29*, 14534-14544.

T. A. MacGillivray, R., Moore, S., Chen, J., F. Anderson, B., Baker, H., Luo, Y., Bewley, M., Smith, C., Murphy, M., Wang, Y., Mason, A., Woodworth, R., D. Brayer, G., and Baker, E. (1998). Two High-Resolution Crystal Structures of the Recombinant N-Lobe of Human Transferrin Reveal a Structural Change Implicated in Iron Release † , ‡, Vol 37.

Takahashi, S., Kubo, K., Waguri, S., Yabashi, A., Shin, H.W., Katoh, Y., and Nakayama, K. (2012). Rab11 regulates exocytosis of recycling vesicles at the plasma membrane. Journal of cell science *125*, 4049-4057.

Takahashi, S., Takei, T., Koga, H., Takatsu, H., Shin, H.W., and Nakayama, K. (2011). Distinct roles of Rab11 and Arf6 in the regulation of Rab11-FIP3/arfophilin-1 localization in mitotic cells. Genes to cells : devoted to molecular & cellular mechanisms *16*, 938-950.

Takai, Y., Sasaki, T., and Matozaki, T. (2001). Small GTP-binding proteins. Physiological reviews *81*, 153-208.

Takami, M., Nagashima, Y., Sano, Y., Ishihara, S., Morishima-Kawashima, M., Funamoto, S., and Ihara, Y. (2009). gamma-Secretase: successive tripeptide and tetrapeptide release from the transmembrane domain of beta-carboxyl terminal fragment. The Journal of neuroscience : the official journal of the Society for Neuroscience *29*, 13042-13052.

Tampellini, D. (2015). Synaptic activity and Alzheimer's disease: a critical update. Frontiers in neuroscience *9*, 423.

Tang, B.L., and Liou, Y.C. (2007). Novel modulators of amyloid-beta precursor protein processing. Journal of neurochemistry *100*, 314-323.

Tang, W., Tam, J.H., Seah, C., Chiu, J., Tyrer, A., Cregan, S.P., Meakin, S.O., and Pasternak, S.H. (2015). Arf6 controls beta-amyloid production by regulating macropinocytosis of the Amyloid Precursor Protein to lysosomes. Molecular brain *8*, 41.

Tang, Y., and Le, W. (2016). Differential Roles of M1 and M2 Microglia in Neurodegenerative Diseases. Molecular neurobiology *53*, 1181-1194.

Tansley, G.H., Burgess, B.L., Bryan, M.T., Su, Y., Hirsch-Reinshagen, V., Pearce, J., Chan, J.Y., Wilkinson, A., Evans, J., Naus, K.E., McIsaac, S., Bromley, K., Song, W., Yang, H.C., Wang, N., DeMattos, R.B., and Wellington, C.L. (2007). The cholesterol transporter ABCG1 modulates the subcellular distribution and proteolytic processing of beta-amyloid precursor protein. Journal of lipid research *48*, 1022-1034.

Tanzi, R.E. (2015). TREM2 and Risk of Alzheimer's Disease--Friend or Foe? The New England journal of medicine *372*, 2564-2565.

Tanzi, R.E., and Bertram, L. (2005). Twenty years of the Alzheimer's disease amyloid hypothesis: a genetic perspective. Cell *120*, 545-555.

Tarawneh, R., and Holtzman, D.M. (2012). The clinical problem of symptomatic Alzheimer disease and mild cognitive impairment. Cold Spring Harbor perspectives in medicine *2*, a006148.

Taylor, C.J., Ireland, D.R., Ballagh, I., Bourne, K., Marechal, N.M., Turner, P.R., Bilkey, D.K., Tate, W.P., and Abraham, W.C. (2008). Endogenous secreted amyloid precursor protein-alpha regulates hippocampal NMDA receptor function, long-term potentiation and spatial memory. Neurobiology of disease *31*, 250-260.

Taylor, D.R., and Hooper, N.M. (2007). Role of lipid rafts in the processing of the pathogenic prion and Alzheimer's amyloid-beta proteins. Seminars in cell & developmental biology *18*, 638-648.

Teich, A.F., Patel, M., and Arancio, O. (2013). A reliable way to detect endogenous murine beta-amyloid. PloS one *8*, e55647.

Thal, D.R., Capetillo-Zarate, E., Del Tredici, K., and Braak, H. (2006). The development of amyloid beta protein deposits in the aged brain. Science of aging knowledge environment : SAGE KE *2006*, re1.

Thinakaran, G., Borchelt, D.R., Lee, M.K., Slunt, H.H., Spitzer, L., Kim, G., Ratovitsky, T., Davenport, F., Nordstedt, C., Seeger, M., Hardy, J., Levey, A.I., Gandy, S.E., Jenkins, N.A., Copeland, N.G., Price, D.L., and Sisodia, S.S.

(1996a). Endoproteolysis of presenilin 1 and accumulation of processed derivatives in vivo. Neuron *17*.

Thinakaran, G., and Koo, E.H. (2008). Amyloid precursor protein trafficking, processing, and function. The Journal of biological chemistry *283*, 29615-29619.

Thinakaran, G., Teplow, D.B., Siman, R., Greenberg, B., and Sisodia, S.S. (1996b). Metabolism of the "Swedish" amyloid precursor protein variant in neuro2a (N2a) cells. Evidence that cleavage at the "beta-secretase" site occurs in the golgi apparatus. The Journal of biological chemistry *271*, 9390-9397.

Tienari, P.J., De Strooper, B., Ikonen, E., Simons, M., Weidemann, A., Czech, C., Hartmann, T., Ida, N., Multhaup, G., Masters, C.L., Van Leuven, F., Beyreuther, K., and Dotti, C.G. (1996). The beta-amyloid domain is essential for axonal sorting of amyloid precursor protein. The EMBO journal *15*, 5218-5229.

Toledo, J.B., Xie, S.X., Trojanowski, J.Q., and Shaw, L.M. (2013). Longitudinal change in CSF Tau and Abeta biomarkers for up to 48 months in ADNI. Acta neuropathologica *126*, 659-670.

Tomaselli, S., Esposito, V., Vangone, P., van Nuland, N.A., Bonvin, A.M., Guerrini, R., Tancredi, T., Temussi, P.A., and Picone, D. (2006). The alpha-to-beta conformational transition of Alzheimer's Abeta-(1-42) peptide in aqueous media is reversible: a step by step conformational analysis suggests the location of beta conformation seeding. Chembiochem : a European journal of chemical biology *7*, 257-267.

Tomita, S., Kirino, Y., and Suzuki, T. (1998). Cleavage of Alzheimer's amyloid precursor protein (APP) by secretases occurs after O-glycosylation of APP in the protein secretory pathway. Identification of intracellular compartments in which APP cleavage occurs without using toxic agents that interfere with protein metabolism. The Journal of biological chemistry *273*, 6277-6284.

Tomita, T., Maruyama, K., Saido, T.C., Kume, H., Shinozaki, K., Tokuhiro, S., Capell, A., Walter, J., Grunberg, J., Haass, C., Iwatsubo, T., and Obata, K. (1997). The presenilin 2 mutation (N141I) linked to familial Alzheimer disease (Volga German families) increases the secretion of amyloid beta protein ending at the 42nd (or 43rd) residue. Proceedings of the National Academy of Sciences of the United States of America *94*, 2025-2030.

Tooyama, I., Kimura, H., Akiyama, H., and McGeer, P.L. (1990). Reactive microglia express class I and class II major histocompatibility complex antigens in Alzheimer's disease. Brain research *523*, 273-280.

Trischler, M., Stoorvogel, W., and Ullrich, O. (1999). Biochemical analysis of distinct Rab5- and Rab11-positive endosomes along the transferrin pathway. Journal of cell science *112 (Pt 24)*, 4773-4783.

Trojanowski, J.Q., and Lee, V.M. (2000). "Fatal attractions" of proteins. A comprehensive hypothetical mechanism underlying Alzheimer's disease and other neurodegenerative disorders. Annals of the New York Academy of Sciences *924*, 62-67.

Tuccari, G., Villari, D., Giuffre, G., Simone, A., Squadrito, G., Raimondo, G., and Barresi, G. (2002). Immunohistochemical evidence of lactoferrin in hepatic biopsies of patients with viral or cryptogenetic chronic liver disease. Histology and histopathology *17*, 1077-1083.

Udayar, V., Buggia-Prevot, V., Guerreiro, R.L., Siegel, G., Rambabu, N., Soohoo, A.L., Ponnusamy, M., Siegenthaler, B., Bali, J., Simons, M., Ries, J., Puthenveedu, M.A., Hardy, J., Thinakaran, G., and Rajendran, L. (2013). A paired RNAi and RabGAP overexpression screen identifies Rab11 as a regulator of beta-amyloid production. Cell reports *5*, 1536-1551.

Ullrich, O., Horiuchi, H., Bucci, C., and Zerial, M. (1994). Membrane association of Rab5 mediated by GDP-dissociation inhibitor and accompanied by GDP/GTP exchange. Nature *368*, 157-160.

Ullrich, O., Reinsch, S., Urbe, S., Zerial, M., and Parton, R.G. (1996). Rab11 regulates recycling through the pericentriolar recycling endosome. The Journal of cell biology *135*, 913-924.

Umeda, T., Maekawa, S., Kimura, T., Takashima, A., Tomiyama, T., and Mori, H. (2014). Neurofibrillary tangle formation by introducing wild-type human tau into APP transgenic mice. Acta neuropathologica *127*, 685-698.

Urbe, S., Huber, L.A., Zerial, M., Tooze, S.A., and Parton, R.G. (1993). Rab11, a small GTPase associated with both constitutive and regulated secretory pathways in PC12 cells. FEBS letters *334*, 175-182.

Urrutia, P., Aguirre, P., Esparza, A., Tapia, V., Mena, N.P., Arredondo, M., Gonzalez-Billault, C., and Nunez, M.T. (2013). Inflammation alters the expression of DMT1, FPN1 and hepcidin, and it causes iron accumulation in central nervous system cells. Journal of neurochemistry *126*, 541-549.

Valenti, P., and Antonini, G. (2005). Lactoferrin: an important host defence against microbial and viral attack. Cellular and molecular life sciences : CMLS *62*, 2576-2587.

Vallabhapurapu, S., and Karin, M. (2009). Regulation and function of NF-kappaB transcription factors in the immune system. Annual review of immunology *27*, 693-733.

van Berkel, P.H., Geerts, M.E., van Veen, H.A., Kooiman, P.M., Pieper, F.R., de Boer, H.A., and Nuijens, J.H. (1995). Glycosylated and unglycosylated human lactoferrins both bind iron and show identical affinities towards human lysozyme and bacterial lipopolysaccharide, but differ in their susceptibilities towards tryptic proteolysis. The Biochemical journal *312 (Pt 1)*, 107-114.

van der Kant, R., and Goldstein, L.S. (2015). Cellular functions of the amyloid precursor protein from development to dementia. Dev Cell *32*, 502-515.

van der Sluijs, P., Hull, M., Webster, P., Male, P., Goud, B., and Mellman, I. (1992). The small GTP-binding protein rab4 controls an early sorting event on the endocytic pathway. Cell *70*, 729-740.

Van Nostrand, W.E., Schmaier, A.H., Farrow, J.S., and Cunningham, D.D. (1990). Protease nexin-II (amyloid beta-protein precursor): a platelet alpha-granule protein. Science *248*, 745-748.

Vanlandingham, P.A., and Ceresa, B.P. (2009). Rab7 regulates late endocytic trafficking downstream of multivesicular body biogenesis and cargo sequestration. The Journal of biological chemistry *284*, 12110-12124.

Vardy, E.R., Catto, A.J., and Hooper, N.M. (2005). Proteolytic mechanisms in amyloid-beta metabolism: therapeutic implications for Alzheimer's disease. Trends in molecular medicine *11*, 464-472.

Vash, B., Phung, N., Zein, S., and DeCamp, D. (1998). Three complement-type repeats of the low-density lipoprotein receptor-related protein define a common binding site for RAP, PAI-1, and lactoferrin. Blood *92*, 3277-3285.

Vassar, R. (2013). ADAM10 prodomain mutations cause late-onset Alzheimer's disease: not just the latest FAD. Neuron *80*, 250-253.

Vassar, R., Bennett, B.D., Babu-Khan, S., Kahn, S., Mendiaz, E.A., Denis, P., Teplow, D.B., Ross, S., Amarante, P., Loeloff, R., Luo, Y., Fisher, S., Fuller, J., Edenson, S., Lile, J., Jarosinski, M.A., Biere, A.L., Curran, E., Burgess, T., Louis, J.C., Collins, F., Treanor, J., Rogers, G., and Citron, M. (1999). Beta-secretase cleavage of Alzheimer's amyloid precursor protein by the transmembrane aspartic protease BACE. Science *286*.

Vela, D. (2018). The Dual Role of Hepcidin in Brain Iron Load and Inflammation. Frontiers in neuroscience *12*.

Velusamy, S.K., Ganeshnarayan, K., Markowitz, K., Schreiner, H., Furgang, D., Fine, D.H., and Velliyagounder, K. (2013). Lactoferrin knockout mice demonstrates greater susceptibility to Aggregatibacter actinomycetemcomitans-induced periodontal disease. Journal of periodontology *84*, 1690-1701.

Vieira, S.I., Rebelo, S., Domingues, S.C., da Cruz e Silva, E.F., and da Cruz e Silva, O.A. (2009). S655 phosphorylation enhances APP secretory traffic. Molecular and cellular biochemistry *328*, 145-154.

Vijayan, M., and Reddy, P.H. (2016). Stroke, Vascular Dementia, and Alzheimer's Disease: Molecular Links. Journal of Alzheimer's disease : JAD *54*, 427-443.

Vitelli, R., Santillo, M., Lattero, D., Chiariello, M., Bifulco, M., Bruni, C.B., and Bucci, C. (1997). Role of the small GTPase Rab7 in the late endocytic pathway. The Journal of biological chemistry *272*, 4391-4397.

von Arnim, C.A., von Einem, B., Weber, P., Wagner, M., Schwanzar, D., Spoelgen, R., Strauss, W.L., and Schneckenburger, H. (2008). Impact of

cholesterol level upon APP and BACE proximity and APP cleavage. Biochemical and biophysical research communications *370*, 207-212.

von Koch, C.S., Zheng, H., Chen, H., Trumbauer, M., Thinakaran, G., van der Ploeg, L.H., Price, D.L., and Sisodia, S.S. (1997). Generation of APLP2 KO mice and early postnatal lethality in APLP2/APP double KO mice. Neurobiology of aging *18*, 661-669.

von Rotz, R.C., Kohli, B.M., Bosset, J., Meier, M., Suzuki, T., Nitsch, R.M., and Konietzko, U. (2004). The APP intracellular domain forms nuclear multiprotein complexes and regulates the transcription of its own precursor. Journal of cell science *117*, 4435-4448.

Vonderheit, A., and Helenius, A. (2005). Rab7 associates with early endosomes to mediate sorting and transport of Semliki forest virus to late endosomes. PLoS biology *3*, e233.

Vulpe, C.D., Kuo, Y.M., Murphy, T.L., Cowley, L., Askwith, C., Libina, N., Gitschier, J., and Anderson, G.J. (1999). Hephaestin, a ceruloplasmin homologue implicated in intestinal iron transport, is defective in the sla mouse. Nat Genet *21*, 195-199.

Waldron, E., Isbert, S., Kern, A., Jaeger, S., Martin, A.M., Hebert, S.S., Behl, C., Weggen, S., De Strooper, B., and Pietrzik, C.U. (2008). Increased AICD generation does not result in increased nuclear translocation or activation of target gene transcription. Experimental cell research *314*, 2419-2433.

Walsh, D.M., Fadeeva, J.V., LaVoie, M.J., Paliga, K., Eggert, S., Kimberly, W.T., Wasco, W., and Selkoe, D.J. (2003). gamma-Secretase cleavage and binding to FE65 regulate the nuclear translocation of the intracellular C-terminal domain (ICD) of the APP family of proteins. Biochemistry *42*, 6664-6673.

Walsh, D.M., Minogue, A.M., Sala Frigerio, C., Fadeeva, J.V., Wasco, W., and Selkoe, D.J. (2007). The APP family of proteins: similarities and differences. Biochemical Society transactions *35*, 416-420.

Walter, J. (2016). The Triggering Receptor Expressed on Myeloid Cells 2: A Molecular Link of Neuroinflammation and Neurodegenerative Diseases. The Journal of biological chemistry *291*, 4334-4341.

Wan, M., van der Does, A.M., Tang, X., Lindbom, L., Agerberth, B., and Haeggstrom, J.Z. (2014). Antimicrobial peptide LL-37 promotes bacterial phagocytosis by human macrophages. Journal of leukocyte biology *95*, 971-981.

Wan, X.Z., Li, B., Li, Y.C., Yang, X.L., Zhang, W., Zhong, L., and Tang, S.J. (2012). Activation of NMDA receptors upregulates a disintegrin and metalloproteinase 10 via a Wnt/MAPK signaling pathway. The Journal of neuroscience : the official journal of the Society for Neuroscience *32*, 3910-3916.

Wang, J., Bi, M., Liu, H., Song, N., and Xie, J. (2015). The protective effect of lactoferrin on ventral mesencephalon neurons against MPP + is not connected with its iron binding ability. Scientific reports *5*, 10729.

Wang, L., Sato, H., Zhao, S., and Tooyama, I. (2010). Deposition of lactoferrin in fibrillar-type senile plaques in the brains of transgenic mouse models of Alzheimer's disease. Neuroscience letters *481*, 164-167.

Wang, Q., Du, F., Qian, Z.M., Ge, X.H., Zhu, L., Yung, W.H., Yang, L., and Ke, Y. (2008). Lipopolysaccharide induces a significant increase in expression of iron regulatory hormone hepcidin in the cortex and substantia nigra in rat brain. Endocrinology *149*, 3920-3925.

Wang, Y., and Ha, Y. (2004). The X-ray structure of an antiparallel dimer of the human amyloid precursor protein E2 domain. Molecular cell *15*, 343-353.

Wang, Y., Tu, Y., Han, F., Xu, Z., and Wang, J. (2005). Developmental gene expression of lactoferrin and effect of dietary iron on gene regulation of lactoferrin in mouse mammary gland. Journal of dairy science *88*, 2065-2071.

Ward, E.S., Martinez, C., Vaccaro, C., Zhou, J., Tang, Q., and Ober, R.J. (2005a). From sorting endosomes to exocytosis: association of Rab4 and Rab11 GTPases with the Fc receptor, FcRn, during recycling. Molecular biology of the cell *16*, 2028-2038.

Ward, P.P., and Conneely, O.M. (2004). Lactoferrin: role in iron homeostasis and host defense against microbial infection. Biometals : an international journal on the role of metal ions in biology, biochemistry, and medicine *17*, 203-208.

Ward, P.P., Mendoza-Meneses, M., Cunningham, G.A., and Conneely, O.M. (2003). Iron status in mice carrying a targeted disruption of lactoferrin. Molecular and cellular biology *23*, 178-185.

Ward, P.P., Paz, E., and Conneely, O.M. (2005b). Multifunctional roles of lactoferrin: a critical overview. Cellular and molecular life sciences : CMLS *62*, 2540-2548.

Ward, R.J., Zucca, F.A., Duyn, J.H., Crichton, R.R., and Zecca, L. (2014). The role of iron in brain ageing and neurodegenerative disorders. The Lancet Neurology *13*, 1045-1060.

Wasco, W., Brook, J.D., and Tanzi, R.E. (1993). The amyloid precursor-like protein (APLP) gene maps to the long arm of human chromosome 19. Genomics *15*, 237-239.

Wasco, W., Bupp, K., Magendantz, M., Gusella, J.F., Tanzi, R.E., and Solomon, F. (1992). Identification of a mouse brain cDNA that encodes a protein related to the Alzheimer disease-associated amyloid beta protein precursor. Proceedings of the National Academy of Sciences of the United States of America *89*, 10758-10762.

Washington, P.M., Villapol, S., and Burns, M.P. (2016). Polypathology and dementia after brain trauma: Does brain injury trigger distinct neurodegenerative diseases, or should they be classified together as traumatic encephalopathy? Experimental neurology *275 Pt 3*, 381-388.

Watanabe, T., Nagura, H., Watanabe, K., and Brown, W.R. (1984). The binding of human milk lactoferrin to immunoglobulin A. FEBS letters *168*, 203-207.

Webb, D.J., Thomas, K.S., and Gonias, S.L. (2001). Plasminogen activator inhibitor 1 functions as a urokinase response modifier at the level of cell signaling and thereby promotes MCF-7 cell growth. The Journal of cell biology *152*, 741-752.

Weidemann, A., Eggert, S., Reinhard, F.B., Vogel, M., Paliga, K., Baier, G., Masters, C.L., Beyreuther, K., and Evin, G. (2002). A novel epsilon-cleavage within the transmembrane domain of the Alzheimer amyloid precursor protein demonstrates homology with Notch processing. Biochemistry *41*, 2825-2835.

Weidemann, A., Konig, G., Bunke, D., Fischer, P., Salbaum, J.M., Masters, C.L., and Beyreuther, K. (1989). Identification, biogenesis, and localization of precursors of Alzheimer's disease A4 amyloid protein. Cell *57*, 115-126.

Weiss, G., and Schaible, U.E. (2015). Macrophage defense mechanisms against intracellular bacteria. Immunological reviews *264*, 182-203.

Weyer, S.W., Klevanski, M., Delekate, A., Voikar, V., Aydin, D., Hick, M., Filippov, M., Drost, N., Schaller, K.L., Saar, M., Vogt, M.A., Gass, P., Samanta, A., Jaschke, A., Korte, M., Wolfer, D.P., Caldwell, J.H., and Muller, U.C. (2011). APP and APLP2 are essential at PNS and CNS synapses for transmission, spatial learning and LTP. The EMBO journal *30*, 2266-2280.

White, K.N., Conesa, C., Sanchez, L., Amini, M., Farnaud, S., Lorvoralak, C., and Evans, R.W. (2012). The transfer of iron between ceruloplasmin and transferrins. Biochimica et biophysica acta *1820*, 411-416.

White, M.R., Kandel, R., Tripathi, S., Condon, D., Qi, L., Taubenberger, J., and Hartshorn, K.L. (2014). Alzheimer's associated beta-amyloid protein inhibits influenza A virus and modulates viral interactions with phagocytes. PloS one *9*, e101364.

Wilcke, M., Johannes, L., Galli, T., Mayau, V., Goud, B., and Salamero, J. (2000). Rab11 regulates the compartmentalization of early endosomes required for efficient transport from early endosomes to the trans-golgi network. The Journal of cell biology *151*, 1207-1220.

Wildburger, N.C., Esparza, T.J., LeDuc, R.D., Fellers, R.T., Thomas, P.M., Cairns, N.J., Kelleher, N.L., Bateman, R.J., and Brody, D.L. (2017). Diversity of Amyloid-beta Proteoforms in the Alzheimer's Disease Brain. Scientific reports *7*, 9520.

Willem, M., Tahirovic, S., Busche, M.A., Ovsepian, S.V., Chafai, M., Kootar, S., Hornburg, D., Evans, L.D., Moore, S., Daria, A., Hampel, H., Muller, V., Giudici, C., Nuscher, B., Wenninger-Weinzierl, A., Kremmer, E., Heneka, M.T., Thal, D.R., Giedraitis, V., Lannfelt, L., Muller, U., Livesey, F.J., Meissner, F., Herms, J., Konnerth, A., Marie, H., and Haass, C. (2015). eta-Secretase processing of APP inhibits neuronal activity in the hippocampus. Nature *526*, 443-447.

Wolfe, M.S., Xia, W., Ostaszewski, B.L., Diehl, T.S., Kimberly, W.T., and Selkoe, D.J. (1999). Two transmembrane aspartates in presenilin-1 required for presenilin endoproteolysis and gamma-secretase activity. Nature *398*, 513-517.

Wong, B.X., Ayton, S., Lam, L.Q., Lei, P., Adlard, P.A., Bush, A.I., and Duce, J.A. (2014a). A comparison of ceruloplasmin to biological polyanions in promoting the oxidation of Fe(2+) under physiologically relevant conditions. Biochimica et biophysica acta *1840*, 3299-3310.

Wong, B.X., and Duce, J.A. (2014). The iron regulatory capability of the major protein participants in prevalent neurodegenerative disorders. Frontiers in pharmacology *5*, 81.

Wong, B.X., Tsatsanis, A., Lim, L.Q., Adlard, P.A., Bush, A.I., and Duce, J.A. (2014b). beta-Amyloid precursor protein does not possess ferroxidase activity but does stabilize the cell surface ferrous iron exporter ferroportin. PloS one *9*, e114174.

Wong, H., and Schryvers, A.B. (2003). Bacterial lactoferrin-binding protein A binds to both domains of the human lactoferrin C-lobe. Microbiology *149*, 1729-1737.

Wood, J.A., Wood, P.L., Ryan, R., Graff-Radford, N.R., Pilapil, C., Robitaille, Y., and Quirion, R. (1993). Cytokine indices in Alzheimer's temporal cortex: no changes in mature IL-1 beta or IL-1RA but increases in the associated acute phase proteins IL-6, alpha 2-macroglobulin and C-reactive protein. Brain research *629*, 245-252.

Wood, W.G., Li, L., Muller, W.E., and Eckert, G.P. (2014). Cholesterol as a causative factor in Alzheimer's disease: a debatable hypothesis. Journal of neurochemistry *129*, 559-572.

Woodman, P.G. (2000). Biogenesis of the sorting endosome: the role of Rab5. Traffic *1*, 695-701.

Wu, C., Zhao, W., Yu, J., Li, S., Lin, L., and Chen, X. (2018). Induction of ferroptosis and mitochondrial dysfunction by oxidative stress in PC12 cells. Scientific reports *8*, 574.

Xiang, Z., Ho, L., Yemul, S., Zhao, Z., Qing, W., Pompl, P., Kelley, K., Dang, A., Teplow, D., and Pasinetti, G.M. (2002). Cyclooxygenase-2 promotes amyloid plaque deposition in a mouse model of Alzheimer's disease neuropathology. Gene expression *10*, 271-278.

Xiong, H., Callaghan, D., Jones, A., Walker, D.G., Lue, L.F., Beach, T.G., Sue, L.I., Woulfe, J., Xu, H., Stanimirovic, D.B., and Zhang, W. (2008). Cholesterol retention in Alzheimer's brain is responsible for high beta- and gamma-secretase activities and Abeta production. Neurobiology of disease *29*, 422-437.

Xiong, X.Y., Liu, L., Wang, F.X., Yang, Y.R., Hao, J.W., Wang, P.F., Zhong, Q., Zhou, K., Xiong, A., Zhu, W.Y., Zhao, T., Meng, Z.Y., Wang, Y.C., Gong, Q.W.,

Liao, M.F., Wang, J., and Yang, Q.W. (2016). Toll-Like Receptor 4/MyD88-Mediated Signaling of Hepcidin Expression Causing Brain Iron Accumulation, Oxidative Injury, and Cognitive Impairment After Intracerebral Hemorrhage. Circulation *134*, 1025-1038.

Xu, W., Fang, F., Ding, J., and Wu, C. (2018). Dysregulation of Rab5-mediated endocytic pathways in Alzheimer's disease. Traffic *19*, 253-262.

Xu, X., Zhou, H., and Boyer, T.G. (2011). Mediator is a transducer of amyloid-precursor-protein-dependent nuclear signalling. EMBO reports *12*, 216-222.

Yamamoto, M., Kiyota, T., Horiba, M., Buescher, J.L., Walsh, S.M., Gendelman, H.E., and Ikezu, T. (2007). Interferon-gamma and tumor necrosis factor-alpha regulate amyloid-beta plaque deposition and beta-secretase expression in Swedish mutant APP transgenic mice. The American journal of pathology *170*, 680-692.

Yamamoto, Y., and Gaynor, R.B. (2001). Therapeutic potential of inhibition of the NF-kappaB pathway in the treatment of inflammation and cancer. The Journal of clinical investigation *107*, 135-142.

Yamazaki, T., Koo, E.H., and Selkoe, D.J. (1996). Trafficking of cell-surface amyloid beta-protein precursor. II. Endocytosis, recycling and lysosomal targeting detected by immunolocalization. Journal of cell science *109 (Pt 5)*, 999-1008.

Yamazaki, T., Koo, E.H., and Selkoe, D.J. (1997). Cell surface amyloid beta-protein precursor colocalizes with beta 1 integrins at substrate contact sites in neural cells. The Journal of neuroscience : the official journal of the Society for Neuroscience *17*, 1004-1010.

Yang, A.J., Chandswangbhuvana, D., Margol, L., and Glabe, C.G. (1998). Loss of endosomal/lysosomal membrane impermeability is an early event in amyloid Abeta1-42 pathogenesis. Journal of neuroscience research *52*, 691-698.

Yang, L.B., Lindholm, K., Yan, R., Citron, M., Xia, W., Yang, X.L., Beach, T., Sue, L., Wong, P., Price, D., Li, R., and Shen, Y. (2003). Elevated beta-secretase expression and enzymatic activity detected in sporadic Alzheimer disease. Nature medicine *9*, 3-4.

Yang, W.M., Jung, K.J., Lee, M.O., Lee, Y.S., Lee, Y.H., Nakagawa, S., Niwa, M., Cho, S.S., and Kim, D.W. (2011). Transient expression of iron transport proteins in the capillary of the developing rat brain. Cellular and molecular neurobiology *31*, 93-99.

Yang, W.S., SriRamaratnam, R., Welsch, M.E., Shimada, K., Skouta, R., Viswanathan, V.S., Cheah, J.H., Clemons, P.A., Shamji, A.F., Clish, C.B., Brown, L.M., Girotti, A.W., Cornish, V.W., Schreiber, S.L., and Stockwell, B.R. (2014). Regulation of ferroptotic cancer cell death by GPX4. Cell *156*, 317-331.

Yang, W.S., and Stockwell, B.R. (2008). Synthetic lethal screening identifies compounds activating iron-dependent, nonapoptotic cell death in oncogenic-RAS-harboring cancer cells. Chemistry & biology *15*, 234-245.

Yang, Z., and Xiong, H.-R. (2012). Culture Conditions and Types of Growth Media for Mammalian Cells. In.

Yao, Z.X., and Papadopoulos, V. (2002). Function of beta-amyloid in cholesterol transport: a lead to neurotoxicity. FASEB journal : official publication of the Federation of American Societies for Experimental Biology *16*, 1677-1679.

Yap, C.C., and Winckler, B. (2015). Adapting for endocytosis: roles for endocytic sorting adaptors in directing neural development. Frontiers in cellular neuroscience *9*, 119.

Yoshikai, S., Sasaki, H., Doh-ura, K., Furuya, H., and Sakaki, Y. (1991). Genomic organization of the human-amyloid beta-protein precursor gene. Gene *102*, 291-292.

You, L.H., Yan, C.Z., Zheng, B.J., Ci, Y.Z., Chang, S.Y., Yu, P., Gao, G.F., Li, H.Y., Dong, T.Y., and Chang, Y.Z. (2017). Astrocyte hepcidin is a key factor in LPS-induced neuronal apoptosis. Cell death & disease *8*, e2676.

Yuyama, K., and Yanagisawa, K. (2009). Late endocytic dysfunction as a putative cause of amyloid fibril formation in Alzheimer's disease. Journal of neurochemistry *109*, 1250-1260.

Zecca, L., Youdim, M.B., Riederer, P., Connor, J.R., and Crichton, R.R. (2004). Iron, brain ageing and neurodegenerative disorders. Nature reviews Neuroscience *5*, 863-873.

Zechel, S., Huber-Wittmer, K., and von Bohlen und Halbach, O. (2006). Distribution of the iron-regulating protein hepcidin in the murine central nervous system. Journal of neuroscience research *84*, 790-800.

Zemankova, N., Chlebova, K., Matiasovic, J., Prodelalova, J., Gebauer, J., and Faldyna, M. (2016). Bovine lactoferrin free of lipopolysaccharide can induce a proinflammatory response of macrophages. BMC veterinary research *12*, 251.

Zerial, M., and McBride, H. (2001). Rab proteins as membrane organizers. Nature reviews Molecular cell biology *2*, 107-117.

Zhang, D., Lee, H.F., Pettit, S.C., Zaro, J.L., Huang, N., and Shen, W.C. (2012). Characterization of transferrin receptor-mediated endocytosis and cellular iron delivery of recombinant human serum transferrin from rice (Oryza sativa L.). BMC biotechnology *12*, 92.

Zhang, D.L., Senecal, T., Ghosh, M.C., Ollivierre-Wilson, H., Tu, T., and Rouault, T.A. (2011). Hepcidin regulates ferroportin expression and intracellular iron homeostasis of erythroblasts. Blood *118*, 2868-2877.

Zhang, F., and Jiang, L. (2015). Neuroinflammation in Alzheimer's disease. Neuropsychiatric disease and treatment *11*, 243-256.

Zhang, W., Guo, H., Jing, H., Li, Y., Wang, X., Zhang, H., Jiang, L., and Ren, F. (2014). Lactoferrin stimulates osteoblast differentiation through PKA and p38 pathways independent of lactoferrin's receptor LRP1. Journal of bone and mineral research : the official journal of the American Society for Bone and Mineral Research *29*, 1232-1243.

Zhang, X., and Song, W. (2013a). The role of APP and BACE1 trafficking in APP processing and amyloid-beta generation. Alzheimer's research & therapy *5*, 46.

Zhang, X., and Song, W. (2013b). The role of APP and BACE1 trafficking in APP processing and amyloid-β generation. Alzheimer's research & therapy *5*, 46.

Zhang, Z., Song, M., Liu, X., Su Kang, S., Duong, D.M., Seyfried, N.T., Cao, X., Cheng, L., Sun, Y.E., Ping Yu, S., Jia, J., Levey, A.I., and Ye, K. (2015). Delta-secretase cleaves amyloid precursor protein and regulates the pathogenesis in Alzheimer's disease. Nature communications *6*, 8762.

Zhao, G., Liu, Z., Ilagan, M.X., and Kopan, R. (2010). Gamma-secretase composed of PS1/Pen2/Aph1a can cleave notch and amyloid precursor protein in the absence of nicastrin. The Journal of neuroscience : the official journal of the Society for Neuroscience *30*, 1648-1656.

Zhao, N., Pang, B., Shyu, C.R., and Korkin, D. (2011). Charged residues at protein interaction interfaces: unexpected conservation and orchestrated divergence. Protein science : a publication of the Protein Society *20*, 1275-1284.

Zheng, H., Jia, L., Liu, C.C., Rong, Z., Zhong, L., Yang, L., Chen, X.F., Fryer, J.D., Wang, X., Zhang, Y.W., Xu, H., and Bu, G. (2017). TREM2 Promotes Microglial Survival by Activating Wnt/beta-Catenin Pathway. The Journal of neuroscience : the official journal of the Society for Neuroscience *37*, 1772-1784.

Zheng, H., Jiang, M., Trumbauer, M.E., Hopkins, R., Sirinathsinghji, D.J., Stevens, K.A., Conner, M.W., Slunt, H.H., Sisodia, S.S., Chen, H.Y., and Van der Ploeg, L.H. (1996). Mice deficient for the amyloid precursor protein gene. Annals of the New York Academy of Sciences *777*, 421-426.

Zheng, H., Jiang, M., Trumbauer, M.E., Sirinathsinghji, D.J., Hopkins, R., Smith, D.W., Heavens, R.P., Dawson, G.R., Boyce, S., Conner, M.W., Stevens, K.A., Slunt, H.H., Sisoda, S.S., Chen, H.Y., and Van der Ploeg, L.H. (1995). beta-Amyloid precursor protein-deficient mice show reactive gliosis and decreased locomotor activity. Cell *81*, 525-531.

Zheng, H., and Koo, E.H. (2011). Biology and pathophysiology of the amyloid precursor protein. Molecular neurodegeneration *6*, 27.

Zhong, L., Chen, X.F., Zhang, Z.L., Wang, Z., Shi, X.Z., Xu, K., Zhang, Y.W., Xu, H., and Bu, G. (2015). DAP12 Stabilizes the C-terminal Fragment of the Triggering Receptor Expressed on Myeloid Cells-2 (TREM2) and Protects against LPS-induced Pro-inflammatory Response. The Journal of biological chemistry *290*, 15866-15877.

Zhou, J., Yu, J.T., Wang, H.F., Meng, X.F., Tan, C.C., Wang, J., Wang, C., and Tan, L. (2015). Association between stroke and Alzheimer's disease: systematic review and meta-analysis. Journal of Alzheimer's disease : JAD *43*, 479-489.

Zhou, Z.D., and Tan, E.K. (2017). Iron regulatory protein (IRP)-iron responsive element (IRE) signaling pathway in human neurodegenerative diseases. Molecular neurodegeneration *12*, 75.

Zhu, G., Wang, D., Lin, Y.H., McMahon, T., Koo, E.H., and Messing, R.O. (2001). Protein kinase C epsilon suppresses Abeta production and promotes activation of alpha-secretase. Biochemical and biophysical research communications *285*, 997-1006.

Zhu, W.Z., Zhong, W.D., Wang, W., Zhan, C.J., Wang, C.Y., Qi, J.P., Wang, J.Z., and Lei, T. (2009). Quantitative MR phase-corrected imaging to investigate increased brain iron deposition of patients with Alzheimer disease. Radiology *253*, 497-504.

Zilberberg, A., Yaniv, A., and Gazit, A. (2004). The low density lipoprotein receptor-1, LRP1, interacts with the human frizzled-1 (HFz1) and down-regulates the canonical Wnt signaling pathway. The Journal of biological chemistry *279*, 17535-17542.

APPENDIX I: CALCULATIONS REQUIRED FOR DISSOCIATION CONSTANTS

Sedimentation velocity analysis

In general, the sedimentation velocity data is fitted to the function:

$$Sw = \frac{1}{c_{tot}} \sum S_i c_i \qquad \text{Eq 1}$$

where Sw is the weight average sedimentation coefficient, c_{tot} is the total concentration of macromolecules, S_i is the sedimentation coefficient of component i, and c_i is the concentration of component i.

The concentration of each component is related to the dissociation constant (Kd) of the complex by standard mass conservation equations:

$$m_A m_L K = m_{AL}, \qquad m_{A,tot} = m_A + m_{AL}, \qquad m_{L,tot} = m_L + m_{AL}$$

$$Sw = \frac{s_A \varepsilon_A m_A + s_L \varepsilon_L m_L + s_{AL}(\varepsilon_A + \varepsilon_L) m_{AL}}{\varepsilon_A m_{A,tot} + \varepsilon_L m_{L,tot}} \qquad 2$$

where m indicates the total (tot) molar concentration m_A, m_L, and m_{AL} of species A (APP), L (lactoferrin) and AL (APP and lactoferrin), respectively. It is assumed that all species are in instantaneous equilibrium following the mass action law with the equilibrium association constant K, with ε denoting each species extinction coefficient. From the analysis of these equations, binding constants as well as an s-value of the complex was determined by nonlinear regression in Sedfit 9.4.

Tryptophan fluorescence analysis

The fluorescence data was analysed using the following equation:

$$I_t = (fA \times IA) + (fL \times IL) + (fAL_1 \times IAL_1) + (fAL_2 \times IAL_2) + \left(fAL_{1,2} \times IAL_{1,2}\right) \qquad 1$$

where the total intensity (I_t) of the sample is given by the fraction (f) of APP alone (A), lactoferrin alone (L), APP and lactoferrin bound at site one (LA_1), APP with lactoferrin bound at site two (LA_2) and APP with lactoferrin bound at site one and

site two ($LA_{1,2}$) multiplied by the intensity of each respective complex. The equilibrium concentration of each complex is determined by:

$$[A]_{free} = \frac{Kd_{1:1}Kd_{1:2}[A]_t}{Kd_{1:1}Kd_{1:2}+Kd_{1:1}[L]+Kd_{1:2}[L]+[L]^2} \quad 2$$

$$AL_1 = \frac{[L][A]}{Kd_{1:1}} \quad 3$$

$$AL_2 = \frac{[L][A]}{Kd_{1:2}} \quad 4$$

$$AL_{1,2} = \frac{[L]^2[A]}{Kd_{1:1}Kd_{1:2}} \quad 5$$

and

$$[L] = \frac{\alpha}{3} + \frac{2}{3}\sqrt{(\alpha^2 - 3b)}\frac{\theta}{3} \quad 6$$

where

$$\alpha = Kd_{1:1} + Kd_{1:2} + 2[A]_t - [L]_t \quad 7$$

$$b = Kd_{1:1}Kd_{1:2} + Kd_{1:1}[A]_t + Kd_{1:2}[A]_t - Kd_{1:1}[L]_t - Kd_{1:2}[L]_t \quad 8$$

$$c = Kd_{1:1}Kd_{1:2}[L]_t \quad 9$$

where $[A]_{free}$ is the free concentration of APP, $[A]_t$ is the total concentration of APP, [L] is the free concentration of lactoferrin, $[L]_t$ is the total concentration of lactoferrin, $Kd_{1:1}$ is the dissociation constant for binding to site one and $Kd_{1:2}$ is the dissociation constant for binding to site two. These equations are a general description of an independent two-site interaction. To apply these equations to the current model we assume that the change in fluorescence intensity is taken to be proportional to the fraction of each complex and that the binding of lactoferrin to site one is taken to provide the same fluorescence change as the binding of lactoferrin to site two.

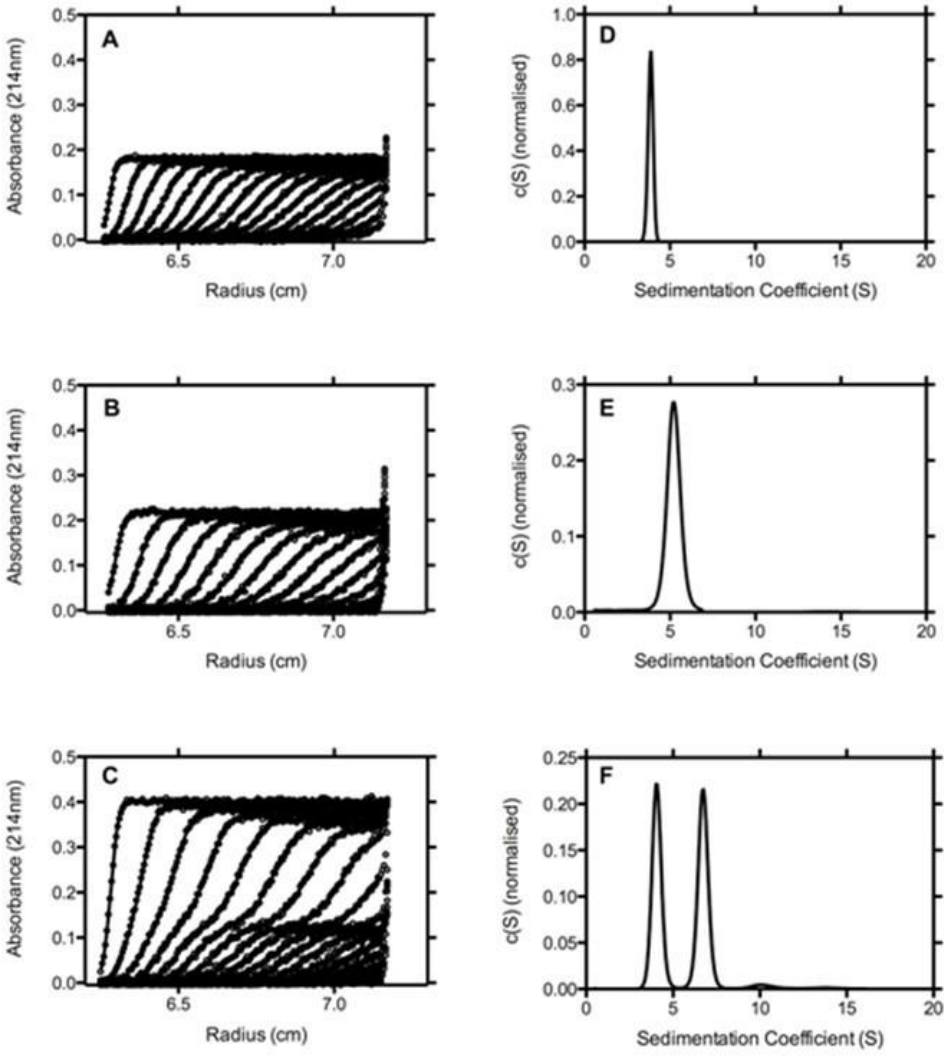

Figure S1. Related to Figure 1A. Sedimentation velocity data for **(A)** APP alone, **(B)** Lf alone and **(C)** a mixture of APP and Lf (circles). **(A, B & C)** The data were fitted using the c(S) model from sedfit 9.4 (solid lines through the data) to obtain the corresponding sedimentation coefficient distributions in **D, E & F**.

APPENDIX II: CURRICULUM VITAE

ANDREW TSATSANIS

EDUCATION

Completed 2004	Honours (Immunology/Pathology) Austin Research Institute, Melbourne, Australia
Completed 2003	Bachelor of Science Majors include: Pathology and Immunology The University of Melbourne, Melbourne, Australia
Completed 2000	Victorian Certificate of Education Lalor North Secondary College, Melbourne, Australia

EMPLOYMENT

Mar 2016 – present	PhD. School of Biomedical Sciences. The University of Leeds, UK
May 2012 – Feb 2016	Senior Research Assistant. Cellular and Molecular Biology. The University of Leeds, UK
Jan 2012 - May 2012	Senior Research Assistant. The Florey Institute of Neuroscience and Mental Health, Australia
Jan 2011 - Jan 2012	Senior Research Technician II. Ontario Cancer Institute, The University Health Network, Toronto, Canada
Jan 2005 - June 2010	Research Assistant. The Mental Health Research Institute of Victoria, Australia
Oct 2007 - Feb 2008	Clinical Trials Assistant. The Mental Health Research Institute of Victoria and Prana Biotechnology, Australia

RESEARCH ARTICLE PUBLICATIONS

(Web of Science report. Total times cited: 888, h-index: 7)

(1) **Tsatsanis A**, Wong BX, Gunn AP, Ayton S, Diouff I, Bush AI, Devos D, Duce JA and the Alzheimer's Disease Neuroimaging Initiative. Amyloidogenic processing of β-amyloid precursor protein increases susceptibility to neuroferroptosis through iron retention. ***Manuscript in preparation.*** 2019.

(2) **Tsatsanis A**, Wong BX, Ryan TM, Evans RW, Bush AI, Sivaprasadarao A, Duce JA. The inflammatory protein lactoferrin internalises APP via an ARF6-dependent pathway to exacerbate Aβ production. ***Manuscript in preparation.*** 2019.

(3) **Tsatsanis A**, Dickens S, Kwok JCF, Wong BX, Duce JA. Post Translational Modulation of β-Amyloid Precursor Protein Trafficking to the Cell Surface Alters Neuronal Iron Homeostasis. ***Neurochem Res.*** 2019 Feb 22. PMID: 30796750

(4) Dean B, **Tsatsanis A**, Lam LQ, Scarr E, Duce JA. Changes in cortical protein markers of iron transport with gender, major depressive disorder and suicide. ***World J Biol Psychiatry.*** 2019 Jan 30:1-8. PMID: 30513246

(5) Lopez Sanchez MIG, Waugh HS, **Tsatsanis A**, Wong BX, Crowston JG, Duce JA, Trounce IA. Amyloid precursor protein drives down-regulation of mitochondrial oxidative phosphorylation independent of amyloid beta. ***Sci Rep.*** 2017 Aug 29:7(1):9835. PMID: 28852095

(6) Workman DG, **Tsatsanis A**, Lewis FW, Boyle JP, Mousadoust M, Hettiarachchi NT, Hunter M, Peers CS, Tétard D, Duce JA. Protection from neurodegeneration in the 6-hydroxydopamine (6-OHDA) model of Parkinson's with novel 1-hydroxypyridin-2-one metal chelators. ***Metallomics.*** 2015 Mar 17. PMID: 25781076

(7) Wong BX, **Tsatsanis A**, Lim LQ, Adlard PA, Bush AI, Duce JA. β-Amyloid precursor protein does not possess ferroxidase activity but does stabilize the cell surface ferrous iron exporter ferroportin. ***PLoS One.*** 2014 Dec 2;9(12):e114174. PMID: 25464026

(8) O'Brien CA, Kreso A, Ryan P, Hermans KG, Gibson L, Wang Y, **Tsatsanis A**, Gallinger S, Dick JE. ID1 and ID3 regulate the self-renewal capacity of human colon cancer-initiating cells through p21. ***Cancer Cell.*** 2012 Jun 12;21(6):777-92. PMID: 22698403

(9) Duce JA, Ayton S, Miller AA, **Tsatsanis A**, Lam LQ, Leone L, Corbin JE, Butzkueven H, Kilpatrick TJ, Rogers JT, Barnham KJ, Finkelstein DI, Bush AI. Amine oxidase activity of β-amyloid precursor protein modulates systemic and local catecholamine levels. ***Mol Psychiatry.*** 2013 Feb;18(2):245-54. PMID: 22212595

(10) Duce JA, **Tsatsanis A**, Cater MA, James SA, Robb E, Wikhe K, Leong SL, Perez K, Johanssen T, Greenough MA, Cho HH, Galatis D, Moir RD, Masters CL, McLean C, Tanzi RE, Cappai R, Barnham KJ, Ciccotosto GD, Rogers JT, Bush AI. Iron-export ferroxidase activity of β-amyloid precursor protein is inhibited by zinc in Alzheimer's disease. ***Cell.*** 2010 Sep 17;142(6):857-67. PMID: 20817278

(11) Faux NG, Ritchie CW, Gunn A, Rembach A, **Tsatsanis A**, Bedo J, Harrison J, Lannfelt L, Blennow K, Zetterberg H, Ingelsson M, Masters CL, Tanzi RE, Cummings JL, Herd CM, Bush AI. PBT2 Rapidly Improves Cognition in Alzheimer's Disease: Additional Phase II Analyses. ***J Alzheimers Dis.*** 2010;20(2):509-16. PMID: 20164561

(12) Smidt K, Jessen N, Petersen AB, Larsen A, Magnusson N, Jeppesen JB, Stoltenberg M, Culvenor JG, **Tsatsanis A**, Brock B, Schmitz O, Wogensen L, Bush AI, Rungby J. SLC30A3 responds to glucose- and zinc variations in beta-cells and is critical for insulin production and in vivo glucose-metabolism during beta-cell stress. ***PLoS One.*** 2009 May 25;4(5):e5684. PMID: 19492079

(13) Strozyk D, Launer LJ, Adlard PA, Cherny RA, **Tsatsanis A**, Volitakis I, Blennow K, Petrovitch H, White LR, Bush AI. Zinc and copper modulate Alzheimer Abeta levels in human cerebrospinal fluid. ***Neurobiol Aging.*** 2009 Jul;30(7):1069-77. PMID: 18068270

BOOK CHAPTER PUBLICATIONS

(1) Wong BX, Lam LQ, **Tsatsanis A**, Duce JA. (2017) Evaluating Iron Flux in the Brain. In: White A. (eds) ***Metals in the Brain.*** Neuromethods, vol 124. Humana Press, New York, NY

LABORATORY EXPERIENCE

I have facilitated a role as a research assistant for over 10 years gaining substantial international experience. I have a strong background in neurodegeneration and am highly experienced at performing a broad range of laboratory procedures using a range of assays, scientific instruments and techniques. Proficiencies includes, but not limited to:

Recombinant DNA technology	Western blotting
Mutagenesis	Light and Confocal Microscopy
PCR	Cell and Tissue culture techniques
Immunofluorescence	Microbiological assays
UV Spectrophotometry	Lentiviral production
Kinetic measurements	Flow Cytometry
Calorimetric assays	Animal experimentation
Protein purification	Animal and human tissue processing
Gel electrophoresis (SDS-PAGE)	Radioactive material handling

AWARDS

(1) Winner - Best oral presentation at The University of Leeds Postgraduate Scientific Symposium, Leeds (May, 2018). ‘The iron-bound form of Lactoferrin directly binds to β-Amyloid Precursor Protein to produce Aβ and increase iron levels inside the cell’

(2) Winner - Young Scientist Travel Award to present oral presentation at The International Society for Neurochemistry (ISN) conference, Paris (August, 2017). ‘Lactoferrin is an iron transporter and key innate immune response protein that directly binds β-Amyloid Precursor Protein to promote amyloidogenic processing’

ORAL PRESENTATIONS

(1) ‘The iron-bound form of Lactoferrin binds to β-Amyloid Precursor Protein to exacerbate Aβ and increase iron levels inside the cell’ *Alzheimer’s Research*

Network meeting, Leeds (June, 2018) and The University of Leeds Postgraduate Scientific Symposium, Leeds (May, 2018)

(2) ‘Lactoferrin is an iron transporter and key innate immune response protein that directly binds β-Amyloid Precursor Protein to promote amyloidogenic processing’ *International Society for Neurochemistry (ISN) conference, Paris (August, 2017) and Alzheimer’s Research Network meeting, Sheffield (June, 2017)*

POSTERS PRESENTED IN PERSON

(1) ‘The iron-bound form of Lactoferrin directly binds to β-Amyloid Precursor Protein to produce Aβ and increase iron levels inside the cell’ *The Alzheimer’s Society Annual Conference, London (May, 2018)*

(2) ‘Lactoferrin is an iron transporter and key innate immune response protein that directly binds β-Amyloid Precursor Protein to promote amyloidogenic processing’ *The Alzheimer's Association International Conference, London (July, 2017) and The Alzheimer’s Society Annual Conference, London (May, 2017)*

(3) ‘The influence of β-Amyloid Precursor Protein proteolytic processing on neuronal iron homeostasis’ *White Rose Dementia Symposium, Sheffield (May, 2016)*

(4) ‘Alzheimer's Disease β-Amyloid Precursor Protein functions as an iron export ferroxidase’ *The International Alzheimer’s Disease/ Parkinson’s Disease Conference, Prague (March, 2009)*

(5) ‘Alzheimer's disease β-amyloid precursor protein is ferroxidase II, a ceruloplasmin-like iron detoxification enzyme’ *The International Conference of Alzheimer’s Disease, Chicago (July, 2008)*

(6) ‘A novel role for the β-amyloid precursor protein of Alzheimer’s disease involving extracellular superoxide dismutase interaction’ *Australia Lorne Proteins Conference (2007)*

(7) ‘Endogenous human β-amyloid precursor protein possesses oxidase activity’ *The International Conference of Alzheimer’s Disease, Madrid (July, 2006)*